

**Pathological and Immunological Changes in  
Host Cells in Response to  
*Leishmania mexicana* Infection**

A Thesis Submitted by

**Salah Mahrous Alhajri**

**Nottingham Trent University, UK**

For the partial requirements for the degree of

Doctor of Philosophy

April 2019



## **Copyright statement**

This work is the intellectual property of the author and may also be owned by the research sponsor (s) and/or Nottingham Trent University. You may copy up to 5% of this work for private study, or personal, non-commercial research. Any re-use of the information contained within this document should be fully referenced, quoting the author, title, university, degree level and pagination. Queries or requests for any other use, or if a more substantial copy is required, should be directed in the first instance to the author.

Salah Alhajri

## **Communications resulting from this study**

### **Conferences**

- Salah Al-Hajri; Gemma Foulds, Abbas Faraj and Selman Ali (2018) A model to study the effect of Leishmania parasite virulence on interaction with Balb/c and C57 mice macrophages Poster presentation at First INTERNATIONAL CAPARICA CONGRESS ON LEISHMANIASIS 29th – 31st October 2018 | Caparica | Portugal
- Salah Al-Hajri; Abbas Faraj, Khdiya Ali and Selman Ali (2016), A model to study the effect of Leishmania parasite virulence on interaction with host cells, Poster presentation at British society for parasitology (BSP) Trypanosomiasis and Leishmaniasis Seminar 2016 České Budějovice (Budweis), Czech Republic.

## **Acknowledgements**

I would like to first thank God for enabling me to complete my Doctor of Philosophy. I am also grateful to number of people whose contributions made this thesis possible.

I would like to sincerely thank my lead supervisor Dr. Ali Selman for his support, guidance and continuous monitoring. Sincere thanks to my other supervisors Dr Sergio Colombo and Dr Shiva Sivasubramaniam as well as my Independent Assessor Dr Luigi De Girolamo for their help and support. I would also like to thank the Saudi Arabia Cultural Bureau and my sponsor, Ministry of Education of Kingdom Saudi Arabia for giving me the opportunity to expand my knowledge in science.

I am also thankful to Gemma Foulds, from The John van Geest Cancer Research Centre at NTU for helping me to use the flow cytometry analysis. I would also like take this opportunity to thank all my colleagues Dr. Reham Balahmar, Alanood Algarni, Adeola grace Akashdeep and Abed Ali, for their help and cooperation in the lab during the implementation for this study. I would particularly like to thank Professor Ahmad Alluwaimi, Dr. Abbas Hameed and James Daubney who have provided me with invaluable help, supports and advices. With special thanks to those who encouraged me with my PhD; Dr. Ibarihm Alshubaith, my brother Mamdooh, my cousin Ehsan, and my friend Ali Albader

I would like to thank my loving father, who taught me the patience and how to achieve my target independently. Last but not the least, I would like to thank my wife Dr. Ahlam Alhajri and my lovely daughters Fatimah, Sarah, Amnah and Mariya, for supporting me spiritually throughout my study.

## **Funding**

I extend my gratitude towards the funding body, the Saudi Ministry of Education, which generously supported and fully funded this work.

## Abstract

**Introduction:** Leishmaniasis is a group of parasitic diseases caused by obligate intracellular protozoa of the genus *Leishmania*, with more than 20 pathogenic species. *Leishmania* infects approximately 12 million people annually in 98 countries. The deaths associated with this disease ranges between 20,000 - 30,000 per year (WHO, 2018). Therefore, the need for treatments or vaccines get more urgent. Macrophages are the ultimate host cell for the *Leishmania* parasite where it survives and multiplies. Though, a lot is known on how the *Leishmania* parasite survives and multiplies inside macrophages, there are still aspects related to pathophysiological and immunological responses to their infection that need further investigation to aid in the development of new vaccines or drugs for this disease. In this study, a virulent and avirulent *L.mexicana* model was developed to examine their interaction with bone marrow derived macrophages (BMDM) from susceptible (Balb/c) and resistant (C57) mice *in vitro*.

**Methods:** Virulent *L.mexicana* parasite MNYC/BZ/62/M379 (P1) was maintained by subcutaneous inoculation of Balb/c mice. Avirulent *L.mexicana* passage twenty (P20) was produced by sub culturing of *L.mexicana* passage one (P1) twenty times *in vitro*. The effects of 20 continuous passages on virulence-associated gene (LPG1, LPG2, A2, CHAT1, CPB2, CPB2.8, CPC, GP63, LACK, and MAPK9) were investigated using qPCR. The expression of LPG and PS was also investigated using flow cytometry and immunofluorescence analysis. Growth characteristics and morphology of avirulent (P20) and virulent (P1) *L.mexicana* parasites grown in two media (Schneider's *Drosophila* and RPMI1640) *in vitro* were investigated under different culture conditions (temperature, and oxygen) using light immunofluorescence microscopy, EM and AFM. Differentiation into amastigotes under several conditions was investigated by estimation of the number of amastigotes. The infectivity of the parasites at each passage was also assessed by hemocytometry and Alamar blue assay. Survival of parasites inside macrophages was assessed visually by labelling the parasites with CFSE stain and the ability to form PV in BMDM from C57 and Balb/c mice. qPCR was used assess the expression pro-inflammatory cytokine expression (TNF-  $\alpha$ , IL-6, IL-1 $\beta$  and TGF- $\beta$ ) and ELISA was used for estimation of TNF- $\alpha$  in the culture supernatants. Annexin V stain and flow cytometry analysis was used to assess apoptosis of infected cells. qPCR was used to assess the expression of genes associated with apoptosis (Bax, BCL 2, Caspase 1, Caspase 8, Caspase 9 and PD 1). The effect of supernatants derived from cultures of infected BMDM on the P1 and P20 promastigotes growth and virulence genes regulation was also investigated by qPCR.

**Results:** Twenty passages of *L.mexicana in vitro* caused significant changes in parasite morphology, ability to differentiate into amastigotes and downregulation of all tested virulence associated genes. Expression of LPG decreased, and PS increased on the surface of *L.mexicana* promastigotes. P20 infected both Balb/c and C57 BMDM but failed to survive inside BMDM both mice strains. P1 survived and inhibited apoptosis accompanied by significant downregulation of Caspase 8 by qPCR. Both P1 and P20 induced the release of TNF- $\alpha$  as confirmed by qPCR and ELISA. P1 promastigotes incubated in conditioned media derived from Balb/c BMDM infected with P1, enhanced their growth accompanied by upregulation of LPG1, CHT1, CPB2 and CPB2.8. While, incubation in conditioned media derived from C57 BMDM infected with P1 inhibited their growth and caused downregulation of LPG1, LPG2 CPB2, CPB2.8, CHT1 and A2.

**Conclusion:** Culturing of *L.mexicana in vitro* for 20 passages has produced significant changes in their ability to differentiate from promastigotes into amastigotes, the ability to survive in macrophages and regulation of apoptosis associated genes. Supernatants produced by BMDM infected with P1 enhanced the growth rate of P1 promastigotes, when derived from Balb/c and inhibited their growth when derived from C57 cells. Understanding differences between P1 and P20 and their interaction with mammalian host may help in identifying the virulence factors of P1 *L.mexicana* which may aid in development of vaccines or drugs against this disease.

## Table of Contents

<b>1</b>	<b>CHAPTER 1: INTRODUCTION</b>	<b>1</b>
1.1	INTRODUCTION	2
1.2	TRANSMISSION	2
1.3	CLINICAL SIGNS	3
1.4	EPIDEMIOLOGY	3
1.4.1	<i>Leishmania</i> parasite species that are known as causative agents of Leishmaniasis in humans	5
1.5	PREVENTION AND CONTROL	6
1.6	TREATMENT	6
1.6.1	Antimony	7
1.6.2	Amphotericin B	7
1.6.3	Miltefosine	8
1.7	VACCINATION	8
1.8	LEISHMANIA PARASITES	8
1.8.1	<i>Leishmania</i> parasite classification	8
1.8.2	<i>L.mexicana</i> genome	9
1.8.3	<i>L.mexicana</i> morphology	9
1.8.4	<i>Leishmania</i> life cycle	11
1.8.5	<i>L.mexicana</i> virulence	12
1.8.6	<i>Leishmania</i> parasite within the vector	13
1.8.7	Role of parasite surface molecules	13
1.8.8	Glycoprotein 63 (GP63)	13
1.8.9	Lipophosphoglycans (LPG)	15
1.8.9.1	LPG1 gene	17
1.8.9.2	LPG2 gene	17
1.8.10	Cysteine peptidases (CP)	17
1.8.11	MAPK9 gene	18
1.9	LEISHMANIA HOST CELL INTERACTION	18
1.9.1	Interaction of <i>Leishmania</i> with host cells	19
1.9.2	Phagocytosis of the <i>Leishmania</i> parasite	20
1.9.3	Phagocytosis of promastigotes by macrophages	21
1.9.4	Phagocytosis of amastigotes by macrophages	21
1.9.5	Receptors and recognition	22
1.9.5.1	Third complement receptor (CR3)	22
1.9.5.2	First complement receptor (CR1)	22
1.9.6	Survival of <i>Leishmania</i> parasite in the blood stream and macrophage	23
1.9.7	LPG and inhibition of phagosome maturation in a macrophage	23
1.9.8	Nitric Oxide	24
1.9.9	Nuclear factor kappa-light-chain-enhancer of activated B cells (NF- $\kappa$ B)	25
1.10	APOPTOSIS	26
1.10.1	Apoptosis pathways	27
1.10.2	Apoptosis mechanism	28
1.10.3	Gene regulation of apoptosis	28
1.10.3.1	BCL 2	28

1.10.3.2	Bax.....	29
1.10.3.3	Macrophage Programmed death 1 receptor.....	29
1.10.3.4	Caspases.....	29
1.11	PYROPTOSIS.....	30
1.12	AUTOPHAGY.....	31
1.13	ROLE OF AUTOPHAGY IN DIFFERENTIATION OF <i>LEISHMANIA</i> PROMASTIGOTES INTO AMASTIGOTES..	31
1.13.1	<i>Paraptosis</i> .....	32
1.13.2	<i>Necrosis</i> .....	32
1.13.3	<i>Apoptosis in Leishmania Parasites</i> .....	32
1.13.4	<i>Apoptosis and immunity</i> .....	33
1.14	PROINFLAMMATORY CYTOKINES.....	35
1.14.1	<i>Interleukin 1 (IL-1)</i> .....	36
1.14.2	<i>Interleukin 6 (IL-6)</i> .....	36
1.14.3	<i>Tumour necrosis factor-<math>\alpha</math> (TNF-<math>\alpha</math>)</i> .....	37
1.14.4	<i>Transforming growth factor beta (TGF-<math>\beta</math>)</i> .....	37
1.15	BALB/C AND C57 MICE.....	39
1.16	AIMS AND HYPOTHESIS.....	40
<b>2</b>	<b>CHAPTER 2: MATERIALS AND METHODS .....</b>	<b>41</b>
2.1	MATERIALS .....	42
2.2	INTRODUCTION.....	48
2.3	VIRULENT AND AVIRULENT <i>L. MEXICANA</i> .....	48
2.3.1	<i>Virulent L. mexicana (P1)</i> .....	48
2.3.2	<i>Avirulent L. mexicana (P20)</i> .....	48
2.4	STORING OF <i>L. MEXICANA</i> PARASITES.....	49
2.5	PREPARATION OF P1 AND P20 <i>L. MEXICANA</i> FOR INFECTION .....	49
2.6	WORKFLOW OF CHARACTERISATION OF P1 AND P20 <i>L. MEXICANA</i> .....	49
2.6.1	<i>Growth and morphology characteristics of P1 and P20 L. mexicana</i> .....	50
2.6.2	<i>Morphology of P1 and P20 L. mexicana Promastigotes</i> .....	50
2.6.3	<i>Slide preparation for Giemsa staining, Atomic Force Microscope and Electronic Microscope</i>	51
2.6.4	<i>Giemsa Stain</i> .....	51
2.6.5	<i>Atomic Force Microscope and Electron Microscope</i> .....	51
2.6.6	<i>Labelling of P1 and P20 L. mexicana promastigotes by CFSE</i> .....	51
2.6.7	<i>Body and flagella measurement of P1 and P20 L.mexicana promastigotes</i> .....	51
2.6.8	<i>Data analysis of P1 and P20 promastigote morphology</i> .....	52
2.6.9	<i>Effect of culture conditions on P1 and P20 L.mexicana differentiation into amastigotes</i> .....	52
2.6.10	<i>Effect of pH 5.5 medium on P1 and P20 L.mexicana differentiation into amastigotes</i> .....	53
2.6.11	<i>Effect of RPMI1640 versus Schneider's Drosophila medium on P1 and P20 L.mexicana promastigotes growth rate using Alamar blue assay</i> .....	53
2.6.12	<i>Effect of L.mexicana concentration on the RPMI1640 medium pH after 2- and 24-hours incubation at 37°C</i> .....	54
2.6.13	<i>Virulence gene regulation of P1 and P20 L.mexicana promastigotes</i> .....	54
2.6.14	<i>Regulation of LPG1, LPG2, GP63, CPB 2, CPB 2.8 and A2 genes of P1 and P20 L.mexicana promastigotes and amastigotes</i> .....	55

2.6.15	Detection of <i>L. mexicana</i> LPG in P1 and P20 promastigotes.....	55
2.6.16	Immunofluorescence staining of LPG .....	55
2.6.17	Detection of LPG by flow cytometry.....	56
2.7	MAMMALIAN CELL INTERACTION WITH P1 AND P20 <i>L. MEXICANA</i> .....	56
2.7.1	Culturing of Balb/c and C57 mice bone marrow macrophage.....	58
2.7.2	Characterisation of Balb/c and C57 mouse bone marrow derived macrophages (BMDM) by flow cytometry .....	60
2.7.3	Infectivity of P1 and P20 <i>L.mexicana</i> .....	60
2.8	INFECTION OF BALB/C AND C57 MICE BMDM WITH P1 AND P20 <i>L. MEXICANA</i> .....	61
2.9	FREE NON-ENGULFED PARASITES .....	61
2.10	SURVIVAL OF P1 AND P20 <i>L.MEXICANA</i> IN BALB/C AND C57 BMDM USING LIGHT MICROSCOPE ....	62
2.11	VIABILITY OF MACROPHAGES POST-INFECTION .....	62
2.12	DETECTION OF PHOSPHATIDYLSERINE IN P1 AND P20 <i>L. MEXICANA</i> PROMASTIGOTES AND AMASTIGOTES BY ANNEXIN V STAINING .....	63
2.13	CYTOKINES GENE REGULATION AFTER INFECTION OF MAMMALIAN CELL WITH P1 AND P20 <i>L. MEXICANA</i> PROMASTIGOTES .....	64
2.13.1.1	Enzyme-linked immunosorbent assay (ELISA).....	64
2.14	EFFECT OF CONDITIONED MEDIUM ON P1 AND P20 <i>L. MEXICANA</i> PROMASTIGOTE GROWTH AND VIRULENCE GENES REGULATION .....	65
2.14.1	Workflow of Effect of conditioned media on P1 and P20 <i>L. mexicana</i> promastigote growth and virulence gene regulation .....	66
2.15	EFFECT OF CONDITIONED MEDIUM ON P1 AND P20 <i>L. MEXICANA</i> PROMASTIGOTE GROWTH AND ASSOCIATED VIRULENCE GENES REGULATION .....	67
2.16	ALAMAR BLUE ASSAY TO ASSESS EFFECT OF CONDITIONED MEDIUM ON P1 AND P20 <i>L. MEXICANA</i> PROMASTIGOTE GROWTH.....	67
2.17	EFFECT OF CONDITIONED MEDIUM ON LPG EXPRESSION BY P1 AND P20 PROMASTIGOTES BY FLOW CYTOMETRY .....	67
2.18	A BRIEF DESCRIPTION OF THE GENE EXPRESSION TECHNIQUE USED IN METHODOLOGY FOR THE CURRENT STUDY .....	68
2.18.1	Preparation of target cells for RNA extraction .....	68
2.18.2	RNA extraction by Qiagene RNeasy mini kit.....	68
2.18.3	cDNA synthesis.....	69
2.18.4	Real time polymerase chain reaction (qPCR) .....	70
2.19	METHOD DEVELOPMENT.....	71
2.19.1	RNA extraction .....	71
2.19.2	LPG staining with CA7AE.....	71
2.19.3	Alamar blue optimisation .....	71
2.19.4	Parasites concentration and pH .....	72
2.20	STATISTICAL ANALYSIS .....	72

### **3 CHAPTER 3: VIRULENT P1 AND AVIRULENT P20 *L. MEXICANA* PROMASTIGOTE GROWTH AND CHARACTERISATION.....73**

3.1	INTRODUCTION.....	74
3.2	RESULTS.....	76
3.2.1	Characterisation of P1 and P20 <i>L. mexicana</i> .....	76
3.2.1.1	Effect of culture conditions on P1 and P20 <i>L. mexicana</i> growth rate.....	76
3.2.2	Morphology of P1 and P20 <i>L. mexicana</i> .....	78
3.2.3	Physical measurements of P1 and P20 promastigotes .....	81

3.2.4	<i>Differentiation of P1 and P20 L. mexicana into amastigotes.</i>	83
3.2.5	<i>Effect of temperature oxygen, medium type, and incubation time on the ability of P1 and P20 L.mexicana to differentiate into amastigotes.</i>	84
3.2.6	<i>Effect of pH on the ability of P1 and P20 L.mexicana promastigotes to differentiate into amastigotes.</i>	86
3.2.7	<i>The ability of P1 and P20 L. mexicana to differentiate into amastigotes.</i>	87
3.2.7.1	Effect of pH 5.5 and 25°C temperature on ability of P1 and P20 <i>L. mexicana</i> to differentiate into amastigotes	87
3.2.7.2	Effect of pH 5.5 and 37°C temperature on ability of <i>L. mexicana</i> P1 and P20 to differentiate into amastigotes	87
3.2.7.3	Effect of incubation time on ability of P1 and P20 <i>L. mexicana</i> to differentiate into amastigotes	88
3.2.7.4	Effect of type of medium on the ability of P1 and P20 <i>L. mexicana</i> to differentiate into amastigotes	88
3.2.8	<i>Effect of parasite concentrations on the RPMI1640 medium pH after 2- and 24-hours incubation at 37°C</i>	88
3.2.9	<i>Effect of parasite concentration on the RPMI1640 medium pH after 2- and 24-hours incubation at 37 °C when incubated with mammalian cells</i>	89
3.2.10	<i>Effect of 20 passages in vitro on virulence-associated gene expression of L. mexicana.</i>	90
3.2.11	<i>The effects of culturing of P1 and P20 L.mexicana in differentiation conditions for 2 and 24 hours on the expression of differentiation-associated genes regulation.</i>	91
3.2.11.1	The effects of incubation of P1 and P20 at 37°C for 2 and 24 hours on GP63, CPB and CPB2.8 genes regulation	91
3.2.11.2	The effects of incubation of P1 and P20 <i>L.mexicana</i> promastigotes at 37°C for 2 and 24 hours on LPG1 and LPG2 gene regulation	94
3.2.11.3	Detection of LPG on P1 and P20 <i>L.mexicana</i> promastigotes by immunofluorescent microscopy and flow cytometry	95
3.2.12	<i>Detection of phosphatidylserine (PS) in P1 and P20 promastigotes by flow cytometry</i>	98
3.2.13	<i>Synopsis of the virulent P1 and avirulent P20 L. mexicana promastigote growth and characterisation results</i>	99
3.3	DISCUSSION	101
3.3.1	<i>Characterisation of P1 and P20 L. mexicana promastigotes.</i>	101
3.3.1.1	Growth Rate	101
3.3.1.2	Morphology of P1 and P20 <i>L.mexicana</i>	102
3.3.1.3	Differentiation of P1 and P20 <i>L.mexicana</i> promastigote to amastigotes	103
3.3.1.4	Role of pH on P1 and P20 <i>L.mexicana</i> differentiation to amastigotes	103
3.3.1.5	Effect of incubation time on ability of P1 and P20 <i>L.mexicana</i> to differentiate into amastigotes	104
3.3.1.6	Effect temperature alteration on the ability of P1 and P20 <i>L.mexicana</i> to differentiate into amastigotes	104

3.3.1.7	Effect of 20 passages on the ability of P1 and P20 <i>L.mexicana</i> promastigotes to differentiate into amastigotes .....	105
3.3.1.8	Effect of 20 passages <i>in vitro</i> on virulent gene expression of <i>L.mexicana</i> by qPCR .....	107
3.3.1.9	Cysteine protease genes .....	108
3.3.1.10	Chitinase 1 (CHT1).....	108
3.3.1.11	MAPK9.....	109
3.3.1.12	A2 Protein.....	110
3.3.1.13	LPG1 and LPG2.....	110
3.3.1.14	GP63 .....	112
3.3.1.15	LACK .....	112
3.3.1.16	Phosphatidylserine (PS) on P1 and P20 .....	113

**4 CHAPTER 4: BALB/C AND C57 BONE MARROW DERIVED MACROPHAGES INFECTED WITH VIRULENT AND AVIRULENT *L.MEXICANA* .....114**

4.1	INTRODUCTION.....	115
4.2	RESULTS.....	118
4.2.1	<i>Infectivity of P1 and P20 L.mexicana in Balb/c and C57 BMDM.....</i>	118
4.2.2	<i>The fate of P1 and P20 L.mexicana in Balb/c and C57 BMDM.....</i>	121
4.2.2.1	<i>Live images of Balb/c and C57 BMDM infected with P1 and P20 L.mexicana .....</i>	121
4.2.3	<i>Fluorescent microscopic images of Balb/c and C57 BMDM infected with P1 and P20 L.mexicana after 24 hours .....</i>	126
4.2.4	<i>The fate of engulfed L.mexicana P1 and P20 in Balb/c and C57 BMDM .....</i>	129
4.2.5	<i>Survival of P1 L.mexicana in Balb/c and C57 BMDM.....</i>	130
4.2.6	<i>Apoptosis in Balb/c and C57 BMDM in response to infection with P1 and P20 L.mexicana promastigotes .....</i>	134
4.2.6.1	<i>The effect of removing GMCSF from Balb/c and C57 BMDM culture on apoptosis.....</i>	134
4.2.6.2	<i>Effect of infection with P1 and P20 L.mexicana on apoptosis in Balb/c and C57 BMDM.....</i>	135
4.2.6.3	<i>Effect of infection with P1 and P20 L.mexicana on apoptosis associated genes regulation in Balb/c and C57 BMDM.....</i>	137
4.2.7	<i>Effect of infection with P1 and P20 L.mexicana on cytokine gene regulation in Balb/c and C57 BMDM .....</i>	138
4.2.8	<i>Synopsis of the infection of Balb/c and C57 BMDM with virulent P1 and avirulent P20 L.mexicana promastigote results.....</i>	140
4.3	DISCUSSION.....	142
4.3.1	<i>Assessment of P1 and P20 L.mexicana infectivity.....</i>	142
4.3.2	<i>Assessment of P1 and P20 L.mexicana parasite survival in the infected macrophage .....</i>	142
4.3.3	<i>Survival of virulent P1 L.mexicana in Balb/c and C57 BMDM.....</i>	143
4.3.3.1	<i>Role of LPG.....</i>	143
4.3.3.2	<i>Role of LPG and oxidative burst.....</i>	144
4.3.3.3	<i>Role of phosphatidylserine in infection and survival.....</i>	145
4.3.3.4	<i>Inhibition of the formation of phagolysosomes .....</i>	146

4.3.3.5	Role of GP63 in parasite survival .....	147
4.3.3.6	Role of cysteine protease in parasite survival .....	148
4.3.4	<i>Parasitophorous vacuoles (PV)</i> .....	149
4.3.4.1	Fusion of parasitophorous vacuoles .....	150
4.3.5	<i>Apoptosis</i> .....	151
4.3.5.1	Apoptosis in Balb/c and C57 BMDM infected with P1 <i>L.mexicana</i> .....	151
4.3.5.2	Apoptotic genes regulation of Balb/c and C57 BMDM infected with P1 and P20 <i>L.mexicana</i> .....	153
4.3.5.3	Caspase 8 .....	154
4.3.5.4	BCL 2 .....	156
4.3.5.5	Caspase 1 .....	157
4.3.5.6	PD-1.....	158
4.3.5.7	Bax.....	159
4.3.5.8	Caspase 9 .....	159
4.3.5.9	Necrosis .....	159
4.3.6	<i>Proinflammatory cytokine gene regulation of Balb/c and C57 BMDM infected with P1 and P20 L.mexicana</i> .....	160
4.3.6.1	TNF- $\alpha$ .....	160
4.3.6.2	IL-6.....	162
4.3.6.3	IL1- $\beta$ .....	162
4.3.6.4	TGF- $\beta$ .....	163

**5 CHAPTER 5: THE EFFECT OF BALB/C AND C57 BMDM CONDITIONED MEDIUM ON P1 AND P20 *L.MEXICANA* PROMASTIGOTES.....164**

5.1	INTRODUCTION.....	165
5.2	RESULTS.....	167
5.2.1	<i>Effect of conditioned media on the growth of P1 and P20 L.mexicana promastigotes</i> .....	167
5.2.1.1	Effect of conditioned media on the growth of P1 and P20 <i>L.mexicana</i> promastigotes measured by haemocytometer .....	167
5.2.1.2	Effect of conditioned media on P1 and P20 growth rate measured by Alamar blue assay.....	169
5.2.2	<i>Effect of conditioned media on P1 and P20 L.mexicana promastigotes virulence associated gene regulation</i> .....	171
5.2.3	<i>Effect of Balb/c and C57 conditioned medium on the expression of LPG in P1 and P20 promastigotes measured by flow cytometry</i> .....	173
5.2.4	<i>Synopsis of effects of conditioned media on the virulent P1 and avirulent P20 L. mexicana promastigotes</i> .....	174
5.3	DISCUSSION.....	176

<b>6</b>	<b>CHAPTER 6: GENERAL DISCUSSION, CONCLUSION AND FUTURE WORK.....</b>	<b>178</b>
6.1	GENERAL DISCUSSION.....	179
6.1.1	Apoptosis.....	180
6.1.2	Role of Balb/c and C57 mouse genetic background in parasite survival.....	181
6.1.3	Limitations of in vitro modelling.....	182
6.1.4	LPG and cytokines.....	184
6.2	CONCLUSION.....	185
6.3	APPLICATION.....	186
6.4	FUTURE WORK.....	186
<b>7</b>	<b>REFERENCES.....</b>	<b>188</b>
<b>8</b>	<b>APPENDICES.....</b>	<b>221</b>

## List of figures

Figure 1.1:	Cutaneous Leishmaniasis Distribution.....	4
Figure 1.2:	Overview of the <i>L. mexicana</i> complex.....	9
Figure 1.3:	<i>Leishmania</i> life stages divided into two stages, promastigotes, and amastigotes. .....	11
Figure 1.4:	Diagram of the <i>Leishmania</i> promastigote and amastigote.....	12
Figure 1.5:	Virulence of P1, P7 and P20 <i>L. mexicana</i> promastigotes.....	13
Figure 1.6:	Structure of the LPG.....	15
Figure 1.7:	Inhibition of phagosome maturation in a macrophage infected with <i>Leishmania</i> promastigote.....	24
Figure 1.8:	The apoptosis pathways.....	27
Figure 1.9:	Chemical structure of the PS.....	34
Figure 1.10:	Immune response necrosis and apoptosis.....	35
Figure 1.11:	Role of proinflammatory cytokines in <i>Leishmaniasis</i> .....	38
Figure 2. 1:	Workflow of P1 and P20 characterisation (Stage-1).....	49
Figure 2. 2:	Workflow of mammalian cell interaction with P1 and P20 <i>L.mexicana</i> (stage-2) .....	57
Figure 2. 3:	Differentiation of bone marrow macrophages <i>in vitro</i> for seven days.....	59

Figure 2. 4 Workflow of the effect of conditioned medium on P1 and P20 <i>L. mexicana</i> promastigote growth and virulent gene regulation (Stage-3).....	66
Figure 3. 1:P1 and P20 growth curve cultured in RPMI 1640 or Schneider's <i>Drosophila</i> medium under aerobic and anaerobic conditions at 25 °C.....	77
Figure 3. 2: Growth curve of P1 and P20 cultured in RPMI 1640 or Schneider's <i>Drosophila</i> medium under aerobic and anaerobic conditions at 37 °C.....	77
Figure 3. 3: Effect of RPMI versus Schneider's <i>Drosophila</i> medium on P1 and P20 <i>L.mexicana</i> growth rate using Alamar blue assay.....	78
<b>Figure 3. 4: Morphology of P1 and P20 <i>L.mexicana</i> promastigotes stained with Giemsa</b> .....	79
Figure 3. 5: Morphology of P1 and P20 <i>L.mexicana</i> promastigotes under the Atomic Force microscopy. ....	80
Figure 3. 6: Morphology of P1 and P20 <i>L.mexicana</i> under the Electronic microscope .....	80
<b>Figure 3. 7: Cell size measurement of P1 and P20 <i>L. mexicana</i> promastigotes.....</b>	81
Figure 3. 8: Percentage of metacyclic promastigotes of P1 and P20 <i>L. mexicana</i> . ....	82
Figure 3. 9: Differentiation of P1 and P20 <i>L. mexicana</i> into amastigotes in absence of mammalian cells.....	83
Figure 3. 10: Effect of incubation of P1 and P20 promastigotes in RPMI 1640 at 37 °C....	84
Figure 3. 11: Differentiation of P1 and P20 <i>L. mexicana</i> promastigotes into amastigotes after 2, 24- and 48-hours incubation at 25 and 37 °C with or without O <sub>2</sub> .....	85
Figure 3. 12: Differentiation of p1 and p20 <i>L. mexicana</i> promastigotes to amastigotes after 2, 24- and 48-hours' incubation in pH 5.5 medium at 25 °C and 37 °C.....	86
Figure 3. 13: Effect of 20 passages <i>in vitro</i> on virulence gene expression.....	91
Figure 3. 14: Effect of 2- and 24-hours incubation at 37°C on GP63, CPB2 and CPB2.8 gene regulation in P1 and P20. ....	92

Figure 3. 15: The effects of culturing P1 and P20 <i>L.mexicana</i> promastigotes under amastigote differentiation conditions for 24 hours on A2 genes regulation.....	93
Figure 3. 16: The effects of culturing of P1 and P20 <i>L.mexicana</i> in amastigote differentiation conditions for 2 and 24 hours on LPG1 and LPG2 gene regulation.....	94
<b>Figure 3. 17: Detection of LPG on the surface of P1 and P20 promastigotes by immunofluorescence</b> .....	95
<b>Figure 3. 18: Detection of LPG on the P1 and P20 promastigotes by flow cytometry</b>	96
Figure 3. 19: Detection of LPG on the surface of P1 and P20 <i>L.mexicana</i> by immunofluorescence after incubation in differentiation conditions for 2 and 24 hours.....	97
<b>Figure 3. 20: P1 and P20 phosphatidylserine expression</b> .....	98
Figure 4. 1: Estimation of numbers of non-engulfed P1 and P20 <i>L. mexicana</i> parasites after interaction with Balb/c and C57 BMDM for 2- and 24-hours at 37 °C by using Neubauer haemocytometer.....	119
Figure 4. 2: Estimation by Alamar blue of percentage non-engulfed P1 and P20 <i>L. mexicana</i> by Balb/c and C57 BMDM after 2 and 24 hours of infection .....	120
Figure 4. 3: Live images of Balb/c BMDM infected with P1 and P20 at 2 hours and 1, 3 and 7 days .....	122
Figure 4. 4: Live images of C57 BMDM infected with P1 and P20 <i>L.mexicana</i> at two 2 and 24 hours. ....	123
Figure 4. 5: Giemsa stained images of Balb/c and C57 BMDM infected with P1 and P20 <i>L.mexicana</i> at 2 and 24 hours. ....	125
Figure 4. 6: Infectivity of P1 and P20 <i>L. mexicana</i> promastigotes in Balb/c BMDM measured by fluorescent microscope after 24 hours .....	127
Figure 4. 7: Infectivity of P1 and P20 <i>L. mexicana</i> promastigotes to C57 BMDM measured by fluorescent microscope after 24 hours .....	128
Figure 4. 8: Fate of P1 and P20 <i>L. mexicana</i> promastigotes in Balb/c and C57 BMDM was measured by fluorescent microscope.....	129

Figure 4. 9: Infectivity of P1 <i>L.mexicana</i> promastigotes in Balb/c and C57 BMDM at 1,3- and 7-days of infection.....	130
Figure 4. 10: Number of PV per Balb/c and C57 BMDM infected with P1 after 1, 3- and 7-days of infection.....	131
Figure 4. 11: Number of amastigotes per PV and cell in Balb/c and C57 BMDM infected with P1 <i>L.mexicana</i> promastigotes .....	132
Figure 4. 12: Infectivity index of P1 in Balb/c and C57 BMDM after 1, 3- and 7-days infection.....	133
Figure 4. 13: Effect of removing of GMCSF from control Balb/c and C57 BMDM culture apoptosis.....	134
Figure 4. 14: Apoptosis in Balb/c and C57 BMDM after infection with P1 and P20 <i>L.mexicana</i> promastigotes.....	136
Figure 4. 15: Apoptosis associated gene expression in Balb/c and C57 BMDM after 24 hours infection with P1 and P20 <i>L. mexicana in vitro</i> . .....	137
Figure 4. 16: qPCR analysis of cytokines genes regulation of Balb/c and C57 BMDM infected with P1 and P20 promastigotes for 2 and 24 hours.....	138
Figure 4. 17: Estimation of TNF- $\alpha$ cytokine concentration in supernatants of Balb/c and C57 BMDM infected with P1 and P20 by ELISA.....	139
Figure 4. 18: Diagram illustrates the possible effect of deactivation of Caspase 8 on both extrinsic and intrinsic apoptosis pathways. ....	154
Figure 4. 19: Effect of activated of BCL 2 on intrinsic apoptosis pathways .....	157
Figure 4. 20: Effect of activated of BCL 2 on intrinsic apoptosis pathways .....	157
Figure 5. 1: Effect of Balb/c and C57 BMDM conditioned medium on P1 and P20 growth by using haemocytometer. ....	168
Figure 5. 2 : Effect of Balb/c and C57 BMDM conditioned medium on P1 <i>L.mexicana</i> promastigotes growth measured by Alamar blue assay. ....	169

Figure 5. 3: Effect of Balb/c and C57 BMDM conditioned medium on P20 <i>L.mexicana</i> promastigotes growth measured by Alamar blue assay.....	170
Figure 5. 4: Effect of Balb/c and C57 BMDM conditioned medium on P1 and P20 virulence gene regulation.....	171
Figure 5. 5: Effect of Balb/c and C57 BMDM conditioned medium on LPG expression on P1 and P20 <i>L.mexicana</i> promastigotes .....	173

## List of tables

Table 1.1: Leishmania parasite species known as causative agents of human Leishmaniasis .....	5
Table 1.2: Morphology of <i>L.mexicana</i> in different stages.....	10
Table 1.3: Comparative analysis of apoptosis, paraptosis and necrosis features .....	33
Table 2. 1: List of equipment used in this study.....	42
Table 2. 2: List of consumables used in this study .....	43
Table 2. 3: List of reagents, chemicals and kits used in this study.....	44
Table 2. 4: List of mice primers used in this study.....	45
Table 2. 5: List of <i>L.mexicana</i> primers used in this study.....	46
Table 2. 6: media and buffers used in this study .....	47
Table 2. 7: staining strategy of P1 and P20 promastigotes using immunofluorescence and flow cytometry.....	56
Table 2. 8: Phenotyping staining of BMD using flow cytometry.....	60
Table 2. 9: Tetro cDNA protocol for super mix preparation for one sample (Bioline, UK). .....	69
Table 2. 10: Real time PCR super mix .....	70
Table 3. 1: Effect of parasite concentration on the RPMI medium pH after 2- and 24-hours' incubation at 37 °C without mammalian cells .....	88

Table 3. 2: Effect of parasites concentration on the RPMI1640 medium pH after 2- and 24-hours' incubation at 37°C with mammalian cells .....	89
Table 3. 3: Growth characteristic of P1 and P20 promastigotes .....	99
Table 3. 4: Morphology of P1 and P20 promastigotes.....	99
Table 3. 5: expression of LPG and PS on the P1 and P20 <i>L.mexicana</i> .....	100
Table 3. 6: Virulence associated gene regulation expression of the P20 promastigotes compared with P1 promastigotes .....	100
Table 3. 7: Effect of incubation of P1 and P20 <i>L.mexicana</i> promastigotes on the amastigote's differentiation conditions for 24 hours on virulence associated gene regulation .....	101
<b>Table 4. 1: Infection and survival of P1 and P20 <i>L.mexicana</i> in Balb/c and C57 BMDM.</b> .....	140
<b>Table 4. 2: Effect of Infection P1 and P20 <i>L.mexicana</i> in Balb/c and C57 BMDM apoptosis</b> .....	140
<b>Table 4. 3: Effect of infection P1 and P20 <i>L.mexicana</i> in Balb/c and C57 BMDM cytokines.</b> .....	141
Table 5. 1: Effect of Balb/c and C57 BMDM conditioned medium on the P1 and P20 <i>L. mexicana</i> promastigotes growth.....	174
Table 5. 2: Effect of conditioned media on P1 and P20 <i>L. mexicana</i> promastigote virulence associated gene regulation.....	175
Table 5. 3: Effect of Balb/c and C57 conditioned medium on P1 and P20 <i>L. mexicana</i> promastigotes LPG expression.....	175

## List of Abbreviations

Ab	antibody
AFM	Atomic Force Microscope
AHAW	Animal Health and Welfare
AKT	a serine/threonine-protein kinase
AP-1	Activating Protein-1
ATP	Adenosine triphosphate
$\beta$ actin	Beta actin
BAD	BCL 2-associated death promoter
Bax	BCL 2 associated X Protein
BCL 2	B-cell lymphoma 2
BID	pro-apoptotic member of the Bcl-2 protein family
BMDM	Bone marrow derived macrophage
Caspase	Cysteine-aspartic acid protease
C3	Complement system component 3
C3b	Cleavage components of C3
C3bi	Cleavage components of C3
C57	C57BL/6J
CD4 <sup>+</sup> T	T Cluster of differentiation 4 T cell
CDC	Centers for Disease Control and Prevention
cDNA	Complementary Deoxyribonucleic Acid
CFSE	Carboxyfluorescein succinimidyl ester
c-Jun	transcription factors protein encoded by the JUN gene
CL	Cutaneous Leishmaniasis.
CO <sub>2</sub>	Carbon dioxide
CP	Cysteine Peptidases
CPB	cysteine peptidases B
CPB2.8	cysteine peptidases B and 2.8 refers to the gene size
CPC	Cysteine Peptidases A
CPC	Cysteine Peptidases C
CR1	Complement receptor1
CR3	Complement receptor3
CRISPR	Clustered regularly interspaced short palindromic repeats
DC medium	Dendritic cell generation medium
DC	Dendritic cell
DISC	Death-inducing signalling complex
DNA	Deoxyribonucleic acid
DOK	Downstream of tyrosine kinases
EFSA	European Food Safety Authority
ELISA	Enzyme-linked immunosorbent assay
ERK	extracellular signal-regulated kinases
EVOS	Digital Inverted Fluorescence Microscope
FADD	Fas-associated death domain
FCS	Foetal calf serum
FITC	Fluorescein isothiocyanate
FnR	fibronectin receptors
Gal	Galactose

GAPDH	Human glyceraldehyde 3-phosphate dehydrogenase mRNA
GIPLs	Glycoinositolphospholipids
Glc	Glucose
GMCSF	Granulocyte macrophage stimulating factor
GN	Glucosamine
GP63	Glycoprotein of 63KD
HIFCS	Heat inactivated foetal calf serum
iC3b	Inactive components of C3
IFN- $\gamma$	Interferon Gamma
IL-1 $\beta$	Interleukin 1 beta
IL-1	Interleukin 1
IL-12	Interleukin 12
IL-4	Interleukin 4
IL-6	Interleukin 6
IL-8	Interleukin 8
iNOS	Inducible nitric oxide
LACK	<i>Leishmania</i> activated C kinase
<i>L. amazonensis</i>	<i>Leishmania amazonensis</i>
<i>L. donovani</i>	<i>Leishmania donovani</i>
<i>L. infantum.</i>	<i>Leishmania infantum</i>
<i>L. major</i>	<i>Leishmania major</i>
<i>L.mexicana</i>	<i>Leishmania mexicana</i>
<i>L. pifanoi</i>	<i>Leishmania pifanoi</i>
<i>L.</i>	<i>Leishmania</i>
LPG	Lipophosphoglycan
LPG1	LPG1 gene
LPG2	LPG2 gene
Man	Mannose
MAPK	Mitogen Activated Protein Kinase
MR	Mannose-fucose Receptor
mRNA	Messenger Ribonucleic acid
mTOR	mechanistic target of rapamycin.
NADPH	Nicotinamide adenine dinucleotide phosphate.
NF- $\kappa$ B	Nuclear factor kappa-light-chain-enhancer of activated B cells
NK	Natural killer cell
NO	Nitric oxide
P1	Passage 1 <i>Leishmania mexicana</i>
P20	Passage 20 <i>Leishmania mexicana</i>
PAMPs	Pathogen associated molecular patterns
PBS	Phosphate buffered Saline
PCD	Programmed cell death
PCR	Polymerase Chain Reaction
PD-1	Programmed Death 1
PRRs	Pattern recognition receptors
P38	Mitogen-activated protein kinases class P38
PG	Phosphoglycans
PI	Propidium Iodide

PPG	Proteophosphoglycan
PS	Phosphatidylserine
PV	Parasitophorous Vacuole
qPCR	Quantitative real time polymerase chain reaction
qRT-PCR	Real time quantitative reverse transcription PCR
RNA	Ribonucleic acid
RNS	Reactive Nitrogen Species
ROS	Reactive oxygen species
TGF- $\beta$	Transforming growth factor beta
Th1	T helper cell type 1
Th17	T helper cell type 17
Th2	T helper cell type 2
TLR	Toll-like receptor
TLR-2	Toll-like receptor 2
TLR-4	Toll-like receptor 4
TNF- $\alpha$	Tumour Necrosis Factor-Alpha
TF	Transcription Factor
VL	Visceral Leishmaniasis
WHO	World Health Organization

# **Introduction**

## 1.1 Introduction

Leishmaniasis describes a group of parasitic diseases caused by obligate intracellular protozoa of the genus *Leishmania* with more than 20 pathogenic species. *Leishmania* infects approximately 12 million people annually in 98 countries, with an estimated 1.3 million new cases every year. The number of deaths associated with this disease range between 20,000 - 30,000 per year according to reports by the WHO (WHO, 2018).

Leishmaniasis has multiple clinical forms which are the outcome of the damage to macrophages caused by the *Leishmania* parasite (CDC, 2018). There are at least three clinical forms; cutaneous, mucocutaneous and visceral with the cutaneous Leishmaniasis or dermal Leishmaniasis as the most common forms of this disease. The cutaneous lesion develops a few weeks or months after infection with the promastigote form of the parasite. Lesions start with papules (nodular plaque) then develop into skin ulcers with rising edges and covered with crust. In some cases, the lesion persists as a nodule stage with no ulcers. Although the ulcerative lesions are usually painless, they could be painful in association with secondary bacterial infection (CDC, 2018). Skin Leishmaniasis can persist for long periods and could last from several months into years causing permanent scars, disfigurement, unaesthetic stigma and disability in some cases (CDC, 2018; WHO, 2013).

The mucocutaneous form is rare, but it is more serious and usually need treatment. Some species of *Leishmania* parasite that can cause cutaneous Leishmaniasis amastigotes can spread from the skin into mucous tissue of the mouth, nostril or even mouth palate causing mucocutaneous Leishmaniasis. This can happen after the healing of a skin ulcer, which usually occurs after several months of cutaneous infection with *Leishmania* (Cafasso, 2019). Visceral Leishmaniasis (kala-azar) caused by, *L. donovani* or *L. infantum* can be a fatal form of the disease; it usually affects the internal organs such as the spleen, bone marrow, and liver (CDC, 2018; Cobo, 2014). The estimated number of new cases annually are about half a million with a mortality rate of 50 000–60 000 per year. Visceral Leishmaniasis is the second most common fatal parasitic disease in the world, after malaria (Reisinger, *et al.*, 2007; Cobo, 2014).

## 1.2 Transmission

*Leishmania* parasite protozoa that cause Leishmaniasis are more than 20 species and can infect approximately 70 animal species in addition to humans, which act as a natural reservoir. The *Leishmania* parasite promastigotes are transmitted to the host through biting by the female sand fly vector (*Phlebotomus Psychodopygus Lutzomyia*), which have more than 90 species or subspecies (WHO, 2018).

The sand fly is most active in hot and humid weather (Killick, 1999) it can also pass through bed nets due to its tiny size (WHO, 2013). The amastigotes transform into promastigote, live and multiply inside the midgut of the female sand fly vector. Usually rats, gerbils, hamsters, dogs and foxes act as reservoirs for these parasites. Therefore, sand flies transmit the promastigote from infected animals into humans. They also can be transmitted by other rare ways such as through damaged skin during dealing with promastigotes at the lab, sharing syringes, blood transfusion, and congenitally from mother to her offspring (WHO, 2013). *Leishmania* also can be transmitted by an anthroponotic way which is from infected human into human by the vector (CDC, 2018).

There are many factors which can contribute to the spreading of Leishmaniasis into new non-endemic areas such as improvements in transportation and climate changes (CDC, 2018). In addition, the lack of effective treatment, reliable vaccines and effective diagnostic programmes which can identify early infections also contribute to its spread (EFSA AHAW, 2015).

### 1.3 Clinical signs

The incubation period is usually between one to two weeks but may be months or years depending on the form of Leishmaniasis. The lesion develops after exposure to sand fly biting in an endemic area. Clinical findings of the skin form are mainly characterized by skin ulcers and may lead to disfigurement if on the face (Reithinger, *et al.*, 2007; Cafasso, 2019). Clinical signs of muco-cutaneous forms appear 1-5 years after healing of skin lesions. It may start with ulcers in the nostril, mouth and lips, progressing to other symptom such as dyspnoea, nasal discharge, and epistaxis (Cafasso, 2019).

Incubation period of visceral Leishmaniasis is between 2-6 months in most cases of this form; symptoms include weight loss, tiredness and weakness, splenomegaly, liver enlargement, decreasing of red blood cell count, fever which may persist for weeks or months, cough, bleeding, night sweats. hair loss, secondary infection by other microorganisms, desquamation (scaly skin) and grey, ashen skin may also present during the disease (Cobo, 2014; Cafasso, 2019).

### 1.4 Epidemiology

The number of deaths associated with this disease ranges between 20,000 -30,000 per year according to WHO estimation (WHO, 2018). Approximately 95% of the Leishmaniasis is the cutaneous form; and is found mostly in Algeria, Afghanistan, Brazil, Iran, Pakistan, Peru, Colombia, Saudi Arabia, Syria, and Tunisia. The visceral form is more common in India,

Bangladesh, Sudan, Brazil, Ethiopia, and Nepal. Mucocutaneous forms mainly occur in Brazil, Peru and Bolivia (90%) (WHO, 2018). The most cases of Leishmaniasis were reported in 2014 by WHO are in India, Brazil, Ethiopia, Somalia, and Sudan (WHO, 2018). In the New World, the most common form is also cutaneous Leishmaniasis, and the most affected countries are Mexico, Argentina, Peru and Brazil.

Status of endemicity of cutaneous leishmaniasis worldwide, 2015

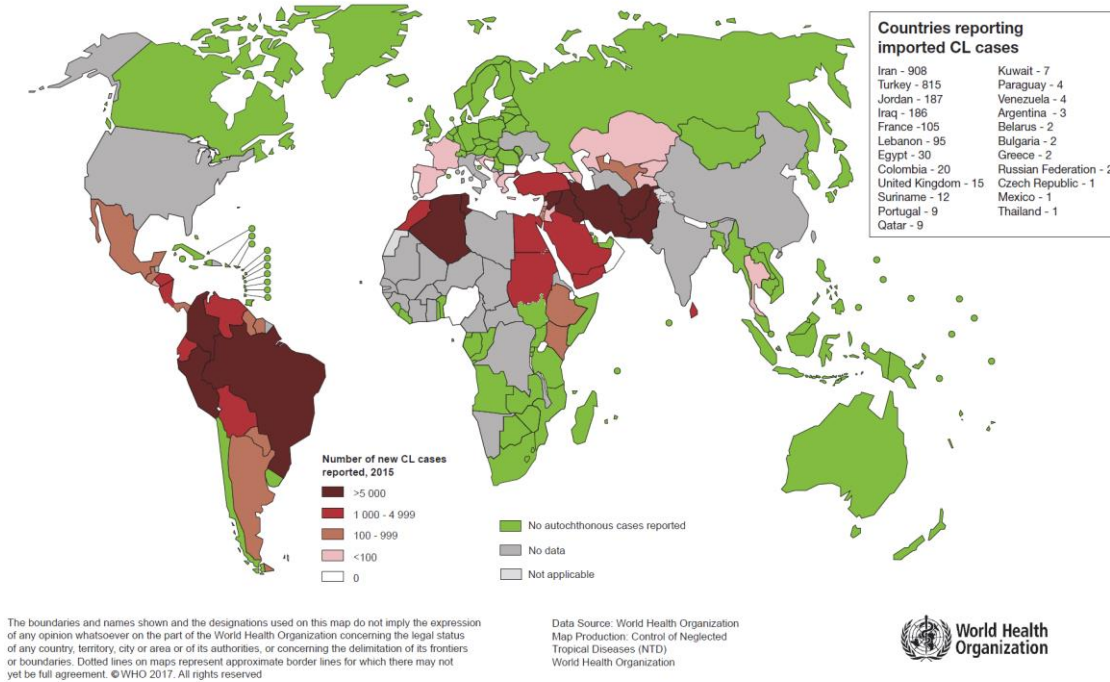


### Figure 1.1: Cutaneous Leishmaniasis Distribution

map illustrated the infected individual numbers cutaneous form Leishmaniasis in different parts of the world (Adapted from WHO, 2018, WWW<sup>1</sup>)

### 1.4.1 *Leishmania* parasite species that are known as causative agents of Leishmaniasis in humans

**Table 1.1: *Leishmania* parasite species known as causative agents of human Leishmaniasis**  
Shows a list of *Leishmania* parasite species known as causative agents of Leishmaniasis in humans. Including classification of New World (NW) and Old World (OW), species of vectors and endemic areas along with type of clinical lesion, Visceral Leishmaniasis (VL), Cutaneous Leishmaniasis (CL), Diffuse Cutaneous Leishmaniasis (DCL) Mucotaneous Leishmaniasis (MCL), and Post-Kala-Azar dermal Leishmaniasis (PKDL) (Gillespie and Pearson 2003, Rogers, 2012).

<i>Leishmania</i> species	Origin	Type of <i>Leishmaniasis</i>	Vector	Endemic area
<i>L. amazonensis</i>	NW	CL, DCL, MCL	Lutzomyia longipalpis	Brazil, Bolivia, Venezuela
<i>L. mexicana</i>	NW	CL, DCL	Lutzomyia longipalpis Lutzomyia diabolica Lutzomyia abboneci	USA, Ecuador, Venezuela, Peru
<i>L. tropica</i>	NW	CL, VL	Phlebotomus arabicus Phlebotomus sergenti	Middle East, Central and North Africa, Central Asia, India
<i>L. venezuelensis</i>	NW	CL		Venezuela Northern South America
<i>L. braziliensis</i>	NW	CL, MCL	Lutzomyia longipalpis	South America, Western Amazon Basin, Brazil, Bolivia, Venezuela, Peru Guatemala
<i>L. guyanensis</i>	NW	CL, MCL		Northern South America, Brazil, Bolivia, French Guiana, Suriname
<i>L. lainsoni</i>	NW	CL		Brazil, Bolivia, Peru
<i>L. lindenbergi</i>	NW	CL		Brazil
<i>L. naiffi</i>	NW	CL		Brazil, French Guyana
<i>L. panamensis</i>	NW	CL, MCL	Lutzomyia gomezi	Central and South America, Venezuela, Brazil, Panama, Colombia

<i>L. peruviana</i>		CL, MCL		Peru, Bolivia
<i>L. shawi</i>	NW	CL		Brazil
<i>L. colombiensis</i>	NW	CL, VL		Colombia
<i>L. donovani</i>	OW	VL, PKDL	Phlebotomus argentipes	Central Africa, Middle East, South Asia, India, China
<i>L. major</i>	OW	CL, DCL	Phlebotomus papatasi Phlebotomus duboscqi	Central and North Africa, Central Asia, Middle East
<i>L. aethiopica</i>	OW	CL, DCL		Ethiopia, Kenya
<i>L. infantum</i>	NW OW	VL, CL	Phlebotomus ariasi	North Africa, Middle East, Mediterranean countries, Central Asia, Central ,South, North America
<i>L. martiniquensis</i>	NW OW	VL, CL		Martinique, Thailand
<i>L. siamensis</i>	NW OW	VL, CL		Central Europe, Thailand, USA

## 1.5 Prevention and control

The most effective Leishmaniasis prevention methods are by controlling of intermediate host sand fly to decrease the transmission of disease. This can be achieved by using insecticides or the use of biological control methods of these insects. Controlling of reservoir species such as dogs or gerbils of infected area is also effective (CDC, 2018).

## 1.6 Treatment

In most cases cutaneous Leishmaniasis heals spontaneously without treatment but after several months or years of infection. According to European Food Safety Authority (2015) currently there is no effective treatment that can absolutely cure the disease and completely eradicate the *Leishmania* parasite. Treatment can usually help in the improvement of clinical manifestations by reducing parasite infiltration into infected body tissues (European Food Safety Authority, 2015). There are many antiparasitic drugs used for Leishmaniasis treatment such as paromomycin, amphotericin B and antimony compounds (sodium stibogluconate and meglumine antimoniate) (Cafasso, 2019). These treatments can help to speed up healing, prevent secondary infection, and prevent or reduce scars especially in face skin lesion. In some cases, facial ulcers can cause disfigurement and may need plastic surgery and grafting. In addition, defaults in treatment of the mucocutaneous form in

mucosal tissues such as the nostril, mouth, soft and hard palate, may cause massive destruction of these tissues (Handler *et al.*, 2015).

### **1.6.1 Antimony**

Antimony is a semi-metal grey coloured compound found naturally as a part of the earth's crust. It was discovered approximately 1600 BC (ATSDR, 2011; Royal Society of Chemistry 2016). Antimony as a chemotherapy drug comes in two forms for treatment of Leishmaniasis; sodium stibogluconate and meglumine antimoniate (Cafasso, 2019). Antimony is the first choice of treatment in human and animal *Leishmaniasis* in endemic areas (Jeddi *et al.*, 2011).

Sodium stibogluconate (Pentostam®) is an injectable medicine which contains 100 mg antimony per mL. It is used for treatment of the three forms of Leishmaniasis (cutaneous, muco-cutaneous and visceral Leishmaniasis). The mode of action of this medicine is still unclear. Antimony reduces energy metabolism in the parasites by reducing ATP (adenosine triphosphate) and GTP (guanosine triphosphate) (ATSDR, 2011).

The drug can be administered by intravenous injection or by the intradermal route at the site of infection. This medicine contains large particles between 20-300 microns so it should be filtered by 5-micron filter before administration. The effectivity of antimony has significantly dropped and has become ineffective in approximately 50% of visceral Leishmaniasis cases (Perry *et al.*, 2015). The treatment requires injection, which may be difficult to do in some tissues; in addition, failure in the treatment of mucocutaneous form in mucosal tissues, such as nostrils and the mouth's soft and hard palates might cause massive destruction of these tissues.

### **1.6.2 Amphotericin B**

Though intravenous injections of Amphotericin B are regularly used for the treatment of *L. mexicana* infection, the experimental administration of this drug fails to induce a positive effect in susceptible Balb/c and 129SVE mice infected with cutaneous *L. mexicana in vivo* (Varikuti *et al.*, 2017). Morizot *et al.*, (2016) reported that the failure of treatment or even relapse by amphotericin B *in vivo* but not *in vitro* is due to immunosuppression of the patient. The medicine has been shown to be effective *in vitro* (Lachaud *et al.*, 2009) therefore, Morizot *et al.*, (2016) suspect that the mechanism of the medicine's efficacy is different from sensitivity of this parasite to antimony.

### 1.6.3 Miltefosine

The active ingredient of Miltefosine is the chemotherapeutic drug alkyldiphosphocholine. It is an exclusively oral drug that used for treatments of Leishmaniasis, it is used for both VL and CL, especially in areas with antimonial resistant *Leishmania* (Sundar *et al.*, 2002). However, relapse or resistance against this drug has also been reported (Perez-Victoria *et al.*, 2003; Pandey *et al.*, 2009; Mishra and Singh, 2013).

## 1.7 Vaccination

Many types of vaccine have been investigated, such as killed promastigotes (either with or without adjuvants) genetically engineered parasites, recombinant antigens, and parasite subunit antigen, but with little success (Modabber, 2010). In addition, using leishmanization by inoculation of healthy individuals with a low dose of live *Leishmania* parasite to develop immunity against this disease is unacceptable because it is associated with development of non-healing lesions (Palatnik-De-Sousa, 2008).

Live attenuated leishmanial vaccines are the best standard for protection against leishmaniasis. Vaccination with live attenuated parasites, which are infectious, but non-pathogenic, has major advantages compared to vaccination with killed parasites or leishmanization (Kedzierski *et al.*, 2006). Attenuated live vaccines are produced by long term incubation *in vitro* (Mitchell *et al.*, 1984) or by using  $\gamma$ -irradiation (Rivier *et al.*, 1993), or by culturing under gentamicin pressure *in vitro* (Daneshvar *et al.*, 2003), or using temperature sensitivity (Gorczynski *et al.*, 1985). Genetic mutations or knock-out of specific virulence associated genes could lead to loss of pathogenicity of the parasite (Streit *et al.*, 2001; Nagill and Kaur, 2011).

Currently there is no effective authorised vaccine against *Leishmania* registered in European countries. Taking evidence from the fact that individuals infected and then recovered from Leishmaniasis can become resistant to re-infections, implies that developing a vaccine against this disease is possible (Khamesipour *et al.*, 2006). However, there is only one authorised vaccine for canine (CaniLeish®) which provide partial protection to dogs against *L. infantum* (EFSA AHAW, 2015).

## 1.8 *Leishmania* Parasites

### 1.8.1 *Leishmania* parasite classification

The *Leishmania* parasite and *Leishmania* vector classification is controversial due to the discovery of new species and new endemic areas, both in the old and new worlds (Akhoundi *et al.*, 2016). The *Leishmania* parasite is a eukaryotic microorganism belonging to the

kingdom *Protista*; sub kingdom *protozoa* order Kinetoplastida, genus *Leishmania* and family *Trypanosomatidae*. There are about 31 species of *Leishmania* known which can infect mammals, 20 of those species are zoonotic. However, 11 of these 20 species have veterinary and medical importance (Gillespie and Pearson, 2003; Rogers, 2012; Akhoundi *et al.*, 2016). The genus *Leishmania* is divided into three subgenera according to where the promastigote phase is found in the sand fly. The subgenus *Leishmania*, in which the promastigote is found in the foregut and midgut of the sand fly alimentary tract, while in the subgenus *Viannia* a promastigote phase develops in the hindgut of the sand fly with later migration of flagellates to the foregut and midgut. *Sauroleishmania* subgenus include species that particularly parasitize lizards (Bates, 2007).

Taxonomy of the *Leishmania* genus, subgenus and species complex of *Leishmania* is demonstrated (Real *et al.*, 2013).

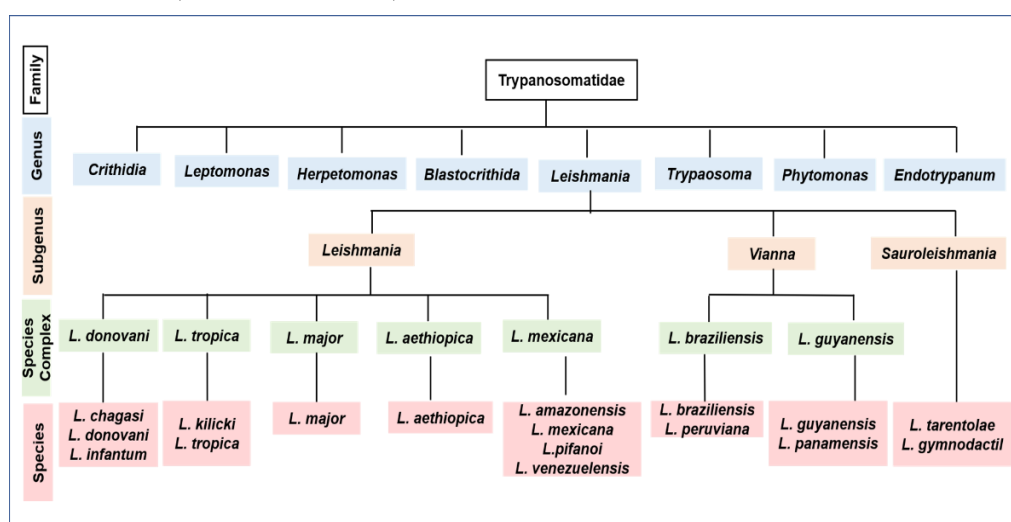


**Figure 1.2: Overview of the *L. mexicana* complex**

Taxonomy of the *Leishmania* genus, subgenus and species complex of *Leishmania*. *L. mexicana* is belongs to the *L. mexicana* complex, and subgenus *Leishmania* (Adapted from Real *et al.*, 2013).

### 1.8.2 *L. mexicana* genome

*L. mexicana* genome has been sequenced at the Sanger Institute. *Leishmania mexicana*, genome size is 32 MBPs with 34 chromosomes. The percentage of nucleobases guanine (G) and cytosine (C) is approximately 59% (Sanger, 2018). However, the gene expression profile during differentiation from promastigote into amastigotes, demonstrates the differential expression of 3,832 genes between these two stages, which include flagellum and surface proteins (Fiebig *et al.*, 2015).

### 1.8.3 *L. mexicana* morphology

*L. mexicana* morphology depends on the stage of the life cycle, with a positive relationship between flagellum length and the growth stage of the parasite and cell cycle (Wheeler *et al.*,

2011). *L. mexicana* morphological stages in general are similar to other *Leishmania* parasites (Tyler and Engman, 2001; Wheeler *et al.*, 2011). The promastigote is defined by its distinctive morphology, measurement of flagellum length, and cell body width and length (Wheeler *et al.*, 2011). The growth of the *Leishmania* parasite is divided into two main stages, amastigote and promastigote. Promastigotes are very motile parasites which have a cylindrical elongated body and flagella, amastigotes have a round body shape but without flagella. Promastigotes differentiate into amastigotes inside mammalian hosts (Pearson and Sousa, 1996). Promastigotes are an extracellular stage of the parasite, long and flagellated which are mainly found in the sand fly vector. Inside the sand fly amastigotes undergo multiple differentiation from procyclic, nectomonad, leptomonad, and then into metacyclic promastigotes (Rogers, 2012). Amastigotes 2-3  $\mu\text{m}$  in size are rounded in shape without flagella and are found intracellularly, inside mononuclear cells of mammalian hosts (Gillespie and Pearson 2003).

**Table 1.2: Morphology of *L.mexicana* in different stages**  
(table adapted from Rogers *et al.*, (2002) with modifications).

Stage	Character	Example
Amastigote	Ovoid body form, no flagellum protruding from flagellar pocket	
Procyclic Promastigote	Body length between 6.5 – 11.5 $\mu\text{m}$ , body width variable, flagellum length shorter than body length.	
Nectomonad Promastigote	Body length more than 12 $\mu\text{m}$ , the width of body and length flagellum are variable	
Leptomonad promastigote	Body length between 6.5 and 11.5 $\mu\text{m}$ , variable body width flagellum is longer than the body length	
Haptomonad promastigote	variable body and flagellar length, flagellar tip look like A Disc expansion	
Metacyclic Promastigote	Body length is less or equal 8 $\mu\text{m}$ , body width less or equal 1 $\mu\text{m}$ , flagellum length is longer than body length	
Paramastigote	Kinetoplast adjacent to nucleus, external flagellum present	

### 1.8.4 *Leishmania* life cycle

*Leishmania* life stages divided into two types, promastigotes and amastigotes.

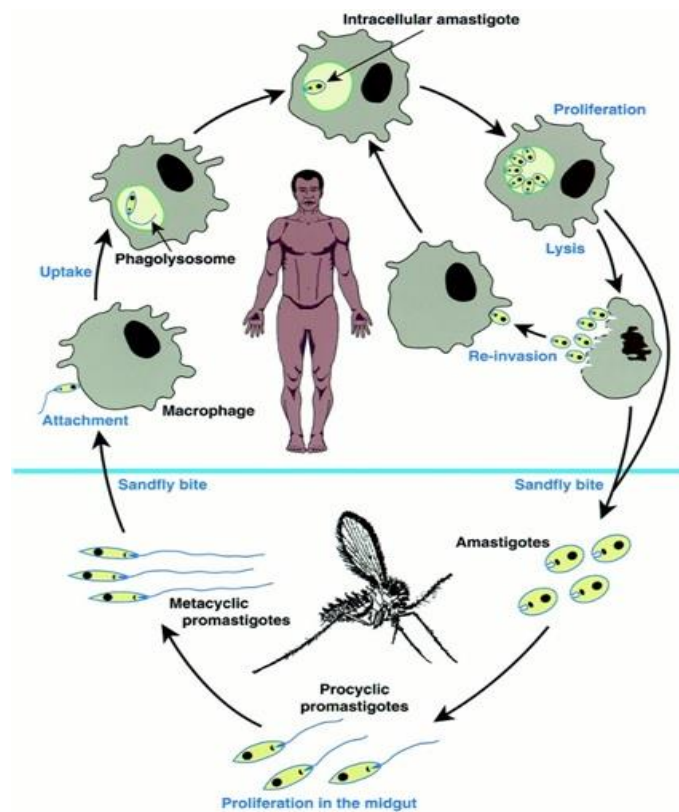


**Figure 1.3: *Leishmania* life stages divided into two stages, promastigotes, and amastigotes.**

*Leishmania* life cycle starts by biting mammalian host and injection of *Leishmania* promastigotes by infected sand fly vector (Sacks and Kamhawi, 2001; Rogers, 2012). Promastigote engulfed by host phagocytic cells (neutrophils, dendritic cells, fibroblasts and macrophages), (Naderer, and McConville, 2011). Promastigote differentiate into amastigotes and replicates inside macrophage by binary fission (Van Zandbergen *et al.*, 2004; Gillespie and Pearson, 2003). When naive sand fly vector bites the infected host and takes a blood meal, amastigotes are sucked in with the blood meal. In the vector midgut, *Leishmania* amastigotes will differentiate into promastigotes to infect another host (Brandão-Filho., 1999). (figure adapted from Handman, 2001).

Distinct forms represent the adaptation of the parasite to the changes of the environmental conditions because the parasite lives in two different hosts, the infected mammalian host's cells, and the sand fly vector. Extracellular spindle shape flagellated promastigotes are found in the sand fly alimentary tract, whereas the intracellular round form amastigotes are found in mammalian host cells. During transition through these two different environments, the parasite is exposed to many environmental changes such as temperature, pH, oxygen and nutrients, combined with changes in the parasite's morphology in promastigotes and amastigotes (Reithinger, *et al.*, 2007). Temperature (37 °C), low pH, and elevated CO<sub>2</sub> can induce the promastigote to differentiate into an amastigote to adapt to these conditions (Barak *et al.*, 2005). *L.mexicana* amastigote structure is characterised by the presence of numerous organelles called megasomes that make up 15% of the total cell volume (Coombs, *et al.*, 1986).

It is of note that the size of megasomes varies between *Leishmania* species, being largest in *L. mexicana* and they are not found in *L. donovani* species (Ueda-Nakamura *et al.*, 2001; Besteiro, *et al.*, 2007).

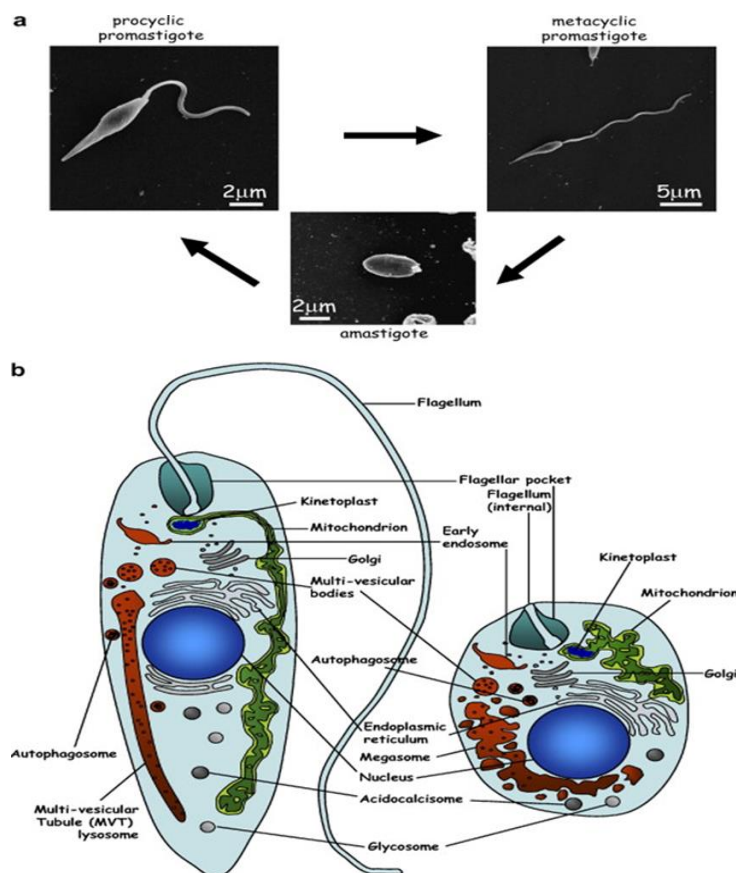


**Figure 1.4: Diagram of the *Leishmania* promastigote and amastigote**

Diagram illustrating the *Leishmania* promastigote and amastigote changes in cell morphology during the *Leishmania* lifecycle (a). The metacyclic promastigote which can differentiate into an amastigote. (b) Graphic representation of the main intracellular organelles from *Leishmania* promastigote (left) and amastigote stages (right) (Adapted from Besteiro, *et al.*, 2007).

### 1.8.5 *L.mexicana* virulence

Previous studies have shown that *L.mexicana* lost virulence after prolonged culture for up to Twenty passages *in vitro* (Ali *et al.*, 2013), in this study parasite virulence was examined at passages 1, 7 and 20 by injecting  $2 \times 10^6$  *L. mexicana* promastigotes intradermally in Balb/c mice. Results clearly show that the parasite completely lost ability to induce lesions in the infected mice after 20 passages (figure 1.5).

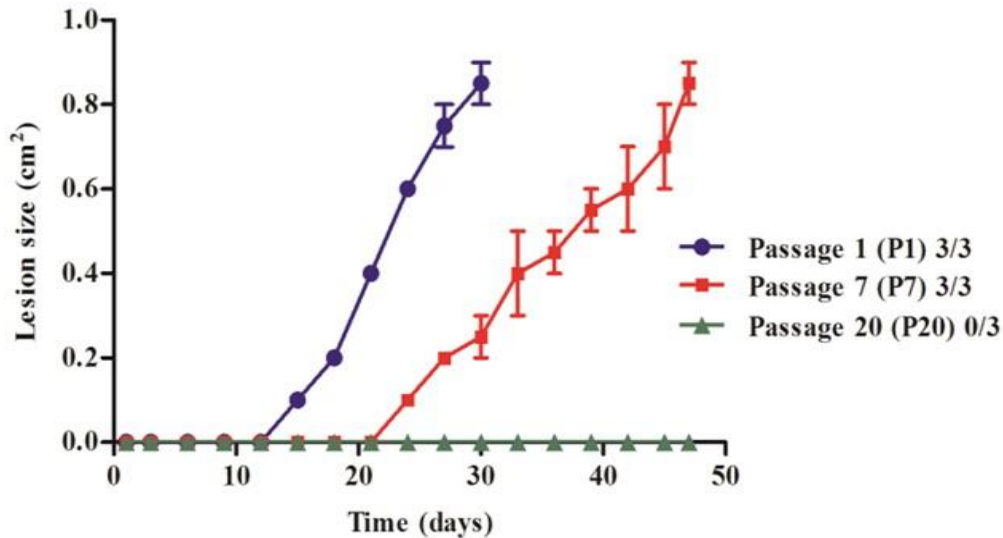


**Figure 1.5: Virulence of P1, P7 and P20 *L. mexicana* promastigotes**  
P1, P7 and P20 *L. mexicana* virulence were assessed by intradermal inoculation of susceptible Balb/c mice. The result showed that no lesion was observed in mice infected with P20 (adapted from Ali *et al.*, 2013).

### 1.8.6 *Leishmania* parasite within the vector

Infection of the female hematophagous sand fly starts in the midgut, which provides the ideal environment for proliferation and maturation of *Leishmania* into the metacyclic stage (Teixeira *et al.*, 2013). The metacyclic promastigote stage parasite migrates from the vector midgut to the oesophagus, and when the vector bites a susceptible animal the parasites are injected intra-dermally, parasites are rapidly phagocytosed by cells such as monocytes, neutrophils, and macrophages (Sacks and Kamhawi, 2001; Rogers, 2012) where they differentiate into amastigotes.

### 1.8.7 Role of parasite surface molecules

*Leishmania* parasites can resist the complement system in the blood stream and become attached and internalized to the macrophages by two main types of ligand molecules, which are found on the parasite surface. These are divided into two major families of phosphoglycans (PG) and zinc metalloprotease glycoprotein (GP63) (Kweider *et al.*, 1987).

### 1.8.8 Glycoprotein 63 (GP63)

The GP63 molecule is a zinc metalloprotease found on the surface of promastigotes associated with complement resistance; it can also be found on the surface of amastigotes, albeit in a small quantity. *Leishmania* parasites attach and enter the macrophage through the binding of their GP63 to macrophage complement receptor CR3, fibronectin receptor and

Mac-1 (Rizvi *et al.*, 1988; Russell *et al.*, 1988; Mosser *et al.*, 1992). GP63 also plays an important role in cell signalling of the host cells and the regulation of the protein tyrosine phosphatase (PTPs) mechanism (Isnard *et al.*, 2012). Therefore, it is identified as a virulence factor of *Leishmania* (Brittingham *et al.*, 1995).

In a study by Thiakaki *et al.*, (2006) to assess the role of GP63 *in vivo*, Balb/c mice were infected with a GP63 downregulated mutant *L. amazonensis*, results showed the mutant parasite became less infective than controls by the formation of delayed and small lesions with less parasite load in lesions and draining lymph nodes. Moreover, the number of CD4+ cells was fewer at the site of inoculation and higher in the draining lymph node than controls, with positive profile of IFN- $\gamma$  cytokine. Hence, this suggests that downregulated GP63 *Leishmania* were efficiently lysed by the complement system, and parasite infectivity has been reduced along with activation of immune response type 1. However, GP63 can induce the release of IL-6 and TNF cytokines by degradation of synaptotagmin, which is a family of membrane proteins, which regulate the fusion process in phagosomes and negatively regulate the release of IL-6 and TNF cytokines (Duque *et al.*, 2014).

Gene methylation is another way that has been recently reported to enable *Leishmania* survival inside the macrophage by turning off genes that control macrophage physiology and microbicidal activity through GP63 (Duque and Descoteaux, 2015). The *Leishmania* cell membrane protease GP63 cleaves AP-1 transcription factor (TF) directly (Contreras *et al.*, 2010) causing protection of infected cells against apoptosis (Wisdom *et al.*, 1999). It is noteworthy that the Activating Protein-1 (AP-1) is a dimeric transcription factor consisting of Jun, Fos proteins that bind to a common DNA site, the AP-1-binding site (Karin, and Zandi, 1997; Ameyar, and Weitzman 2003). c-Jun and AP-1 are involved in regulation of extracellular stimuli such as stress, cytokines, growth factors, and infection. AP-1 is a transcription factor that controls gene expression in response to different stimuli (Hess and Schorpp-Kistner 2004). In addition, AP-1 play a central role in a wide range of cellular processes, such as cell growth, differentiation, and apoptosis. (Ameyar and Weitzman 2003). AP-1 plays an important role as a transcription factor in regulation and expression of many genes that are involved in activation of macrophage functions such as TNF $\alpha$ , iNOS, and IL-12 (Newell, and Lopez-Berestein, 1994; Contreras *et al.*, 2010). However, it should be mentioned that transcription factor (TF), also called sequence-specific DNA-binding factor, is a type of protein that has a function in controlling transcription of genetic information from DNA to mRNA by binding to a specific DNA sequence (Karin, 1990).

### 1.8.9 Lipophosphoglycans (LPG)

All *Trypanosoma* family member are characterized by the presence of a glycocalyx, also called glycoconjugate coat, covering the parasite surface (Ferguson, 1999). The main components of the glycocalyx are glycoinositolphospholipids, and lipophosphoglycans. These surface glycolipids are important virulence factors of pathogens such as bacteria, fungi and protozoa (Ferguson, 1999). LPG is essential for *Leishmania* survival and multiplication within the mammalian host and intermediate host environments. *Leishmania* parasites must undergo morphological and biochemical adaptations including expression of glycoconjugates, which are composed of molecules attached by a glycosylphosphatidylinositol (GPI) anchor (Turco and Descoteaux, 1992). They anchor GPI molecules such as LPG, glycoproteins 63 (GP63), glycoinositolphospholipids (GIPLs) and the proteophosphoglycan (PPG), or they are secreted as proteins that contain phosphoglycans (PGs), including the secreted acid phosphatase (McConville, and Menon, 2000; Naderer *et al.*, 2004).

The dominant surface component of *Leishmania* promastigote is LPG, a large glycoconjugate which together associated with cell surface PPG forms a dense glycocalyx to protect the *Leishmania* parasite from the innate immune response (Naderer *et al.*, 2004). LPG is a glyco-phospholipid complex that plays an important role in parasite survival in host cell phagosomes and the sand fly gut (Descoteaux and Turco, 2002). The Lipophosphoglycan (LPG) is a *Leishmania* dominant surface molecule which is found on all *Leishmania* promastigotes species. LPG consists of lipid and polysaccharide (glycan) linked by a phosphodiester bond, so it is called lipophosphoglycan such as phosphoglycosylated and proteophosphoglycans (PPG). Glycoconjugates are the most common surface coat on the promastigote surfaces with around  $5 \times 10^6$  copies per cell (Turco and Descoteaux, 1992), while GP63 is found on the promastigote plasma membrane with approximately  $5 \times 10^5$  copies per cell.

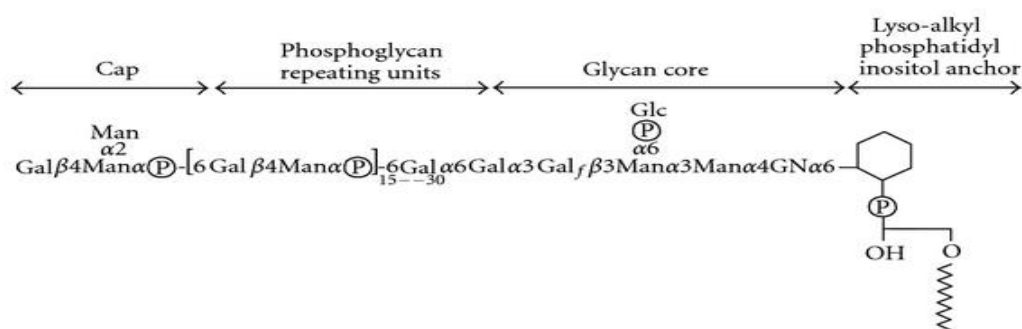


**Figure 1.6: Structure of the LPG**

The LPG consists of four domains: cap, PG repeating units, glycan core and lipid anchor. The number of PG repeating units increases during metacyclogenesis of the parasite promastigotes. The structure of the cap is different among parasite species. Where Gal is galactose; Man is Mannose; GN is glucosamine; and Glc is glucose (Adapted from Franco, *et al.*, 2012).

Parasite surface LPG modulates the immune interaction between the host macrophage and the *Leishmania* parasite. LPG is a pathogen-associated molecular pattern (PAMP), which plays a crucial role in modulation of the host immune response during interaction and establishment of macrophage infection by the parasite. In addition, it plays a role in the binding of the parasite to the vector gut wall, which protects the parasite from degradation (Desjardins and Descoteaux, 1997; Duque *et al.*, 2014).

The first interface between parasite and host immune system takes place in the dermis of the mammalian host immediately after parasite inoculation by the sand fly vector, it is through the interface between *Leishmania* LPG and the immune system. More precisely, LPG is a coat protecting *Leishmania* from attack by the host immune system and, at the same time, it is the first target for immune detection.

Human macrophages and dendritic cells recognise *Leishmania* through LPG (Favila *et al.*, 2015). When procyclic parasites bind to mannan-binding proteins in the serum through LPG, this will activate the complement system (C1q) and kill the parasite in the procyclic stage. On the other hand, LPG protects the metacyclic stage by its repeating units which increases the phosphorylated disaccharide which increases thickening of glycocalyx (Sacks *et al.*, 1995). This will subsequently reduce the binding of the parasite surface to endosomes and lysosomes inside the vacuoles. Exposure of murine macrophages to LPG extracted from purified *L. donovani* confirms that the strategy used by the parasite to establish infection of the macrophage is through LPG repeating units (Desjardins and Descoteaux, 1997). The LPG repeating unit plays an essential role in the transmission of the parasite from vector midgut to macrophage phagolysosome and during the early stages of macrophage infection. In addition, it inhibits phagolysosome activation, which protects promastigotes from degradation and provides a good environment for differentiation into amastigotes (Desjardins and Descoteaux, 1997). This has been demonstrated in *L. major* LPG deficient mutants, which lost virulence to infect mice either *in vivo* or *in vitro* (McConville and Homans, 1992; Späth *et al.*, 2003). A recent study by Zamora-Chimal *et al.*, (2016) examined the effect of LPG extracts from *L. mexicana* on bone marrow macrophages derived from Balb/c and C57BL/6 mice *in vitro*. On the basis of their results they concluded that LPG binds to TLR2 in dendritic cells which indirectly activates NK cells to release IFN- $\gamma$  and IL-4, which provide protection against the parasite. Another study by Favila *et al.*, (2015) reported that *Leishmania* LPG induces the release of IL-12 from infected macrophages and dendritic cells. However, LPGs differ among parasite species; peritoneal Balb/c C57BL/6 macrophages stimulated with *L. braziliensis* LPG produce higher IL-1 $\beta$ , TNF- $\alpha$ , IL-6 and NO than one stimulated with *L. infantum* (Ibraim *et al.*, 2013).

The genes responsible for LPG synthesis are LPG1, LPG2, LPG3, and LPG5 (Ryan *et al.*, 1993) However, the studies did not achieve a complete characterisation of LPG structure, function and gene regulation of LPG synthesis (Forestie *et al.*, 2015).

#### **1.8.9.1 LPG1 gene**

Ilg (2000) has reported that, *L. mexicana* LPG1 mutant parasites produced by gene deletion failed to synthesize LPG protein, but still expressed a variety of phosphoglycan molecules on their surface. The study concluded that LPG1 deficient *L. mexicana* mutants did not affect parasite infectivity to Balb/c and C57 macrophage suggesting that LPG1 is not to be considered as a virulence factor. In another study by Turco *et al.*, (2001) who compared between *L. mexicana* and *L. major* LPG biosynthetic genes knock-outs, reported that *L. major* but not *L. mexicana* lost virulence. Another study by Beneke, *et al.*, (2017) reported that deletion of the LPG1 gene from *L. mexicana* by using clustered regularly interspaced short palindromic repeats (CRISPR) technology caused loss of LPG from the parasite surface. More recently, deletion of LPG1 from *L. infantum* impaired the outcome of C57BL/6 bone marrow derived macrophage infection and the survival of parasites was reduced significantly after 72 hours of infection, coinciding with strong induction of NF- $\kappa$ B- and activation of iNOS (Lázaro-Souza *et al.*, 2018).

#### **1.8.9.2 LPG2 gene**

The synthesis of a phosphoglycan molecule is dependent on the Golgi GDP-mannose (GDP-Man) transporter that is encoded by LPG2. Golgi GDP-Man transporter plays a major role in the synthesis of phosphoglycan-containing glycoconjugates in eukaryotic microorganisms such as the *Leishmania* parasite. LPG2 plays an essential role in this process, either because it encodes the GDP-Man transporter or by the transportation of GDP-Man into the lumen of the Golgi apparatus (Ma *et al.*, 1997).

A study by Gaur *et al.*, (2009) reported that *L. donovani*, *L. major* and *L. mexicana* null of LPG2 were highly sensitive to complement mediated lysis *in vivo*. Amastigotes and promastigotes from *L. donovani* and *L. major* but not *L. mexicana* failed to infect macrophages *in vitro*.

#### **1.8.10 Cysteine peptidases (CP)**

There are 19 genes of CP, including CPB and CPB2.8, which are significantly different from the remaining 17 genes (CPB 3 to CPB 19) (Mottram *et al.*, 1997). CPB is a single isoform array whereas, CPB2.8 is an isoform encoded by a gene internal to the array; and 2.8 refers to the gene size. *L. mexicana* amastigotes are rich in cysteine peptidases which play central

roles in facilitating growth and survival of the parasites in mammalian cells. CPB of *L. mexicana* amastigotes plays a central role in the ability of the *Leishmania* parasite to modulate signalling via NF- $\kappa$ B which leads to inhibition of IL-12 production (Cameron *et al.*, 2004). CPB activities are predominantly expressed in promastigotes at the metacyclic stage (Bates *et al.*, 1992). Balb/c mice infected with mutants of *L. mexicana* lacking CPB enzymes have greatly reduced infectivity of this parasite despite having the ability to induce subcutaneous lesions, but lesions of slower growth rate and smaller size. Also, they have decreased infectivity of Balb/c macrophages *in vitro* compared with wild-type parasites (Mottram *et al.*, 1996; Frame *et al.*, 2000).  $\Delta$ CPB promastigotes can infect Balb/c macrophages in large numbers but they are unable to survive in the majority of the infected cells (Frame *et al.*, 2000).

### 1.8.11 MAPK9 gene

Parasite flagellar morphogenesis is associated with mitogen activated protein kinase homologue (MAPK9) and its mRNA was found in all *L. mexicana* stages (Bengs, *et al.*, 2005; Reddy *et al.*, 2017). Phosphorylation is a reversible reaction for modification of protein and protein function. Protein Phosphorylation is catalysed by kinases enzyme, while the reverse reaction (dephosphorylation) is carried out by phosphatases. During differentiation of promastigotes into amastigotes, the flagellum length shortens and it has been shown that overall phosphorylation indicated by abundance of phosphoprotein in kinetoplastids (which is could be due to phosphatases and protein kinases) is involved in the amastigote differentiation processes (Mukhopadhyay *et al.*, 1988; Parsons *et al.*, 1995; Bengs, *et al.*, 2005).

## 1.9 *Leishmania* host cell interaction

The mammalian immune system is divided into two types, innate or nonspecific immunity and adaptive or specific immunity (Janeway *et al.*, 2001). Innate immunity in addition to anatomical barriers consists of phagocytes such as neutrophils, macrophages, and dendritic cells which engulf the invader to protect the host. Phagocyte recognise the foreign invader through pattern recognition receptors (PRRs) on the phagocytes cell surface and pathogen-associated molecular patterns (PAMPs) which are found on the microorganism, while adaptive immunity consists of B and T lymphocytes and the response of adaptive immunity to the antigen is through the recognition by specific antigen receptors of antigen that are expressed by antigen presenting cell (APCs) of the innate immunity. Interestingly, the adaptive immune system, unlike innate immunity, has a specific memory for every antigen (Janeway *et al.*, 2001; Chaplin, 2010).

Successful infection of *Leishmania* depends on both the immune system and the species of the parasite. On the parasite side, the promastigotes enter the host's blood stream to invade host cells and to differentiate into amastigotes. The interaction between the host immune system and the virulence potential of the parasite will dictate the fate of this disease.

The macrophage is one of the mononuclear phagocytic cells which plays a vital role in the immune system. It regulates immune response and participates in both the innate and adaptive immune system and is the main target of *Leishmania* infection (Zhang *et al.*, 2008). The host's immune response against the *Leishmania* parasite is highly complicated and while these may accelerate healing some responses worsens the disease. Both these responses depend on the immune status of the infected host the stage of the disease, and species of *Leishmania* (Antonelli *et al.*, 2004).

In the infected tissues, macrophages will be activated to differentiate into specialized functional phenotypes. The main factors that affect this differentiation are cytokines and pathogenic products. The macrophages phenotypes are M1 and M2 (Martinez and Gordon, 2014). M1 and M2 macrophages represent the major activities of macrophages. Whereas M1 inhibits cell proliferation and causes tissue damage, M2 promotes cell proliferation and repair tissue. M1 macrophages promote Th1, while M2 promote Th2 responses, therefore they are known as M1 and M2 (Mills, 2012). Understanding pathophysiological and immunological responses of different hosts is important for the researcher to developed vaccines or drugs for this disease.

### **1.9.1 Interaction of *Leishmania* with host cells**

Infection of host cells with the *Leishmania* parasite stimulates immune responses to recruit a wide range of cells such as neutrophils, mast cells, monocytes, dendritic cells and macrophages. Macrophages and dendritic cells are the main immune cells that interact with *Leishmania*. On the entry of *Leishmania* promastigotes, they differentiate into non-motile amastigotes which can survive and multiply inside phagosomes of macrophages (Liu, and Uzonna, 2012).

Amastigotes are internalised inside parasitophorous vacuoles (PV) of macrophages, where they start multiplication by binary fission, subsequently leading to, rupturing of macrophages and release of amastigotes to infect other surrounding macrophages (Liu, and Uzonna, 2012). Intracellular amastigotes can infect other macrophages upon lysis of the host cell (Naderer, and McConville, 2008). Naïve sand fly vectors get infected when they bite the infected host and take a blood meal containing these amastigotes. In the vector midgut, *Leishmania* amastigotes will differentiate into infectious promastigotes to infect another host during a blood meal (Brandão-Filho., 1999; Liu, and Uzonna, 2012). Knowing how the *Leishmania*

parasite survives and multiplies inside macrophages would help in designing the right treatment or vaccines.

Monocytes and macrophages are the main cellular component of the reticuloendothelial system. Macrophages are produced by differentiation of monocytes when they leave the blood stream and enter tissues. A macrophage is a phagocytic cell that is found in different body tissues and plays a main role in the innate immune system and inflammation (Beutler, 1999). Macrophages play a main role in the immune system's response against pathogens. They engulf and destroy pathogens and direct the immune response from innate into adaptive (Elhelu, 1983). A macrophage is a phagocyte that engulfs extracellular antigens and debris, which can include parasite derived features such as flagella and it is found in all tissues and is responsible for the inflammatory and immunological response (Unanue and Allen, 1987). When a macrophage engulfs a pathogen, it secretes a variety of proteins, cytokines, and bioactive molecules to activate or suppress other tissues or immune cells, which regulate immune responses, such as activation or inhibition of lymphocytes. T helper cells are activated or inhibited by interaction with protein presented on the surface of macrophages or other phagocytic cells. The interaction between macrophages and T cells involves major histocompatibility complex and growth-differentiating proteins (Unanue, and Allen, 1987).

### **1.9.2 Phagocytosis of the *Leishmania* parasite**

The phagocytosis process of the *Leishmania* parasite consists of two steps: attachment and internalization. Infection with *Leishmania* starts when the female sand fly injects metacyclic promastigotes intradermally into a susceptible mammalian host. Most *Leishmania* parasites will be killed in interstitial tissues by the complement system; some of them can escape into phagocytic cells (Solbach and Laskay, 2000).

The first defence against the *Leishmania* parasite is the complement system, which can kill the parasite before they escape into phagocytic cells. It has been shown that phosphate buffered Saline (PBS) containing 25% normal sera can kill *Leishmania* promastigotes by activation of complement through the alternative pathway; however, 8% of normal sera enhanced attachment of parasites to macrophages (Mosser, and Edelson, 1984). The first phagocytic cells that infiltrate into the site of infection are neutrophils. It starts a few hours after parasite inoculation by vector bite (MuÈller *et al.*, 2001).

Van Zandbergen *et al.*, (2004) have reported that neutrophils infected with *Leishmania major* secrete an enriched amount of MIP-1 $\beta$  chemokine in large quantities, which acts as a macrophage chemo-attractant to the site of infection. Macrophages will phagocytose apoptotic neutrophils along with free *Leishmania* parasites and they become the final host cell for the *Leishmania* parasite where it survives and multiplies. Multiplication of the

parasite leads to the rupture of macrophages and the release of amastigotes that can infect other macrophages (Peters *et al.*, 1995).

When *Leishmania* promastigotes are recognized and phagocytosed by macrophages they transform inside phagosomes into amastigotes. The *Leishmania* parasite can survive in neutrophils but it cannot multiply, therefore macrophages are the ultimate final host for *Leishmania* parasites. Accordingly, Leishmaniasis is the outcome of a successful invasion of macrophages by *Leishmania* parasites (Van Zandbergen *et al.*, 2004).

The immunological effective pathway against this disease is dependent on macrophage responses to the parasites, on the activation of CD4<sup>+</sup> Th1 cells that is accompanied with IFN- $\gamma$  and IL-12 production, which can lead to the production of Inducible Nitric Oxide (iNOS) in macrophages to produce NO to kill the parasites and healing of Leishmaniasis, while activation of Th2 can lead to the suppression of IFN- $\gamma$  and IL-12 production and subsequent inhibition of NO causing exacerbation of Leishmaniasis (Scott, 1991; Chatelain *et al.*, 1999).

### **1.9.3 Phagocytosis of promastigotes by macrophages**

Parasite LPG and GP63 molecules play a main role in the attachment and internalisation in macrophages. The main receptors of macrophages that deal with *Leishmania* parasites are the complement receptors (CR)1, CR1, CR3, mannose-fucose receptor (MR) and fibronectin receptors (FnRs). The attachment of the promastigote starts when the GP63 molecule cleaves C3 opsonin into C3b and subsequently, CR1 cleaves C3b into iC3b and then iC3b facilitates binding of promastigote to CR3. In addition, attachment can be enhanced by binding of GP63 to fibronectin, which acts as a bridge to connect GP63 to FnRs. In addition, GP63 may bind directly to the CR3 but this is still unclear (Ueno and Wilson, 2012).

### **1.9.4 Phagocytosis of amastigotes by macrophages**

Amastigotes bind to macrophages by two methods; by the binding of amastigote surface GP63 molecules to iC3b, which subsequently bind to the CR3. Or by binding of host IgG antibodies to amastigote epitopes and Fc $\gamma$ Rs of macrophages. Although, GP63 molecules are less expressed on amastigote surfaces, the GP63 can bind to fibronectin, which in turn binds to FnR of macrophages (Ueno and Wilson, 2012).

Fc receptor can bind to IgG antibodies on the surface of the parasite which plays a role in macrophage infection by amastigotes. In a study to examine the role of the Fc receptor by Kima *et al.*, (2000) mice deficient with circulating antibodies by genetic alteration were poorly infected with *L. mexicana*, *L. pifanoi* and *L. amazonensis*, suggesting the role of antibodies in the attachment of parasites to macrophages.

## 1.9.5 Receptors and recognition

The *Leishmania* parasite binds to host cell membrane receptors which play a major role in the attachment of *Leishmania* to macrophages, such as TLR, Fc $\gamma$ R, CR3, CR1, (Mac-1), fibronectin receptor and mannose-fucose receptor (MR) (Ueno and Wilson, 2012).

### 1.9.5.1 Third complement receptor (CR3)

CR3 receptor is found on phagocytic cells such as neutrophils and macrophages; it has a role in adhesion and internalisation of the *Leishmania* pathogen. When *Leishmania* parasites are recognised by the macrophage, parasite GP63 surface protein converts soluble serum component opsonin C3 to C3b. Then, factor 1 cleaves C3b to iC3b which leads to binding of parasite to CR3. *Leishmania* promastigotes can directly bind CR3 receptor by opsonised iC3b (Ueno and Wilson, 2012).

The role of complement protein was investigated in a study by Wozencraft *et al.*, (1986) who reported that incubation of promastigotes and amastigotes from *L. donovani* with murine macrophages in a medium without serum led to the binding of these parasites by macrophages. In this regard, Blackwell (1985) suggested that macrophages secrete complement to bind to the parasite that activates the alternative pathway.

Using CR3 receptor could allow the *Leishmania* parasite to escape from an innate immune response, Ricardo *et al.*, (2013) reported that binding of *L. major* to CR3 mediates and inhibits production of IL-12 cytokines that activate Th1. In line with this, Marth and Kelsall (1997) have reported that signalling through CR3 without any infection suppresses the production of IL-12 and IFN- $\gamma$ . However, blocking of CR3 and CR1 receptors never prevents attachment of the parasite to macrophages (Rosenthal *et al.*, 1996; Ueno and Wilson, 2012). Therefore, promastigotes may bind to the CR3 through other yet unknown antigenic determinants on the promastigote surface (Ueno and Wilson, 2012).

### 1.9.5.2 First complement receptor (CR1)

CR1 is found on the surface of monocytes, macrophages and neutrophils. CR1 recognises C3b, C4b. It facilitates the cleavage of C3b into iC3b. Rosenthal *et al.*, (1996) have reported that the blocking of CR1 receptor never prevents parasite attachment to macrophages. However, there is a cooperation between CR1 and CR3 to enhance parasite attachment. In addition, there is a cooperation between CR1 and Mac-1 on monocytes to mediate adhesion between human monocytes and promastigote metacyclic stage through complement (Rosenthal *et al.*, 1996). In a recent study on human monocytes, Machado de Oliveira (2016) reported that blocking of CR1 leads to reduced *Leishmania* phagocytosis and increased *Leishmania* survival.

### **1.9.6 Survival of *Leishmania* parasite in the blood stream and macrophage**

In the blood stream *Leishmania* parasites have to survive the humoral immune system before infecting macrophages. *Leishmania* parasites can resist the complement system mainly by two molecules, LPG and GP63, which are found on the parasite surface (Kweider *et al.*, 1987) while antibodies, on their own have no effect on the parasite's early stage of interaction in the blood stream. Promastigote parasites attach to the macrophage after complement opsonisation to CR3, fibronectin receptor and mannose receptor (Mosser and Rosenthal, 1994). *Leishmania* survive and proliferate inside macrophages in the acidic phagolysosome vacuoles.

Inside macrophages, *Leishmania* should be protected from reactive oxygen species (ROS) which are reactive chemical molecules produced by phagocytes as part of a defence mechanism against intracellular pathogens (Hancock *et al.*, 2001) and reactive nitrogen species (RNS) derived from NO. RNS and ROS can induce changes in protein expression profile of *Leishmania* which is important for the survival of promastigotes (Sardar *et al.*, 2013). In recent study by Roma *et al.*, (2016), comparing wild type and genetically deficient ROS C57BL/6 mice and wild-type mice infected with *L. amazonensis*, it was reported that ROS play a role in the regulation of inflammatory responses without effect on parasite killing, so the mechanism that protects parasites to avoid degradation is still unclear.

Both promastigotes and amastigotes survive inside PV through internalization in the macrophage, and maturation of the PV. Mature PV is an adapted environment within the macrophage, which supplies the parasite shelter with nutrients and protects the parasite from the host immune system and macrophage microbicides. Thus, parasites survive and differentiate into an amastigote form (Liévin-Le Moal, and Loiseau, 2016). Intracellular amastigotes can infect other macrophages by release from lysed host cell or by cell division (Naderer, and McConville, 2011).

### **1.9.7 LPG and inhibition of phagosome maturation in a macrophage**

LPG which covers promastigote surfaces has the ability to inhibit phagolysosome biogenesis which causes accumulation of periphagosomal filamentous actin (F-actin). It should be mentioned that F-actin is a protein found in most eukaryotic cells as a part of the cytoskeleton and plays a crucial role in cell functions such as cell division, migration, endocytosis, stability and morphogenesis (Stossel, 1978; Stricker *et al.*, 2010).

Accumulation of F-actin may form a physical barrier that prevents *Leishmania* promastigote-harboured phagosomes from interaction with early lysosomes and endosomes. Therefore, LPG is not necessary for parasite survival at this stage while internalised in the macrophages, after preventing the formation of the phagolysosome. *Leishmania* promastigotes hijack the infected macrophage cytoskeleton early during the infection process (Stricker *et al.*, 2010).

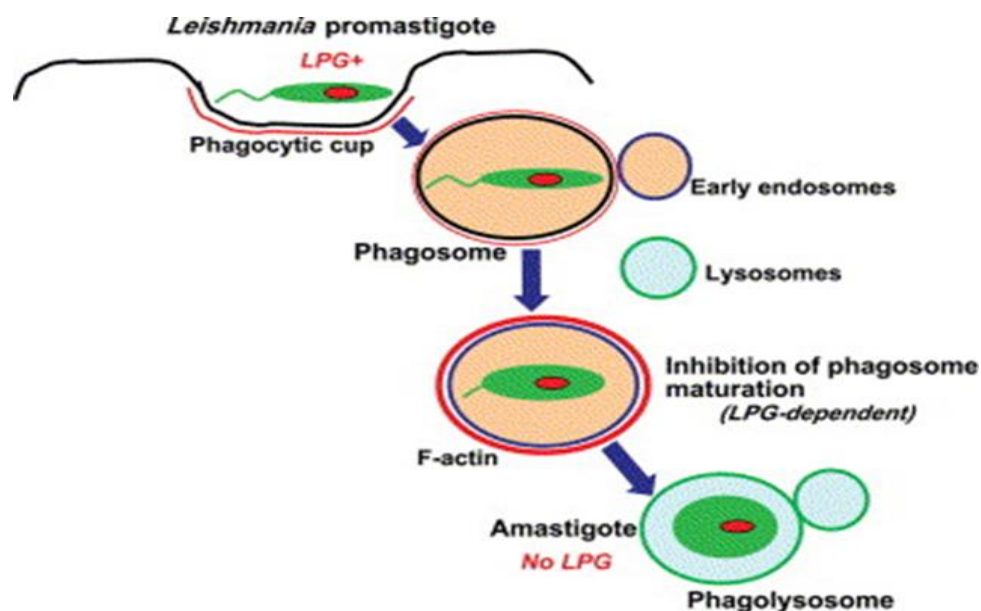


**Figure 1.7: Inhibition of phagosome maturation in a macrophage infected with *Leishmania* promastigote.**

After engulfment of *Leishmania* promastigotes by the macrophage, F-actin (red circle) accumulates around the phagosome which contain the parasite and acts as a barrier. This F-actin barrier prevents phagosomes interacting with early endosomes (blue circle) or lysosomes (green circle) until completing the differentiation of the promastigotes into amastigotes. (Adapted from Stricker, *et al.*, 2010).

### 1.9.8 Nitric Oxide

*Leishmania* parasites have several mechanisms for escaping host immune responses. An important one is the ability of the parasite to interfere with NO production, by suppressing the expression of iNOS in infected macrophages, which results in NO depletion (Calegari-Silva *et al.*, 2009). Nitric Oxide (NO) plays a vital role in many biological activities, it suppresses T lymphocytes in chronic inflammation, destroys tumour cells, and protects host cells from destruction by pathogens such as bacteria, fungi, viruses and protozoa (Nathan and Hibbs, 1991; Marletta, 1993). Liew, *et al.*, (1990a) have demonstrated that the main effector agent to kill *L. major* inside macrophages is NO. Moreover, NO kills *Leishmania* parasites when cultured in PBS *in vitro* at room temperature. A preparation of amphotericin B, DETA and NO can kill 98% of promastigotes and 76% of amastigotes after 12 hours' incubation *in vitro* (Pandya *et al.*, 2016).

NO is an important microbicide effector *in vivo* and *in vitro*. Synthesis of NO by enzymatic oxidation of L-arginine is activated by IFN- $\gamma$  (Töttemeyer *et al.*, 2006). It has been reported that the *Leishmania* parasites can inhibit production of lethal NO in infected cells (Olivier *et al.*, 2005). This was confirmed in mutant mice lacking iNOS where they fail to control *L. major* infection *in vivo* (Wei *et al.*, 1995). It is noteworthy that iNOS is a key mediator of the leishmanicidal process, which can impair the replication of *Leishmania* (Calegari-Silva *et al.*, 2009). It was also shown that the iNOS can be purified from mice macrophages treated with lipopolysaccharide and IFN-  $\gamma$  (Marletta, 1993).

Stenger *et al.*, (1994) reported that iNOS is significantly released in high quantities earlier in resistant C57BL/6 mice compared to susceptible Balb/c mice when infected with *L. major*. Moreover, none to very low parasite numbers were detected in skin lesion of C57BL/6 mice which was accompanied by high levels of iNOS in the lymph nodes. Almeida-Souza *et al.*, (2016) have reported that the treatment of Balb/c peritoneal macrophages with *Morinda citrifolia* increased of NO production and killing of intracellular *L. amazonensis*. However, de Moura *et.al*, (2016) demonstrated that there is a resistance against the antimonial drugs and NO in relapse human cases of *L. infantum*.

### **1.9.9 Nuclear factor kappa-light-chain-enhancer of activated B cells (NF- $\kappa$ B)**

Nuclear factor NF- $\kappa$ B is a protein complex found in almost all animal cells. NF- $\kappa$ B is involved in cellular responses to stimuli such as in case of infection. It is playing a central role in many macrophage functions and plays a key role in regulation of the immune response to infection (Gilmore., 2006), and the expression of proinflammatory genes including chemokines, cytokines, and adhesion molecules by controlling DNA transcription by modulating the expression of genes involved in the immune response of the host. The nuclear factor NF- $\kappa$ B pathway has been considered a pro-inflammatory signalling pathway, it is based on the activation of NF- $\kappa$ B by proinflammatory cytokines such as IL-1 and TNF- $\alpha$  (Gilmore, 2006; Perkins, 2007). It has been reported that *L. amazonensis* has developed a strategy to survive in the infected cell by escaping from host defences by stimulation of the NF- $\kappa$ B repressor complex p50/p50 of a gene which subsequently regulates the expression of iNOS negatively and enables the parasite to establish a successful infection of human monocytes (Calegari-Silva *et al.*, 2009).

## 1.10 Apoptosis

Generally, cell death is of two types, necrosis and apoptosis (Edinger, and Thompson, 2004). Apoptosis or programmed cell death (PCD) is one of the most highly regulated physiological processes of cell tissue homeostasis which is essential for development in most organisms (Fadeel, and Orrenius., 2005; Edinger, and Thompson, 2004; Kerr *et al.*, 1972). Apoptosis was first described by Kerr *et al.*, in 1972. It occurs in multicellular organisms to aid development, immune responses and, to dispose of cells that are no longer required e.g. in case of infected or transformed cells (Evan and Littlewood 1998).

Apoptosis is induced by the activation of caspases which are either triggered by the release of apoptotic mediators from mitochondria or ligation of death receptors. During apoptosis, the nucleus is condensed, fragmented, and chromosomal DNA cleaved into internucleosomal fragments and packaging of the apoptotic cell into bleb bodies without plasma membranes. Bleb bodies are recognized and engulfed by phagocytic cells without activation of inflammation around the apoptotic cell (Danial, and Korsmeyer., 2004; Edinger, and Thompson., 2004).

Apoptosis can be induced by a variety of intrinsic and extrinsic signals in response to physiological and pathological stimuli (Fadeel, and Orrenius., 2005; Edinger, and Thompson, 2004; Kerr *et al.*, 1972). Many mammalian diseases are caused by direct or indirect defects in apoptosis, leading to accumulation of undesired cells, or impaired normal function of cells.

Apoptosis can be detected by morphological and biochemical changes in cell tissues. It can be identified morphologically by loss of adhesion to flasks of adherent cells such as macrophages, loss of normal appearance of the cells, the presence of nuclear fragmentation, chromatin condensation and membrane blebs (Rodrigues *et al.*, 2006).

Plasma membrane blebbing is the morphological feature which appears in a late stage of the apoptotic process. It is due to localisation of the plasma membrane cytoskeleton and characterised by irregular bulging of the cell plasma membrane. Subsequently, blebs separate from the cell with a part of the cell cytoplasmic nuclear fragments (Stillwell, 2016). The apoptotic plasma cell membrane is distinguishable from that of a normal cell. Apoptotic cell membrane is triggered and lose integrity (Stillwell, 2016). However, it has been reported that blebs are also found in normal cell processes during cell division or locomotion.

Early apoptosis can be detected biochemically, by the detection of the upregulation of phosphatidylserine (PS) by staining with annexin V stain and flow cytometry analysis. PS expression on the plasma membranes of apoptotic cells enhances macrophages to engulf them (Krahling *et al.*, 1999. Huynh *et al.*, 2002) and subsequently the suppression of the release of pro-inflammatory mediators and promote the release of anti-inflammatory agents

like the TGF- $\beta$ 1. Engulfment of apoptotic cells with low PS expression such as human monomyelocytic cells cause reduced level of TGF- $\beta$ 1 and subsequently the acceleration of inflammation resolution (Huynh *et al.*, 2002).

### 1.10.1 Apoptosis pathways

Apoptosis is divided into two main pathways, intrinsic and extrinsic pathways, (Rodrigues *et al.*, 2006; Rampal *et al.*, 2012). a brief description for these pathways is given in figure.1.8

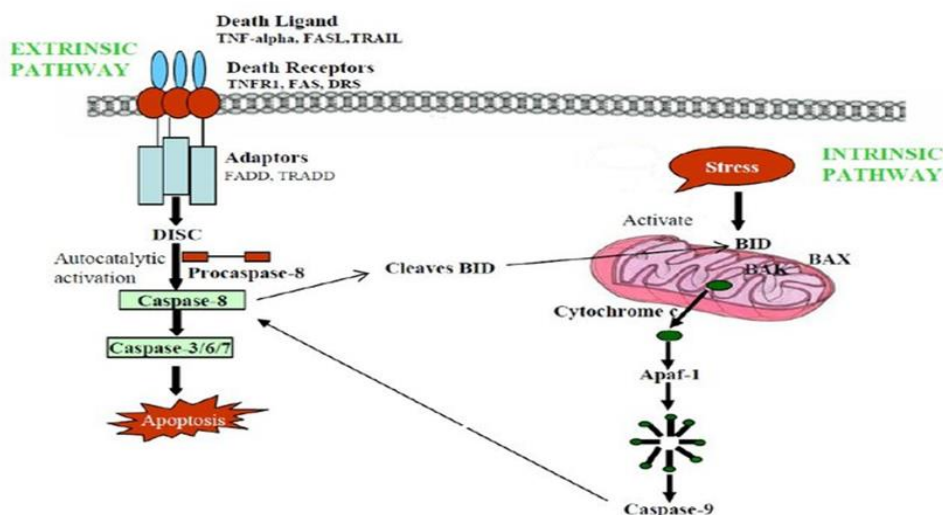


**Figure 1.8: The apoptosis pathways**

In apoptosis there are two pathways, the intrinsic and extrinsic pathways

**The extrinsic pathway** is initiated by activation of death receptors, such as TNF- $\alpha$  and Fas (on the cell intended to die) when bound with the death ligands on the plasma membrane. (Binding between the ligand and the receptors). Thus, fas-associated death domain (FADD) induces the formation of death inducing signalling complex (DISC) which activates caspase 8. Active caspase 8 is a mediator that cleaves pro-apoptotic BID protein, which subsequently releases mitochondrial pro-apoptotic factors linking these two pathways. The results of caspase 8 activation are activation of the cascade and apoptosis.

**In the intrinsic pathway**, activation is by cellular stresses which activate one of the BCL 2 family that initiate apoptosis signalling and induce release of Bax and or BAK to promote loss of mitochondrial outer membrane potential, cytochrome c release and activation of caspase 9 that activate caspase 3, caspase 6, caspase 7 and apoptosis. Disruption of the outer mitochondrial membrane and release of cytochrome C are important markers indicating triggering of apoptosis (Abhishek *et al.*, 2018).

**In cross talk between these two apoptotic pathways**, stress signals lead to the binding of BID and Bax to the outer membrane of mitochondria. Subsequently, BID and Bax will bind with BAK (mitochondrial protein) causing releasing of cytochrome C into the cytosol. This, in turn binds to the apoptotic protease activating factor-1 (Apaf-1) leading to formation of an apoptosome which triggers the activation of pro-caspase 9. Activated caspase 9 leads to further initiation of the caspase cascade leading to apoptosis. (Adapted from Rampal *et al.*, (2012) with minor changes).

## 1.10.2 Apoptosis mechanism

The extrinsic pathway is initiated by binding of death ligand to TNF- $\alpha$  and Fas death receptors (Adams, 2003). The death receptors contain death domain ligand which bind to FADD causing formation of DISC which cleaves and activate pro-caspase 8 to become activated caspase 8 which in turn cleaves and activates a cascade of caspases such as caspase 3, caspase 6 and caspase 7 and induces apoptosis which is called the mitochondrial independent pathway. Also, caspase 8 can cleave BID which is a BCL 2 family member, cleaved BID can induce mitochondria to release cytochrome C which will activate caspase 9. Eventually, activated caspase 9 causes activation of caspase 3 and triggers apoptosis (Luo *et al.*, 1998; Chandra *et al.*, 2004; Reyland and Bradford, 2010) which is called the mitochondrial dependent pathway.

## 1.10.3 Gene regulation of apoptosis

It is known that activation of apoptosis plays an essential role in elimination of intracellular pathogens such as viruses, bacteria and parasites e.g. *Mycobacterium tuberculosis* and *Leishmania* parasite species (Dragovich *et al.*, 1998; Moore and Matlashewski, 1994; Park *et al.*, 2006; Donovan, *et al.*, 2009).

### 1.10.3.1 BCL 2

B-cell lymphoma 2 (BCL 2), is a gene that belongs to the BCL 2 family and the BCL 2 protein is localized to the outer membrane of mitochondria. BCL 2 regulates proteins that are involved in apoptosis regulation in two different ways, by inducing or inhibiting apoptosis through the intrinsic apoptosis pathway (Tsujimoto *et al.*, 1984; Cleary ML *et al.*, 1986). It activates apoptosis by release of the pro-apoptogenic factor cytochrome c from the mitochondria, which is essential for caspase activation (Kuwana and Newmeyer., 2003) and suppresses apoptosis by formation of a heterodimer of anti-apoptotic BCL 2 or Bcl-xL proteins, with pro-apoptotic proteins such as Bax and BAK. Therefore, the ratio of pro-apoptotic BCL 2 to anti-apoptotic BCL 2 proteins is important to determine the cell fate (Reyland and Bradford, 2010). The BCL 2 gene encodes an anti-apoptotic protein (Solano-Gálvez *et al.*, 2018). Bcl-xL and BCL 2 are found in the outer membrane of mitochondria and their role is to prevent the release of cytochrome c, while the pro-apoptotic proteins such as Bax, and Bad, are in the cytosol, but under certain stimuli are translocated into the mitochondria, and induce the release of cytochrome c (Frenzel *et al.*, 2009).

### **1.10.3.2 Bax**

Bax or BCL 2 like protein is an apoptosis regulator that also belongs to BCL 2 family. These family members act as anti or pro-apoptotic regulators which are involved in a wide variety of cellular activities. It has been reported that the function of this protein is to increase the opening of mitochondrial voltage dependent anion channels, which in turn leads to the loss in membrane potential and release of cytochrome c which is involved in initiation of apoptosis. Mitochondria play a central role in cell survival through their generation of energy through ATP via oxidative phosphorylation. Loss of cytochrome C from the mitochondria prevents production of energy causing apoptosis (Oltval and Korsmeyer, 1993; Westphal and Dewson, 2014).

### **1.10.3.3 Macrophage Programmed death 1 receptor**

Programmed death 1 (PD-1) is a receptor expressed in many immune cells including macrophages. It is known that the function of PD-1 is the triggering of T-cell exhaustion. Infection of Balb/c macrophages with *L. donovani* causes downregulation of PD-1 and subsequently causes activation of pro-survival AKT by phosphorylation and resulting inhibition of the proapoptotic protein BAD and inhibition of apoptosis (Roy *et al.*, 2017). However, BAD protein belongs to the proapoptotic BCL 2 family that plays an important role in apoptosis regulation (Forde and Dale, 2007).

### **1.10.3.4 Caspases**

Cysteine-aspartic acid protease (caspase) family are proteases that need the presence of cysteine to perform their catalytic activity. The proteases target hundreds of proteins for controlled proteolysis of target proteins which minimizes damage and disruption to neighbouring cells and avoids activation by release of immunostimulatory molecules (Taylor *et al.*, 2008; Solano-Gálvez *et al.*, 2018). There are many types of caspases classified according to their function: caspase 2, caspase 8, caspase 9 and caspase 10 are initiator caspases. While caspase 3, caspase 6, caspase 7, classified as executor caspases. caspase 1, caspase 4, and caspase 5 are inflammatory caspases. In addition, other caspases such as caspase 11, are responsible for regulation of cytokines during septic shock, caspase 12 is associated with endoplasmic reticulum stress apoptosis, and caspase 14, is found in embryonic tissue (McLuskey and Mottram, 2015 ; Solano-Gálvez *et al.*, 2018).

The caspases are normally found in the cell as inactive proenzymes and they can be activated by a selective proteolytic cleavage. When the cells are stimulated with an apoptotic stimulus, this causes activation of initiator caspases which are activated through the extrinsic and intrinsic pathways (two main apoptotic pathways).

The extrinsic pathway is activated upon stimulated by death receptors, which causes activation of caspase 8. In the intrinsic pathway, the activation is by several stimuli which damage mitochondria and lead to release of cytochrome c which activates procaspase 9 thus in turn activating cascades of executioner caspases, such as caspase 3 caspase 6 and caspase 7 (Thornberry, 1998; Cianciulli *et al.*, 2018).

caspase 1 is one of the cysteine-aspartic acid protease (caspase) family, which is also described as an interleukin-1 $\beta$ -converting enzyme. It plays a central part in the inflammatory process by activation of pro-inflammatory cytokines IL1- $\beta$  and IL-18 (Fantuzzi and Dinarello, 1999) and inducing cell apoptosis. Initiation of caspase 1 can be triggered by a number of stimulants either from the host or foreign sources, which are mainly associated with components of pathogenic microorganisms (Firestein *et al.*, 2016). Caspase 1 play a role in triggering pyroptosis in infected host immune cells such as macrophages. Pyroptosis is a highly inflammatory form of programmed cell death with involvement of DNA fragmentation and membrane permeabilization causing the elimination of infected cells (Fink and Cookson 2006). In contrast to apoptosis, the cell death due to pyroptosis results from rupture of the plasma-membrane and the release of DAMP molecules (Baroja-Mazo *et al.*, 2014).

Caspase 8 is a member of caspase family. It plays a main role in the execution phase of cell apoptosis. This protein is involved in the apoptosis induced by Fas receptor and various apoptotic stimuli. Fas receptor may interact with Fas-associated death domain (FADD), which then recruits caspase 8 (Kruidering, and Evan, 2000).

Caspase 9 is member of the caspase family; it is implicated in cytokine and apoptosis processing. Caspase 9 is activated in the early stage of apoptosis after stimulation of cells by apoptotic stimuli which in turn stimulates mitochondrial release of cytochrome C and production of ROS (Kuida, 2000). After activation of mitochondria by caspase 9, caspase 3 inhibits production of ROS and is required for execution of apoptosis (Brentnall *et al.*, 2013).

## 1.11 Pyroptosis

Pyroptosis is the highly inflammatory form of programmed cell death with involvement of DNA fragmentation and membrane permeabilization causing the elimination of the infected cells (Fink and Cookson, 2006). Inflammasomes are multiprotein which are formed after cellular infection or stress. The inflammasome is responsible for triggering the maturation and secretion of proinflammatory cytokines such as IL-1 $\beta$  and IL-18. In addition, the inflammasome can trigger caspase 1 resulting in pyroptotic lysis of the infected cell (Fink and Cookson, 2005).

Pyroptosis plays an important role in the clearance of intracellular infection by removing intracellular replication niches and promoting the host's immune defensive responses (Fink and Cookson 2006). In infected macrophages, pyroptosis is initiated by the recognition of pathogen associated molecular patterns (PAMPs) by plasma membrane receptors such as toll-like receptors (TLRs), which recognize antigens found inside the cell. In contrast to apoptosis, cell death due to pyroptosis results in plasma-membrane rupture and is characterised by release of Damage Associated Molecular Pattern (DAMP) molecules (Baroja-Mazo *et al.*, 2014). However, both apoptotic and pyroptotic cell express PS on the outer membrane leaflet, therefore Annexin V cannot differentiate between apoptotic and pyroptotic cells (McIlwain, *et al.*, 2013).

## 1.12 Autophagy

Autophagy or type-II cell death is a self-degradative process of damaged or unnecessary cell organelles which maintains normal cell functions. Autophagy is induced through cellular stress when there is starvation and /or reduction in growth factors. Thus, autophagy may provide an alternative source of energy and building blocks obtained from defective or aged macromolecules to enable cells to survive. However, mediators and pathways of autophagy differ from apoptosis. (Overholtzer *et al.*, 2007; Yang *et al.*, 2010).

## 1.13 Role of autophagy in differentiation of *Leishmania* promastigotes into amastigotes

Autophagy can occur during differentiation of amastigotes by self-digestion of some cell organelles by degradative enzymes originating from inside of the parasite infected cell. Autophagy is important for defence against starvation conditions after changes in the environmental conditions, and also as for protein and organelle degradation during cellular differentiation and recycling of damaged organelles in order to survive in extreme environmental conditions (Reggiori and Klionsky, 2005; Cull, *et al.*, 2014).

The *Leishmania* parasite has two largely different morphological stages, promastigote and amastigote. Within the mammalian host, the metacyclic promastigotes are engulfed by macrophages, and then promastigotes differentiate to the amastigote form which survives and multiplies. Differentiation between these forms involves extensive reorganisation of the cellular structure and large changes in overall parasite size. Accordingly, these changes are crucial for the parasite's survival. Therefore, it has been hypothesized that autophagy plays an essential role in amastigote differentiation processes and *Leishmania* would be an

excellent model organism for studies of autophagy in cellular differentiation (Williams *et al.*, 2006).

### **1.13.1 Paraptosis**

Paraptosis is a type of programmed cell death characterized morphologically by the presence of vacuolization in the cytoplasm. Vacuolization begins with the physical swelling of endoplasmic reticulum and mitochondria (Sperandio *et al.*, 2000). It should also be pointed out that paraptosis does not involve the activation of caspases, apoptotic bleb body formation, or other morphological characteristics of apoptosis such as nuclear fragmentation and chromatin condensation. In addition, it is insensitive to apoptotic inhibitors such as Bcl-xL which are members of the BCL 2 family (Sperandio *et al.*, 2000, 2004).

### **1.13.2 Necrosis**

Necrosis is a premature cell death caused by cell injury induced by pathological factors such as trauma or physical damage, infection, toxins, heat, cancer, infarction, inflammation, and particularly failure of energy supply to the cells (Proskuryakov *et al.*, 2003). Necrosis is characterised morphologically by cellular swelling and vacuolation of the cytoplasm and breakdown of plasma cell membrane. Subsequently, there is release of cellular contents and proinflammatory molecules which lead to induction of inflammation around the necrotic cells. Apoptosis is caspase dependent whereas necrosis is caspase independent. Morphologically, necrotic cells are characterised by changes in the nuclear condensation and fragmentation of DNA. However, there are morphological similarities between necrosis and apoptosis (Edinger, and Thompson, 2004).

Secondary necrosis is a process which occurs in apoptotic cells when they are not engulfed by phagocytes, in this case the plasma membrane is broken down and the cell contents are released (Kono, and Rock, 2008). It is also pointed out that necrosis, secondary necrosis and necroptosis, followed by apoptosis represent different forms of cell death that eventually lead to similar cellular morphological features, including cytoplasmic swelling, rounding of the cell, loss of plasma cell membrane integrity and release of intracellular contents outside the cell (Berghe *et al.*, 2010).

### **1.13.3 Apoptosis in *Leishmania* Parasites**

Apoptosis is also observed in eukaryotic microorganisms such as protozoa and yeast, with a common feature of apoptosis in mammalian cell which is mainly the appearance of plasma membrane blebs, chromatin condensation and mitochondrial swelling (Planchon *et al.*, 2001;

Rodrigues *et al.*, 2006). The differences between apoptosis, paraptosis and necrosis of mammalian *Leishmania* cell and are summarised in Table 1.3.

**Table 1.3: Comparative analysis of apoptosis, paraptosis and necrosis features**

Comparative analysis of apoptosis, paraptosis and necrosis features observed in mammalian cells and *Leishmania* parasite (adapted from Rodrigues, *et al.*, 2006).

Cell type death	mammalian cells	<i>Leishmania</i> parasite
<b>Apoptosis</b>	-Exposure of phosphatidylserine on the cell membrane -Alteration of mitochondria -Activation of caspases -Fragmentation of DNA -Membrane blebbing Cell membrane lost integrity	-not depend on apoptosis activation -Alteration of mitochondria -Activation of caspase -Fragmentation of DNA -Membrane blebbing
<b>Paraptosis</b>	-Cytoplasmic vacuolation -No fragmentation of DNA -No activation of caspases -Swelling of mitochondria	-Cytoplasmic vacuolation -No fragmentation of DNA -No activation of caspases -Swelling of mitochondria
<b>Necrosis</b>	-Plasma membrane breakdown -Integrity of cell membrane	-Plasma membrane breakdown -Integrity of cell membrane

#### 1.13.4 Apoptosis and immunity

Apoptosis is a self-suicide of cells to eliminate infected or damaged cells therefore, apoptosis play an important role in immune responses and haemostasis (Jacobson *et al.*, 1997). Apoptosis is a defence mechanism by neutrophils, eosinophils, lymphocytes, monocytes and macrophages without triggering immune and inflammatory response (Savill *et al.*, 2003). Moreover, the viability of macrophages to engulf and degrade dead cells may also contribute to tissue imbalance. Therefore, abnormal apoptosis can contribute to several types of diseases ranging from autoimmunity to cancer (Fadeel, and Orrenius, 2005).

Phosphatidylserine (PS), which is found on the cell membrane consists of fatty acid, glycerol and amino acid. PS plays a role in signalling and engulfing of target cells by macrophages (Verhoven *et al.*, 1995). It is found on mature macrophages, and monocytes (Verhoven *et al.*, 1995; Appelt *et al.*, 2005). PS is found in the inner leaflet of cellular membranes of eukaryotic cells; it plays an important role in many biological and immunological processes. In the case of apoptosis, PS is translocated from the inner leaflet into the outer leaflet of plasma membranes (Schroit and and Zwaal., 1991).

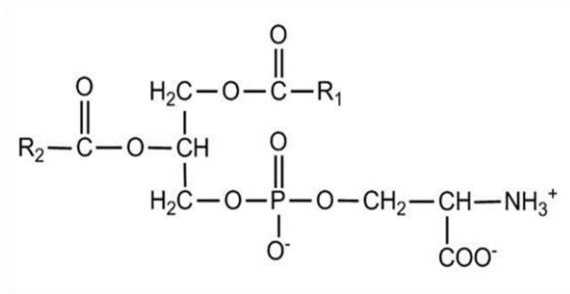


**Figure 1.9: Chemical structure of the PS**

PS is an acidic phospholipid has three ionizable groups. The generation of ROS occurs during apoptosis, which together with the cytochrome c cussing oxidation of the fatty acids in the PS before this lipid is externalized. Adapted from (the lipidweb, 2019).

In apoptosis the normal structure of cell membranes will change permanently to control and eliminate the damaged cells; senescent and activated cells will act as an 'eat me' signal to activate phagocytic cells to recognise the apoptotic cells. Subsequently, recognition of PS activates phagocytic cells to produce IL-10 and TGF- $\beta$  cytokines. (Kerr *et al.*, 1972). However, both live and dead *L. mexicana* parasites express high levels of PS on their surface (van Zandbergen *et al.*, 2006; Séguin, and Descoteaux, 2016). Therefore, PS may activate phagocytic cells to engulf these parasites via apoptotic receptors which prevents activation of immune response and releasing of proinflammatory cytokines against this pathogen (van Zandbergen *et al.*, 2006).

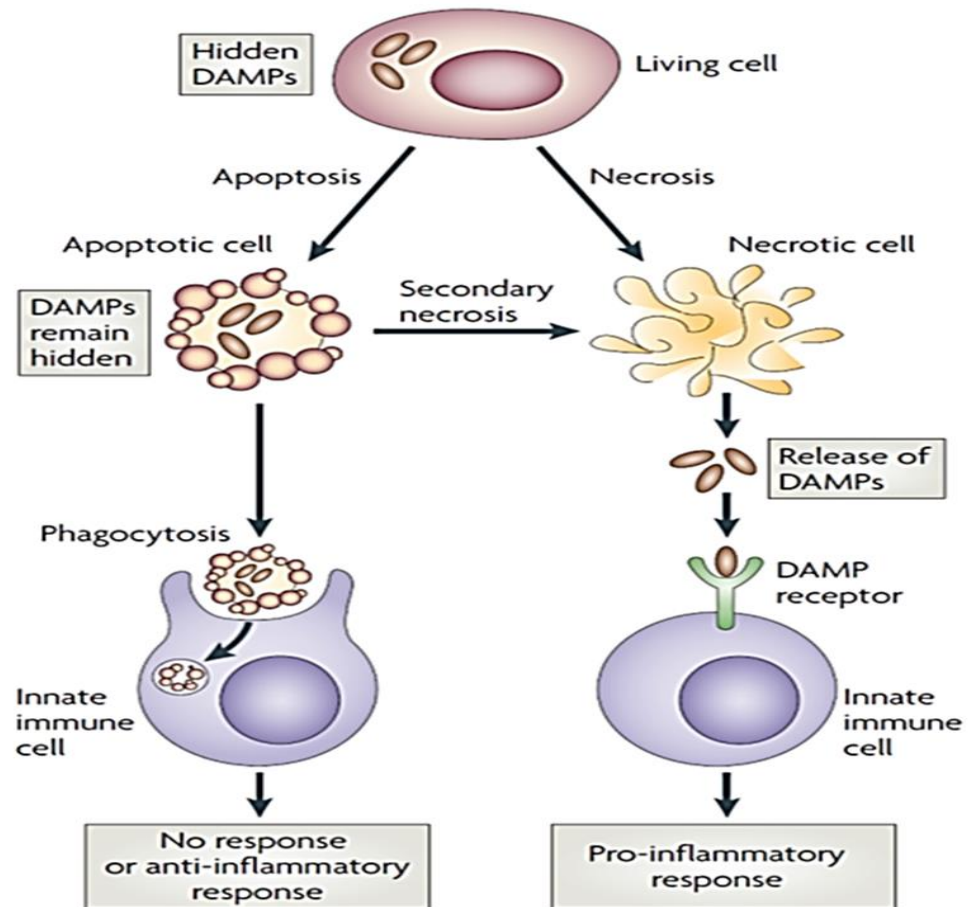


**Figure 1.10: Immune response necrosis and apoptosis**

Damage associated molecular patterns (DAMPs) are intracellular molecules which are normally hidden in the interior of cells and that are only detected after necrosis. Innate immune cells have receptors that can detect certain intracellular DAMPs. In necrosis, cells always lose the membrane integrity and release their intracellular contents including DAMPs, whereas in apoptosis, cells initially maintain membrane integrity including DAMPs. When the apoptotic cells are engulfed by phagocytes, the apoptotic cells do not release their intracellular DAMPs which will not stimulate the immune system. However, if the apoptotic cells are not rapidly engulfed, they will undergo secondary necrosis which causes releasing of DAMPs and then stimulation of the innate immune system. In the case of necrosis, DAMPs will be recognised by innate immune cells which will stimulate the immune system. Adapted from ( Kono, and Rock, 2008).

Understanding the signalling pathways of Balb/c and C57 BMDM infected with P1 and P20 that govern the execution of apoptosis and comparing between different pathways in these two strains in addition to the role of P20 in apoptosis, may thus yield novel targets for therapeutic intervention in a wide range of mammalian diseases.

## 1.14 Proinflammatory cytokines

Cytokines play a major role in the regulation of host immune responses to infection and inflammation. TNF, IL-1, and IL-6, IL-8, and IL-12 are defined as proinflammatory

cytokines which are produced mainly by macrophages and monocytes (Beutler, 1999). In this regard, cytokines play a vital role in health and disease. Proinflammatory cytokines (IL-1  $\beta$ , IL-6 and TGF- $\beta$ ) can regulate endothelial cell adhesion molecule levels, and leucocytes trafficking to inflammation sites, causing tissue damage (Mul *et al.*, 2000; Gomes *et al.*, 2014).

### **1.14.1 Interleukin 1 (IL-1)**

The family of interleukin 1 is mainly produced by macrophages and monocytes after activation. These cytokines are pleiotropic and are involved in the inflammatory process, immune responses and trigger apoptosis (NCBI RefSeq, 2008). There are 11 members that belong to the IL-1 cytokine family such as IL-1 $\alpha$ , IL-1  $\beta$  and IL-1Ra. IL-1  $\beta$  is one of the strongest pro-inflammatory cytokines in this family.

The secretion of IL-1 $\beta$  in a response to PAMPs is influenced by type and strength of pathogen stimulator (Le Feuvre *et al.*, 2002; Lopez-Castejon and Brough, 2011), as shown in a recent study which confirmed that amastigotes but not promastigotes of *L. braziliensis* can induce IL-1 $\beta$  cytokines (Gomes *et al.*, 2014). IL-1 $\beta$  is the main player in determining the severity of diffuse cutaneous Leishmaniasis along with a positive relationship between levels of this cytokine and severity of Leishmaniasis (Fernández-Figureueroa *et al.*, 2012). It is also pointed out that Gomes *et al.*, (2014) confirmed that only amastigote of *L. braziliensis* can induce the release of IL-1 $\beta$ .

IL-1 $\beta$  and TNF are produced in an early innate immune response to PAMPs. Although the main sources of IL-1 $\beta$  are macrophages and monocytes, it is also produced by epithelial cells, dendritic cells, NK cells, B cells, and fibroblasts (Ben-Sasson *et al.*, 2009; Lopez-Castejon and Brough, 2011). IL-1 $\beta$  stimulates the liver to produce acute phase proteins that induce the central nervous system to secrete prostaglandins and induce fever. IL-1 $\beta$  stimulates mast cells to produce histamine which acts as a vasodilator and granulocyte chemoattractant during inflammation (Ben-Sasson *et al.*, 2009).

### **1.14.2 Interleukin 6 (IL-6)**

The main producers of this cytokine *in vivo* are antigen presenting cells such as monocytes, macrophages, in addition to other cells including fibroblasts, T-cells and B-cells. Stimulation of IL-6 secretion can be triggered by IL-1, TNF- $\alpha$ , TNF- $\beta$ , and infection with pathogens. Stimulation of human monocytes with bacterial lipopolysaccharides can activate them and increase IL-6 production. However, inhibition or blocking of IL-6 leads to a delay or prevention of maturation of plasma and B-cells which will increase progressive cases (Scheller *et al.*, 2011; NCBI RefSeq, 2017). Antigen presenting cells secrete either IL-6 or

IL-12, in response to a particular pathogen, which are the main factors that determine the type of immune response (activate type of CD4<sup>+</sup> T cells). In the case of secretion of IL-6, this will activate Th2, and may activate the release of IL-4, which also in turn activates Th2 as well (Rincón *et al.*, 1997). In contrast, in mucosal but not cutaneous Leishmaniasis, Castellucci *et al.*, (2006) demonstrated that IL-6 could play a role in the regulation of type 1 inflammatory responses. IL-6 plays two roles, it promotes Th2 and inhibits Th1. It inhibits Th1 either by activation of naive CD4<sup>+</sup> T cells to produce IL-4 which helps in differentiation of T cell into Th2 or by interfering with IFN- $\gamma$  signalling (Diehl and Rincón, 2002). Another study has also reported that low levels of IL-6 were shown to enhance human macrophage activity against the *Leishmania* parasite (Hatzigeorgiou, He *et al.*, 1993).

### **1.14.3 Tumour necrosis factor- $\alpha$ (TNF- $\alpha$ )**

The TNF- $\alpha$  family is produced in the early stages of immune response by macrophages and is also produced by epithelial cells, dendritic cells, NK cells, B cells and fibroblasts (Ben-Sasson *et al.*, 2009). TNF plays a role in regulation of wide biological processes such as differentiation, proliferation and apoptosis (NCBI RefSeq, 2016) and plays a significant role against cutaneous Leishmaniasis. Liew *et al.*, (1990b) infected mice with *L. major* and injected them with anti TNF which caused exacerbation of the lesions, whereas mice injected with TNF in the lesion had a reduction in lesion size. In this regard Zwingenberge *et al.*, (1991) compared serum cytokine levels of infected and control patients with *L. donovani* in Brazil. The results showed that the TNF- $\alpha$  level in patients was increased ten-fold than controls. The secretion of TNF, IL-1 and IL-6 by leucocytes in early infection by parasites is a result of the combination of cytokines which regulate acute inflammation and fever (Titus *et al.*, 1991). The early release of TNF by macrophages in response to infection with promastigotes is more than that in response to that with amastigotes either *in vivo* or *in vitro* (Duque *et al.*, 2014). This was associated with the expression of GP63 which is abundant on the promastigote surface and can degrade membrane proteins in phagosomes called synaptotagmin. Degradation of synaptotagmin leads to the release of IL-6 and TNF (Duque *et al.*, 2014).

### **1.14.4 Transforming growth factor beta (TGF- $\beta$ )**

TGF- $\beta$  is a protein superfamily consisting of three members TGF- $\beta$ 1, TGF- $\beta$ 2 and TGF- $\beta$ -3. TGF- $\beta$  is a protein that regulates cell functions such as growth, proliferation, differentiation and activates other cytokines such as TNF- $\alpha$  and IFN- $\gamma$  (NCBI RefSeq, 2016). In *Leishmania* infection TGF- $\beta$  is produced in response to infection with amastigotes (Gomes *et al.*, 2014) and increases susceptibility to Leishmaniasis by inhibiting activation

of macrophages and decreasing IFN- $\gamma$ . Barral *et al.*, (1995) compared human macrophages infected with *L. braziliensis* in *in vitro* culture medium containing TGF- $\beta$ , the results showed that the number parasites in the TGF- $\beta$  treated flask was 50% higher than controls, suggesting TGF- $\beta$  had reduced macrophage activity. Moreover, TGF- $\beta$  is capable of changing the immune response toward Th2 by upregulation of IL-10 either *in vivo* or *in vitro* (Barral *et al.*, 1993). TGF- $\beta$  activates Th17 which is associated with chronic inflammation and damaged tissues (Belkaid and Tarbell, 2009). The regulation of TGF- $\beta$  is associated with two factors, the parasite burden and the host; it is higher in mucosal Leishmaniasis than cutaneous Leishmaniasis Bacellar *et al.*, (2002), and there is a wide range of variation in TGF- $\beta$  levels among different individual infected with *Leishmania* (Gomes *et al.*, 2014). The secretion of TNF, IL-1 and IL-6 by leucocytes in response to early infection with *Leishmania* parasite regulates the acute inflammation and fever (Titus *et al.*, 1991) and the activation of Th17 which is associated with chronic inflammation and tissue damage (Acosta-Rodriguez *et al.*, 2007). However, there is a big individual variation in the levels of IL-6 and TGF- $\beta$  cytokines between samples in response to Leishmaniasis (Gomes *et al.*, 2014).

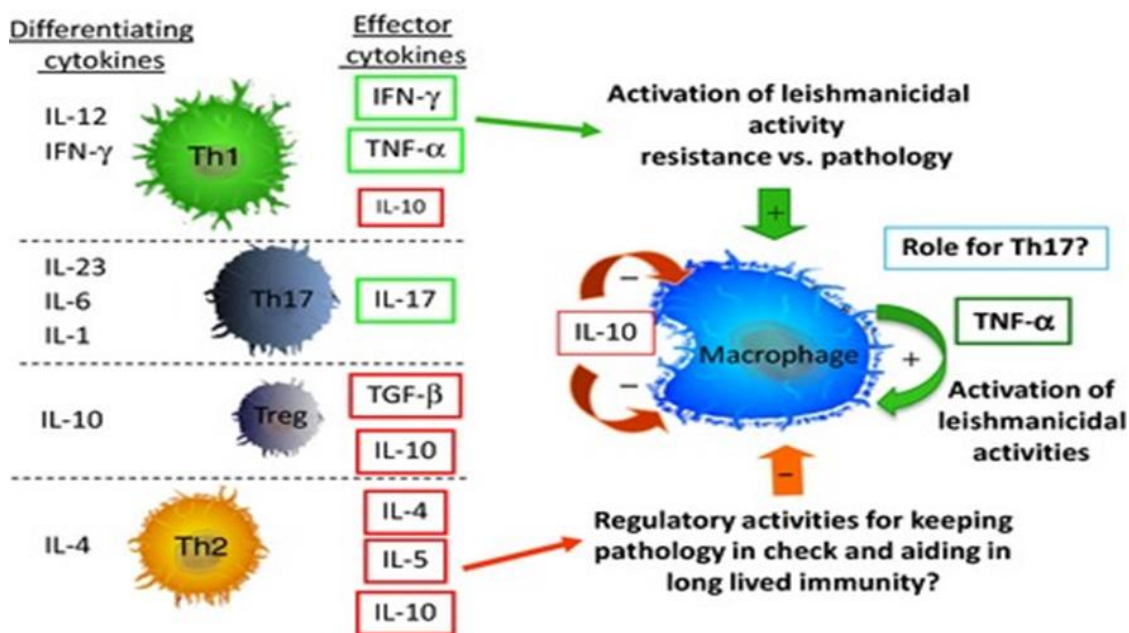


**Figure 1.11: Role of proinflammatory cytokines in *Leishmaniasis***

Cytokines play a central role in activation or suppression of host monocytes and macrophages in response to *Leishmania* infection and subsequent immunopathology of this disease. Effective cellular response against *Leishmania*, depend on CD4<sup>+</sup> T cell subset formation. CD4<sup>+</sup> T cell subsets are able to activate leishmanicidal responses by host monocytes and macrophages.

The cytokine microenvironment is the main factor that cause initial activation of naïve CD4<sup>+</sup> T cell differentiation of CD4<sup>+</sup> T cell subsets (Th1, Th2, Th3, Treg and Th17).

Adapted from (Gollob and Dutra. 2014).

## 1.15 Balb/c and C57 mice

Two inbred mouse strains have been widely used in research to study the biology of the host's response to *Leishmania* infection. C57BL/6J mice (C57) is an inbred strain of 20 generations by inbreeding between offspring and parents or brothers and sisters, therefore the individuals have 98.6% homozygous similarity. This strain is characterised with a black colour coat and are most popular sub-strains mice for cancer and immune research (Beck *et al.*, 2000). The *Leishmania* resistant C57 mice display a localized, small and self-healing infection lesion combined with Th1 cytokines such as IL-4 IL-10, TNF- $\alpha$  and IFN- $\gamma$  production. Activation of Th1 is capable of activating macrophages to generate and release microbicidal factors leading to resistance and recovery from infection (Sher *et al.*, 2003; Soong, 2012). On the other hand, *Leishmania* susceptible Balb/c mice strain is an albino strain of house mouse, it is widely used in immune research around the world, inbred for 200 generations (Informatics.jax.org, 2019). Balb/c mice have a different response to *Leishmania* infection characterised with a production of Th2 cytokines (IL-4, IL-10, and IL-13). This difference in the genetic background as a basis of susceptibility or resistance was instrumental in the development of the Th1/Th2 paradigm (Reiner, and Locksley., 1995; Gollob *et al.*, 2014).

Developing safe, effective, and affordable vaccines for the prevention of this disease become an urgent need. Therefore, it becomes important to understand the immunological and pathophysiological mechanisms to help researchers develop vaccines or treatments. Many studies have focussed on mouse models that are susceptible and resistant to *Leishmania* infection, in order to broaden understanding of the immune responses such as mediators of protection, primarily a Th1 and Th2 -biased response, but to best of my knowledge there is no study comparing between P1 and P20 parasites and Balb/c and C57 BMDM.

To understand fully the infectivity and survival of the *Leishmania* parasite it is necessary to study the interaction between the host mammalian cells and the parasite. Therefore, using BMDM from resistant and susceptible model animals and virulent and avirulent parasites may lead to a more complete understanding of the underlying mechanisms of the disease.

## 1.16 Aims and hypothesis

A literature review reported that the *L.mexicana* parasites lost virulence after 20 passages. On the other hand, there are two strains of mice, Balb/c which is susceptible and C57BL which is naturally resistant to Leishmaniasis. However, macrophages are the ultimate final host for *Leishmania* parasites where parasite can survive and multiply. Accordingly, Leishmaniasis is the outcome of a successful invasion of macrophages by *Leishmania* parasites. Therefore, knowing how the *Leishmania* parasite survives and multiplies inside macrophages would help in designing the right treatment or vaccines. Establishing an *in vitro* model system using macrophage cells isolated from Balb/c and C57 mice and infected with virulent and avirulent *Leishmania* parasites could be helpful for understanding the survival strategy of parasites inside macrophages.

### Aims

- 1 - To generate an avirulent *Leishmania* parasite by prolonging *in vitro* culture for 20 passages to study parasite growth, virulence rate and parasite characteristics.
- 2 - Studying infectivity of virulent (P1) and avirulent (P20) *Leishmania* parasites in susceptible Balb/c and resistant C57 mice bone marrow derived macrophages. This will involve survival of virulent and avirulent *L.mexicana* in susceptible Balb/c and resistant C57 mice, macrophages cell interaction and gene regulation of apoptosis and proinflammatory cytokines.
- 3 - To investigate the effect of molecules produced by animal host cells during interaction with *L.mexicana* parasites on the parasite growth and virulence gene regulation P1 and P20 promastigotes.

# **Materials and Methods**

## 2.1 Materials

**Table 2. 1: List of equipment used in this study**

Number	Equipment name	Manufacturer	Catalogue Number
1	-20 freezer	Les	2C0000062
2	4°C fridge	Les	2C0000062
3	-20°C freezer	Denely	9811271100
4	4°C fridge	Denely	9811271100
5	-80°C freezer	Sanyo	0870722
6	Micro centaur centrifuge	Sanyo	SG94/02/284
7	Nano drop 800R spectrophotometer	Lab tech	0388
8	Autoclave	Rodwell	
9	Bench-top vortex mixer	Scientific industries	
10	Block heater	Stuart	SBH130D
11	CK2 Microscope	Olympus	110605
12	Hotplate with stirrer, aluminium plate analogue	Geneflow	SB162
13	Class II microbiological safety cabinet	Envair	C14299
14	Class II microbiological safety cabinet	Walker	C1496
15	O <sub>2</sub> /CO <sub>2</sub> incubator 37°C	Sanyo	
16	Cooled incubator 25°C	LMS	9140/06LR
17	Real time PCR machine	Rcorbett	R070571
18	Surgical Forceps		
19	Surgical Scissors		
20	Disposable sterile scalpel	Swann Morton	
21	Pellet pestle	Sigma	Z359971
22	Nikon eclipse TS100 microscope	Nikon	
23	Nikon digital net camera DN100	Nikon	
24	Microscope	Olympus	
25	CMEX 5 camera	Euromex	DC. 5000C
26	Heraeus Megafuge 8 centrifuge	Thermo Scientific	75007210
27	Flow cytometer	Beckman Coulter	AN31109
28	Fluorescent microscope EVOS	Thermo Fisher Scientific	AMF4300
29	Automatic counter	BIORAD	TC20
30	pH meter	thermos Scientific	OR10N STAR
31	Clario star plate reader	BMG LABTECH	

**Table 2. 2: List of consumables used in this study**

Number	Name of product	Manufacturer	Catalogue Number
1	10 mL syringes	Becton Dickinson	
2	Needles (25 G <sup>5/8</sup> ) x 1"	Becton Dickenson	SKU: ND400
3	Sterile Petri dishes	Sarstedt	
4	Pipettes 5 mL	Sarstedt	
5	Pipettes tips 1000 µL blue	Sarstedt	
6	Pipettes tips 200 µL yellow	Sarstedt	
7	15 mL centrifuge tubes	Sarstedt	
8	20 mL centrifuge tubes	Sarstedt	
9	50 mL centrifuge tubes	Sarstedt	
10	Tissue culture flasks T75 vented (red cap)	Sarstedt	83.1813.00
11	Tissue culture flasks T25 vented (red cap)	Sarstedt	83.3910.002
12	Tissue culture flasks T25 unvented (green cap)	Sarstedt	83.3910.500
13	Neubauer haemocytometer	Nano EnTek	4359B233
14	Pasteur pipettes	SLS	
15	6 well tissue culture plates	Sarstedt	
16	96 well tissue culture plates	Sarstedt	83.3924
17	24 well tissue culture plates	Sarstedt	83.1836
18	Pipette tips biosphere 10 µL (white rack) with filter	Sarstedt	70.116.210
19	Pipette tips biosphere 20 µL (yellow rack) with filter	Sarstedt	70.760.122
20	2 mL micro tubes	Sarstedt	72.695.500
21	1.5 mL micro tubes	Sarstedt	12.690
22	0.5 mL micro tubes	Sarstedt	72.699
23	CryoPure Tube	Sarstedt	72.377
24	Cell scraper (Small)	Fisher	08-100-241
25	Strip Tubes and Caps 0.1 mL	Qiagen	981103
26	0.25 µm minisart syringe filter	Sartorius	16534

**Table 2. 3: List of reagents, chemicals and kits used in this study**

Number	Reagent/chemical	Manufacturer	Catalogue Number
1	Foetal bovine serum heat inactivated	Gibco	10500-064
2	Dimethyl Sulphoxide (DMSO)	Sigma	D2650
3	Ethanol absolute	Sigma	E7023
4	Phosphate- buffered saline(PBS)	Lonza	BE17-512F
5	Paraformaldehyde (PFA)	Sigma	158127
6	RPMI1640 media with L-glutamine	Lonza	BE12-702F/U1
7	Foetal bovine serum	Gibco	10270-106
8	Penicillin-streptomycin	LONZA	DE17-603E
9	Tetro cDNA synthesis kit	Bioline	BIO-65043
10	RNase-Free DNase set	QIAGEN	792554
11	Glacial acetic acid	Sigma	
12	RNeasy mini kit	Qiagen	74104
13	Beta mercaptoethanol	Sigma	M3148
14	Giemsa stain modified solution	Sigma	BCBQ8217V
15	Ethanol anhydrous	Sigma	676829
16	Schneider's <i>Drosophila</i> medium	Lonza	04-351Q
17	SsoAdvanced™ universal SYBR® Green Supermix	Biorad	172-5271
18	Nuclease-Free Water	Qiagen	129115
19	Albumin from bovine serum	Sigma	A2153
20	1 M Hepes	Lonza	17-737F
22	RAT ANTI MOUSE F4/80	AbD Serotec	MCA497GA
23	Goat F(ab') <sup>2</sup> ANTI RAT IgG: FITC (MOUSE ADSORBED)	AbD Serotec	STAR69
24	Mouse anti <i>Leishmanial</i> LPG (CA7AE)	Biorad	OBT2002
25	Alexa fluor 488 goat anti-mouse IgG (H+L)	Thermo Fisher Scientific	A32723
26	Alexa fluor 647 Annexin V	BioLegend	640911
27	propidium iodide	Sigma	P4170-10mg
28	Trypan Blue Dye,0.4%	BIORAD	145-0013
29	Trypan Blue Solution	Sigma	TB154
30	Mouse IL-6 ELISA development kit	MABTECH	3361-1H-6
31	Mouse TNF- $\alpha$ ELISA development kit	MABTECH	3511-1H-6
32	Glycerol for molecular biology	Sigma	G5516

**Table 2. 4: List of mice primers used in this study**

<b>Primer</b>	<b>Sequence</b>	<b>Annealing temperature</b>
IL-6 forward primer	TGG AGT CAC AGA AGG AGT GGC TAA G	63.8°C
IL-6 reverse primer	TCT GAC CAC AGT GAG GAA TGT CCA C	63.8°C
IL-1 $\beta$ forward prime	GCC TTG GGC CTC AAA GGA AAG AAT C	63.8°C
IL-1 $\beta$ reverse primer	GGA AGA CAC AGA TTC CAT GGT GAA G	63.8°C
TNF- $\alpha$ forward primer	ATA GCT CCC AGA AAA GCA AGC	63.8°C
TNF- $\alpha$ reverse primer	CAC CCC GAA GTT CAG TAG ACA	63.8°C
TGF- $\beta$ forward primer	CTC CCA CTC CCG TGG CTT TGA	63.8°C
GAPDH forward primer	GTT CCA CAT GTT GCT CCA CAC TTG	63.8°C
TGF- $\beta$ reverse prime	TTC ACC ACC ATG GAG AAG GC	63.8°C
GAPDH reverse primer	GGC ATG GAC TGT GGT CAT GA	63.8°C
b-actin forward primer	TCA CCC ACA CTG TGC CCA TCT ACG A	63.8°C
b-actin reverse primer	GGA TGC CAC AGG ATT CCA TAC CCA	63.8°C
Bax forward primer	CTG AGC TGA CCT TGG AGC	60°C
Bax reverse primer	GAC TCC AGC CAC AAA GAT G	60°C
BCL 2 forward primer	GAC AGA AGA TCA TGC CGT CC	60°C
BCL 2 reverse primer	GGT ACC AAT GGC ACT TCA AG	60°C
IL-1 $\alpha$ forward primer	CAC CTT ACA CCT ACC AGA GTG ATT TG	64 °C
IL-1 $\alpha$ reverse primer	TGT TGC AGG TCA TTT AAC CAA GT	64°C
PD1 forward primer	CCA GCA ACC AGA CTG AAA AAC	64°C
PD1 reverse primer	TCT CCT CGA TTT TTG CCT TG	64°C
CASP1 forward primer	GAG ATG GTG AAA GAG GTG AA	60°C
CASP1 reverse primer	GTG TTG AAG AGC AGA AAG CA	60°C
CASP8 forward primer	TGC CCT CAA GTT CCT GTG CTT GGA	60°C
CASP8 reverse primer	GGA TGC TAA GAA TGT CAT CTC C	60°C
CASP9 forward primer	GCC ATG GAC GAA GCG GAT CGG CGG	64°C
CASP9 reverse primer	GGC CTG GAT GAA GAA GAG CTT GGG	64°C

**Table 2. 5: List of *L.mexicana* primers used in this study**

<b>Primer</b>	<b>Sequence</b>	<b>Annealing temperature</b>
GP63 forward primer	ACA TCC TCA CCG ACG AGA AG	60°C
GP63 reverse primer	ACC TTG AAG TCG CCA CAG AT	60°C
LPG1 forward prime	CCA GAA TCT CTT TAT CAT TCA CC3	60°C
LPG1 reverse prime	GTA GTC GTG ATC TTC GCC GTA	60°C
LPG2 forward primer	CAT TTG GTA TCC TGG	60°C
LPG2 reverse prime	GAG GAA GCC ACT GTT	60°C
GAPDH forward primer	CCA TCT GTG ACC AGG GTC TT	60°C, 58°C, 68.8°C
GAPDH reverse primer	TGC TGC TTC ATC ATC TGG TAT GC	60°C, 58°C, 68.8°C
MPK9 forward primer	GTT GGA TCC ATG GAG CGC TAC ACG GTG ATG	68.8°C
MPK9 reverse primer	ATG AAG CTT CCC GGG TCA GAA GTT GAA CTC	68.8°C
A2 forward primer	ACT GCG GGT CAA CAG AGAG	58°C
A2 reverse primer	ATG AAG ACA CTC AGC TTG CG	58°C
CBP2 forward primer	ACGTGTTGATCGGAAGCAG	60°C
CBP2 reverse primer	CAG CGT GGT TCA CCT CTT TA	60°C
CPB2.8 forward primer	CGT GCC TGC TCA GTG AAT AC	60°C
CPB2.8 reverse primer	GAT CAC CTG CTC CAC CAT C	60°C
LACK forward primer	GGT CGT ACA TCA AGG TGG TG	60°C
LACK reverse primer	GAC CGT AGT CGC TGT CCA C	60 °C
CHT1 forward primer	TCA GGA CTC GTT CCA CTA CG	58°C
CHT1 reverse primer	ACC TCG GCA CTG AAG AAG AT	58°C
CPC forward primer	GTG ACA ACG TCG AGA TGG AG	58°C, 60°C
CPC reverse primer	TAC ACC TGC ATG GCT ACC TC	58°C, 60°C

**Table 2. 6: media and buffers used in this study**

Reagent	Recipe
Annexin V buffer	PBS plus 10mM HEPES (pH 7.4), 150mM NaCl, 5mM KCl, 5mM MgCl <sub>2</sub> , 1.8mM CaCl <sub>2</sub>
DC medium	RPMI1640 with glutamine, 5% v/v FCS, 10 mM hepes, 20µM β Mercaptoethanol, 50 U/ml Penicillin/Streptomycin ,5 ng/mL GMCSF
RPMI 1640 10% HIFCS medium	RPMI1640 with glutamine, 10% v/v HIFCS
RPMI1640 10% HIFCS medium 5.5 pH	R HCL A PMI 1640 with glutamine, 10% v/v HIFCS, HCL A until pH become 5.5
Schneider's <i>Drosophila</i> 10% HIFCS medium	Schneider's <i>Drosophila</i> with glutamine 10% v/v HIFCS
Schneider's <i>Drosophila</i> 10% HIFCS medium 5.5 pH	Schneider's <i>Drosophila</i> with glutamine 10% v/v HIFCS, HCL A until pH become 5.5
Flow cytometry Fluid	1 x PBS containing 0.1% w/v BSA plus 0.1% NaN <sub>3</sub>
White blood cell count fluid	Glacial acetic acid 2% s/v, Gentian Violet 1% w/v in Distilled water
PBS-Tween20 (PBS-T)	1 litre 1 X PBS, 5 ml Tween 20
Antibody Buffer	3% BSA, 0.02% Sodium Azide in PBS
Blocking Buffer	100 µL tween 20 + 5% BSA + 100 mL PBS

## 2.2 Introduction

Three methods were examined to achieve the aim of this study including; (i) P1 and P20 characterisation, (ii) interaction between virulent P1 and avirulent P20 *L. mexicana* and two types of mammalian cells, susceptible Balb/c and resistant C57 mice bone marrow derived macrophages (BMDM), and (iii) effect of supernatants derived from these mammalian cells infected with P1 and P20 for 24 hours on *L. mexicana* P1 and P20. This chapter starts with explanation of the production methods of avirulent *L. mexicana*. A brief description of both P1 and P20 and effect of culture conditions on growth and differentiation into amastigotes was also introduced and highlighted. It should be mentioned that the main approach used in the methodology consists of three stages. In the first stage, P1 and P20 parasites are compared in parasite culture conditions and infection conditions which included type of medium (Schneider *drosophila* and RPMI1640), presence and absence of oxygen, and temperature (25°C and 37°C) to understand the difference between them without the presence of mammalian cells before investigating the ability of P1 and P20 to survive and multiply in the infected cell. Infectivity of P1 and P20 are compared by infection of *Leishmania* susceptible Balb/c and resistant C57 BMDM *in vitro* is described in stage-2. Stage-3 investigates whether infected mammalian cells produce molecules that may affect P1 and P20 growth and virulence by using supernatant produced from stage-2 for preparation of conditioned medium.

## 2.3 Virulent and Avirulent *L. mexicana*

### 2.3.1 Virulent *L. mexicana* (P1)

*L. mexicana* parasite MNYC/BZ/62/M379 strain, was obtained from Dr V. Yardley, London School of Hygiene and Tropical Medicine and kept in liquid nitrogen. The parasite was maintained by subcutaneous inoculation of Balb/c mice. Parasite was harvested from Balb/c mice lesions and cultured *in vitro* in Schneider's *Drosophila* medium. Parasites at P1 of *in vitro* culture were highly virulent as was showed by Ali *et al.*, (2013).

### 2.3.2 Avirulent *L. mexicana* (P20)

*L. mexicana* passage twenty (P20) was produced by sub culturing of *L. mexicana* passage one (P1) twenty times *in vitro* (Ali *et al.*, 2013). Briefly,  $5 \times 10^5$  P1 *L. mexicana* was cultured in unvented T25 tissue culture flasks (Sarstedt, UK) containing 5 mL Schneider's *Drosophila* media (Lonza, UK) supplemented with 10% v/v heat inactivated foetal calf serum (HIFCS) (Gibco, UK) at 25°C (Jaffe *et al.*, 1984). Sub-culturing was repeated when the parasites was at decline phase (Approximately after 7 days) by discarding all medium containing parasites and keeping remaining parasites in the flask's base and walls, and 5 mL

new fresh Schneider's *Drosophila* medium 10% v/v HIFC was added. Subculturing of parasite was continued approximately every 7 days for 20 times.

## 2.4 Storing of *L. mexicana* parasites

P1 and P20 cultures in Schneider's *Drosophila* medium supplemented with 10% HIFCS v/v at 25°C in unvented T25 flask at stationary phase, parasites were harvested and washed 3 times with PBS. They were resuspended in storage media (10% v/v glycerol, 20% HIFCS and 70% RPMI1640 medium). Approximately 20 x10<sup>6</sup> P1 and P20 per mL were transferred into cryotubes and kept under -80°C before being transferred into liquid nitrogen containers for further usage during this study.

## 2.5 Preparation of P1 and P20 *L. mexicana* for infection

Promastigotes at the stationary phase were obtained by culturing the parasites from liquid nitrogen in Schneider's *Drosophila* medium supplemented with 10% HIFCS at 25°C in unvented T25 tissue culture flasks until they reach the concentration of  $\geq 20 \times 10^6$  per mL which usually happened at days 3 to 5 (see figure 3.1) (Ali *et al.*, 2013). Before infection, parasites were washed by RPMI1640 and centrifuging at 2000g for 10 minutes and re-suspended in RPMI1640 medium with 10% HIFCS v/v and counted by haemocytometer.

## 2.6 Workflow of characterisation of P1 and P20 *L. mexicana*

Figure 2.1 summarises the flow work of P1 and P20 characterisation. Therefore, P1 and P20 characterisation was investigated without the presence of mammalian cells *in vitro*.

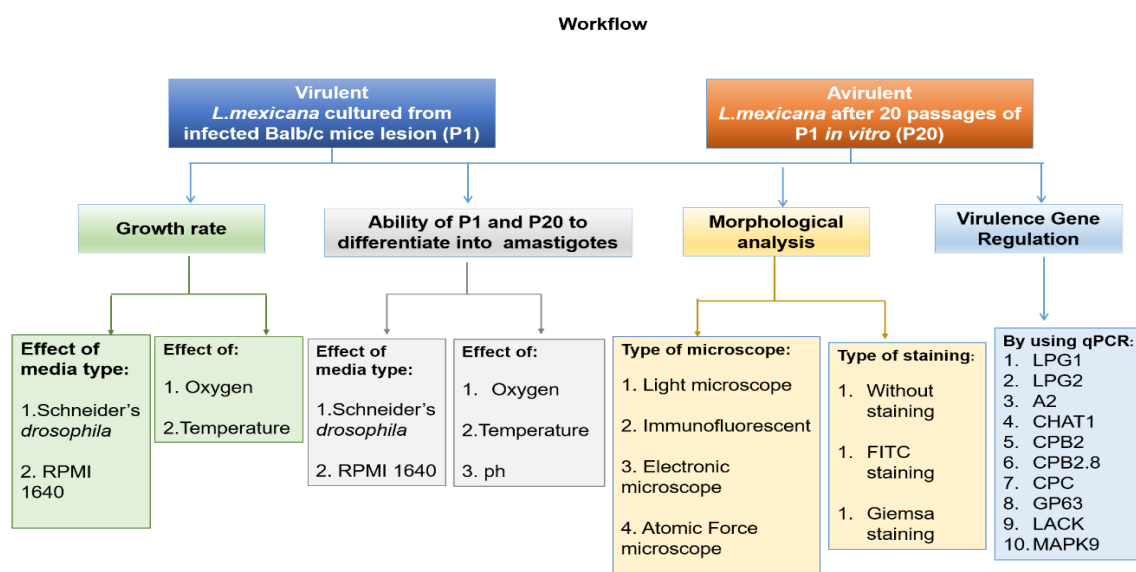


**Figure 2. 1: Workflow of P1 and P20 characterisation (Stage-1)**

Differences between P1 and P20 have investigated which include the effect of the media (Schneider *drosophila* and RPMI1640), the temperature and oxygen levels on the growth rate. The morphology of P1 and P20 was studied in a stationary phase of parasite growth using three different configurations (without staining, FITC staining and Giemsa staining). In these experiments, various types of microscope were used including light, immunofluorescent, electronic and atomic force microscope.

A series of experiments were conducted to study the ability of P1 and P20 to differentiate into amastigotes considering the effect of Schneider *drosophila* and RPMI1640 media, the temperature, oxygen and pH. Ten virulence genes were examined in P20 compared with P1 promastigotes at stationary phase using qPCR. The details of the above workflow are described in the following subsections.

### **2.6.1 Growth and morphology characteristics of P1 and P20 *L. mexicana***

The growth curve of virulent (P1) and avirulent passage (P20) *L. mexicana* were compared under different conditions including effect of type of medium, oxygen concentration, incubation temperature and infection conditions in the absence of mammalian cells. P1 and P20 were cultured at a concentration of  $1 \times 10^5$  per mL in two types of media, Schneider's *Drosophila* which is the standard parasite medium and RPMI1640 medium which is used for infection of mammalian cells. Both media were supplemented with 10% HIFCS. In order to investigate the effect of oxygen, parasites were cultured in the presence (aerobically) and absence of oxygen (anaerobically) by using vented and unvented T25 tissue culture flasks (Sarstedt UK) respectively. All flasks were incubated at two different temperatures, 25°C and 37°C. The number of P1 and P20 parasites were counted every two days by adding 10 µL of parasite culture to 90 µL of 1% w/v paraformaldehyde (Sigma, UK) using a Neubauer haemocytometer (Nano EnTek UK).

### **2.6.2 Morphology of P1 and P20 *L. mexicana* Promastigotes**

Parasite cultures of P1 and P20 at the stationary phase were analysed by four staining methods; by Giemsa stain and light microscope, staining with FITC and analysed by EVOS (life technology UK), Atomic force microscope analysis and Electron microscope examination.

### **2.6.3 Slide preparation for Giemsa staining, Atomic Force Microscope and Electronic Microscope**

*L. mexicana* promastigotes were cultured in Schneider's *Drosophila* in unvented flask until they reached stationary phase.  $20 \times 10^6$  of P1 and P20 promastigotes were collected and centrifuged at 800 g for 10 minutes. Smears were prepared, dried at room temperature and fixed with 100% methanol.

### **2.6.4 Giemsa Stain**

The prepared slides were stained with 5% w/v modified Giemsa stain (sigma UK) for 15-20 minutes, washed with distilled water and left to air dry at room temperature; slides were mounted by dpx and visualised by light microscope (Olympus UK) connected with camera (CMEX 5 Holland) using 100 x power and oil immersion.

### **2.6.5 Atomic Force Microscope and Electron Microscope**

Some of the dried smear slides without staining were also examined by Atomic Force Microscope (AFM). To examine slides by an electron microscope, slides were fixed to the stage by carbon sticky pad and covered by 10  $\mu\text{m}$  gold using Quorum (Q15OR ES) with 19.32g/m<sup>3</sup>.

### **2.6.6 Labelling of P1 and P20 *L. mexicana* promastigotes by CFSE**

Carboxyfluorescein succinimidyl ester (CFSE) stain at concentrations 10, 20, 50 and 100 ng/ml were tested, with the optimum results achieved at 100 ng/ml in RPMI1640 media containing  $20 \times 10^6$  P1 and P20 promastigotes for 30 minutes at 25°C. The optimal concentration of the selected stain was non-toxic as determined by motility test.

P1 and P20 promastigotes at stationary phase were stained with CFSE at a concentration of 100 ng/ml and incubated for 30 minutes at 25°C. The parasites were washed 3 times with PBS to remove the extra stain and resuspended in 50  $\mu\text{L}$  4% paraformaldehyde. Wet smears were prepared and fixed with a coverslip, sealed with nail polish and examined by fluorescent EVOS life technology microscope UK (40X).

### **2.6.7 Body and flagella measurement of P1 and P20 *L.mexicana* promastigotes**

To estimate the body size and flagella length of P1 and P20 parasites, Parasite cultures at stationary phase were centrifuged at 800 g for 10 minutes and re-suspended in 50  $\mu\text{L}$  of 1% w/v paraformaldehyde. Wet smears were prepared from parasites pellet and sealed with a

coverslip using nail polish. Pictures were taken using EVOS microscope (Life technology UK) in transmission mode. Measurements of parasite sizes were taken using NI vision assistant software (UK). Measurements were converted from pixels into  $\mu\text{m}$  ( $1\mu\text{m} = 4.72$  pixels) according to the scale of the picture defined by EVOS microscope (Appendix 1 A and B).

### **2.6.8 Data analysis of P1 and P20 promastigote morphology**

The pictures collected for P1 and P20 promastigotes with or without CFSE stain were analysed using NI vision assistant software. The metacyclic stage of P1 and P20 was determined by two methods: first, by determining “flagellum/body ratio” which is defined by: If ratio is  $\geq 2$ , the promastigotes were considered at metacyclic stage (da Silva *et al.*, 2015). Second, the metacyclic stage of P1 and P20 can be considered at metacyclic stage if the product of {Body length ( $\mu\text{m}$ ) X body width ( $\mu\text{m}$ )} is  $\leq 12$ , (Zakai, 1998). The percentage of metacyclic promastigotes, for both methods, were then calculated from 300 parasites.

In addition, the initial calculation was also performed by dividing the average length of the flagellum by the average length of the body for 300 promastigotes. It was found that the results obtained by this initial calculation were in good agreement with the results obtained from the above two methods.

### **2.6.9 Effect of culture conditions on P1 and P20 *L.mexicana* differentiation into amastigotes**

Two types of media; Schneider's *Drosophila* and RPMI1640 supplemented with 10 HIFCS v/v. and two incubation temperatures  $25^{\circ}\text{C}$  and  $37^{\circ}\text{C}$  and aerobic and anaerobic conditions were assessed for their effect on differentiation from promastigotes to amastigotes.

For these studies 20 million P1 and P20 promastigotes at stationary phase were cultured in 2.5 mL RPMI1640 or Schneider's *Drosophila* media containing 10 v/v HIFCS, in vented and unvented flasks, and incubated at  $25^{\circ}\text{C}$  or  $37^{\circ}\text{C}$  and in 95% v/v humidity in 5% v/v  $\text{CO}_2$  incubator, all flasks were incubated for 2, 24, and 48 hours.

Parasites were spun down at 200 g for 10 minutes at room temperature and resuspended in 50  $\mu\text{L}$  1% w/v paraformaldehyde. Wet smears were prepared, and slides were fixed with coverslips using nail polish. Pictures were taken using EVOS (life technology) 40 X microscopic transmission light (Appendix 4). Rounded parasites without flagellum were counted as amastigotes, and parasites cylindrical elongated body with flagella counted as promastigotes (Pearson and Sousa, 1996). Amastigotes and promastigotes were counted per microscopic field and average percentages of amastigotes were calculated.

### **2.6.10 Effect of pH 5.5 medium on P1 and P20 *L.mexicana* differentiation into amastigotes**

This experiment has been designed in order to investigate the ability of P20 to differentiate into amastigotes in the ideal differentiation conditions. Effect of pH medium on the ability of P1 and P20 to differentiate to amastigotes described above (in section 2.6.9) was performed under a manufacturer defined pH of  $6.9 \pm 0.3$  for RPMI1640 and  $6.5 \pm 0.3$  for Schneider's *Drosophila* medium respectively (both pH values are after supplementation with 10% v/v HIFC respectively).

Bates, (1994) reported that at 5.5 pH, *Leishmania* parasites differentiate into amastigotes. Therefore, to verify this, another test (using similar conditions described in (section 2.6.9) was performed at 5.5 pH to study the ability of P1 and P20 to differentiate into amastigotes. The pH was adjusted to pH 5.5 by using a pH meter (Thermos Scientific) and Hydrochloric acid (Sigma, UK). All media was sterilised by filtrating using 0.25- $\mu$ m filters and used accordingly. The procedure of preparing the slides and taking pictures is described above (section 2.6.7).

### **2.6.11 Effect of RPMI1640 versus Schneider's *Drosophila* medium on P1 and P20 *L.mexicana* promastigotes growth rate using Alamar blue assay**

Due to the significant difference found in growth rate between P1 and P20 in RPMI1640 media (Results section 3.2), additional tests were conducted to study, the effect of RPMI 1640 versus Schneider's *Drosophila* medium on P1 and P20 growth rate, in more detail.

To confirm the effect of RPMI1640 medium on P1 and P20 growth,  $1 \times 10^6$  parasites were seeded in 96 well plate in 100  $\mu$ L per well using RPMI1640 or Schneider's *Drosophila* with 10% HIFCS. Plates were sealed with cling film and incubated at 25°C for 48 hours and 3 days. The concentration of promastigotes was estimated by Alamar blue assay. 10  $\mu$ L Alamar blue (Biorad UK) was added in each well then, the plate sealed and wrapped with foil to protect it from light and O<sub>2</sub>. After 2 hours, the plate was read by spectrophotometry plate reader (Clarion star Europe) at 570 nm and 600 nm. Staining with Alamar blue was also repeated after 3 days of incubation. Results were calculated according to the manufacturer's protocol as percentage difference in reduction between treated and control cells using the following equation:-

$$\text{Percentage difference between treated and control cells} = \frac{(O2 \times A1) - (O1 \times A2)}{(O2 \times B1) - (O1 \times B2)} \times 100$$

Where: -

O1 = molar extinction coefficient of oxidized Alamar blue (Blank) at 570 nm wavelength

O2 = molar extinction coefficient of oxidized Alamar blue (Blank) at 600 nm wavelength

A1 = absorbance of test wells at 570 nm wavelength

A2 = absorbance of test wells at 600 nm wavelength

B1 = absorbance of control well at 570 nm wavelength

B2 = absorbance of control well at 600 nm wavelength

The results were normalised against RPMI1640 medium for both P1 and P20.

### **2.6.12 Effect of *L.mexicana* concentration on the RPMI1640 medium pH after 2- and 24-hours incubation at 37°C**

In order to investigate whether parasite concentration has any effect on the media pH which may have impact on parasite differentiation, P1 and P20 parasites at a stationary phase were cultured in RPMI1640 supplemented with 10% HIFCS (Because this medium will be used for parasite mammalian host cell interaction experiments, as it is more analogous to host mammalian cell environments) at four different concentrations  $2 \times 10^6$ ,  $4 \times 10^6$ ,  $6 \times 10^6$ ,  $8 \times 10^6$  per mL and incubated in 95% v/v humidity at 37 °C in 5% v/v CO<sub>2</sub> incubator for 2 and 24 hours. pH of medium was measured after 2 and 24 hours in each concentration using litmus paper.

### **2.6.13 Virulence gene regulation of P1 and P20 *L.mexicana* promastigotes**

The regulation of 10 virulence genes including LPG1, LPG2, A2, CHAT1, CPB2, CPB2.8, CPC, GP63, LACK, (Ali, *et al.*, 2013) and MAPK9 (Bengs, *et al.*, 2005) were assessed by qPCR; in P20 compared with P1 promastigotes. P1 and P20 were cultured at 25°C in Schneider's *Drosophila* media containing 10% v/v HIFCS for three days. At stationary phase,  $40 \times 10^6$  parasites were harvested, and total mRNA was extracted (as mentioned in 2.8.1), then converted into cDNA and subjected to qPCR. qPCR results were normalized using the housekeeping gene GAPDH and Ct values were calculated as  $2^{-\Delta\Delta Ct}$ .

#### **2.6.14 Regulation of LPG1, LPG2, GP63, CPB 2, CPB 2.8 and A2 genes of P1 and P20 *L.mexicana* promastigotes and amastigotes**

Further experiments were conducted to determine the effect of *in vitro* passaging on expression of 6 virulence genes associated with differentiation of promastigotes into amastigotes after 2 and 24 hours of both P1 and P20 by qPCR. In addition, detection of LPG on P1 and P20 by using Immunofluorescence staining and flow cytometry using anti-LPG monoclonal antibodies was carried out.

P1 and P20 promastigotes were cultured at 25°C in Schneider's *Drosophila* media containing 10% v/v HIFCS. 20 x 10<sup>6</sup> P1 and P20 at stationary phase were cultured in RPMI1640 medium 10% v/v HIFCS and incubated in 95% v/v humidity at 37 °C in 5% v/v CO<sub>2</sub> incubator for 2 and 24 hours in vented flasks. 40 x 10<sup>6</sup> parasites were harvested from each flask, and total RNA was extracted, then converted into cDNA and subjected to qPCR by using LPG1, LPG2 GP63, CPB 2, CPB 2.8 and A2 primers. qPCR results were normalized using the housekeeping gene GAPDH and Ct values were calculated as 2<sup>-ΔΔCt</sup>.

#### **2.6.15 Detection of *L. mexicana* LPG in P1 and P20 promastigotes**

Immunofluorescence and flow cytometry staining were used in this study to check for the presence of *L. mexicana* LPG on P1 and P20 promastigotes.

#### **2.6.16 Immunofluorescence staining of LPG**

In order to investigate LPG on the P1 and P20 promastigote cell membrane, anti-LPG antibody, primary antibody CA7AE Mouse anti-Leishmanial LPG (Bio-Rad) was used by immunofluorescence and flow cytometry. FITC Alexa fluor goat anti-mouse IgG (Thermo Fisher Scientific) was used as secondary antibody.

According to the manufacturer's protocol and adopted from Bee, *et al.*, (2001); and Ali *et al.*, (2013) with a minor change by staining the parasites in the tube instead of coverslip to avoid loss of parasites during staining and after optimisation of the primary anti body and testing them by flow cytometry by using 4 different concentrations (1,2, 4, and 6 μL/mL). Briefly, 8 x10<sup>6</sup> *L. mexicana* at stationary phase were washed twice with PBS and divided into three tubes one for parasites without staining, the second tube was stained with secondary antibody only and the third one was stained with both primary and secondary antibodies as shown in Table-2.7. Nonspecific binding sites were blocked by 200 μL blocking buffer (100 μL tween 20 + 5% BSA + 100 mL PBS) and incubated for 1 hour at room temperature. Blocking buffer was removed by washing with PBS. 0.5 μL diluted

(1/500) CA7AE anti-LPG antibody was added with 0.5µl (1µg/mL) to the parasite except conditioned control parasite and incubated at 4°C for overnight. Tubes were washed twice with PBS and shaken for 3 minutes. 0.5µl secondary anti-mouse antibody was added into all tubes and incubated at room temperature. Non-binding antibodies were removed by double washing with PBS. Smears were prepared from each tube and visualised by EVOS microscope fluorescence at power 40.

**Table 2. 7: staining strategy of P1 and P20 promastigotes using immunofluorescence and flow cytometry**

phenotyping staining strategy of P1 and P20 promastigotes using Immunofluorescence and flow cytometry where 2° ab control to correct for non-specific binding and unstained to correct for autofluorescence.

Tube	Primary anti body	Secondary anti body
1- (assay)	CA7AE Mouse anti <i>Leishmanial</i> Igm	Goat anti-mouse IgG :FITC
2- (2° Ab control)	--	Goat anti-mouse IgG :FITC
3- (unstained control)	--	--

### 2.6.17 Detection of LPG by flow cytometry

0.5 x 10<sup>6</sup> P1 and P20 promastigotes at stationary phase and divided into three tubes one for parasites without staining, the second tube was stained with secondary antibody only and the third one was stained with both primary and secondary anti bodies as shown in Table-2.7.

Parasites were washed with PBS and resuspended in 500 µL blocking buffer and incubated with 0.5 µL primary anti body CA7AE Mouse anti-*Leishmanial* LPG (Bio-Rad) for 30 minutes at 25 °C. All tubes were washed with PBS to remove non-binding antibodies, then resuspended in 500 µL blocking buffer and stained with 0.5 µl secondary antibody Alexa fluor goat anti-mouse IgG (Thermo Fisher Scientific) and incubated in the dark at 25°C for 30 minutes. All tubes were washed 3 times with PBS to remove non-binding secondary antibodies and resuspended in 400 µL flow cytometry fluid (1 x PBS containing 0.01% w/v BSA plus 0.1% NaN<sub>3</sub>) and read by flow cytometry.

## 2.7 Mammalian cell interaction with P1 and P20 *L. mexicana*

In order to investigate the early pathological and immunological changes in immune cells after infection with *L. mexicana*, the next stage in the methodology of the current study was designed to study the interaction between virulent (P1) and avirulent (P20) *L. mexicana* infection using two types of mammalian cells, *L. mexicana* susceptible Balb/c and resistant C57 mice bone marrow derived macrophages. Immunological changes in infected cells were investigated at two times, after 2- and 24-hours post-infection *in vitro*.



### 2.7.1 Culturing of Balb/c and C57 mice bone marrow macrophage

To generate bone marrow derived macrophages, 6–8 week of age susceptible Balb/cN (Balb/c) and resistant C57BL/6J (C57) mice were purchased from Charles River UK and maintained at Nottingham Trent University lab animal unit. Mice were sacrificed by spinal cord displacement and soaked in 70% v/v ethanol by an expert before being transported into the tissue culture lab. All preparations of bone marrow extraction were performed under sterile conditions using a class II microbiological safety cabinet in level 2 containment tissue culture lab. Mice were subjected to removing of skin and muscles from hind limbs using scalpel, forceps and scissors. Femurs and tibia bones were cracked at the middle and bone marrows were flushed by RPMI1640 medium using a 10 mL syringes with a 27G needle in a sterile petri dish. Bone marrow cells were transferred into 50 mL sterile tube and passed through 27G needle to separate cells from each other. Bone marrow cells were centrifuged at 400 g for 5 minutes. The pellet was suspended in DC medium, 10  $\mu$ L cells were diluted in white blood fluid (Glacial acetic acid 2% s/v, Gentian Violet 1% w/v in Distilled water) and counted by Neubauer hemocytometer. Approximately  $1.5 \times 10^6$  Bone marrow cells were cultured in T25 tissue culture flasks in 7 mL DC medium, in (RPMI1640 with glutamine, 5% v/v FCS, 10 mM hepes, 20  $\mu$ M  $\beta$ mercaptoethanol, 50 U/ml Penicillin/Streptomycin, 5 ng/mL GMCSF) per flask and incubated at 37 °C in 5% v/v CO<sub>2</sub>. All flasks were washed at 2<sup>nd</sup> and 4<sup>th</sup> and 6<sup>th</sup> day by replacing 5 mL by fresh DC medium. Figure 2.3 shows differentiation of bone marrow macrophage *in vitro* which usually needs seven days. It is seen from this figure that at day-1, the cells are found to be small, suspended and rounded. During this time, the cells start to change their morphology into a star shape and become larger. In addition, as the days proceed, the cells adhered to the flask. On day-7, all suspended cells were removed with the DC media and only adhered cells were kept for infection.

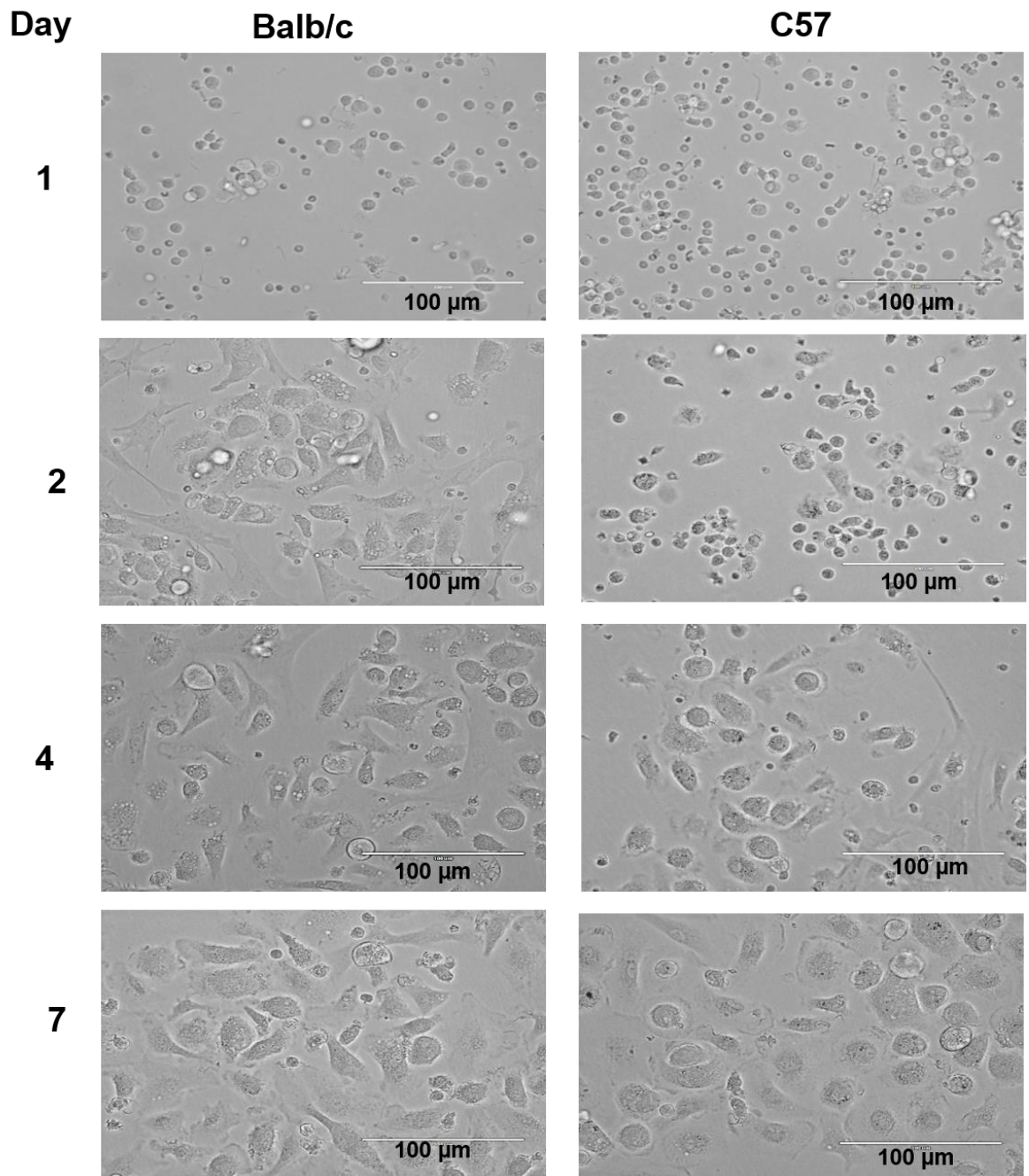


**Figure 2. 3: Differentiation of bone marrow macrophages *in vitro* for seven days**

All preparations were performed under sterile conditions, mice were euthanised, their skin and muscles of hind limb were removed using scalpel, forceps and scissors. Femurs and tibia bones were removed and cracked at the middle and bone marrows were flushed by RPMI 1640 medium using a 10 mL syringe with a 27G needle in a sterile petri dish. Bone marrow cells were transferred into a 50 mL sterile tube then, centrifuged at 400g for 5 minutes. The pellet was suspended in DC medium stained with white blood cell count fluid and counted by Neubauer hemocytometer. Approximately  $2.6 \times 10^6$  Bone marrow cells were cultured in T25 tissue culture flask in a 7 mL DC medium (RPMI 1640 with glutamine, 5% v/v FCS, 10 mM hepes, 20µM βmercaptoethanol, 50 U/ml Penicillin/Streptomycin, 5 ng/mL GMCSF) per flask and incubated at 37 °C in 5% v/v CO<sub>2</sub>. All flasks were washed at 2<sup>nd</sup>, 4<sup>th</sup> and 6<sup>th</sup> day by replacing 5ml by fresh DC medium. Pictures were taken using light (EVOS life technology) microscope transmission power 40.

## 2.7.2 Characterisation of Balb/c and C57 mouse bone marrow derived macrophages (BMDM) by flow cytometry

To make sure that the adhered cells are differentiated into macrophage, Macrophage phenotyping was assessed by analysing the expression of the F4/80 marker using flow cytometry for both Balb/c and C57 BMDM. At the 7th day of macrophage differentiation, DC media was discarded, and flasks were rinsed twice by PBS. Adhered macrophages were detached using a tissue culture scraper. Macrophages were washed with PBS by centrifugation at 300 g for 5 minutes.

Pellets were re-suspended in 1 mL PBS. 10  $\mu$ L cells were stained using trypan blue by mixing of 90  $\mu$ L trypan blue and 10  $\mu$ L cells. Cells were divided into three Eppendorf tubes 2.5  $\times 10^5$  cells per tube. The first tube was stained with rat anti mouse F4/80 and incubated on ice for 30 minutes, then washed. Tubes number one and two were stained by secondary antibody Goat anti-rat F(ab')<sub>2</sub> IgG:FITC and incubated on ice for 30 minutes. Control tube 3 was used without staining macrophages, as shown in Table- 2.8 All tubes were washed and resuspended in 500  $\mu$ L sheath fluid and subjected to flow cytometry analysis and the results were analysed by flow cytometry (Beckman Coulter USA). flow cytometry results were analysed by Beckman Coulter Kaluza software USA (Appendix 2).

**Table 2. 8: Phenotyping staining of BMD using flow cytometry**

phenotyping staining strategy of Balb/c and C57 BMDM using flow cytometry where 2° ab control to correct for non-specific binding and unstained to correct for auto fluorescence.

Tube	Primary anti body	Secondary anti body
1- (assay)	Rat anti mouse F4/80	Goat anti rat IgG:FITC
2- (2° Ab control)	--	Goat anti rat IgG:FITC
3- (unstained control)	--	--

## 2.7.3 Infectivity of P1 and P20 *L.mexicana*

Infectivity of P1 and P20 was assessed by infection of two types of mammalian host cells *Leishmania* susceptible Balb/c mice and *Leishmania* resistant C57 mice BMDM at two time points: 2- and 24-hours post-infection. Ability of P1 and P20 to infect mammalian host was assessed by estimation of non-engulfed parasites by using Neubauer haemocytometer and Alamar blue assay compared with parasite controls cultured in the absence of mammalian cells.

## 2.8 Infection of Balb/c and C57 mice BMDM with P1 and P20 *L. mexicana*

For optimisation of RNA extraction from BMDM several cell densities of BMDM were used:  $200 \times 10^5$ ,  $500 \times 10^5$ ,  $1 \times 10^6$  and  $2 \times 10^6$  and  $3 \times 10^6$  per T25 flask to be used for *L. mexicana* infection. The  $2 \times 10^6$  and  $3 \times 10^6$  were selected for further experiments for their optimum value of RNA concentration. To obtain enough concentration of RNA, two flasks of T25 were used for each treatment. Experiments were designed to let bone marrow cells grow and differentiate and to infect in the same tissue culture flasks.

At the 7<sup>th</sup> day, each T25 tissue culture flask contained approximately  $1 \times 10^6$  BMDM. T25 flasks were washed with RPMI1640 three times and then infected with  $20 \times 10^{10}$  of P1 and P20 *L. mexicana* promastigotes in a total volume of 2.5 ml RPMI1640 medium supplemented with 10% v/v HIFCS. Non-infected macrophages, P1 and P20 *L. mexicana* culture alone were used as controls. All flasks were incubated in 95% v/v humidity at 37 °C in 5% v/v CO<sub>2</sub> incubator for 2 and 24 hours. Supernatants were collected for further analysis and cells were lysed for total RNA extraction using a Qiagen kit. The quality of the extracted RNA was assessed using a Nano Drop®8000 Spectrophotometer. 1 µg of the extracted RNA was transcribed into cDNA using a Tetro cDNA synthesis kit (Bioline, UK), and then subjected to qPCR. Regulation of apoptotic genes Bax, BCL 2 (Vukosavic *et al.*, 1999), caspase 1 (Wang *et al.*, 2012), caspase 8 (Perl *et al.*, 2005), caspase 9 (Tsujimoto *et al.*, 2005) and PD 1 (Roy *et al.*, 2017) was investigated using qPCR.

## 2.9 Free non-engulfed parasites

After 2 and 24 hours, the number of non-engulfed parasites in infected and parasite alone cultures was assessed by two methods: manual counting by Neubauer hemocytometer (Nano EnTek UK) and Alamar blue assay. Free (unphagocytosed) parasites were counted and compared with control P1 and P20 cultures without mammalian cells. 10 µL of parasites was diluted with 1% (90 µL) paraformaldehyde and counted by Neubauer hemocytometer. Average of four chambers count was multiplied by  $10^5$ .

Alamar blue assay was also used to confirm infectivity of P1 and P20 to BMDM. Therefore, after infection of macrophages for specific times of 2 hours or 24 hours, all medium which containing the unphagocytosed P1 and P20 parasites was collected. In addition, the parasite control cultured in the absence of mammalian cells were collected in centrifuge tubes and spun at 2000g for 10 minutes. Pellets were then re-suspended in 300 µL RPMI1640 supplemented with 10% HFCS. Each parasite tube was divided into 3 wells, 100 µL per well, in a flat bottom 96 well plate. 10 µL Alamar blue was added into each well and after

incubation for 2 hours at 25°C, the plate was read at 570 and 600 nm. It should be noted that to avoid the effect of RPMI1640 media on P1 and P20 growth rate, staining was used only for 2 hours.

## **2.10 Survival of P1 and P20 *L.mexicana* in Balb/c and C57 BMDM using light microscope**

To investigate the survival of parasites inside susceptible Balb/c and resistant C57 BMDM for 7 days,  $1 \times 10^6$  Balb/c and C57 BMD were infected with  $20 \times 10^6$  P1 and P20 and incubated at 95% v/v humidity at 37 °C in a 5% v/v CO<sub>2</sub> incubator. Cells were then examined without staining by taking live images using EVOS microscope (life technology) at transmission 40 x objective after 2 hours, 24 hours, 3 days and 7 days of infection. Qualitative data obtained by EVOS was then analysed and converted into quantitative data by calculating the percentage of infected cells. In addition, the numbers of parasites inside the cells were also counted. Moreover, the number of parasitophorous vacuoles (PV) per cell and the number of parasites per PV were also quantified. It was observed that under light microscope, engulfment of P1 but not P20 was clear (see results sections 4.2.2,1 and 4.2.2.2). Therefore, to ensure whether P20 was engulfed and lysed or even not engulfed by macrophages, extra experiments using two stains (CFSE and Giemsa) were carried out.

For Giemsa staining, infected macrophages (see section 2.6.4) were stained with 6% w/v Giemsa stain (sigma, UK) and visualised by an Olympus microscope connected with a Nikon Camera at 40 x objective after 2- and 24-hours infection.

For FITC staining,  $20 \times 10^6$  P1 and P20 promastigotes at stationary stage were stained with 50 ng CFSE in 500 µL RPMI1640 medium supplemented with 10% v/v HIFCS and incubated at 25°C for 30 minutes to allow parasites to absorb the stain. Promastigotes were washed three times with 7 mL PBS to remove the residual stain from the medium.

Approximately  $1 \times 10^6$  Balb/c and C57 BMDM were infected with CFSE stained promastigotes and incubated at 95% v/v humidity at 37°C in a 5% v/v CO<sub>2</sub> incubator for 24 hours. After 24 hours, media containing free parasites were removed and replaced by fresh medium. Cells were examined by fluorescent microscope EVOS (life technology).

## **2.11 Viability of macrophages post-infection**

The viability of BMDM (for the infected cells) was assessed by flow cytometry after 2 and 24 hours infection. For more details on BMDM infection procedure, (see section 2.8). BMDM infected with P1, P20 and the non-infected control were divided into two groups. The first group was treated with removal of GM-CSF to induce apoptosis while the second

group was used as a control with GMCSF to investigate the effect of P1 and P20 on infected cell apoptosis (Zhang *et al.*, 2003; Akarid *et al.*, 2004). All flasks were incubated for 24 hours.

Macrophages (in both groups) were detached using cell scrapers. Detached cells were collected along with floating cells and were subjected to a viability test by using flow cytometry analysis. For cell viability staining Annexin V (Biolegend USA) to stain early apoptotic cells and Propidium Iodide (PI) (sigma) for dead cells have been used. During early cell apoptosis phosphatidylserine (PS) which found only in inner plasma membrane, it is translocated into the external leaflet of cell membranes. Annexin V is a protein that binds to PS in a calcium-dependent affinity manner therefore Annexin V is used for identification of apoptotic cells. PI is an intercalating DNA dye. It is a fluorescent dye that intercalates into double-stranded nucleic acid. It is excluded from viable cells but can penetrate cell membranes of dead or dying cells. Therefore, it is widely used for evaluation of cell death and apoptosis or for determination of DNA content in cell cycle analysis.

Macrophages were detached using cell scrapers. Detached, and floating cells were transferred into centrifuge tubes. Cells were spun down at 300 g for 5 minutes and resuspended in 500  $\mu$ L Annexin V buffer (PBS plus 10mM HEPES (pH 7.4), 150mM NaCl, 5mM KCl, 5mM MgCl<sub>2</sub>, 1.8mM CaCl<sub>2</sub>). Cells were washed again and resuspended in 100  $\mu$ L Annexin V buffer. 5  $\mu$ L Annexin V stain was added into each tube and incubated in the dark at room temperature for 15 minutes. Cells were stained with PI at 10  $\mu$ L per tube (10  $\mu$ L PI with 190  $\mu$ L Annexin V buffer). Finally, 200  $\mu$ L of Annexin V buffer was added and cells were analysed by flow cytometry (Beckman Coulter USA). flow cytometry results were analysed by Beckman Coulter Kaluza software (USA). Cells were stained with PI by dilution of PI stain 1:20 by mixing of 10  $\mu$ L PI with 190  $\mu$ L Annexin V buffer and adding 10  $\mu$ L diluted PI in each tube. For running flow cytometry, the total volume was increased by adding 200  $\mu$ L Annexin V buffer and analysed by flow cytometry (Beckman Coulter USA). flow cytometry results were analysed by Beckman Coulter Kaluza software USA.

## **2.12 Detection of phosphatidylserine in P1 and P20 *L. mexicana* promastigotes and amastigotes by Annexin V staining**

França-Costa *et al.*, (2012) reported that phosphatidylserine is naturally expressed on the outer membrane of *Leishmania* parasites. Therefore, expression was compared in the P1 and P20 at stationary phase promastigotes coming from 25°C incubation culture and after incubation at 37°C for 2 and 24 hours. 20 x 10<sup>6</sup> of P1 and P20 *L. mexicana* parasites in stationary phase in a total volume of 2.5 mL RPMI1640 supplemented with 10% v/v HIFCS

in vented T25 tissue culture flasks were incubated in 95% v/v humidity at 37 °C in 5% v/v CO<sub>2</sub> incubator for 24 hours for amastigote differentiation. P1 and P20 stationary phase promastigotes were cultured in Schneider's *Drosophila* medium supplemented with 10% v/v HIFCS in unvented T25 tissue culture flasks and incubated in a 25°C incubator. After 24 hours incubation at 37°C, both P1 and P20 parasites were visualised by EVOS microscope to check the differentiation into amastigotes. Human U937 monocytes were used as a negative control. Cells were stained with Annexin V according to the manufacturer's guidelines, briefly, 0.5 x 10<sup>6</sup> parasites were centrifuged at 800 g for 10 minutes and resuspended in 500 µL Annexin V buffer. The same staining procedure described in section 2.11 was used.

## 2.13 Cytokines gene regulation after infection of mammalian cell with P1 and P20 *L. mexicana* promastigotes

Pellets of infected mammalian cells from Balb/c and C57 mice (see Section 2.8) were subjected to total RNA extraction, cDNA synthesis and then qPCR analysis (see Section 2.18.2). Supernatants were collected and assessed for the presence of TNF- $\alpha$  by ELISA. Cytokine gene regulation of IL-6, TNF- $\alpha$ , IL-1 $\beta$  (Wang *et al.*, 2008), IL-1 $\alpha$  (von Stebut *et al.*, 2003) and TGF $\beta$  (Sullivan *et al.*, 2009), was evaluated by using qPCR.

### 2.13.1.1 Enzyme-linked immunosorbent assay (ELISA)

It is worthwhile to use ELISA assay to confirm qPCR results used in gene regulation of cytokines. ELISA approaches were used to estimate the concentration of cytokines. Samples were supernatants collected from mammalian cells infected with P1 and P20 and non-infected controls for 2 and 24 hours.

The ELISA assays were carried out following the manufacturer's instructions, briefly a flat-bottomed 96-well plate (Sarstedt, UK) was coated with 100 µL per well of coating buffer (1x PBS, pH 7.2-7.4) containing 2 µg per mL capture antibodies (2 µg / mL). The plates were covered and incubated at 4 °C overnight. After 2 washes with washing buffer (1 x PBS and 0.05% v/v Tween 20), the plates were blocked with 250 µL blocking buffer (1 x PBS, 5% BSA) for 2 hours at room temperature. Plates were washed 3 times with washing buffer, and 100 µL per well of the fresh standard added (with 5 dilutions). 100 µL of supernatants samples were added in appropriate wells in triplicate. Plates were covered and incubated at room temperature for 2 hours. After 2 washes with washing buffer, 50 µl of detection antibodies (1 µg / mL) were added in all wells, then the plates were covered and incubated for 1 hour at room temperature. Plates were washed twice with washing buffer. 100 µL

diluted streptavidin-HRP (1.5  $\mu$ L streptavidin, 10 mL HRP diluent buffer (1 x PBS, 1% BSA, 0.1% Tween) was added to all wells and the plate was incubated for 30 minutes at room temperature, then washed twice. 100  $\mu$ L TMB of the substrate HRP solution was added into all wells and incubated in the dark for 10 minutes. Reaction was stopped by adding 100  $\mu$ L of 1M H<sub>2</sub>SO<sub>4</sub> into all wells. Absorbance was read immediately by spectrophotometer at 450 nm. The average of absorbance values was calculated of each duplicate of standard and triplicate of the samples. A linear standard curve was generated and the level of cytokines for each sample was determined by extrapolating absorbance values against cytokines standard concentrations using the standard curve.

## **2.14 Effect of conditioned medium on P1 and P20 *L. mexicana* promastigote growth and virulence genes regulation**

In order to investigate whether infected mammalian cells modulate the release of growth inhibitory factors that may affect P1 and P20 growth and virulence by using supernatant produced from stage-2, a series of experiments have been conducted which will be described in stage-3, as discussed in this section.

As mentioned earlier in stage-2, the supernatants were produced as follows.  $1 \times 10^6$  mammalian cells (Balb/c and C57 BMDM) were cultured in RPMI1640 supplemented with 10% v/v HIFCS and infected with  $20 \times 10^6$  P1 and P20 promastigotes at stationary phase. Non-infected mammalian cells and parasites alone were used as control. All flasks were incubated at 37 °C in 5% CO<sub>2</sub> v/v and 95% v/v humidity for 24 hours.

After 24 hours supernatants were collected and centrifuged at 2000g for ten minutes; supernatants were collected and filtered through 0.25  $\mu$ L filter for sterilization and removal of any parasites. Supernatants were stored at -20 °C.

It should be mentioned that the conditioned media used for the experiments described in stage-3 was prepared by dilution of the supernatants 1:1 with fresh RPMI1640 medium supplemented with 10% HIFCS. In other words, prepared condition media contains 50% of supernatants (which was already produced from infected cells described in stage-2) and 50% of fresh RPMI1640 medium supplemented with 10% HIFCS.

### 2.14.1 Workflow of Effect of conditioned media on P1 and P20 *L. mexicana* promastigote growth and virulence gene regulation

The workflow which describes the methods used in stage-3 is shown in figure 2.4, the supernatant obtained previously from stage 2 from mammalian cell infected with P1 and P20 was only for 24 hours. In this stage, the effect of the condition media on; (i) parasite growth rate by using Haemocytometer and Alamar blue, (ii) parasite virulence gene regulation, and (iii) abundance of LPG, were studied.

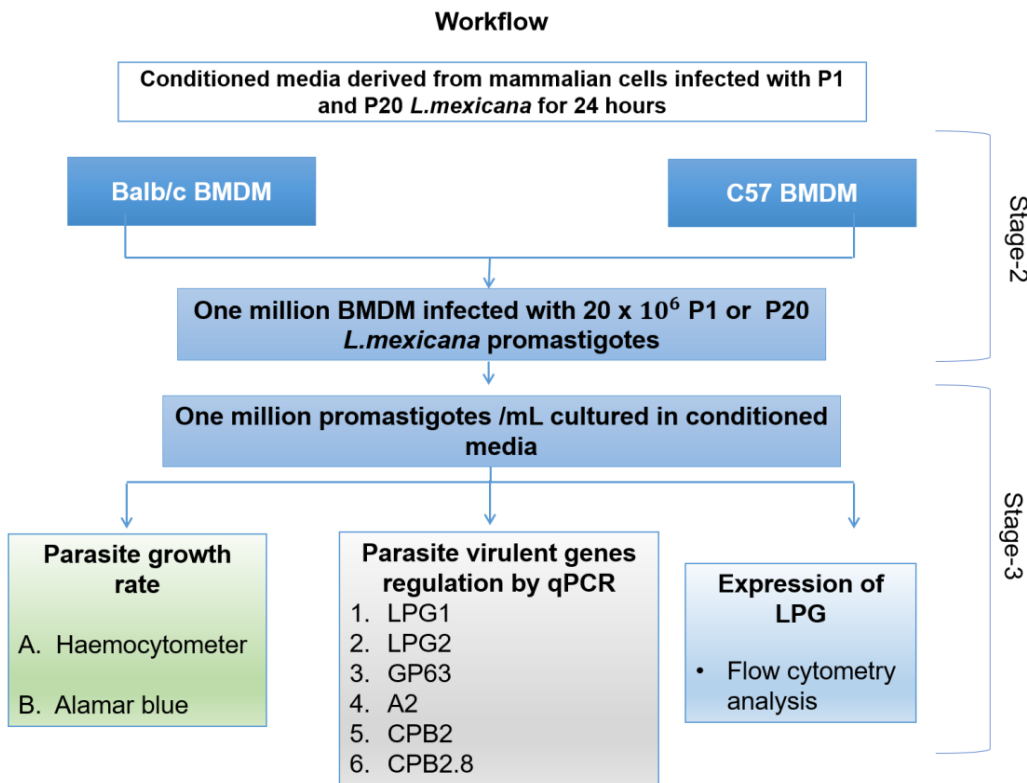


**Figure 2. 4 Workflow of the effect of conditioned medium on P1 and P20 *L. mexicana* promastigote growth and virulent gene regulation (Stage-3)**

Supernatants obtained previously were used for preparation of conditioned medium, and effect of conditioned medium on the parasite growth and virulence associated genes were investigated.

## **2.15 Effect of conditioned medium on P1 and P20 *L. mexicana* promastigote growth and associated virulence genes regulation**

40 x10<sup>6</sup> P1 and P20 *L. mexicana* promastigotes in their stationary phase were cultured in unvented tissue culture flasks containing 4 mL conditioned medium (Derived from mammalian cells infected with P1 or P20 for 24 hours) and incubated at 25°C for 24 hours. P1 and P20 control were cultured in fresh 4 mL RPMI1640 supplemented with 10% v/v HIFCS. After 24 hours' incubation media containing parasites were collected and passed through, an 18G needle to disperse clumped parasites and counted by a Neubauer hemocytometer. Parasite pellets were washed 3 times with PBS and subjected to mRNA extraction, cDNA synthesis and qPCR. 6 virulence associated genes were tested by qPCR: LPG1, LPG2, A2, CHAT1, CPB2, CPB2.8 and GP63.

## **2.16 Alamar blue assay to assess Effect of conditioned medium on P1 and P20 *L. mexicana* promastigote growth**

The brief method of Alamar blue staining was as follow, in sterile flat bottom 96 well plate (Sarstedt UK), 1 x 10<sup>6</sup> P1 or P20 stationary phase promastigotes were seeded per well in 100 µL conditioned medium with three different concentrations 75%, 50% and 25%. Conditioned medium derived from control 1 x 10<sup>6</sup> mammalian cells or infected with 20 x 10<sup>6</sup> P1 or P20 promastigotes. The control medium was RPMI1640 supplemented with 10% HIFCS without supernatant. The plate was sealed with cling film and incubated at 25°C for 48 hours. 10 µL Alamar blue (Biorad) was added to each well, then sealed with cling film and wrapped with foil to protect it from light and O<sub>2</sub>. After 2 hours plates were read by spectrophotometry plate reader (Clarion Star Europe) at 570-600 nm. The results were calculated according to the manufacturer as a percentage difference between wells treated and untreated with conditioned medium, as mentioned above in section 2.9.

## **2.17 Effect of conditioned medium on LPG expression by P1 and P20 promastigotes by flow cytometry**

0.5 X 10<sup>6</sup> P1 and P20 promastigotes at stationary phase incubated in conditioned and control media (as mention above in 2.13) were divided into three tubes, one for parasites without staining, the second tube was stained with secondary antibody only and the third one was stained with both primary and secondary anti bodies.

Parasites were washed with PBS and resuspended in 500 µL blocking buffer and incubated with 0.5 µL primary anti body CA7AE Mouse anti *Leishmanial* LPG (Bio-Rad) for 30 minutes at 25 °C. All tubes were washed with PBS to remove non-binding antibodies, then resuspended in 500 µL blocking buffer and stained with 0.5µL secondary antibody Alexa fluor goat anti-mouse IgG (Thermo Fisher Scientific) and incubated in the dark at 25°C for 30 minutes. All tubes were washed 3 times with PBS to remove non-binding secondary antibodies and resuspended in 400 µL flow cytometry fluid and read by flow cytometry

## **2.18 A brief description of the gene expression technique used in methodology for the current study**

At the end of this chapter, it is worthwhile to give the readers a brief description of the gene expression technique used in the methodology of this study. This includes, RNA extraction, cDNA synthesis and qPCR.

### **2.18.1 Preparation of target cells for RNA extraction**

Preparation of cells for RNA extraction are different between various types of cells. Macrophages are adherent cells and parasites are suspended cells. In addition, parasites have the ability to quickly disperse during the removal of the washing buffer, which presents challenges in RNA extraction.

For adherent BMDM the RNA extraction procedure was slightly modified according to cell adhesion properties, therefore, to avoid dilution of lysis buffer and losing cells, all medium should be removed. Three flasks of the adherent Balb/c or C57 BMDM were washed, media drained and lysed in the flask. Macrophages were then lysed directly in the tissue culture flask by covering all adherent cells with 350 µL lysis buffer (346.5 µL RLT and 3.5 µL β-mercaptoethanol) (sigma, UK). Lysates from 3 flasks where then pooled and were centrifuged in one spin column for 30 seconds for each flask lysate to provide a sufficient yield of RNA for reverse transcription. For suspension of parasite cultures, 40 x 10<sup>6</sup> Parasites were washed twice with 2-3ml PBS at 2000 g for 10 minutes. Parasites were washed for the third time with 500 µl PBS at 2000 g for 10 minutes, and then all PBS was removed carefully in one pipetting action without touching the pellets with the pipette tip.

### **2.18.2 RNA extraction by Qiagene RNeasy mini kit**

Infected and control cells were subjected to RNA extraction using RNeasy mini kit (Qiagene, UK) according to the manufacturer with minor changes. Approximately 3 x 10<sup>6</sup> macrophages were lysed by lysis buffer (346.5 µL RLT and 3.5 µL β-mercaptoethanol) (sigma, UK). Cells

were vortexed and homogenised using homogenizer and Pellet Pestle (Sigma, UK) for 30 seconds. Lysate was mixed with 350  $\mu$ L 70% v/v ethanol (sigma, UK), mixed and transferred into the provided RNeasy spin column. The spin columns were spun at 8000 g for 15 seconds at room temperature. Flow-through was discarded then 350  $\mu$ L RW1 buffer was added and incubated for 3 minutes at room temperature in order to allow RNA to bind to the silica membrane of the spin column. The RW1 buffer was removed by centrifugation of the spin columns at 8000 g for 2 minutes.

The samples were subjected to on-Column DNase digestion using RNase-Free DNase (Qiagen, UK) to remove DNA contamination. 70  $\mu$ L of RDD buffer and 10  $\mu$ L DNase were mixed together and gently loaded onto the spin column silica membrane and incubated at room temperature for 15 minutes. 350  $\mu$ L of RW1 buffer was added; and this was centrifuged for 1 minute at 8000 g in order to remove the of RDD buffer. Spin column membrane was washed twice by 500  $\mu$ L of RPE buffer. To remove carryover of RPE buffer; collection tube and flow-through was discarded and replaced by a new collection tube and spun at 11000 g for 1 minute. The RNA was eluted in a new sterile collection tube and loading 30  $\mu$ L RNase-free water onto the RNeasy silica-gel membrane and spun at 8000 g for 1 minute. The quality and quantity of the extracted mRNA were assessed using Nano Drop@8000 Spectrophotometer (Appendix 6). 1  $\mu$ g high quality RNA was transcribed into cDNA using Tetro cDNA synthesis kit (Bioline, UK) for gene expression real time PCR.

### 2.18.3 cDNA synthesis

1  $\mu$ g of RNA was transcribed to complementary DNA (cDNA) (because the mRNA is unstable and easily degradable) by using Tetro cDNA synthesis kit (Bioline, UK). The protocol of reverse transcription (RT) of mRNA was performed according to the manufacturers and the preparation of super mix for each tube according to this table.

**Table 2. 9: Tetro cDNA protocol for super mix preparation for one sample (Bioline, UK).**

Product Name	Measurement
Primer: Oligo (dT) <sub>18</sub>	1 $\mu$ L
10mM dNtP mix	1 $\mu$ L
5x RT Buffer	4 $\mu$ L
Ribosafe RNase Inhibitor	1 $\mu$ L
Tetro Reverse Transcriptase (200u/ $\mu$ L)	1 $\mu$ L
DEPC-treated water	To 20 $\mu$ L

Each reaction was carried out on ice and under sterile conditions. The volumes of 1  $\mu$ g of each RNA were calculated and mixed with 8  $\mu$ L of super mix containing 1  $\mu$ L Oligo (dT) to

prime cDNA synthesis. 1 µl of 10 mM dNTPs, 4 µl of 5 x RT buffer, 1µl of Ribosafe RNase Inhibitor for reducing template degradation and increasing PCR yield products and 1µl of Tetro Reverse Transcriptase, and the total volume was adjusted to 20 µl using DEPC-treated water. The tubes were mixed and incubated at 45 °C in a block heater for 30 minutes. The reaction was terminated by incubation at 85°C for 5 minutes to de-activate the enzymes and then chilled on ice. The synthesised cDNA quality and quantity were assessed by Nanodrop 8000 Spectrophotometer and the cDNA was kept at -20°C for PCR.

### 2.18.4 Real time polymerase chain reaction (qPCR)

To analyse changes in gene expression of mRNA, qPCR was performed in a total volume of 12.5µL per PCR tube by adding the following volumes:

**Table 2. 10: Real time PCR super mix**

Reagent	volume
SsoAdvanced™ Universal SYBR® Green Supermix	6.75 µL
10µM Forward primer	0.5 µL
10µM Reverse primer	0.5 µL
cDNA template	0.5 µL (50 ng/µl)
Nuclease-free water	4.25 µL
Total volume	12.5 µL

All qPCR reactions were prepared as duplicates, 11.5 µL of super mix was added in strip tubes and caps (Qiagen UK) and mixed with 0.5 µL Forward primer and 0.5 µL Reverse primer of assay primers for investigation of the gene expression profile of control and infected or treated cells using GAPDH as a housekeeping gene.

The qPCR was run under standard conditions using a Corbett® Rotor-Gene as follows: a holding temperature for initial denaturation is 95°C for 10 minutes; followed by 40 cycles at 95°C for 30 seconds each. Annealing step for 30 seconds with melting temperature for each primer as in Table 4, 5, and 6. Extension step at 72°C for 20 seconds. Ramp temperature between melting temperature for each primer and 93°C was used for melting curves rising by 1 with waiting for 5 minutes. After calculating the mean of duplicate results.

qRT-PCR data were analysed, by using comparative threshold method (Ct). Ct values of genes of interest were compared with the Ct values of housekeeping genes (GAPDH). Relative expression was calculated as  $2^{-\Delta\Delta CT}$  for each gene of interest (Rao *et al.*, 2013).

## 2.19 Method development

Techniques were developed in this present study to optimise the study of the *L.mexicana* parasite, with regard to gene expression, surface proteins and the viability of the parasite after co-incubation with host cells, conditioned media and growth conditions.

### 2.19.1 RNA extraction

In order to extract a high concentration of RNA from the cell cultures differentiation, infection and lysing of BMDM was done by lysing cells from a single flask, in addition lysates from 2 or 3 tissue flasks were pooled and spun in a single spin column during RNA extraction.

### 2.19.2 LPG staining with CA7AE

It has been reported before that anti-LPG monoclonal anti bodies (CA7AE) bind specifically to epitopes of the LPG molecule by using ELISA and immunofluorescence (Tolson *et al.*, 1990, Sundar *et al.*, 2001) However at the time of writing there is no study which examined this antibody by using flow cytometry, staining of the parasites with CA7AE primary Ab for flow cytometry analysis. According to the manufacturer's protocol and adopted from Bee, *et al.*, (2001); and Ali *et al.*, (2013) with a minor change by staining the parasites in the tube instead of the coverslip avoids loss of the parasite during staining and washing. Optimisation of the primary antibody by using 4 different concentrations (1µg, 2µg, 4µg, and 6µ g per mL). According to the results, 1µg/mL was the choice for staining. Using flow cytometry over ELISA in this present study was done principally as the standard recombinant protein required for ELISA was difficult to source and was costly. By using a negative control in the flow cytometry alongside the evidence from previous studies, that CA7AE binds specifically to *L.mexicana* LPG protein, specific and selective staining of parasite LPG is assumed.

### 2.19.3 Alamar blue optimisation

Alamar blue was used to test the effect of conditioned medium on P1 and P20 parasite viability. Alamar blue contains resazurin dye which is a non-toxic weakly fluorescent blue indicator (O'Brien *et al.*, 2000). This assay measures the reduction-oxidation which is an indicator for colorimetric changes in cells as a result of reduction of cellular metabolism subsequently, the amount of fluorescence produced by the cells is proportional to the number of living cells. However, the sensitivity of Alamar blue *Leishmania* parasite viability has been tested before and it was not toxic to the parasite (Mikus and Steverding. 2000).

Alamar blue is used in cell proliferation cytotoxicity, viability and toxicity by using absorbance or fluorescence for measuring cell respiration and oxidation-reduction as an indicator for cytotoxicity and proliferation of *Leishmania* parasites. The absorbance increased with higher density of cells using 10% Alamar blue which is a non-toxic stain for *Leishmania mexicana* (Mikus and Steverding, 2000). For optimisation of Alamar blue assay different concentrations of the parasite and a range incubation times with Alamar blue stain was used. In 96 well plates  $10 \times 10^6$  *L. mexicana* promastigotes in 100  $\mu$ L RPMI1640 supplemented with 10% HIFCS were seeded and titrated down in serial dilution, 1:2. 10  $\mu$ L Alamar blue was added into each well. Plates were wrapped with cling film and foil to protect from O<sub>2</sub> and light, then incubated at 25°C for 2, 4, 6, 24, and 72 hours. Plates were then read at 570 nm and 600 nm after each time point of incubation (Appendix 3).

The optimisation study showed that 10% Alamar blue was non-toxic for *L.mexicana* confirming results reported by Mikus and Steverding, (2000). The optimum incubation time is between 2 and 4 hours with a parasite concentration between  $10$  to  $0.3 \times 10^6/100\mu$ L.

#### **2.19.4 Parasites concentration and pH.**

Using  $8 \times 10^6/$  mL concentration of promastigotes is enough to reduce the pH of infection media from 7 to 6 to induce parasite differentiation into amastigotes. In addition, it is useful to evaluate the parasite virulence and infective stage of parasite culture through testing their ability to differentiate into amastigotes (see section 3.2.4).

## **2.20 Statistical analysis**

Data are depicted as mean values  $\pm$  standard error of mean (SEM) using GraphPad Prism 7. Statistical significance of the data was analysed using unpaired student's t-test with GraphPad Prism software 7.

**Virulent P1 and avirulent P20  
*L. mexicana* promastigote growth and  
characterisation**

### 3.1 Introduction

*Leishmania* parasites have a complex lifecycle with several developmental forms. These forms represent the adaptation of the parasite to changes in the environmental conditions, as the parasite lives in two different hosts, mammalian host cells, and the sand fly vector. During the transition through these two different environments, the parasite is exposed to many environmental conditions such as temperature, pH, oxygen and nutrients. Incubation at 37 °C, low pH (lower than 7), and elevated CO<sub>2</sub> induce the promastigote to differentiate into the amastigote form in order to adapt to these conditions (Barak *et al.*, 2005; Reithinger, *et al.*, 2007).

Several studies have already reported that long-term (approximately 12 months) *in vitro* cultivation of *Leishmania* parasite species causes a total loss of the virulence of the promastigote population (Grimm *et al.*, 1991; Segovia *et al.*, 1992). Moreira *et al.*, (2012) demonstrated that 21 passages are enough to lose *L. infantum* virulence. Similarly, *L. mexicana* lost virulence after 20 passages *in vitro* and failed to induce lesions in Balb/c mice *in vivo* (Ali *et al.*, 2013). The effect of 20 passages on *L. mexicana* morphology has been investigated before by comparing virulent and avirulent promastigote morphology (Ali *et al.*, 2013). In addition, estimation of physical measurement of the parasite's flagellum length, body length and width by calibrated micrometre slide (Ali *et al.*, 2013) or by using Open lab software from Improvision (Heidelberg, Germany) on Apple Macintosh computer has been used to investigate changes in morphology (Bengs *et al.*, 2005). In this present study, additional comparable software has been used (NI vision assistant software).

The promastigotes at the metacyclic stages are the infective stage as this is the stage where promastigotes can differentiate into amastigotes (Solbach and Laskay, 2000). The metacyclic stage of the promastigote is determined by its physical measurements, body length should be less or equal to 8 µm, body width less or equal to 1 µm, and flagellum length longer than body length (Rogers *et al.*, 2002). Few studies have focused on the parasite metacyclogenesis and its relation to attenuation of the parasite. Investigation of P1 and P20 morphology may lead to explanations of the reasons for losing virulence.

In recent years various methods have been used for the identification of surface proteins expressed by the *Leishmania* parasite cell membrane under specific conditions at different growth stages. Parasite proteomics is the most promising approach for analysing the complexity of *Leishmania* virulence. Lipophosphoglycan (LPG) is one of most studied molecules of *Leishmania* species as it regulates host cell signalling pathways and it is most the abundant molecule on promastigotes and amastigotes (Olivier *et al.*, 2005; Aguirre-Garcia *et al.*, 2018) However, although LPG is one virulence factor expressed on the *Leishmania* parasites, such as *L. major*, its role is still controversial in *L. mexicana*.

Phosphatidylserine (PS) is another molecule that is expressed on *Leishmania* parasites and plays an important role in suppression of the host immune response. PS is naturally expressed on the outer membrane of *Leishmania* parasite and it is associated with the increase of parasite metacyclic stage infectivity (Tripathi and Gupta *et al.*, 2003; França-Costa *et al.*, 2012). *Leishmania* parasite external membranes contain relatively high levels of phosphatidylserine which may provide a mechanism for a silent entry to the host cells via apoptotic cell receptors without activating the immune system or proinflammatory responses (Wanderley *et al.*, 2006). Increasing PS expression has an important role as a mechanism for parasite survival within host macrophages (Balb/c and C57) and its dissemination and disease outcome and is associated with more severe cases and persistent disease state (França-Costa *et al.*, 2012).

This chapter explains the results of P1 and P20 characterisation when parasites are grown in the absence of a mammalian host cell *in vitro*. The data presented in this chapter relate to the results obtained from stage-1 (section 2.6). The main aim of this chapter is to study the effect of long-term *in vitro* passaging of *L. mexicana in vitro* on growth rate, morphology, the ability to differentiate into amastigotes and virulence gene regulation. For this purpose, a fresh parasite isolated from Balb/c lesions was cultured for 20 passages *in vitro*. The effect of 20 passages was investigated by comparing the parasite at the initial passage (P1) and 20 passages (P20) This comparison includes the effect of culture conditions such as; temperature, pH, presence/absence of oxygen and the type of media, as Schneider's *Drosophila* is a standard growth medium for the parasite and RPMI1640 a media used for the analysis of parasite mammalian cells interaction. The effect of oxygen on parasite growth was also investigated as ordinarily the parasite lives under anaerobic conditions, while infection of mammalian cells is carried out in an aerobic environment. Also, the effect of temperature on P1 and P20 were explored because parasite optimum incubation temperature is 25°C and infection of mammalian cells is carried out at 37 °C. In addition, the effect of parasite concentration on media pH was also studied. All these factors were investigated prior to testing parasite-mammalian cell interaction. Understanding these differences could be helpful in designing a parasite-mammalian cells interaction model.

## 3.2 Results

### 3.2.1 Characterisation of P1 and P20 *L. mexicana*

#### 3.2.1.1 Effect of culture conditions on P1 and P20 *L. mexicana* growth rate

*L. mexicana* parasites isolated from fresh Balb/c lesions were subjected to 20 passages *in vitro* culture. *Leishmania* parasite growth characteristics *in vitro* were investigated at passages 1 and 20 at the stationary phase. To assess the effect of media type, oxygen and temperature, one million P1 and P20 promastigotes at stationary phase were cultured in 5 mL growth medium (Schneider's *Drosophila* and RPMI1640) in vented and unvented T25 flasks under incubation at 25°C and 37°C. The parasites were counted by Neubauer hemocytometer after 48 hours of incubation and continuous counting was carried out every 2 days until day 18 (figure 3.1 and figure 3.2).

No growth of P1 and P20 promastigotes was observed under 37 °C incubation irrespective to the media type and aerobic condition, while increase in growth was detected at 25°C incubation. There was no significant difference between the growth rate of P1 and P20 in Schneider's *Drosophila* under aerobic condition (figure 3.1 A). The optimal conditions for P1 and P20 were observed in Schneider's *Drosophila* under anaerobic conditions. P20 reached a maximum growth peak faster ( $\sim 60 \times 10^6$  at 3 days) compared to P1 ( $\sim 100 \times 10^6$  at 5 days), moreover, their growth rate also decreased faster (figure 3.1 B). An interesting feature in figure 3.1 (B) is that at about day 3, the parasite concentration of both P1 and P2 is approximately  $45 \times 10^6/\text{mL}$  (as can be seen by the crossing point between P1 and P20). This indicates that the infective stage of both P1 and P20 are similar which is known as stationary phase (i.e. when the parasite reaches  $20 \times 10^6$  or higher per mL). More precisely, both P1 and P20 promastigotes reach stationary phase approximately at day-3 of culture, which will subsequently be used for infection of the mammalian cells in this study.

In figure 3.1 (C) using RPMI1640 media supplemented with 10% HIFCS P1 but not P20 are able to grow significantly under aerobic condition. It is worth remembering that this condition (i.e. RPMI1640 with O<sub>2</sub>) will be used for mammalian cell infection of both P1 and P20. The growth rate in RPMI1640 media without O<sub>2</sub> (figure 3.1 D) was not sufficient for both P1 and P20.

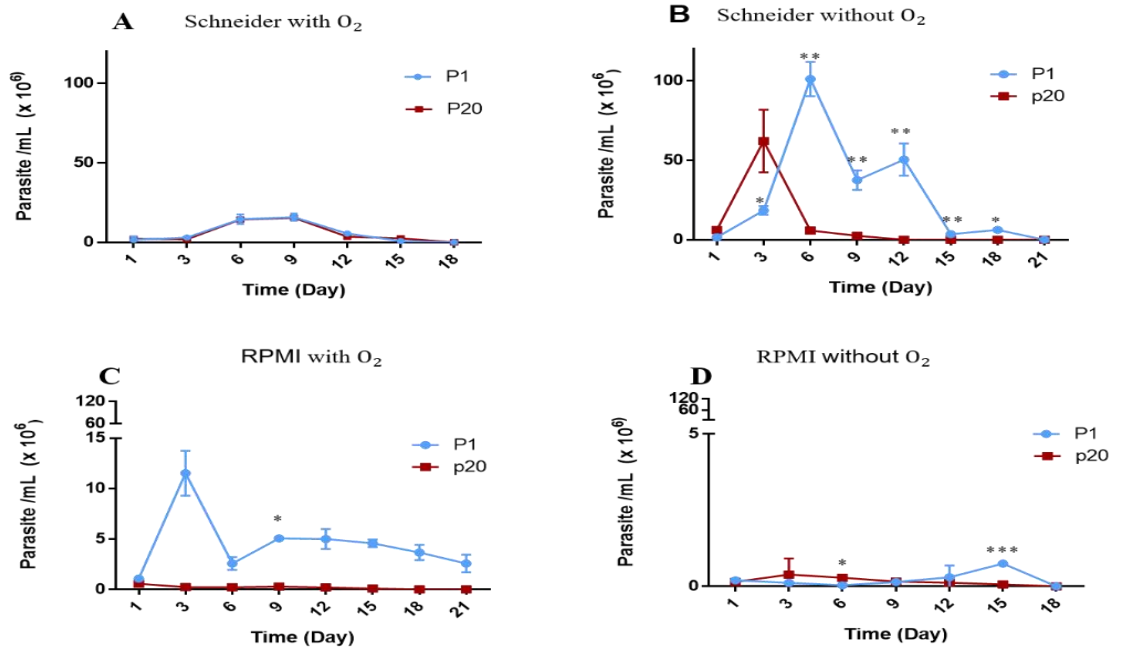


**Figure 3. 1: P1 and P20 growth curve cultured in RPMI 1640 or Schneider's *Drosophila* medium under aerobic and anaerobic conditions at 25°C**

One million P1 and P20 were cultured in 5 mL RPMI and Schneider's *Drosophila* media containing 10% v/v HIFCS, in vented and unvented flasks, incubated at 25°C. Parasites were counted by Neubauer hemocytometer after 48 hours of incubation. Data was analysed by using GraphPad Prism 7. Statistically significant differences between each represented by \* $p < 0.05$  \*\* $p < 0.001$ . \*\*\* $p < 0.0001$ , P value was determined by unpaired t-test. The results are the average of three independent experiments and the error bars represent  $\pm$  standard error of mean.

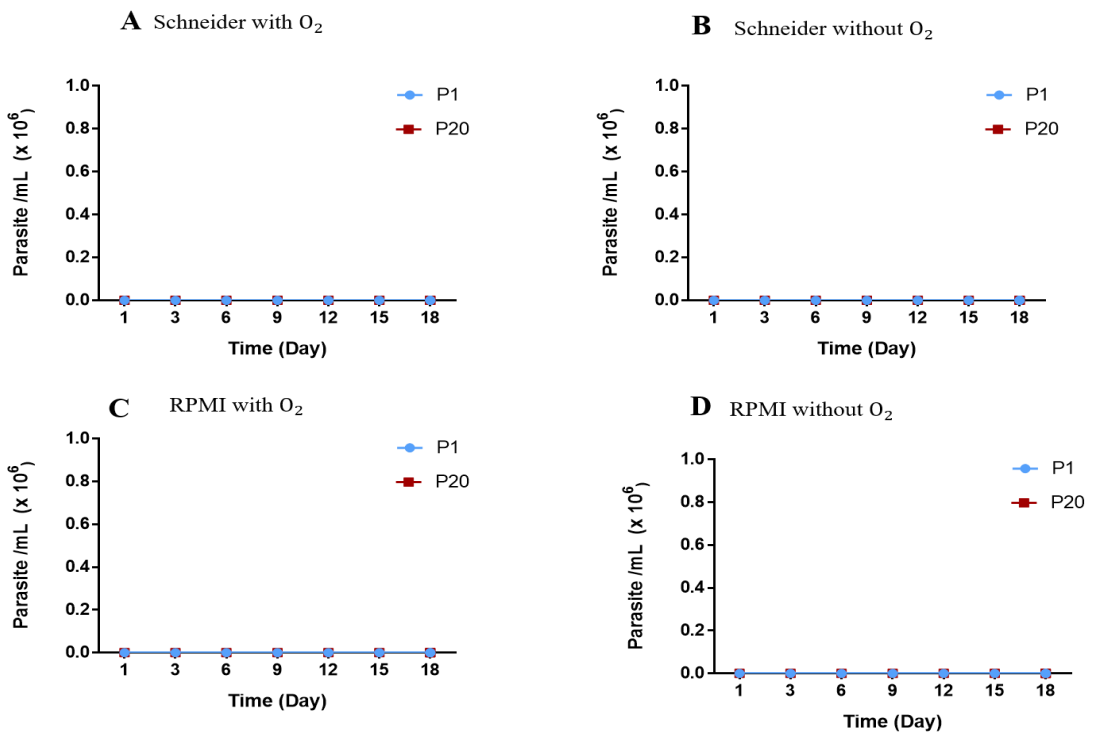


**Figure 3. 2: Growth curve of P1 and P20 cultured in RPMI 1640 or Schneider's *Drosophila* medium under aerobic and anaerobic conditions at 37°C**

One million P1 and P20 stationary phase promastigotes cultured under different conditions to assess the effect of media type (Schneider's *Drosophila* and RPMI1640 medium), oxygen in the volume of 5 mL ( $0.2 \times 10^6$  per mL). Parasites were counted by Neubauer hemocytometer after 48 hours of incubation. The data were analysed by using GraphPad Prism 7.

To confirm the effect of the RPMI1640 medium on the growth of P20 compared with P1, Alamar blue assay was used and the results are shown in figure 3.3., it should be mentioned that the RPMI1640 media was used as a control while Schneider's *Drosophila* medium was used as a growth test condition for P1 and P20 and the results were normalised to RPMI1640 media. It is clear from this figure that the growth of P20 was much greater than the control RPMI1640 medium, approximately 3 times greater than that of RPMI1640 medium. P1 does not show a significant difference between these two media at 25°C.

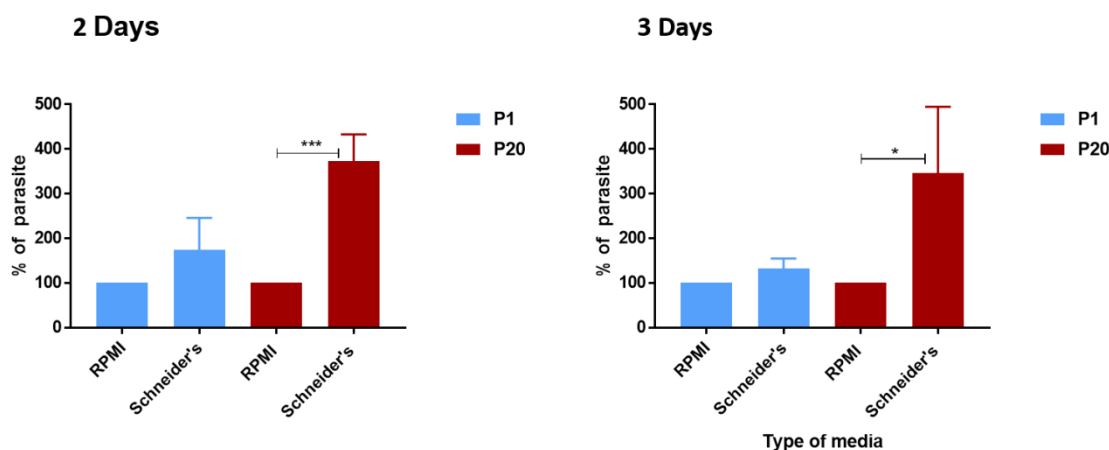


**Figure 3. 3: Effect of RPMI versus Schneider's *Drosophila* medium on P1 and P20 *L.mexicana* growth rate using Alamar blue assay**

One million P1 and P20 in stationary phase were seeded in 96 well plates, in 100  $\mu$ L volume, using RPMI or Schneider's *Drosophila* 10% HIFCS. Plates were covered and incubated at 25°C for 2 or 3 days. All wells were then stained with 10  $\mu$ L Alamar blue wrapped with foil for light protection. The percentage of parasites were calculated as recommended by the manufacturer and the results were normalised to control RPMI1640 medium. The data were analysed by using GraphPad Prism 7. Statistically significant differences between pairs of groups represented by \* $p < 0.05$ , \*\*\* $p < 0.0001$ , the P value was determined by unpaired t-test. The results are the average of three independent experiments and the error bars represent  $\pm$  standard error of mean.

### 3.2.2 Morphology of P1 and P20 *L. mexicana*

This experiment investigated the morphology of P1 and P20 parasites in the stationary phase cultured in Schneider's *Drosophila* and incubated anaerobically at 25°C (See the methodology, section 2.6).

Morphology was assessed by using a light microscope without staining, immunofluorescent FITC staining and Giemsa staining, electronic and atomic force microscopes were also used. By comparing morphology of P1 and P20, it was clear that the bodies of P20 promastigotes were larger than P1 (figure 3.4, 3.5, 3.6, 3.7, and 3.8). The difference between the body sizes of P1 and P20 was confirmed by physical measurement of the body length and width. The results showed that P20 width and length were significantly higher than that of P1. Regarding

the length of the flagellum, the results clearly showed that there was no significant difference between P1 and P20 (figure.3.9).

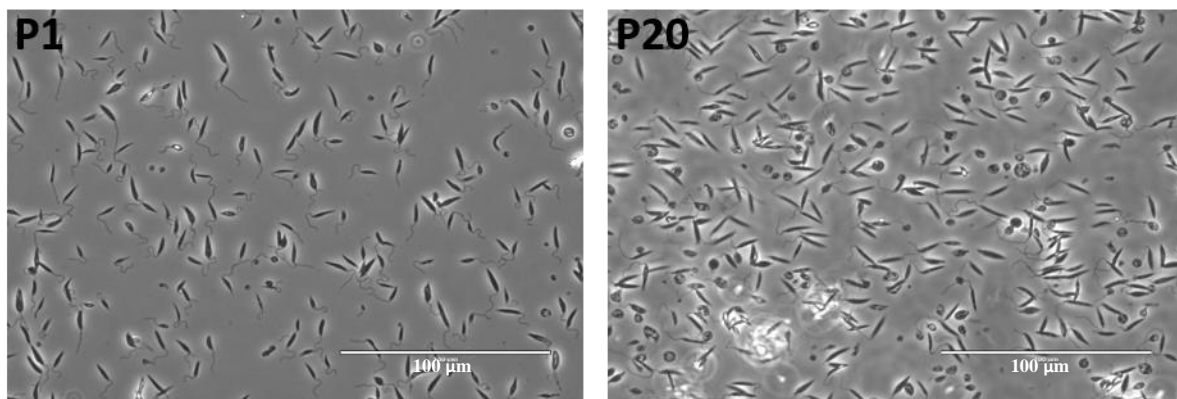


**Figure 3. 4 Morphology of P1 and P20 *L.mexicana* promastigotes under the light microscope.** P1 and P20 *L.mexicana* cultured in Schneider’s *Drosophila* medium at a concentration of  $1 \times 10^6$  promastigote/ mL for 3 days. 2 mL from each flask was collected and centrifuged at 200 g for 10 minutes and resuspended in 50 µL 1% paraformaldehyde. Wet slides were prepared and mounted with a cover slip and sealed by nail polish. Pictures were visualised by EVOS life technology microscope (40 X) transmitted light.

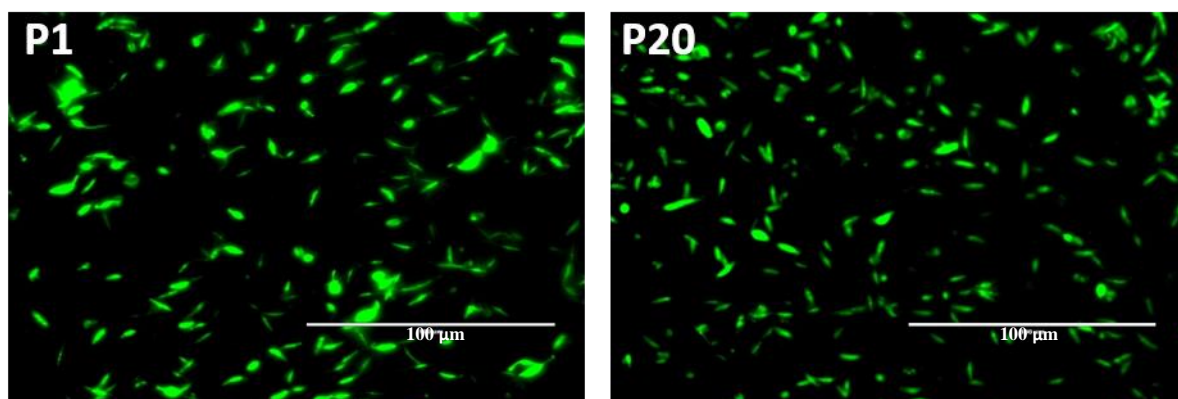


**Figure 3. 5: Morphology of P1 and P20 *L.mexicana* promastigotes stained with CFSE.** P1 and P20 *L.mexicana* cultured in Schneider’s *Drosophila* medium,  $20 \times 10^6$  were centrifuged at 200 g for 10 min and resuspended in 500µL RPMI 1640 10% HIFCS and stained with 10 ng CFSE and incubated for 30 minutes at 25°C. The parasites were washed 3 times with PBS and resuspended in 50 µL 1% paraformaldehyde. Wet slides were prepared and fixed with a cover slip by nail polish. Pictures were visualised by EVOS life technology microscope (40 X) GFP light (470/22 nm Excitation; 510/42 nm Emission)

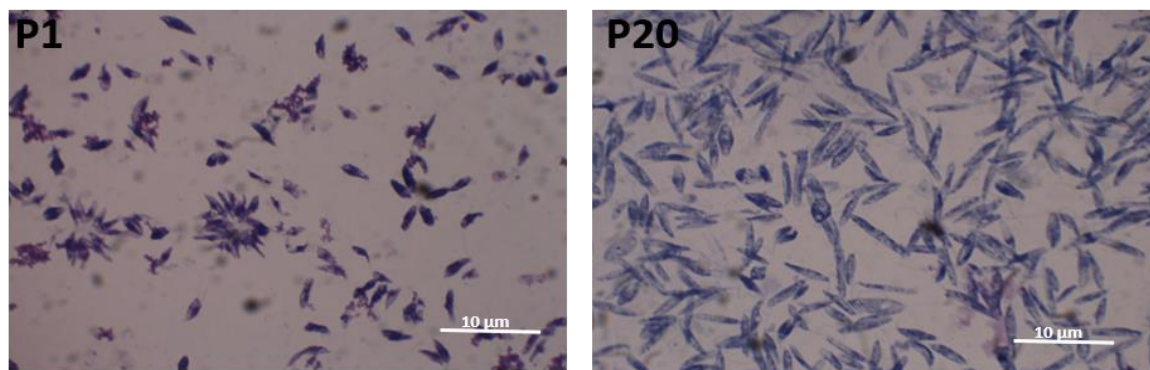


**Figure 3. 4: Morphology of P1 and P20 *L.mexicana* promastigotes stained with Giemsa** P1 and P20 *L. mexicana* cultured in Schneider’s *Drosophila* medium,  $20 \times 10^6$  were spun down at 200g for 10 min. direct smears were prepared. After drying at room temperature, slides were fixed with 100% methanol. Slides were stained with Giemsa modified stain and visualised by light microscope (Olympus) with oil immersion (100 X) and pictures were taken by euromax camera.

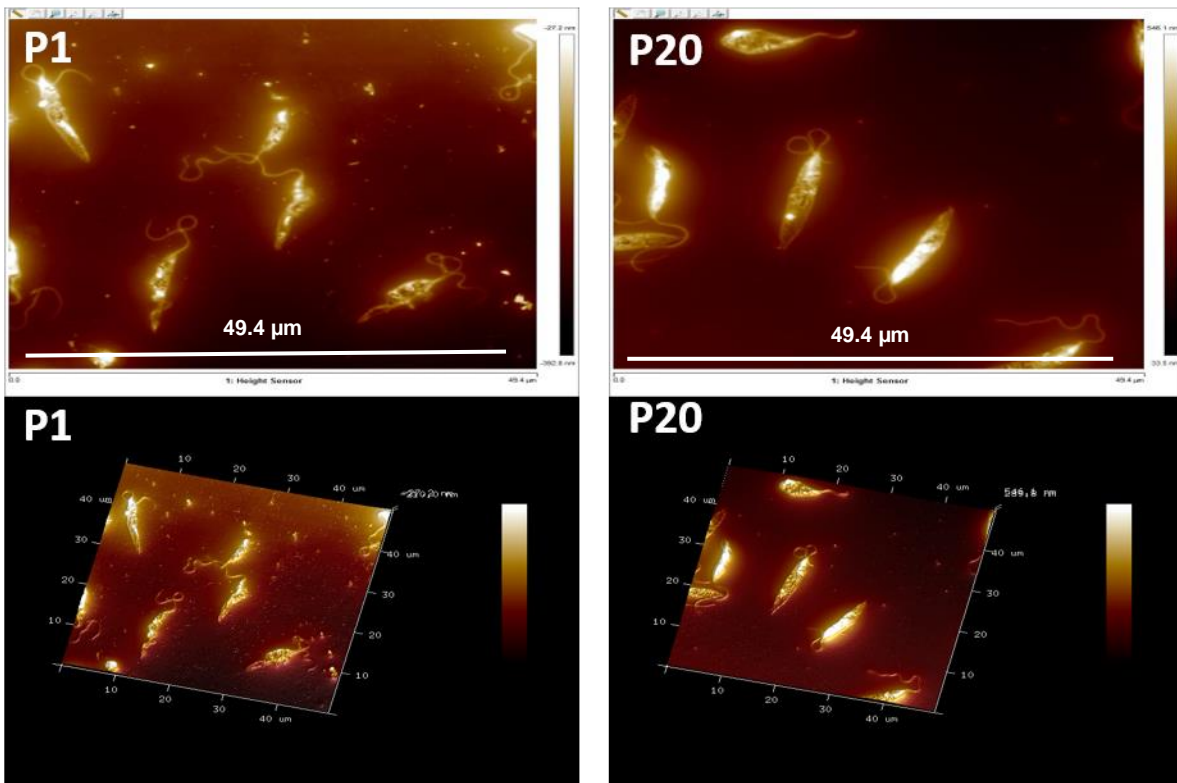


**Figure 3. 5: Morphology of P1 and P20 *L.mexicana* promastigotes under the Atomic Force microscopy.**

P1 and P20 *L.mexicana* cultured in Schneider's *Drosophila* medium,  $20 \times 10^6$  were spun down at 200g for 10 min. direct smears were prepared. After drying at room temperature, slides were fixed with 100% methanol. Pictures were taken by AFM (Atomic Force microscopy). The P20 body size are larger than P1 and the scale bar is 49.4  $\mu\text{m}$ .

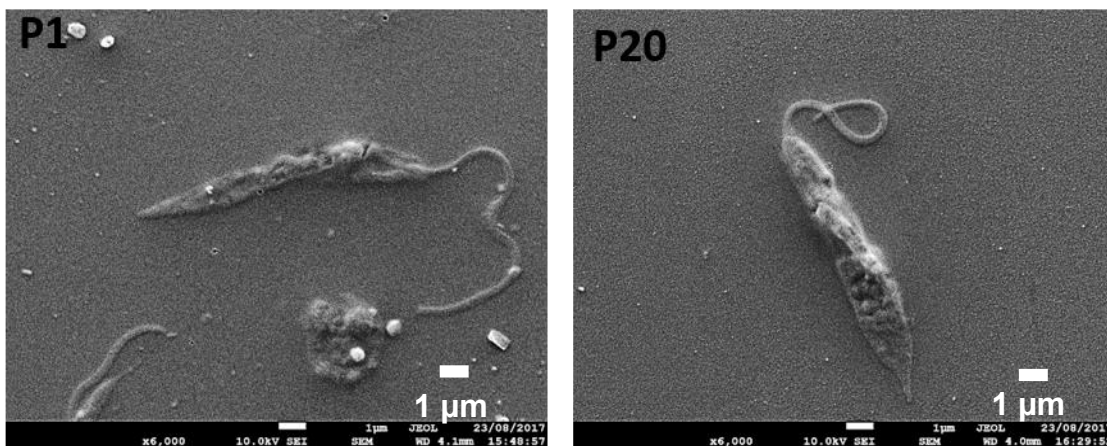


**Figure 3. 6: Morphology of P1 and P20 *L.mexicana* under the Electronic microscope**

P1 and P20 *L.mexicana* cultured in Schneider's *Drosophila* medium,  $20 \times 10^6$  were spun down at 200g for 10 min. Direct smears were prepared. After drying at room temperature, slides were covered by 10  $\mu\text{m}$  gold using Quorum (Q15OR ES) with  $19.32\text{g}/\text{m}^3$ . Pictures were taken by the Electron microscope. The P20 body is larger than P1.

The morphology of P1 and P20 promastigotes was investigated by using a light microscope (figure 3.4), CFSE staining (figure 3.5), Giemsa staining (figure 3.6), atomic force microscope (figure 3.7) and an electron microscope (figure 3.8). The results show that P20 promastigotes were larger than P1 where P1 average length is 8  $\mu\text{m}$  and P20 is 13  $\mu\text{m}$  (figure 3.9 B). The shape of P20 was rounded, elongated and looked more consistent than P1 while, P1 was spindle shape with the narrow end as demonstrated by AFM and Giemsa stain. Results from microscopy showed that the P20 appear larger than P1. This has been confirmed by taking measurements; length and width of the parasites which are shown below (figure 3.9).

### 3.2.3 Physical measurements of P1 and P20 promastigotes

The graphs below (figure 3.9) illustrate the physical measurements of P1 and P20 promastigote. Regarding the length of the flagellum, the results clearly show that there was no significant difference between P1 and P20 (figure 3.9A). Interestingly the length and width of P20 are significantly higher than P1 (figure 3.9 A). More precisely, P20 is larger than P1 significantly ( $p < 0.0001$ ). Because of P20 having a longer body length than P1, its flagellum to body length ratio was lower. The flagellum body ratio in P20 is approximately 1:1.5 compared with P1 1:1.

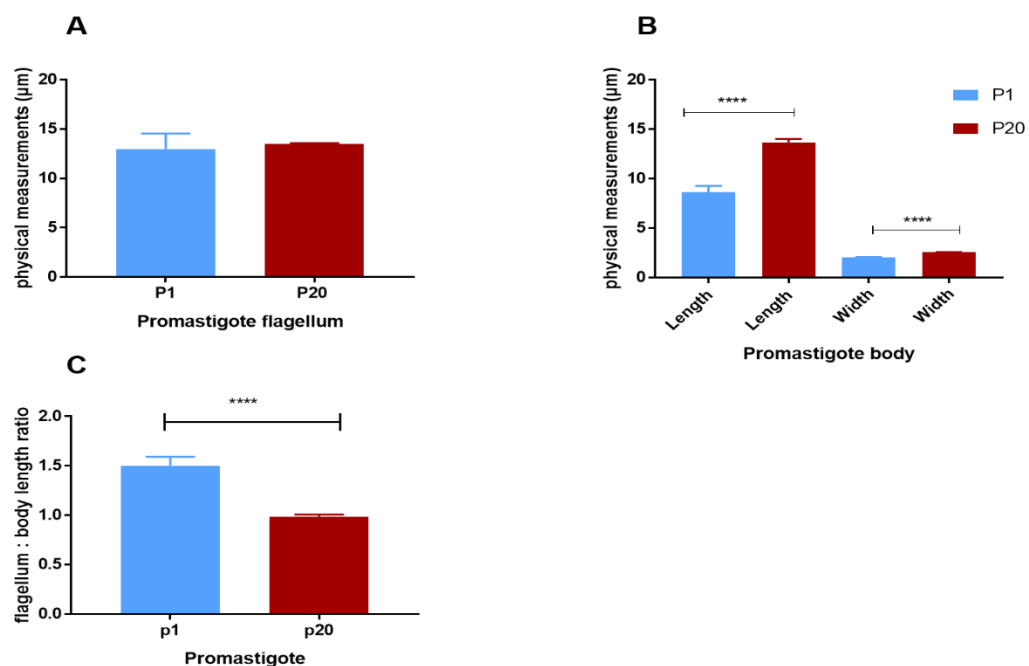


**Figure 3. 7: Cell size measurement of P1 and P20 *L. mexicana* promastigotes**

P1 and P20 were cultured at 25°C in Schneider's *Drosophila* medium containing 10% v/v HIFCS for three days. Pictures were taken using EVOS life technology microscope. Measurement of parasites was taken using NI vision assistant software. The measurement was converted from pixel to  $\mu\text{m}$  ( $1\mu\text{m} = 4.72$  pixel) according to scale given by EVOS microscope picture. Flagellum body ratio was calculated by dividing average flagellum length by average body length of 300 promastigotes. The data were analysed by using GraphPad Prism 7. Statistically significant differences between pairs of groups was represented by\*\*\* $p < 0.0001$ . P value was determined by unpaired t-test. The results are average of three independent experiments and the error bars represent  $\pm$  standard error of mean.

The physical measurements of P1 and P20 promastigotes were used to calculate the metacyclic stage using two different methods. Method, A, P1 has 21% of metacyclic promastigotes. While method B shows that P1 has 28% metacyclic promastigotes (figure 3.10 A). Interestingly, both methods show no metacyclic stage in P20.

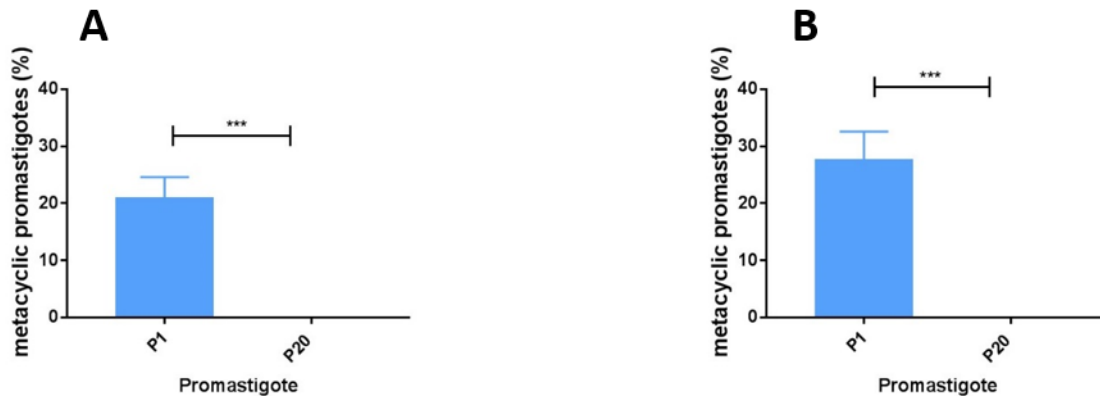


**Figure 3. 8: Percentage of metacyclic promastigotes of P1 and P20 *L. mexicana*.**

P1 and P20 were cultured at 25°C in Schneider's *Drosophila* media containing 10% v/v HIFCS for three days. Pictures were taken using EVOS life technology microscope. Measurement of parasites was estimated using NI vision assistant software. The measurement was converted from pixel into  $\mu\text{m}$  ( $1\mu\text{m}=4.72\text{pixel}$ ) according to scale given by EVOS microscope picture. Metacyclic stage of P1 and P20 was calculated by two methods. (A) calculation of flagellum: body ratio. Metacyclic promastigotes when the ratio is 2 or more (metacyclic forms promastigotes  $\frac{\text{Flagellum length}}{\text{Body length}} \geq 2$ ). The percentage of metacyclic was calculated. (B) by multiplying of Body length X body Width  $\leq 12$  (Body length  $\mu\text{m}$  X body width  $\mu\text{m}$ ) if its less or equal to 12 it is counted as metacyclic and then the percentage of metacyclic promastigotes were calculated in 100 parasites.

The data were analysed by using GraphPad Prism 7. Statistically significant differences between pairs of groups represented by\*\*\* $p < 0.0001$ , The P value was determined by unpaired t-test. The results are the average of three independent experiments and the error bars represent  $\pm$  standard error of mean.

### 3.2.4 Differentiation of P1 and P20 *L. mexicana* into amastigotes.

P1 but not P20 *L. mexicana* promastigotes can differentiate following a temperature shift from 25°C into 37°C into non-flagellated round form amastigotes (figure 3.11). This differentiation was accompanied by a number of morphological changes, such as cell size reduction, and modulation of gene expression of LPG1, LPG2, GP63, CPB2, CPB2.8 and A2. Changes in surface LPG expression were also observed.

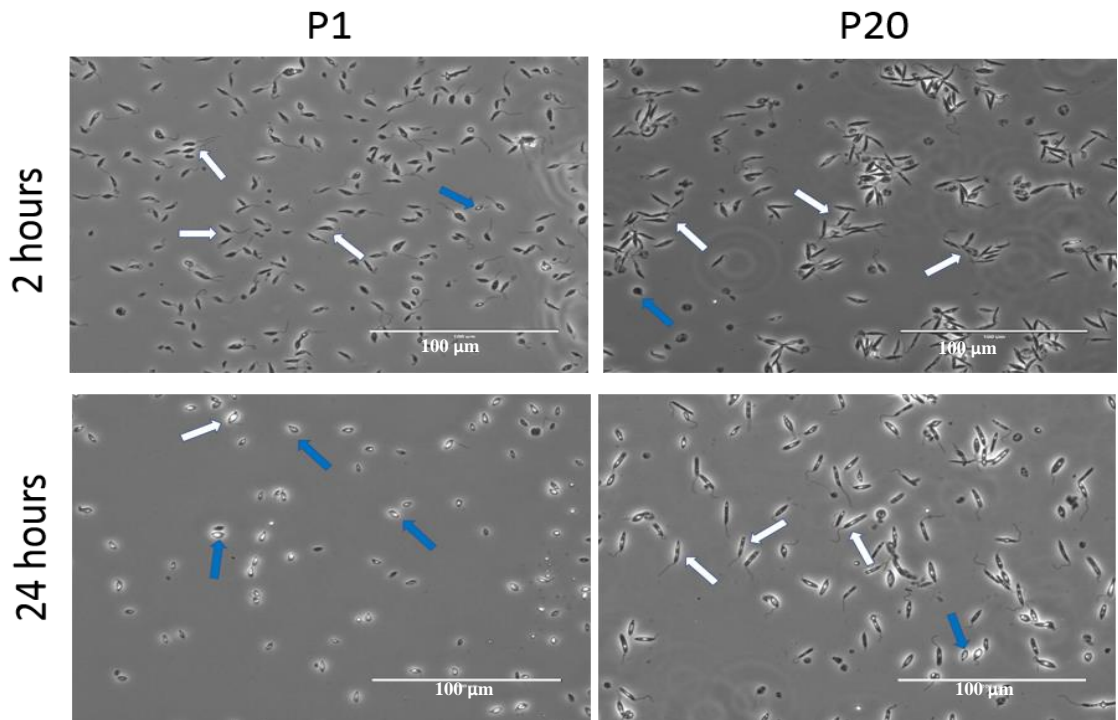


**Figure 3. 9: Differentiation of P1 and P20 *L. mexicana* into amastigotes in absence of mammalian cells**

20 x 10<sup>6</sup> of P1 and P20 *L. mexicana* promastigotes were cultured in 2.5 mL RPMI 1640 medium (10% v/v HIFCS) in vented T25 flasks. P1 and P20 parasites were incubated in 95% v/v humidity at 37 °C in 5% v/v CO<sub>2</sub> incubator for 2 and 24 hours. 2 mL from each flask was collected and centrifuged at 200g for 10 min and resuspended in 50 μL of 1% paraformaldehyde. Wet slides were prepared and mounted with a cover slip and sealed by nail polish. Pictures were visualised by EVOS life technology (40 X) transmitted light microscope. The white arrows indicate promastigotes and blue arrows indicate amastigotes.

Therefore, the number of promastigotes in both P1 and P20 decreased after incubation at 37°C for 24 hours as determined by Neubauer hemocytometer counting. The number of promastigotes of P1 but not P20 declined after 2 hours of incubation. At 24 hours the number P1 promastigotes are significantly lower than P20 (figure 3.12).

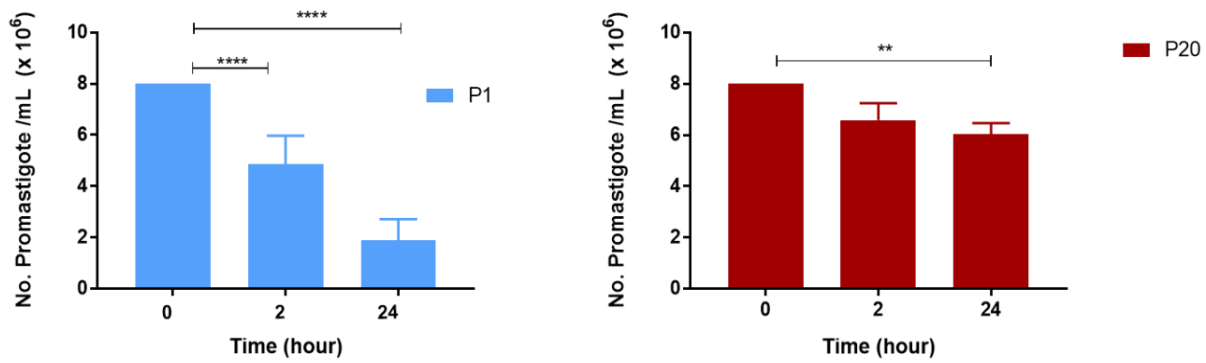


**Figure 3.10: Effect of incubation of P1 and P20 promastigotes in RPMI 1640 at 37°C**

8 x 10<sup>6</sup> /mL P1 and P20 *L. mexicana* promastigotes at stationary phase were cultured in RPMI 1640 medium (10% v/v HIFCS) in vented T25 flasks. P1 and P20 parasites were incubated in a 95% v/v humidity at 37 °C in 5% v/v CO<sub>2</sub> incubator. Promastigote parasite number before incubation was used as a control. Numbers of promastigotes were counted after 2 and 24 hours of incubation using Neubauer hemocytometer. The data were analysed by GraphPad Prism 7. Statistically significant differences between each group represented by \*\*p<0.001, \*\*\*p<0.0001 \*\*\*\*p<0.00001, and P value was determined by unpaired t-test. The results are average of three independent experiments and the error bars represent ± standard error of mean.

By counting the number promastigotes after incubation using Neubauer hemocytometer, the results show that after 2 hours the number of P1 but not P20 promastigote had decreased significantly compared to the control. Although, both P1 and P20 decreased significantly after 24-hour incubation, P1 was significantly lower than P20.

### 3.2.5 Effect of temperature oxygen, medium type, and incubation time on the ability of P1 and P20 *L.mexicana* to differentiate into amastigotes.

In order to examine the ability of P1 and P20 promastigotes to differentiate into amastigotes, the effect of 2- and 24-hour incubation at 37°C compared with 25°C on the differentiation of P1 and P20 promastigotes into amastigotes was investigated by counting the percentage of amastigotes at each incubation time point using EVOS life technology microscope transmission power 40 where rounded parasites without flagellum counted as amastigotes and elongated ones with flagellum counted as promastigotes.

The results show that there was no significant difference in the ability of P1 and P20 *L.mexicana* to differentiate from promastigote into amastigotes when cultured at 25°C either in RPMI1640 or Schneider's *Drosophila* with or without O<sub>2</sub> at the three different time points 2, 24 and 48 hours (figure 3.13 and 3.14). However, when the temperature shifted to 37°C differentiation was observed at 24 and 48 but not 2 hours. Interestingly the percentage of

amastigotes in P1 reached approximately 80% while in P20 is 10% without the effect of media type and O<sub>2</sub>.

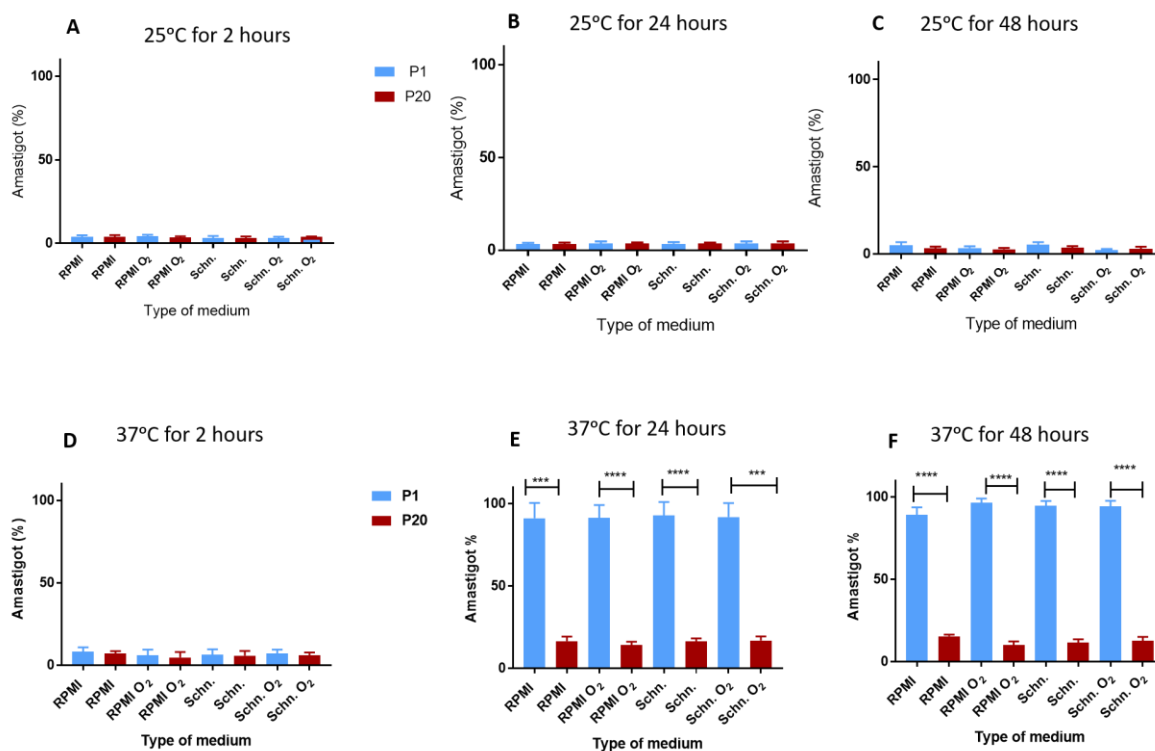


**Figure 3. 11: Differentiation of P1 and P20 *L. mexicana* promastigotes into amastigotes after 2, 24- and 48-hours incubation at 25 and 37°C with or without O<sub>2</sub>**

8 x 10<sup>6</sup> /mL P1 and P20 *L. mexicana* promastigotes at stationary phase were cultured in RPMI 1640 and Schneider's *Drosophila* medium (10% v/v HIFCS). P1 and P20 were cultured in vented or unvented T25 tissue culture flasks and incubated at 25°C and 95% v/v humidity at 37 °C in 5% v/v CO<sub>2</sub> incubator for 2, 24, and 48 hours. Amastigotes and promastigotes were counted per microscopic field and, percentage of amastigotes was calculated. The pictures were taken using EVOS life technology microscope transmission power 40 at 3 different time points. Amastigotes and promastigotes were counted per microscopic field and, percentage of amastigotes were calculated for 100 parasites. The data were analysed by using GraphPad Prism 7. Statistically significant differences between each represented by \*\*\*p<0.0001, \*\*\*\*p<0.00001. The P value was determined by unpaired t-test. The results are average of three independent experiments and the error bars represent ± standard error of mean.

*Leishmania* parasites were exposed to two different conditions that differ significantly between insect vector and mammalian host in temperature, pH and nutrients. The effect of RPMI1640 and Schneider's *Drosophila* media, temperature and oxygen on the ability of P1 and P20 promastigotes to differentiate into amastigotes was investigated at 3 incubation time points. The results clearly show that both P1 and P20 *L.mexicana* were unable to differentiate into amastigotes when cultured at 25°C after 2, 24 and 48 hours (figure 3.13 A, B and C). When P1 and P20 were incubated at 37°C, the results show that after 2 hours there was also no significant difference. After 24 and 48 hours, the results show a significant difference in both P1 and P20 without being affected by oxygen or type of media (figure 3.13 D, E and F).

### 3.2.6 Effect of pH on the ability of P1 and P20 *L.mexicana* promastigotes to differentiate into amastigotes.

In order to examine the ability of P20 promastigotes to differentiate into amastigote under the ideal conditions (5.5 pH and 37 °C), the effect of pH on the ability of P1 and P20 promastigotes to differentiates into amastigotes was investigated, like the previous experiment was designed but with pH 5.5 medium.

20 x 10<sup>6</sup> P1 or P20 *L. mexicana* promastigotes were cultured in media of 5.5 pH. RPMI1640 and Schneider's *Drosophila* medium (10% v/v HIFCS), in vented and unvented T25 tissue culture flasks and incubated at 25°C and 95% v/v humidity at 37 °C in 5% v/v CO<sub>2</sub> incubator for 2, 24, and 48 hours. The culture was examined under microscope and pictures were taken using EVOS life technology microscope transmission power 40. Amastigotes and promastigotes were counted per microscopic field and the percentages of amastigotes were calculated.

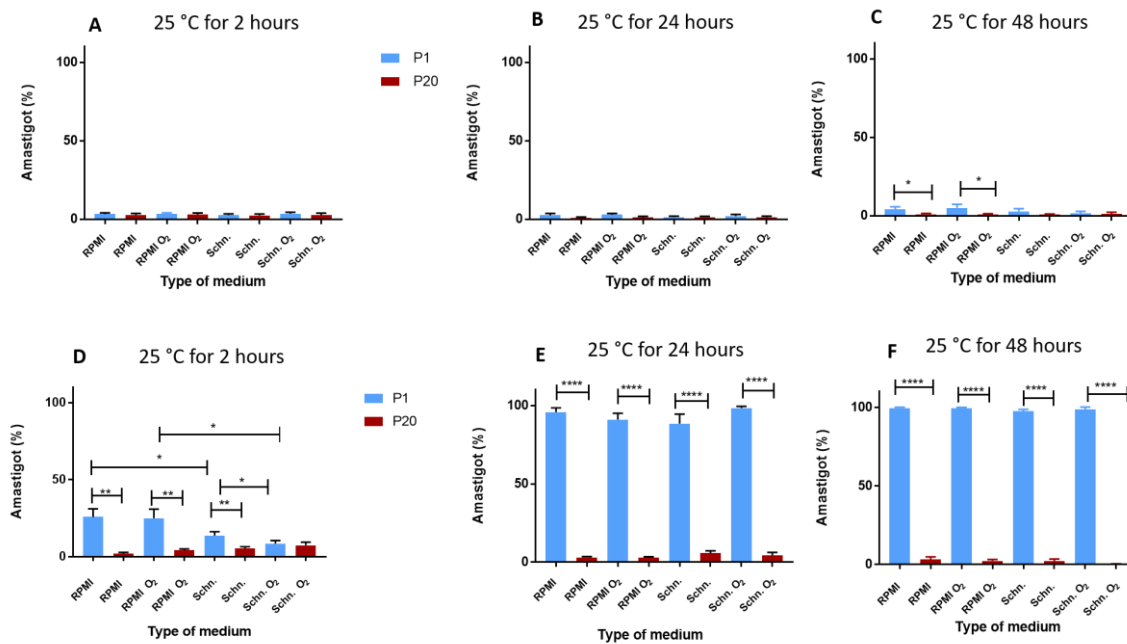


**Figure 3.12: Differentiation of p1 and p20 *L. mexicana* promastigotes to amastigotes after 2, 24- and 48-hours' incubation in pH 5.5 medium at 25°C and 37°C.**

20 x 10<sup>6</sup> P1 and P20 *L. mexicana* promastigotes were cultured in 2.5 mL RPMI 1640 or Schneider's *Drosophila* medium 10% v/v HIFCS and pH was adjusted to 5.5 in vented or unvented T25 tissue culture flasks. P1 and P20 parasites were incubated at two different temperatures, in a 25°C incubator and 95% v/v humidity at 37°C in 5% v/v CO<sub>2</sub> incubator.

The pictures were taken using EVOS life technology microscope transmission power 40 at 3 different time points. Amastigotes and promastigotes were counted per microscopic field and, percentage of amastigotes were calculated in 100 parasites.

The data were analysed by using GraphPad Prism 7. Statistically significant differences between each group are represented by \*p<0.05, \*\*p<0.001, \*\*\*\*p<0.00001. P value was determined by unpaired t-test. The results are average of three independent experiments and the error bars represent ± standard error of mean.

There was no significant observable differentiation of P1 and P20 promastigotes into amastigotes when cultured at 25°C for 2 or 24 hours. However, there was a slight increase

in P1 differentiation into amastigotes at 48 hours incubation in RPMI1640 but not Schneider's *Drosophila* medium either with or without O<sub>2</sub> and pH 5.5. When P1 but, not P20 promastigotes were incubated at 37°C, P1 differentiated into the amastigote form at lower pH medium earlier than normal medium and, the ability of P1 to differentiate into amastigotes was significantly higher than P20 when cultured in either RPMI1640 with or without O<sub>2</sub> and in Schneider's *Drosophila* medium without O<sub>2</sub> and pH 5.5.

The results show that the ability of P1 promastigote to differentiate into amastigotes was increased with incubation time, with a sharp increase after 24 hours either at normal pH (figure 3.13 E) or in acidic medium (figure 3.14 E). The ability of P1 promastigotes to differentiate into amastigotes was significantly higher than that of P20 under all tested conditions, whether they were cultured at 25°C or 37°C in either RPMI1640 with or without O<sub>2</sub> or in Schneider's *Drosophila* medium without O<sub>2</sub> and pH 5.5. It is noteworthy that the Schneider's *Drosophila* medium pH is 6.5 to 6.8 while, pH of RPMI1640 medium is 6.8 to 7. From the results of these experiments it is evident that the main factor in the ability of parasites to differentiate into amastigotes is temperature.

### **3.2.7 The ability of P1 and P20 *L. mexicana* to differentiate into amastigotes**

Another interesting phenomenon reported in this study is that the ability of P1 to differentiate into a round form amastigote is significantly higher in P1 than P20 in all experimental conditions. The effect of RPMI1640 and Schneider media at a pH of 5.5, temperature and oxygen on the ability of P1 and P20 to differentiate into amastigotes was investigated at 3-time points (figure 3.13 and 3.14).

#### **3.2.7.1 Effect of pH 5.5 and 25°C temperature on ability of P1 and P20 *L. mexicana* to differentiate into amastigotes**

After decreasing media pH to 5.5 the results show that there was no significant difference in the ability of P1 and P20 to differentiate into amastigotes when they were cultured at 25°C at 2 and 24 hours of incubation. After 48 hours incubation in RPMI1640 medium but not Schneider's *Drosophila* either with or without O<sub>2</sub>, there was a slight increase in the percentage of amastigotes in P1 but not P20 (figure 3.14 F).

#### **3.2.7.2 Effect of pH 5.5 and 37°C temperature on ability of *L. mexicana* P1 and P20 to differentiate into amastigotes**

After 2 hours incubation at 37°C, the percentage of amastigotes of P1 but not P20 increased significantly in RPMI1640 medium either with or without O<sub>2</sub>. In Schneider's *Drosophila*

medium, the percentage of amastigotes was higher in P1 than P20 when incubated without oxygen. After 24 and 48 hours, the percentage of P1 amastigote increased rapidly and reached approximately 100% under all the experimental conditions.

*L. mexicana* lost the ability to differentiate into amastigotes after 20 passages and the main factor that affects differentiation in P1 is temperature rather than pH. The presence or absent of O<sub>2</sub> did not affect the differentiation except the absence of oxygen showed a slight increase in Schneider's *Drosophila* medium after 2-hour incubation at 37 °C (figure 3.14 D).

### 3.2.7.3 Effect of incubation time on ability of P1 and P20 *L. mexicana* to differentiate into amastigotes

There was an effect of incubation time on the differentiation of promastigotes into amastigotes as after 24 hours the percentage of amastigotes in P1 sharply increased to reach between 80% and 100%. Therefore, the differentiation of promastigotes into amastigotes requires at least 24 hours of incubation at 37°C (figure 3.13 E and 3.14 E).

### 3.2.7.4 Effect of type of medium on the ability of P1 and P20 *L. mexicana* to differentiate into amastigotes

The ability of *Leishmania* to differentiate into amastigotes is higher in RPMI1640 1640 than Schneider's *Drosophila* only when parasites were incubated at 37 °C for 2 hours at pH 5.5.

## 3.2.8 Effect of parasite concentrations on the RPMI1640 medium pH after 2- and 24-hours incubation at 37°C

**Table 3. 1: Effect of parasite concentration on the RPMI medium pH after 2- and 24-hours' incubation at 37 °C without mammalian cells**

Incubation time	Parasite concentration	pH of P1	pH of P20
2 hours	2 x 10 <sup>6</sup> /mL	7	7
	4 x 10 <sup>6</sup> /mL	7	7
	6 x 10 <sup>6</sup> /mL	7	7
	8 x 10 <sup>6</sup> / mL	7	7
24 hours	2 x1 0 <sup>6</sup> /mL	7	7
	4 x 10 <sup>6</sup> /mL	7	7
	6 x 10 <sup>6</sup> /mL	7	7
	8 x 10 <sup>6</sup> / mL	6	6

In T25 P1 and P20 *L. mexicana* promastigotes were incubated in RPMI1640 medium 10% v/v HIFCS at four different concentrations 2 x 10<sup>6</sup>, 4 x 10<sup>6</sup>, 6 x 10<sup>6</sup> and 8 x 10<sup>6</sup> /mL and incubated at 95% v/v humidity at 37°C in a 5% v/v CO<sub>2</sub> incubator. pH of the media was measured after 2- and 24-hours incubation.

The concentration of parasites may affect the pH of the media which may reflect on the differentiation of parasites into amastigotes. Therefore, this experiment was designed to study effect of pH at four different concentrations of the parasite in RPMI1640 media supplemented with 10% v/v HIFCS. Litmus paper was used in order to estimate the pH of the medium. This medium will be also used for parasite-mammalian host cell interaction experiments. The results show that after 2 hours incubation, the pH of the RPMI1640 medium did not change for both P1 and P20 parasites at all concentrations tested. After 24 hours, the pH decreased to 6 in both P1 and P20 with a concentration of  $8 \times 10^6$ / mL. Therefore, this concentration which has been used in these experiments may offer the pH that may help parasites to differentiate into amastigotes.

### 3.2.9 Effect of parasite concentration on the RPMI1640 medium pH after 2- and 24-hours incubation at 37°C when incubated with mammalian cells

**Table 3. 2: Effect of parasites concentration on the RPMI1640 medium pH after 2- and 24-hours' incubation at 37°C with mammalian cells**

Incubation time	<i>L. mexicana</i>	pH
2 hours	P1 control	7
	P20 control	7
	P1 / Balb/c	7
	P20 / Balb/c	7
	P1 / C57	7
	P20 / C57	7
24 hours	P1 control	6
	P20 control	6
	P1/ Balb/c	6
	P20 / Balb/c	6
	P1 / C57	6
	P20 / C57	6

$1 \times 10^6$  Balb/c and C57 macrophages infected with  $1 \times 10^6$  P1 and P20 at concentration  $8 \times 10^6$  /mL in RPMI1640 medium 10% v/v HIFCS. Parasites alone without mammalian cells were used as a control. All flasks were incubated at and 95% v/v humidity at 37 °C in 5% v/v CO<sub>2</sub> incubator. pH of the media was measured after 2- and 24-hours incubation. The results clearly showed that using  $8 \times 10^6$  /mL parasite concentration lead to a decrease the medium pH from 7 into 6 either with or without mammalian macrophages.

Another experiment was designed to examine the effect of parasite concentration with or without Balb/c and C57 BMDM after 2- and 24-hours incubation at 95% v/v humidity at 37°C in 5% v/v CO<sub>2</sub> incubator. In T 25 vented flasks, 8 x10<sup>6</sup> /mL P1 and P20 promastigotes were seeded in RPMI1640 medium 10% v/v HIFCS with and without 8 x10<sup>6</sup> mammalian macrophages.

The pH of RPMI1640 medium did not change when P1 and P20 at a concentration of 8 x10<sup>6</sup> /mL were incubated for 2 hours. Similarly, when the same number of P1 and P20 parasites was incubated with Balb/c and C57 macrophage cell lines for 2 hours no change in pH occurred. Based on these results it can be concluded that the 8 x10<sup>6</sup> /mL concentration of parasite led to a decrease in the medium pH from 7 to 6, which provides a good medium for differentiation of the parasite into amastigotes.

P1 and P20 that were cultured in the same conditions but without oxygen were faster and higher in growth rate than with oxygen. In addition, P20 cultured in Schneider's *Drosophila* medium without oxygen at 25°C reached its growth peak faster than P1.

### **3.2.10 Effect of 20 passages *in vitro* on virulence-associated gene expression of *L. mexicana***

Gene expression analysis is a powerful tool for understanding the molecular mechanisms that regulate *Leishmania* life cycle progression and host-parasite interactions. The effects of 20 continuous passages of *L. mexicana in vitro* on virulence-associated gene regulation was assessed by qPCR. Briefly, total RNA was extracted from the stationary phase at passages P1 and P20, and transcribed into cDNA, which was used for qPCR analysis. All virulence associated genes of P20 promastigotes examined (LPG1, LPG2, A2, CHAT1, CPB2, CPB2.8, CPC, GP63, LACK, and MAPK9) were significantly downregulated compared to control P1 promastigotes; though MAPK9 was the least downregulated (figure 3. 15).

Further experiments were conducted on P1 and P20 to determine the effect of *in vitro* passaging on the expression of differentiation-associated genes (LPG1, LPG2, CPB2, CPB2.8, and A2) which aids transformation from promastigotes into amastigotes after 2 and 24 hours by qPCR. In addition, Immunofluorescence and flow cytometry staining using anti-LPG monoclonal antibodies were used to estimate the expression of LPG protein.

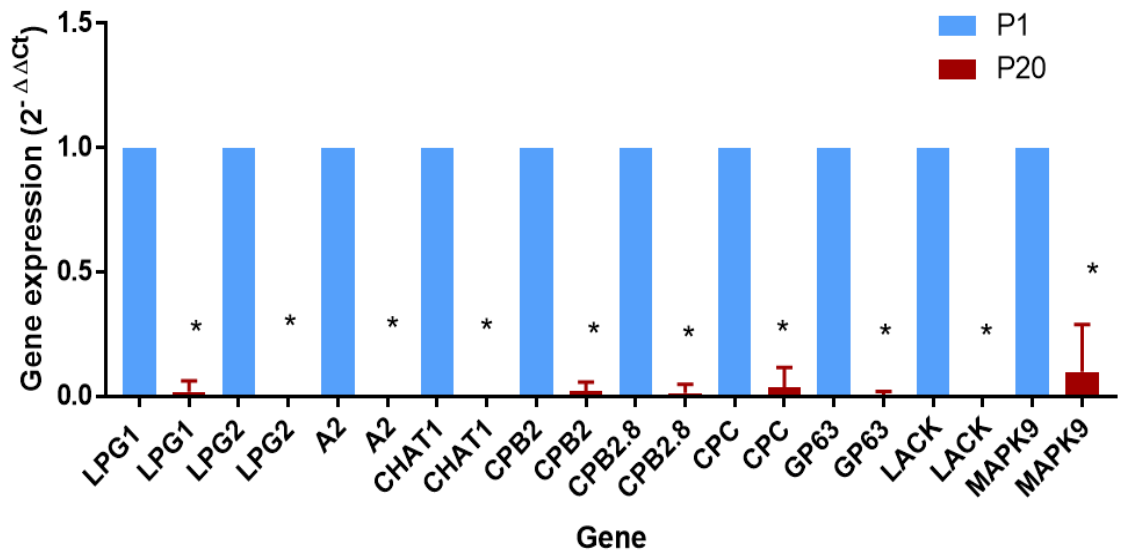


**Figure 3. 13: Effect of 20 passages *in vitro* on virulence gene expression**

Virulence gene regulation of P20 compared with P1 was assessed by qPCR. P1 and P20 were cultured at 25°C in Schneider’s *Drosophila* media containing 10 v/v HIFCS for three days. At stationary phase, 40 x 10<sup>6</sup> parasites were harvested, and total mRNA was extracted, then converted into cDNA and subjected to qPCR. qPCR results were normalized using the housekeeping gene “GAPDH” and Ct values were calculated as 2<sup>-ΔΔCt</sup>.

The data were analysed by using GraphPad Prism 7. Statistically significant differences between pairs of groups represented by \*p<0.0001. The p value was determined by unpaired t-test. The results are average of four independent experiments and the bars represent ± standard error of mean.

### 3.2.11 The effects of culturing of P1 and P20 *L.mexicana* in differentiation conditions for 2 and 24 hours on the expression of differentiation-associated genes regulation

#### 3.2.11.1 The effects of incubation of P1 and P20 at 37°C for 2 and 24 hours on GP63, CPB and CPB2.8 genes regulation

The results clearly show that GP63 was downregulated when P1 and P20 promastigotes were incubated in differentiation conditions (37 °C) for 2 and 24 hours. After 2 hours incubation, GP63 in P1 was significantly lower than that in P20, while, at 24 hours incubation, GP63 in both P1 and P20 was downregulated compared with promastigote control.

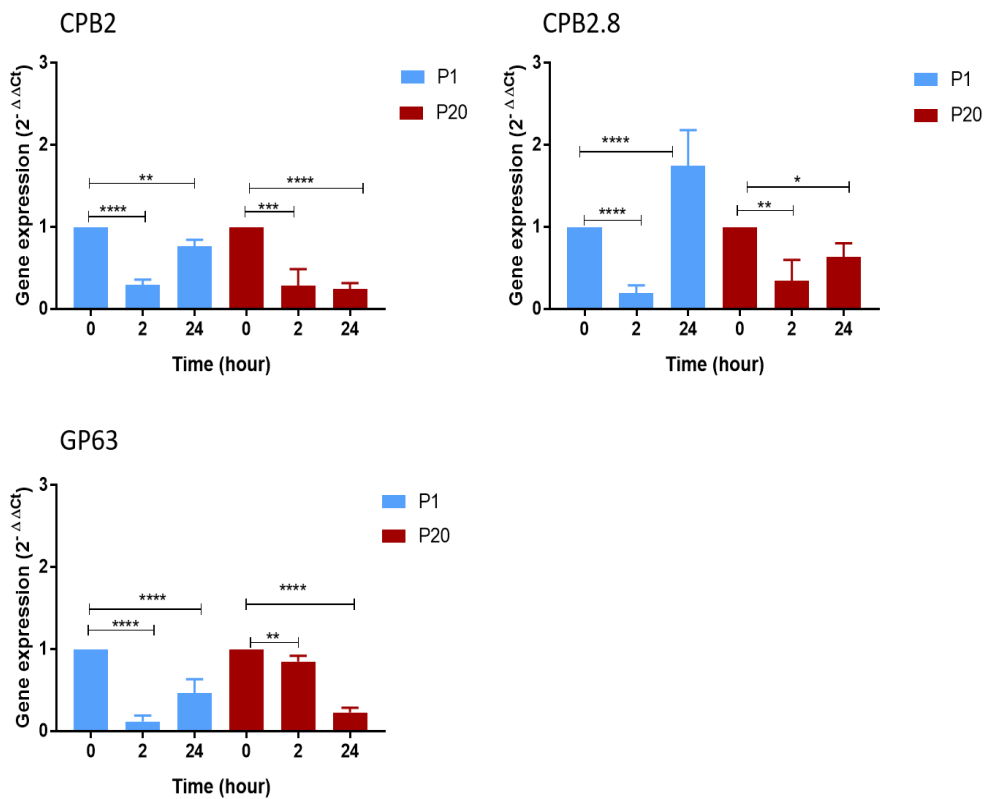


**Figure 3. 14: Effect of 2- and 24-hours incubation at 37°C on GP63, CPB2 and CPB2.8 gene regulation in P1 and P20.**

P1 and P20 were cultured at 25°C in Schneider's *Drosophila* media containing 10 v/v HIFCS for three days. At stationary phase, 40 x 10<sup>6</sup> parasites were harvested, and subjected to total RNA extraction for the control group, another 40 x 10<sup>6</sup> parasites were cultured in RPMI 1640 media containing 10% v/v HIFCS, in vented flask and incubated in 95% v/v humidity at 37 °C in 5% v/v CO<sub>2</sub> incubator for 2 and 24 hours. Total mRNA was extracted, converted into cDNA and subjected to qPCR. qPCR results were normalized using the housekeeping gene GAPDH and Ct values were calculated as 2<sup>-ΔΔCt</sup>.

The data were analysed by using GraphPad Prism 7. Statistically significant differences between pairs of groups represented by \*\*\*\*p<0.00001 and \*\*p<0.001. P value was determined by unpaired t-test. The results are the average of three independent experiments and the error bars represent ± standard error of mean.

Incubation of P1 and P20 promastigotes at 37°C for 2 and 24 hours, caused downregulation of CPB2 in both parasite populations. Only CPB2.8 was significantly upregulated in P1 parasites when cultured for 24 hours but not 2 hours at 37°C. The gene expression of LPG1, LPG2, GP63 and CPB were downregulated in promastigotes when the temperature of the culture was shifted from 25°C to 37°C.

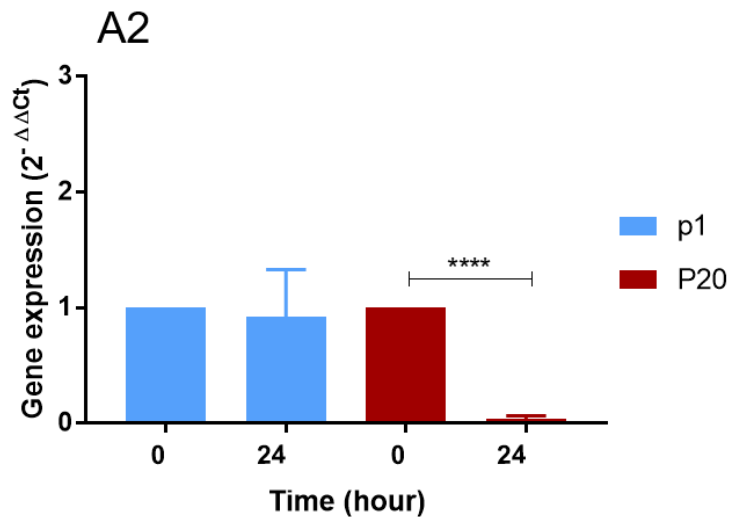


**Figure 3. 15: The effects of culturing P1 and P20 *L.mexicana* promastigotes under amastigote differentiation conditions for 24 hours on A2 genes regulation**

P1 and P20 promastigotes were cultured at 25°C in Schneider's *Drosophila* media containing 10 v/v HIFCS for three days. At stationary phase, 40 x 10<sup>6</sup> parasites were harvested, and subjected to total RNA extraction for the control group, another 40 x 10<sup>6</sup> parasites were cultured in RPMI 1640 media containing 10% v/v HIFCS, in a vented flask and incubated in 95% v/v humidity at 37 °C in 5% v/v CO<sub>2</sub> incubator for 24 hours. Differentiation of P1 and P20 were checked by a light microscope. Total mRNA was extracted, converted into cDNA and subjected to qPCR. qPCR results were normalized using the housekeeping gene GAPDH and Ct values were calculated as 2<sup>-ΔΔCt</sup>.

The data were analysed by using GraphPad Prism 7. Statistically significant differences between pairs of groups represented by \*\*\*\*p<0.00001. P value was determined by unpaired t-test. The results are average of three independent experiments and the error bars represent ± standard error of mean.

### 3.2.11.2 The effects of incubation of P1 and P20 *L.mexicana* promastigotes at 37°C for 2 and 24 hours on LPG1 and LPG2 gene regulation

The effects of incubation of P1 and P20 at 37°C on LPG1 and LPG2 gene regulation for 2 and 24 hours was investigated by qPCR. The results show that incubation of *L. mexicana* at 37°C modified LPG1 expression (figure 3.18). After 2 and 24 hours of incubation, LPG in both P1 and P20 was significantly downregulated compared to the control which was incubated at 25°C. Moreover, after 24 hours of incubation, LPG1 and LPG2 regulation of P1 is significantly lower than P20.

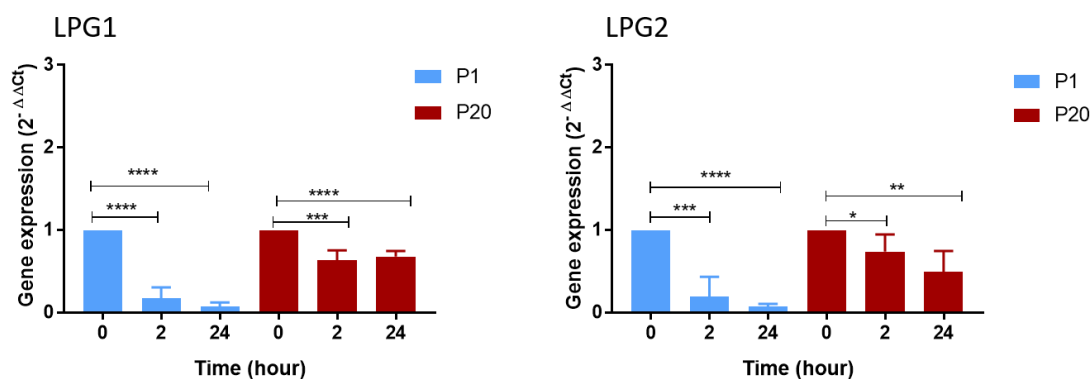


**Figure 3. 16: The effects of culturing of P1 and P20 *L.mexicana* in amastigote differentiation conditions for 2 and 24 hours on LPG1 and LPG2 gene regulation**

P1 and P20 promastigotes were cultured at 25°C in Schneider's *Drosophila* media containing 10% v/v HIFCS for three days. At stationary phase, 40 x 10<sup>6</sup> parasites were harvested, and subjected to total RNA extraction for the control group, another 40 x 10<sup>6</sup> parasites were cultured in RPMI 1640 media containing 10% v/v HIFCS, in a vented flask and incubated in 95% v/v humidity at 37 °C in 5% v/v CO<sub>2</sub> incubator in for 2 and 24 hours. Total mRNA was extracted, converted into cDNA and subjected to qPCR. qPCR results were normalized using the housekeeping gene GAPDH and Ct values were calculated as 2<sup>-ΔΔCt</sup>.

The data were analysed by using GraphPad Prism 7. Statistically significant differences between pairs of groups represented by \*\*\*\*p<0.00001, \*\*\*p<0.0001, \*\*p<0.001 and \*p<0.05 P value was determined by unpaired t-test. The results are the average of three independent experiments and the error bars represent ± standard error of mean.

### 3.2.11.3 Detection of LPG on P1 and P20 *L.mexicana* promastigotes by immunofluorescent microscopy and flow cytometry

Expression of LPG on the surfaces of P1 and P20 promastigotes was assessed by immunofluorescence and flow cytometry by using LPG antibody CA7AE. The CA7AE antibody can recognise LPG epitopes on both P1 and P20 *L.mexicana* (Favila *et al.*, 2015). The results clearly showed that the expression of LPG was significantly higher in P1 than P20 as assessed by immunofluorescent microscopy (figure 3.19) and flow cytometry (figure 3.20), where approximately 60% of P1 and 10% of P20 promastigotes stained positive with this antibody.

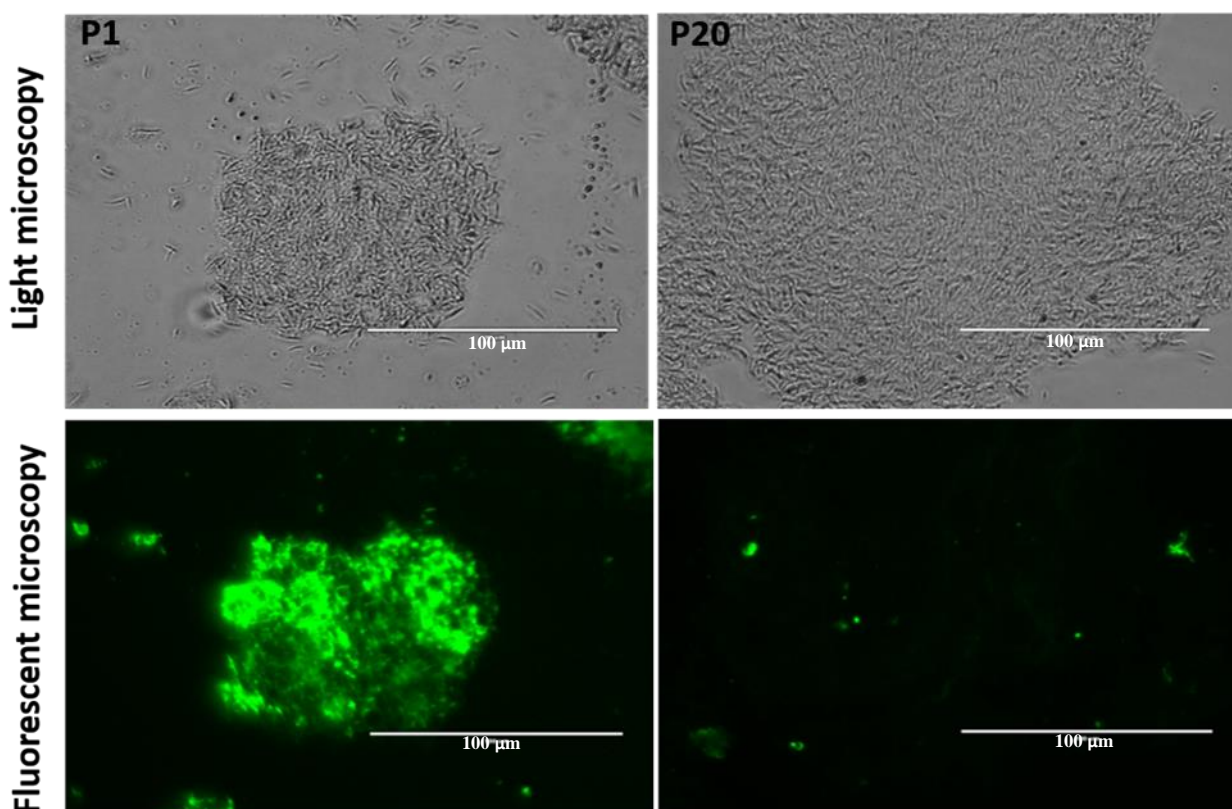


**Figure 3. 17: Detection of LPG on the surface of P1 and P20 promastigotes by immunofluorescence**

$8 \times 10^6$  P1 and P20 *L mexicana* promastigotes at stationary phase were washed twice with 1xPBS, stained with CA7AE anti LPG primary and incubated at 4°C overnight. Cells were washed twice with 1x PBS and stained with Alexa fluor FITC goat anti-mouse IgG secondary antibody and incubated at room temperature for 30 minutes. Non-binding antibodies were removed by washing with PBS. Smears were prepared from each tube and visualised by EVOS microscope fluorescence at power 40.

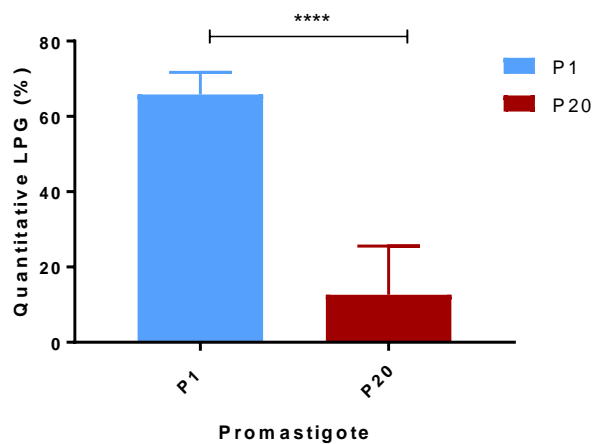
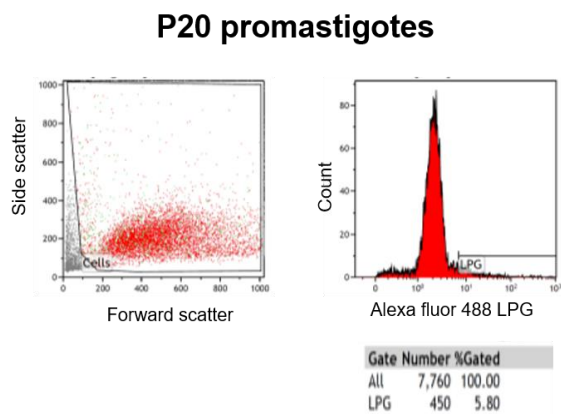
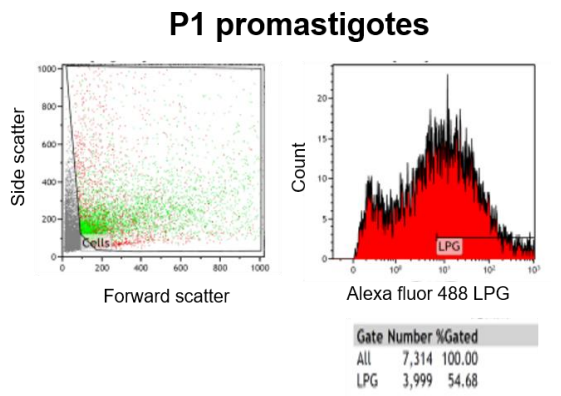


**Figure 3. 18: Detection of LPG on the P1 and P20 promastigotes by flow cytometry**

0.5 X 10<sup>6</sup> of P1 and P20 promastigotes at stationary phase were washed twice with PBS, stained with anti LPG CA7AE primary antibody and incubated at 4°C for 30 minutes. Tubes were washed twice with PBS and stained with Alexa fluor FITC goat anti-mouse IgG secondary antibody and incubated at room temperature for 30 minutes. All tubes were washed 3 times with PBS to remove non-binding secondary antibodies and resuspended in 400 µL flow cytometry fluid and read by flow cytometry.

The flow cytometry results were analysed by Beckman Coulter Kaluza software. The data were analysed by using GraphPad Prism 7. Statistically significant differences between groups represented by \*\*\*\*p<0.00001. The P value was determined by unpaired t-test. The results are the average of four independent experiments and the error bars represent ± standard error of mean.

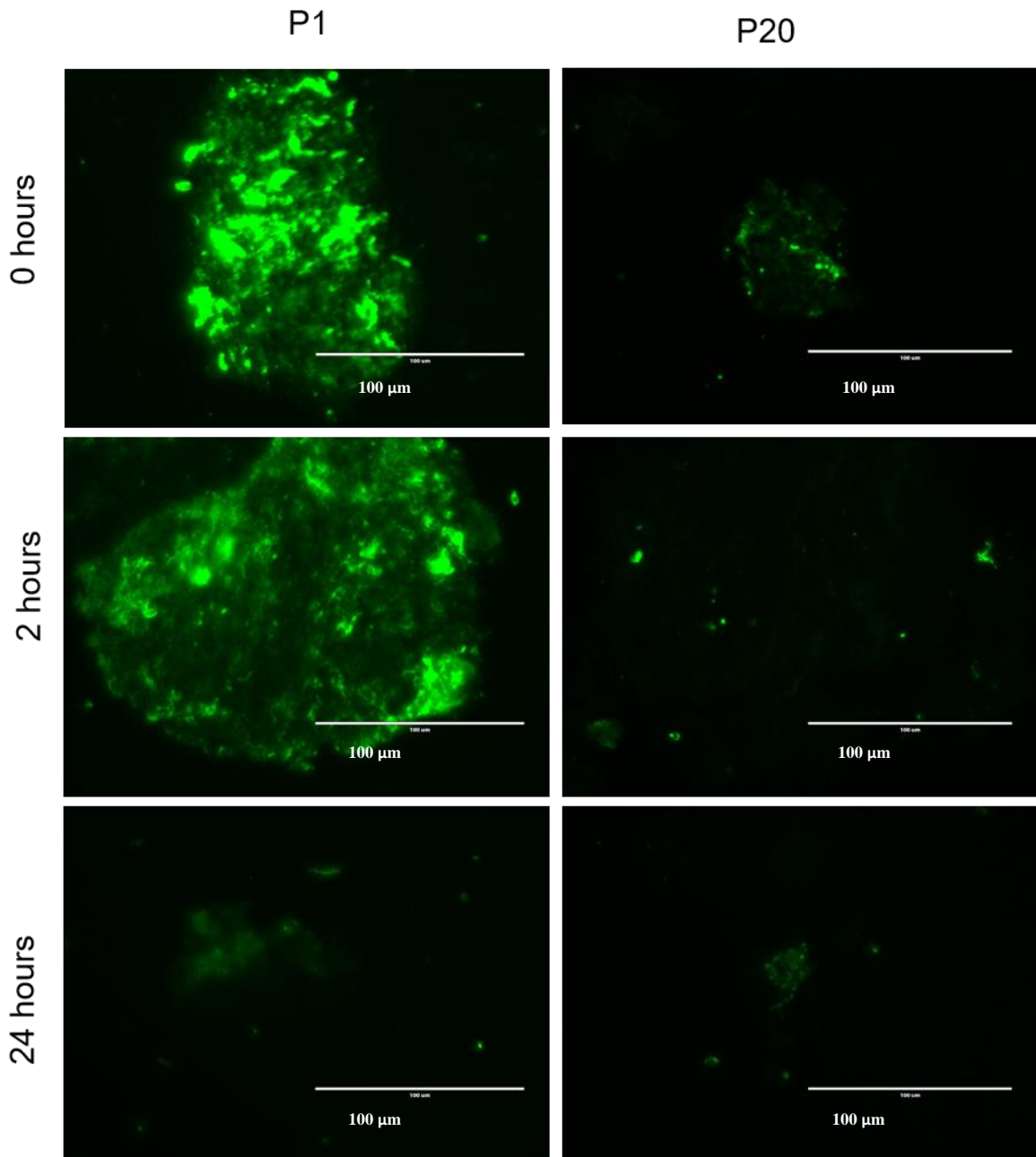


**Figure 3. 19: Detection of LPG on the surface of P1 and P20 *L.mexicana* by immunofluorescence after incubation in differentiation conditions for 2 and 24 hours**  
 $8 \times 10^6$  P1 and P20 *L mexicana* promastigotes at stationary phase were washed twice with 1 x PBS and cultured in RPMI 1640 media containing 10% v/v HIFCS, in a vented flask and incubated in 95% v/v humidity at 37 °C in 5% v/v CO<sub>2</sub> incubator in for 24 hours.  
P1 and P20 *L mexicana* promastigotes at stationary phase were washed twice with 1xPBS, stained with CA7AE anti LPG primary and incubated at 4 °C for overnight. Cells were washed twice with 1xPBS and stained with Alexa fluor FITC goat anti-mouse IgG secondary antibody and incubated at room temperature for 30 minutes. Non-binding antibodies were removed by washing with PBS. Smears were prepared from each tube and visualised by EVOS microscope florescence at power 40 and 470/22 nm Excitation; 510/42 nm Emission.

### 3.2.12 Detection of phosphatidylserine (PS) in P1 and P20 promastigotes by flow cytometry

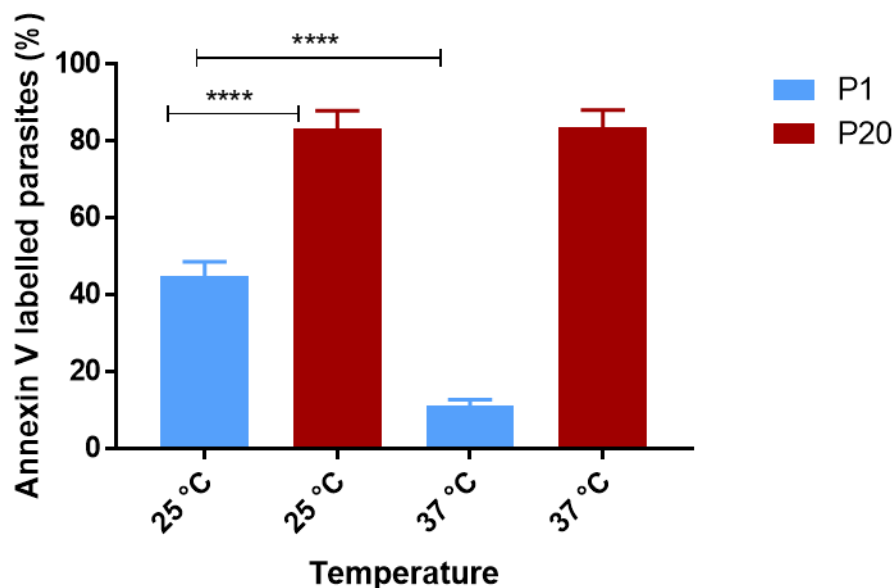


**Figure 3. 20: P1 and P20 phosphatidylserine expression**

In this experiment,  $20 \times 10^6$  P1 and P20 *L. mexicana* parasites at stationary phase were incubated in 95% v/v humidity at 37°C in 5% v/v CO<sub>2</sub> incubator for 24 hours in vented flasks for 24 hours in 2.5 mL RPMI 1640 supplemented with 10% v/v HIFCS for amastigote differentiation. In addition, another  $20 \times 10^6$  P1 and P20 promastigotes at stationary phase were cultured in Schneider's *Drosophila* medium supplemented with 10% v/v HIFCS in unvented T25 tissue culture flasks and incubated in a 25°C incubator. After 24 hours incubation at 37°C, both P1 and P20 parasites were visualised by EVOS microscope to check the differentiation into amastigotes. Human U937 monocytes were used as a negative control. Cells were stained with Annexin V, according to the manufacturer's guidelines and examined by flow cytometry (appendix 6). The results are representing three independent experiments.

The data were analysed by using GraphPad Prism 7. Statistically significant differences between pairs of groups represented by \*\*\* $p < 0.0001$ . The p value was determined by unpaired t-test and the error bars represent  $\pm$  standard error of mean.

phosphatidylserine was expressed in higher amounts on the P20 than P1 *L. mexicana* promastigotes. After incubation at 37°C for 24 hours phosphatidylserine expression was decreased in P1 but not P20 (figure 3.22, appendix 5 A and B).

### 3.2.13 Synopsis of the virulent P1 and avirulent P20 *L. mexicana* promastigote growth and characterisation results

**Table 3. 3: Growth characteristic of P1 and P20 promastigotes**

	Test	P1	P20
<b>Growth rate on schneider's <i>drosophila</i> medium</b>	-Neubauer hemocytometer  -Alamar blue assay	Grow well	Grow well
<b>Growth rate on RPMI 1640 medium</b>	-Neubauer hemocytometer  -Alamar blue assay	Grow well	Did not grow well
<b>Stationary phase</b>	-Neubauer hemocytometer	Between 3 <sup>rd</sup> to 5 <sup>th</sup> day	Between 3 <sup>rd</sup> to 5 <sup>th</sup> day
<b>Effect of 25°C and 37°C temperature and O<sub>2</sub></b>	-Neubauer hemocytometer	Grow at 25°C anaerobically	Grow at 25°C anaerobically

**Table 3. 4: Morphology of P1 and P20 promastigotes**

	Test	P1	P20
<b>Morphological analysis</b>	Light microscope	Body length and width are less than P20	Body length and width are larger than P1
<b>The ability of P1 and P20 to differentiate into amastigotes at 37°C for 24 hours</b>	Light microscope	Approximately 80%	Approximately 20%
<b>The effect of O<sub>2</sub>, CO<sub>2</sub> and type of media on the ability of P1 and P20 to differentiate into amastigotes</b>	Light microscope	No effect	No effect
<b>Metacyclic stage promastigotes</b>	By calculation of physical measurement of body length, width and flagellum	At least 20% metacyclic promastigotes	0% metacyclic promastigotes

**Table 3. 5: expression of LPG and PS on the P1 and P20 *L.mexicana***

	Test	P1	P20
<b>Promastigotes LPG</b>	Flow cytometry	Approximately 65%	Approximately 15%
<b>Promastigote LPG</b>	Immunofluorescence	High	Low
<b>LPG after incubation in the amastigote differentiation conditions for 24 hours</b>	immunofluorescence	Decreased	Did not affected
<b>Promastigote PS</b>	Flow cytometry	Approximately 45%	Approximately 80%
<b>PS after incubation in the amastigote differentiation conditions for 24 hours</b>	Flow cytometry	Approximately 15%	Approximately 65%

**Table 3. 6: Virulence associated gene regulation expression of the P20 promastigotes compared with P1 promastigotes**

	Test	P1	P20
<b>Virulence associated genes regulation of LPG1, LPG2, A2, CHAT1, CPB2, CPB2.8, CPC, GP63, LACK and MAPK9</b>	qPCR	Used as a control	Down regulated

**Table 3. 7: Effect of incubation of P1 and P20 *L.mexicana* promastigotes on the amastigote's differentiation conditions for 24 hours on virulence associated gene regulation**

	Test	P1	P20
CPB2.8	qPCR	Upregulated	Downregulated
CPB2	qPCR	Downregulated	Downregulated
A2	qPCR	Not affected	Downregulated
LPG1 and LPG2	qPCR	Downregulated	Downregulated
GP63	qPCR	Downregulated	Downregulated

### 3.3 Discussion

#### 3.3.1 Characterisation of P1 and P20 *L. mexicana* promastigotes

Continuous passaging of *L.mexicana* for 20 passages *in vitro* has caused major morphological and functional changes. Cells became rounded and elongated, increased in body size, and their growth was inhibited in RPMI1640 medium. This was accompanied by a loss of virulence, downregulation of all ten virulence-associated genes tested and loss of the ability to differentiate into amastigotes under different growth condition.

##### 3.3.1.1 Growth Rate

Transmission of *L.mexicana* promastigotes from the intermediate host insect vector to the mammalian host is affected by a temperature shift from 25°C into 37°C *in vivo*. The question is whether P1 and P20 would similarly grow at 37°C. Both P1 and P20 promastigotes were able to grow at 25°C but not at 37°C (figure 3.2). It has been previously reported that *L.mexicana* was sensitive to temperature change and did not grow at 37°C (Biegel *et al.*, 1983).

In this study, P20 but not P1 promastigotes did not grow in RPMI1640 medium supplemented with 10% HIFCS (figure 3.2) and at 25°C, as assessed by manual counting using a hemocytometer and confirmed by the Alamar blue assay (figure 3.2). No significant difference in P1 promastigote growth rate was observed whether they were cultured in Schneider's *Drosophila* medium or in RPMI1640 medium. However, P20 concentration in Schneider's *Drosophila* medium was approximately 3 times higher than P1 when cultured in RPMI1640 medium after 2 days incubation (figure 3.2); this could be due to significant differences in their nutrient requirements and food metabolism or RPMI1640 medium may contains some growth inhibitors for P20 but not P1; presently no study has addressed this phenomenon.

Studying the ingredients of both media and metabolism pathway of P1 and P20 could give a clue to their growth requirements. It is noteworthy that both RPMI1640 (Lonza) and Schneider's *Drosophila* (Lonza) contains L-glutamine and are routinely supplemented with 10% HIFCS. These results are in line with a previous study by O'Daly, and Rodriguez, (1988) who reported that the nutrient requirements for growth and differentiation to amastigotes are varied among *Leishmania* species including *L.mexicana* and varied with continuous passages *in vitro* (passage 30) as a result of the incubation temperature and the protein content of the culture medium.

### 3.3.1.2 Morphology of P1 and P20 *L.mexicana*

By comparing the morphology of P1 and P20 promastigotes, P1 is spindle-shaped while P20 is elongated with a rounded end (See results figure 3.6, 3.7 and 3.8), the body size of P20 was larger than P1 (figure 3.4, 3.5, 3.6, 3.7, and 3.8). The body length and width of P20 was significantly greater than that of P1 promastigotes, with no significant difference between their flagella. These results are similar to those reported by Ali *et al.*, (2013). It is worthy to note that NI vision assistant software was used in this study compared with the calibrated micrometre slide that was used by Ali *et al.*, (2013). However, the present results of flagellum length are in contrast with another study by Wheeler *et al.*, (2011) who noticed a significant morphological change in *L.mexicana* when cultured *in vitro* over multiple cell cycles. Contrary to the flagellar length findings Wheeler *et al.*, (2011) reported that there was a remarkable increase in flagellum length after multiple cell cycles.

It is noteworthy to mention that the promastigotes are infectious when they are at metacyclic stages because this is the stage where promastigotes are able to differentiate into amastigotes (Solbach and Laskay, 2000). The average of the body length of P1 (8.6  $\mu\text{m}$ ) was significantly shorter than P20 (13.6  $\mu\text{m}$ ) and the width was significantly higher in P20 (2.58  $\mu\text{m}$ ) than P1 (2.04  $\mu\text{m}$ ) promastigotes. Collectively, the P1 body size is smaller than P20 promastigotes and P1 promastigotes are close to metacyclic stage parasite measurements (Rogers *et al.*, 2002; Zakai, *et al.*, 1998). Therefore, the possible explanation for the failure of P20 to differentiate into amastigotes is due to omission of the metacyclic stage.

Failure of P20 to differentiate to metacyclic promastigotes stage was confirmed by two calculation methods: (i) by calculation of flagellum: body size ratio and (ii) multiplying body length by body width (figure 3.10). The changes may be used as an indicator for differentiation into amastigotes (See results section 3.2.6 and 3.2.7). Interestingly, the results confirmed the absence of metacyclic stages in P20 promastigotes (figure 3.10). Absence of the metacyclic infective stage after cultivation of *L.mexicana* for 20 passages *in vitro*, is in line with previous findings of lost virulence and failure of *L.mexicana* after 20 passages *in*

*vitro* to induce lesions in Balb/c mice by Ali *et al.*, (2013) and *L. infantum* (Moreira *et al.*, 2012). Therefore, this is a point to consider when preparing a vaccine from old cultures.

### **3.3.1.3 Differentiation of P1 and P20 *L.mexicana* promastigote to amastigotes.**

The life cycle of *Leishmania* alternates between two main morphological forms: flagellated motile promastigotes in the sand fly vector and intracellular non-flagellated amastigotes in the infected mammalian host (Van Zandbergen *et al.*, 2004). Differentiation from promastigotes to amastigotes is a critical step in the process of infection, and the molecular basis for this differentiation is still poorly understood. Therefore, in this part of this study, the ability of P1 and P20 promastigotes to differentiate into amastigotes was explored, in order to understand how it was influenced by culture conditions which include type of medium, temperature, pH and time of incubation. Results show that P20 lost the ability to differentiate to amastigotes under different culture conditions and even failed to differentiate in 5.5 pH media when incubated at 37°C for 24 and 48 hours. In addition, P20 lost the ability to differentiate into metacyclic promastigotes when cultured at 25°C in Schneider's *Drosophila* medium supplemented with 10% HIFCS. Failure of P20 to differentiate into amastigotes was accompanied by downregulation of A2 gene expression after 24 hours incubation at 37°C as assessed by qPCR. It is noteworthy that the A2 protein is amastigote specific (Zhang *et al.*, 1996).

### **3.3.1.4 Role of pH on P1 and P20 *L.mexicana* differentiation to amastigotes**

To investigate the effect of parasite concentration alone on the ability of P1 and P20 *L.mexicana* promastigotes to differentiate into amastigotes, the promastigotes were subjected to 37°C incubation (5% CO<sub>2</sub> and 95% v/v humidity) for 24 hours. The pH was decreased with time (which might be due to parasite concentration and incubation conditions) to pH 6 (See results 3.2.10 and 3.2.10.1). Under these conditions, the differentiation rate of P1 increased approximately up to 90 % after 24 hours. However, it has been reported that *L.mexicana* promastigotes can adapt and differentiate into amastigotes in cultures at pH 4.5, 5.0, and 6.0 (Bates *et al.*, 1992; Zilberstein *et al.*, 1994). However, using pH 5.5 medium produced approximately 10 % more amastigotes from P1 than regular RPMI 1640 medium. It was reported that *L. mexicana* amastigotes prefer acidic growth medium of pH 5.4 (Bates *et al.*, 1992). In a study conducted by Dagger *et al.*, (2018), who compared between RPMI1640, 199 and LIT modified media, the ability of *L.mexicana* to differentiate was better in RPMI1640 medium compared with 199 or LIT modified medium under similar conditions (pH 5.5 and 37°C). However, the current study findings report that there is no

significant effect from the type of medium on *L.mexicana* differentiation rate into amastigotes.

P20 promastigotes were unable to differentiate into amastigotes when cultured in growth media of pH 5.5 (See results 3.2.9). According to the current study results, the key factor that affects parasite differentiation into amastigotes was the temperature changing from 25°C into 37°C either at pH 5.5 or 6 which is consistent with the recent study of Dagger *et al.*, (2018). The main difference between virulence and avirulence is the capacity of the virulent parasite (P1) to differentiate into the amastigote form; this finding is in line with the study of Moreira *et al.*, (2012) who reported that the avirulent parasite could not properly differentiate into amastigotes *in vitro*. Results in this study confirm that culturing of parasites at concentrations of  $8 \times 10^6$  per mL was enough to reduce the media pH from 7.0 to 6 and induce differentiation of parasites.

#### **3.3.1.5 Effect of incubation time on ability of P1 and P20 *L.mexicana* to differentiate into amastigotes**

Regarding the time of incubation, results of this study show that, P1 differentiates into amastigotes after 24 hours but not at 2 hours which is consistent with previous finding of Williams *et al.*, (2006) who reported that *L.mexicana* needs 18 to 72 hours to differentiate into amastigotes and autophagy appeared after 18 to 72 hours by increasing number of autophagosomes which was consistent with time of incubation for differentiation of parasites. The differentiation into amastigotes which is found in P1 but not P20 may be due to autophagy; it has been reported that there was a large increase in autophagosome production during differentiation of *L.mexicana* metacyclic stage promastigotes to amastigotes *in vitro* (Williams *et al.*, 2006).

#### **3.3.1.6 Effect temperature alteration on the ability of P1 and P20 *L.mexicana* to differentiate into amastigotes**

The effect of temperature alteration on the differentiation of promastigotes into amastigotes was varied between P20 and P1 promastigotes. The temperature change from 25°C to 37°C can cause differentiation of P1 but not P20 into the non-flagellated round form. However, the differentiation is accompanied by several morphological changes, cell size reduction, loss of the flagellum, organelle modification gene expression and surface LPG and PS expression, which may include protein and fat metabolism (Dagger *et al.*, 2018).

Regardless of other factors tested in this study (pH, media types, presence and absence of O<sub>2</sub>), the temperature shifting from 25°C to 37°C is the main factor that induces differentiation of promastigotes into amastigotes. It has been previously reported that incubation of the

parasite at 37°C for 24 hours in the presence of CO<sub>2</sub> can be used for the establishment of an axenic amastigote culture of *L.donovani* (Zilberstein *et al.*, 1994; Alcolea *et al.*, 2010), however in this study there was no effect of the presence or absence of O<sub>2</sub> and CO<sub>2</sub> on the ability of the parasite to differentiate into amastigotes. It is known that the main factors affecting differentiation of *L.mexicana* and *Leishmania* species into amastigotes are the temperature of 37°C and pH of 5.5 (Biegel *et al.*, 1983; Bates *et al.*, 1992). The current results confirm that P1 *L.mexicana* promastigotes can differentiate into amastigotes when incubated at 37°C but not 25°C for 24 hours; in addition, differences of gene regulation profile after 20 passages of *L.mexicana*, such as A2 which is associated with amastigote protein was downregulated after 24 hours incubation in P20 but not P1 (figure 3.17).

### **3.3.1.7 Effect of 20 passages on the ability of P1 and P20 *L.mexicana* promastigotes to differentiate into amastigotes**

One of the aims of this experiment was to investigate the biological characteristics of P1 and P20 isolates before investigation of their interactions with mammalian host cells. Differentiation into amastigotes is a parasite survival strategy to adapt to environmental changes. Although the environmental factors that trigger virulent *Leishmania* differentiation into amastigotes *in vitro* were partially identified several years ago, relatively little is known about the ability of avirulent *Leishmania* parasites (P20) to differentiate into amastigotes and to the best of the author's knowledge there is no other study that has investigated this phenomenon by comparing between these two strains (P1 and P20) of the parasite and their gene regulation except the single study by Ali *et al.*, (2013). The differentiation of promastigotes into amastigotes is essential for the parasite's adaptation to new host environmental conditions. There are many variations between parasite culture growth conditions and mammalian host cell infection conditions such as nutrients (type of medium), temperature, pH, as well as the availability of oxygen which mimics the phagolysosome-like environment. It has been reported that there was a similarity between *in vivo* and *in vitro* conditions for the differentiation of *L.mexicana* into amastigotes, in addition to similarities between amastigotes that differentiated *in vitro* outside mammalian cells to those that differentiated inside macrophages (Hernandez *et al.*, 1981).

The ability of *Leishmania* parasites to differentiate into amastigotes is a key factor for their survival against starvation conditions after changing the environmental conditions (Reggiori and Klionsky, 2005; Cull, *et al.*, 2014). Differentiation into amastigotes takes place by an autophagic-like process (Dagger *et al.*, 2018), which was found in P1 but not P20 *L.mexicana* parasites in the results of this study.

The preceding findings in the literature show that the shifting from promastigotes into amastigotes is combined with large differences in metabolism; at the promastigote stage there is exhibition of high metabolic activity, with excessive rates of consumption of amino acid and glucose, in addition to secretion of metabolic end-products, while the amastigote stage has increased metabolism with low levels of amino acid and glucose consumption and increases in fatty acid catabolism. This phenotype of metabolism is not induced by nutrient limitation (Saunders *et al.*, 1994), because P1 and P20 were cultured in a similar medium (RPMI 1640 and Schneider *Drosophila*), although P20 failed to differentiate into amastigotes in both types, while with changing temperature of incubation from 25°C to 37°C induced the differentiation into amastigotes. Therefore, this study suggests that comparing between P1 and P20 metabolism before and after incubation at 37°C could clarify *Leishmania* parasite metabolism pathways during differentiation into amastigotes.

This aspect of parasite metabolism could be a key in understanding the ability of the amastigote to survive in macrophage phagolysosomes and parasitophorous vacuoles (PV). Therefore, targeting parasite food metabolism of amastigotes could be a key for drug designs. In addition, research on vaccines based on attenuation of the parasite by prolonging incubation must consider that attenuation of parasites leads to loss of the metacyclic stage of the parasite and subsequent infectivity stages (amastigotes), although this may not activate the immune response properly.

The differentiation of *L.mexicana* promastigotes into amastigotes *in vitro* takes place through a selective autophagic-like process. These processes are characterised by deep folding of the plasma membrane and the presence of numerous cytoplasmic lipid droplets which may be the product of changes in lipid metabolism. Autophagy is mainly regulated by the mechanistic target of rapamycin (mTOR). Autophagy is commonly regulated by two signalling pathways; mTOR-dependent and mTOR-independent. In the classical pathway, activation of mTOR leads to inhibition of cellular autophagy, while mTOR independent regulation leads to enhanced autophagy (Ravikumar *et al.*, 2010).

Autophagy is initiated by engulfing particles or organelles into the cytoplasm by double-membrane vesicles in the case of early autophagic vacuoles or single membrane vesicles in the case of late autophagic vacuoles, which leads to autophagosomes eventually fusing with lysosomes, where their contents are degenerated (Liou *et al.*, 1997; Ravikumar, *et al.*, 2010). The autophagosome is a vesicle with a single or double membrane containing cellular materials that will be degraded by autophagy (Liou *et al.*, 1997; Ravikumar, *et al.*, 2010). However, Williams *et al.*, (2006) have reported that *L.mexicana* is lacking cysteine peptidases (CPB and CPA which are necessary for lysosomal function), losing their ability to differentiate to metacyclic promastigote and amastigote forms, due to a defect in

autophagy. Thus, they concluded that lysosomal function and autophagy are crucial for differentiation of *L.mexicana*. In line with this, the qPCR results of the current study show that CPB 2, CPB 2.8 and CPC were downregulated in P20.

Drugs blocking the autophagic-like process of the parasite could be useful as new strategy to combat the disease (Dagger *et al.*, 2018). Comparison between P1 and P20 could be helpful in this regard, as the lost ability of P20 to differentiate into amastigotes may be due to a defect in the autophagic-like process. However, it has been hypothesised before that autophagy plays an essential role in the amastigote differentiation processes and *Leishmania* parasites would be an excellent model for studies on the role of autophagy in cellular differentiation (Williams *et al.*, 2006).

Another possible reason for the failure of P20 promastigotes to differentiate into amastigotes is the lack of sphingolipids which are essential for undergoing metacyclogenesis and differentiation to amastigotes (Zhang *et al.*, 2003; Williams *et al.*, 2006). Sphingolipids are lipids containing a backbone of sphingoid bases, aliphatic amino alcohols including sphingosine which is a cell membrane lipid class. Sphingolipids play an important role in signal transmission and cell recognition (Chun *et al.*, 2010). However, the interplay between sphingolipids and autophagy in *Leishmania* is still unclear. Therefore, this study suggests that the comparison between P1 and P20 could be helpful to study metacyclogenesis, amastigote differentiation and autophagy.

The failure of P20 to differentiate into amastigotes is an interesting phenomenon which needs more in-depth research to understand the factors and mechanisms of gene regulation affecting this process, hence this may lead to designing drug strategies to interfere with the autophagic-like process (Dagger *et al.*, 2018).

### **3.3.1.8 Effect of 20 passages *in vitro* on virulent gene expression of *L.mexicana* by qPCR**

Gene regulation is a powerful tool for understanding the molecular mechanisms that regulate *Leishmania* parasite life cycle progression which will reflect on an understanding of host-parasite interactions. Therefore, in this study, ten genes associated with virulence (LPG1, LPG2, A2, CHAT1, CPB2, CPB2.8, CPC, GP63, LACK and MAPK9) were investigated by qPCR analysis. In addition, 6 genes (LPG1, LPG2, GP63, CPB2, CPB2.8 and A2) associated with amastigote differentiation were also analysed following exposure of parasites to amastigote differentiation conditions. Furthermore, detection of LPG on P1 and P20 by FITC Immunofluorescence staining and flow cytometry analysis using mouse anti-LPG monoclonal antibodies (CA7AE) was used in this study for the first time. Results

showed that all genes tested were significantly downregulated in P20 compared with P1 promastigotes.

### 3.3.1.9 Cysteine protease genes

Results clearly showed downregulation of all virulence-associated genes tested, which may explain the reason behind the reduced infectivity of P20 parasites and ability upon inoculation to induce lesions in Balb/c mice (Ali *et al.*, 2013). CPB2, CPB2.8 and CPC genes play an important role in parasite survival in infected mammalian host cells at the amastigote stage and its interaction with host cells (Mottram *et al.*, 2004). It must be noted that CPB plays a vital role in the autophagic pathway during parasite differentiation into metacyclic and amastigote stages (Mottram *et al.*, 1996; Williams *et al.*, 2006; Gomes *et al.*, 2017). CPB activity is predominantly expressed in promastigotes at their metacyclic stage (Bates *et al.*, 1992) and P20 did not have a metacyclic stage according to the current study results (figure 3.10). It has been reported that virulent *L.mexicana* amastigotes were rich in cysteine peptidases which play a central role in facilitating growth and survival of the parasites in mammalian cells, suggesting multiple cysteine peptidase genes may have a complementary function (Mottram *et al.*, 2004). Mutant *L.mexicana* lacking CPB enzymes have greatly reduced infectivity Balb/c mouse macrophages either *in vivo* or *in vitro* compared with wild-type parasites (Mottram *et al.*, 1996; Frame *et al.*, 200). In addition, inhibitors of cysteine proteases have some efficacy against *Leishmania*, both *in vitro* and *in vivo* (Selzer *et al.*, 1999), which is in line with current study results, where CPB2.8 level in P1 but not P20 were significantly upregulated after 24 hours incubation at 37°C (Section 3.2.11.1). Downregulation of CPB gene expression, loss of metacyclic stage and failure of P20 to differentiate into amastigotes may suggest a defect in the P20 autophagy pathway that interferes with metacyclogenesis and differentiation. However, CPB deficient *L.mexicana* have lost the ability to replicate inside susceptible Balb/c mice macrophages and form large communal PVs by fusion between PVs (Casgrain *et al.*, 2016). However, the potential of cysteine proteases as virulence factors and as potential drug and vaccine targets has been implicated (Mottram *et al.*, 1996). Targeting *L.mexicana* CBP2.8 by CBP2.8 inhibitor drugs is a promising treatment of this disease, and it may kill the intracellular amastigotes *in vitro* (De Luca, *et al.*, 2018) which also agrees with the current study finding in regard to (CPB2, CPB2.8 and CPC) gene regulation.

### 3.3.1.10 Chitinase 1 (CHT1)

Chitinase 1(CHT1) was downregulated in avirulent P20 promastigotes compared with P1. It is noteworthy that CHT enzyme produced by *Leishmania* parasites enables them to infect

epithelial cells by the sand fly vector biting. Also, *L.mexicana* CHT enzyme plays an important role in the development of the parasite and its survival in the mammalian host (Pimenta *et al.*, 1997. Schlein *et al.*, 1991). It has been reported that there is a significant positive relationship between CHT1 and mouse lesion size (Joshi, *et al.*, 2005). Therefore, P20 may lack chitinase enzyme due to downregulation of the CHT1 gene, which is in line with Ali *et al.*, (2013) who reported that CHT1 is downregulated in P20 and which failed to induce lesions in susceptible Balb/c mice *in vivo*.

### 3.3.1.11 MAPK9

Parasite flagellar morphogenesis is associated with mitogen activated protein kinase homologue (MAPK9) and its mRNA was found in all *L.mexicana* stages (Bengs, *et al.*, 2005; Reddy *et al.*, 2017). Long *in vitro* incubation (20 passages) of *L.mexicana* caused significant downregulation of MAPK9 gene (figure 3.15) after which they kept their long flagellum after 24 hours incubation at 37 °C. Therefore, this finding is supported by the study conducted by Bengs, *et al.*, (2005) who reported that in a null mutant MAPK9 promastigotes have elongated flagella, while promastigotes that have overexpression of MAPK9 display very short or no flagella when they differentiated into amastigotes. Accordingly, P20 promastigotes keep their flagella length when incubated at amastigote differentiation conditions (37°C and pH 5.5 medium) which could be due to downregulation of MAPK9.

It is known that amastigotes size are smaller than promastigotes and they have a primitive flagellum embedded in the flagellar pocket. In addition, *L.mexicana* amastigotes have large megasomes (lysosome-like organelles), which are absent in promastigotes (Besteiro, *et al.*, 2007). Pupkis *et al.*, (1986) have found that *L.mexicana* amastigotes contain much higher activities of cysteine proteinase than promastigotes. The unique and huge structure of megasomes in wild *L.mexicana* may provide an excellent model for researches to focus on the enzyme. However, megasomes are potential pharmacologic and immunologic targets for disease control, (McMahon-Pratt and Traub-Csekö., 2010) and studying of P1 and P20 in this regard could be helpful.

Moreover, the promastigote surface membrane is composed of LPG, gp63 and GIPL as dominant surface markers (McConville and Ferguson, 1993; Wiese, 1998; McConville, and Menon, 2000). While *L.mexicana*, amastigotes express GIPLs and glycosphingolipids on their surface, there was very low expression of LPG and GP63 (Bahr *et al.*, 1993; Winter *et al.*, 1994; Wiese, 1998). A possible explanations for this results of the current study in this regard is that, the role of megasomes in P20 may be affected by long *in vitro* passages affecting protein and fat metabolism (Dagger *et al.*, 2018); it is noteworthy that *L.mexicana*

amastigotes have the largest megasomes among all *Leishmania* parasite species (Ueda-Nakamura *et al.*, 2001; Besteiro, *et al.*, 2007).

Behavioural and morphological modulation of *Leishmania* during their life cycle is the result of gene regulation in response to external environmental pressure. However, details of the signal transduction pathways involved in differentiation of promastigotes into amastigotes and specific gene regulation are still unknown (Wiese, 1998). However more recently, the first evidence for post-translational regulation of stage-specific expression of LdAAP24 (proline-alanine transporter) which is expressed exclusively in promastigotes only was reported in *L.donovani* (Liburkin-Dan *et al.*, 2018). However, the kinase is essential for the survival and multiplication of *L.mexicana* amastigotes in infected mammalian host cells (Wiese, 1998).

#### **3.3.1.12 A2 Protein**

A2 protein is essential for amastigote survival in a mammalian host. A2 was identified as the first amastigote stage-specific virulence factor in *Leishmania* (Zhang *et al.*, 1997), A2 protein has been detected in patients' blood infected with VL and CL due to *L.mexicana* and the A2 gene was detected in *L.mexicana* (Ghedini, *et al.*, 1997). According to this study, A2 was downregulated in P20 and slightly upregulated in P1 after 24 hours incubation at amastigote differentiation conditions (figure 3.17) which confirm that the differentiation into amastigotes has been in P1 but not P20. However, it has been shown that A2 deficient *L.donovani* amastigotes lost virulence (Zhang *et al.*, 1997). Immunisation of mice with recombinant A2 protein produced significant protection against *L.donovani* (Ghosh *et al.*, 2001). Therefore, A2 protein is considered one potential antigen that induces an immune response against this disease through the release of IFN- $\gamma$  (Ghosh *et al.*, 2001). Therefore, long *in vitro* culture of *L.mexicana* (P20) made them lose the ability to differentiate into amastigotes which may be as a result of downregulation of A2 genes in P20 promastigotes. Moreover, A2 gene expression is downregulated after 24 hours incubation at 37°C which is observed in P20 but not P1. Notably, A2 protein is an amastigote specific protein (Zhang *et al.*, 1996).

#### **3.3.1.13 LPG1 and LPG2**

All the *Trypanosoma* family is characterised by the presence of a lipophosphoglycan (LPG) coat covering the parasite surface which is an important virulence factor of *Leishmania* protozoa (Ferguson, 1999). It is the most abundant surface coat glycoconjugate on the promastigote surface with approximately  $5 \times 10^6$  copies per cell (Turco and Descoteaux, 1992). LPG protects the parasite at the metacyclic stage by its repeating units which

increases the phosphorylated disaccharide that increases thickening of glycocalyx (Sacks *et al.*, 1995). LPG is a pathogen-associated molecular pattern (PAMP) that plays a crucial role in modulation of host immune responses during the establishment of macrophage infection by the *Leishmania* parasite (Desjardins and Descoteaux, 1997; Duque *et al.*, 2014). In the bloodstream, LPG protects *Leishmania* parasites from the humoral immune system before infecting macrophages (Kweider *et al.*, 1987). Therefore, the regulation of LPG1 and LPG2 genes were assessed by qPCR in P20 compared with P1.

Differentiation of parasite into amastigotes is the adaptation strategy taken by parasites to survive after their exposure to changes in environmental conditions including temperature and pH. Differentiation into amastigotes causes several changes in temperature tolerance, morphogenesis, and parasite surface molecules such as LPG. According to the current study finding, both LPG1 and LPG2 genes were downregulated in P20 compared with P1 promastigotes. LPG is a surface coat protecting *Leishmania* from attack by the host immune system and at the same time, it is the first target for immune detection. LPG is essential for survival during the initial stage of establishment successful macrophage infection, downregulation of LPG1 and LPG2 in P20 is in line with a study by Turco *et al.*, (2001) who compared between *L. major* knock-outs for LPG1 alone or LPG1 and LPG2 together which showed decreased virulence in susceptible mice infections of parasites knocked out for LPG1 and LPG2 together. On the contrary, Ilg (2000) reported that LPG1 is not a virulence factor for *L. mexicana* during infection and survival, it was reported that infection of Balb/c and C57 mice *in vivo* and peritoneal macrophages *in vitro* with *L. mexicana* lacking the LPG1 gene was normal. It must be noted that the Ilg (2000) results were on *L. mexicana* mutant LPG1 only but the genes responsible for LPG synthesis are not only LPG1, there are others such as LPG2, LPG3, and LPG5 (Ryan *et al.*, 1993) However, studies in the literature did not achieve a complete picture of LPG gene regulation or LPG synthesis (Forestie *et al.*, 2015).

LPG2 gene knock-out mutant *L. mexicana* is able to bind, infect, survive and multiply inside host macrophages despite being deficient in phosphoglycan without a significant difference to a wild type strain (Ilg *et al.*, 2001). Turco *et al.*, (2001) who compared between the role of lipophosphoglycan in *L. major* and *L. mexicana* reported that *L. major* but not *L. mexicana* lost virulence after depleting of lipophosphoglycan. However, this study showed that P20 has downregulated LPG1 and LPG2 gene expression and P20 has lost virulence, however losing virulence may be due to downregulation of other virulence genes. Incubation of P1 at 37°C for 24 hours induced differentiation of P1 into amastigotes (figure 3.13 and 3.14) which was accompanied with downregulation of LPG1 and LPG2 (figure 3.18). Similar findings

have been reported where LPG and other surface macromolecule expression was downregulated in the amastigotes (Naderer *et al.*, 2004)

LPG epitopes were detected on P1 and P20 parasites cell membranes by immune fluorescence and flow cytometry analysis using mouse anti-LPG (CA7AE). However, results show that lipophosphoglycan was high in P1 and low in P20 promastigotes (figure 3.19 and 3.20). Turco *et al.*, (2001) found that traces of LPG can be detected during the amastigote stage. Lysis of P20 but not P1 in the macrophages (figure 4.8) could be due to the absence of LPG epitopes on the P20 membrane, which protects promastigotes from a ROS generated during phagocytosis (Spath *et al.*, 2003). LPG may inhibit macrophage signalling pathways to produce ROS (Lodge *et al.*, 2006).

#### **3.3.1.14 GP63**

Results show GP63 gene expression was downregulated in P20 compared with P1 promastigotes. However, it has been reported that *Leishmania* parasites can resist the complement system by two main types of ligand molecules, LPG and GP63, which are found on the parasite surface (Kweider *et al.*, 1987). In recent years, substantial evidence has suggested that both GP63 and CPB are key virulence factors in *L.mexicana*. CPB play a central role in the formation of lesions, PVs, and survival of parasites in the macrophage. However, GP63 expression was inhibited in the absence of CPB (Casgrain *et al.*, 2016). In addition, GP63 plays an important role in prevention of apoptosis of infected mammalian cells. The parasite can inactivate infected macrophages by inhibition of Activating Protein-1 (AP-1) transcription factors which are involved in genes coding transcription for antimicrobial functions of macrophages. In infected macrophages, GP63 can cleave c-Jun protein and AP-1 transcription factors (Contreras *et al.*, 2010). GP63 enters the macrophage through lipid raft microdomains, and after reaching the nuclear compartment it degrades and cleaves c-Jun and AP-1 proteins (Contreras *et al.*, 2010). This protects cells from induced apoptosis, and if it cooperates with NF- $\kappa$ B can prevent apoptosis by TNF $\alpha$ . (Wisdom *et al.*, 1999).

#### **3.3.1.15 LACK**

LACK (*Leishmania* activated C kinase) proteins are found in many *Leishmania* species and in both stages of promastigote and amastigote (Gurunathan *et al.*, 1997). *Leishmania* LACK can stimulate the production of IFN- $\gamma$  and IL-10 in peripheral blood mononuclear cells including CD4<sup>+</sup> T cells derived from patients during early cutaneous Leishmaniasis (CL) (Bourreau, *et al.*, 2002; Bourreau, *et al.*, 2003)

LACK has been used as a vaccine antigen to induce Th1 responses; Bourreau, *et al.*, (2002) have shown that LACK vaccine produced protection against *L. major* CL in a murine model, and against *L. infantum* VL infection in a canine model (Sánchez-Sampedro *et al.*, 2013; Ramos *et al.*, 2008). However, according to this study's findings, LACK gene expression was downregulated in P20 promastigotes which may cause loss of LACK protein. Notably, LACK protein plays a role in activation of Th1 and CD4<sup>+</sup> T and inducing production of IFN- $\gamma$  which eventually induces NO production (Töttemeyer *et al.*, 2006). However, maybe there is downregulation in other untested virulence genes or even mutation in *L. mexicana* after 20 passages (P20) *in vitro* should be taken into consideration.

#### **3.3.1.16 Phosphatidylserine (PS) on P1 and P20**

PS act as ligand for parasite endocytosis and macrophage modulation, causing opsonisation by macrophages in a mechanism called apoptotic mimicry (Wanderley *et al.*, 2006; Wanderley *et al.*, 2013). After subjection of P1 to differentiation conditions phosphatidylserine (PS) was decreased in P1 (figure 3.22) These findings supported in some way the study conducted by Tripathi and Gupta, (2003) who reported that promastigotes in the stationary stage contain significantly higher amounts of PS than other stages. Interestingly, results of this study showed that, PS was more highly expressed on P20 than P1 *L. mexicana* promastigotes, however, no significant changes were noticed in P20 after they were subjected to amastigote differentiation incubation conditions, (37°C). On the other hand, Weingärtner *et al.*, (2012) reported that *Leishmania* promastigote cell membranes lack any detectable PS and they have many phospholipid classes which are stainable by Annexin V stains such as phosphatidic acid, phosphatidylinositol, phosphatidylglycerol and phosphatidylethanolamine.

**Interaction of Balb/c and C57 bone marrow derived macrophages with virulent and avirulent *L.mexicana***

## 4.1 Introduction

Several studies have already reported that long-term *in vitro* cultivation of *Leishmania* parasites species (approximately 12 months) causes a total loss of virulence in promastigote populations (Grimm *et al.*, 1991; Segovia *et al.*, 1992). Moreira *et al.*, (2012) have demonstrated that 21 passages were enough to lose *L. infantum* virulence. *L. mexicana* lost virulence after 20 passages *in vitro* and failed to induce lesions in Balb/c mice *in vivo* (Ali *et al.*, 2013).

Outcomes of *Leishmania* infection depend on both pathogen and host factors that are involved in a molecular interaction where competent cells will survive. Whether *Leishmania* parasites manage to survive in mammalian cells depends on their capacity to suppress host immune mechanisms. The survival strategies of *Leishmania* are dependent on the manipulation of specific functions of the host cell, including the modulation of cell signalling pathways through phosphorylation and dephosphorylation mechanisms (Escalona-Montano *et al.*, 2017). Accordingly, this study was designed to investigate virulent P1 and avirulent P20 *L. mexicana* infectivity to susceptible Balb/c and resistant C57 BMDM *in vitro* in order to understand the survival of this parasite in the infected cells.

The importance of the role of LPG in establishing successful Leishmaniasis is still controversial. It has been pointed out that for *Leishmania* survival in macrophages it needs to change the phagosome into a parasitophorous vacuole (PV) by pathological changes through LPG and GP63 and by inducing Th2 cytokines (Séguin and Descoteaux, 2016). Gene expression and the abundance of GP63 on *L. mexicana* P20 have been investigated before (Ali *et al.*, 2013) therefore LPG1 and LPG2 gene regulation of P20 were investigated in this study by using qPCR. In addition, abundance of LPG was estimated in P1 and P20 by using anti-LPG antibody, CA7AE Mouse anti-Leishmanial LPG (Bio-Rad) by Immunofluorescence and by flow cytometry. The *L. mexicana* parasite does not differ from other intracellular pathogenic promastigotes; it prevents the maturation process of the phagosome and creates an environment for the differentiation of promastigotes to amastigotes where the LPG surface plays a central role in this process. Comparing between P1 and P20 may provide new insights into our knowledge of the biology of *Leishmania* parasites, as well as the biology of phagolysosome biogenesis.

PS is another cell membrane molecule that is associated with apoptosis that was investigated in this study. The recognition of PS expressed on the parasite surface plays a role in deactivation of DC functions after engulfment of the parasites, in a matter like that of apoptotic cell clearance (Wanderley *et al.*, 2013). It plays a role in signalling and engulfing of the cells by macrophages (Verhoven *et al.*, 1995; Appelt *et al.*, 2005). PS conserves immunosuppressive signals that prevent local and systemic immune activation in

microbial and parasitic infection (Birge *et al.*, 2016). Therefore, abundance of PS on P1 and P20 promastigotes and after being subjected to amastigote differentiation conditions were investigated in this study (figure 3.22), in this chapter expression of PS was investigated on the infected macrophages.

The main function of macrophages is to phagocytose antigens that invade the body and apoptotic cell debris, therefore, macrophages are important for immunity. Macrophages are responsive to stimuli during immune activation and they are considered as a first-line-of-defence against infection (Tauber, 2003). Activated macrophages secrete cytokines such as TNF, IL-1, IL-6, IL-8, and IL-12. However, it is known that pro-inflammatory cytokines are produced in the early stages of the immune response during infections particularly TNF- $\alpha$  and IL-1 $\beta$  and they are considered as alarm-call cytokines (Charmoy *et al.*, 2015; Maspi *et al.*, 2016). It is very well-known that C57 mice are resistant to infection with *Leishmania* but with small lesions and self-healing, while Balb/c are susceptible to *Leishmania* infection (Locksley *et al.*, 1992; Allenbach *et al.*, 2006). Resistance or susceptibility to *Leishmania* infection depends on the type of anti-inflammatory cytokines that regulate Th1 or Th2. However, TNF- $\alpha$  plays an important mediation role in host-protection against cutaneous Leishmaniasis (Titus *et al.*, 1989; Carrada *et al.*, 2007; Manna *et al.*, 2014).

However, most studies have focused on measuring cytokines at one time point post-infection; to the best of the author's knowledge, there is no study that has investigated changes in cytokine levels /profiles at different time points post-infection. Therefore, this study tried to answer questions related to differences between Balb/c and C57 when they encounter P1 and P20 *L.mexicana* parasites by comparing this change after 2 and 24 hours post-infection. Therefore, cytokine gene regulation (TNF-  $\alpha$ , IL-6, IL-1 $\beta$  and TGF- $\beta$ ) was investigated at two time points: 2 and 24 hours post-infection in order to study the effect of infection.

Although C57 and Balb/c for studying immunology of *Leishmania* infection *in vitro* infected murine model are widely used, there is very little known on the role of TNF-  $\alpha$  in hostile Balb/c and C57 strains. Little is known on the effect of *L.mexicana* infection (virulent and avirulent; P1 and P20, respectively) *in* Balb/c and C57 on the modulation of the proinflammatory cytokines at multiple time points.

This chapter explains the results of P1 and P20 infectivity in bone marrow derived macrophages (BMDM) of susceptible Balb/c and resistant C57 mice. In addition, interaction, survival and multiplication with mammalian cells were investigated along with the effect on apoptosis and regulation of their associated genes. Infectivity of P1 and P20 was examined by counting non-engulfed parasites by Neubauer hemocytometer (see the methodology in chapter 2, section 2.9, for more details). In addition, an Alamar blue assay was used to assess

the growth rate using parasite alone as a control. In addition, counting the percentage of infected macrophages in C57 compared with Balb/c BMDM. To investigate that fate of the parasite inside the macrophage, parasites were labelled with CFSE, by staining of P1 and P20 before infection and examined by a fluorescent microscope (see the methodology in chapter-2, section 2.10, for more details). The activation of apoptosis can play an essential role in the elimination of intracellular pathogens such as *Leishmania* parasite species (Dragovich *et al.*, 1998; Moore and Matlashewski, 1994; Park *et al.*, 2006; Donovan, *et al.*, 2009). It has been reported that *Leishmania* parasites protect polymorphonuclear cells including macrophages from apoptosis in order to survive (Akarid *et al.*, 2004; Aguirre-Garcia *et al.*, 2018). The macrophage is a major target cell for the obligate intracellular *L.mexicana* parasite. Therefore, inhibition of macrophage apoptosis is a method employed by *Leishmania* parasites to ensure their survival inside the infected host cell. Apoptosis can be triggered through different intracellular signalling pathways that lead to cell death in order to maintain tissue homeostasis, regulation by inhibition or activation of these mechanisms are under cell control. During infection with intracellular microorganisms, these same pathways are utilized by the pathogen to evade recognition by the immune system and therefore the microorganism can survive and multiply inside the host.

In this study, the viability of C57 and Balb/c BMDM infected with virulent P1 and avirulent P20 was assessed by two stains: Annexin V and PI by using flow cytometry analysis. In addition, regulation of apoptotic genes (Bax, BCL 2, caspase 1, caspase 8, caspase 9 and PD 1) was also investigated using qPCR. Annexin V was used for detection of early apoptotic cells and PI for estimation of dead cells after 24 hours infection. (see the methodology in chapter-2, section 2.11, for more details). Although these genes were investigated before in some *Leishmania* species, the apoptotic machinery of apoptotic signalling pathways of infected cell modulated by *Leishmania* parasites is still unclear. Various *Leishmania* species might activate different pathways in different host cells (Cianciulli *et al.*, 2018). Investigation of these genes by comparing Balb/c and C57 BMDM infected with P1 and P20 could shed some light on the mechanism of how parasites interfere with apoptosis in infected macrophages.

Recently, the role of macrophage PD-1 receptor has been investigated in Balb/c macrophages infected with *L. donovani* and the results showed that downregulation of PD-1 may cause the activation of pro-survival AKT by phosphorylation that causes inhibition of the proapoptotic BAD protein and inhibition of apoptosis (Roy *et al.*, 2017). Therefore, gene regulation of macrophage PD-1 receptor was investigated in this study in Balb/c and C57 BMDM infected with P1 and P20 for 24 hours by qPCR.

However, to the best of my knowledge, there is no study that has compared the regulation of PD-1 in Balb/c and C57 BMDM after 24 hours infection with both P1 and P20 *L.mexicana*. The aims of this chapter are to investigate the molecular mechanisms involved in apoptosis inhibition by comparing between susceptible Balb/c and resistant C57 BMDM infected with virulent P1 and avirulent P20 *L.mexicana*.

## 4.2 Results

### 4.2.1 Infectivity of P1 and P20 *L.mexicana* in Balb/c and C57 BMDM

Two methods were used to assess the infectivity of P1 and P20 *L.mexicana* promastigotes in Balb/c and C57 BMDM, by manual counting of free non-engulfed parasites after 2- and 24-hours' infection by haemocytometer and by Alamar blue assay.

The results showed that the number of free non-engulfed P20 in both Balb/c and C57 BMDM cultures was significantly less than the number of P20 cultured alone (control) whereas, no significant difference between the number of P1 when cultured alone (control) and Balb/c and C57 infected with P1 for 2 hours (figure 4.1) and (Appendix 7). By using Alamar blue assay the results showed that the number of both P1 and P20 were significantly reduced after incubation with Balb/c and C57 BMDM for 2 hours (figure 4.2) which suggests that both P1 and P20 were engulfed by macrophages. After 24 hours of infection, there was a significant reduction in the number of non-engulfed P1 and P20 parasite compared with controls (parasites cultured without mammalian cells).

After 2 hours of infection, there was a significant reduction in the number of P20 free parasites in infected Balb/c and C57 BMDM cultures compared with P20 cultured alone (control flasks). This reduction indicates that the P20 promastigotes were engulfed by BMDM from both mouse strains (figure 4.1). After using Alamar blue, the results showed that both P1 and P20 were engulfed by Balb/c and C57 BMDM after 2 hours of infection (figure 4.2).

After 24 hours, there was a clear significant reduction in free (non- engulfed) P1 and P20 parasites in both Balb/c and C57 BMDM suggesting efficient engulfment by macrophages from the two mice strains. Regarding the effect of mice strains, there was no significant difference between Balb/c and C57 BMDM, as there were no significant differences in parasite survival when interaction with Balb/c and C57 BMDM was assessed by Alamar blue assay (figure 4.2).

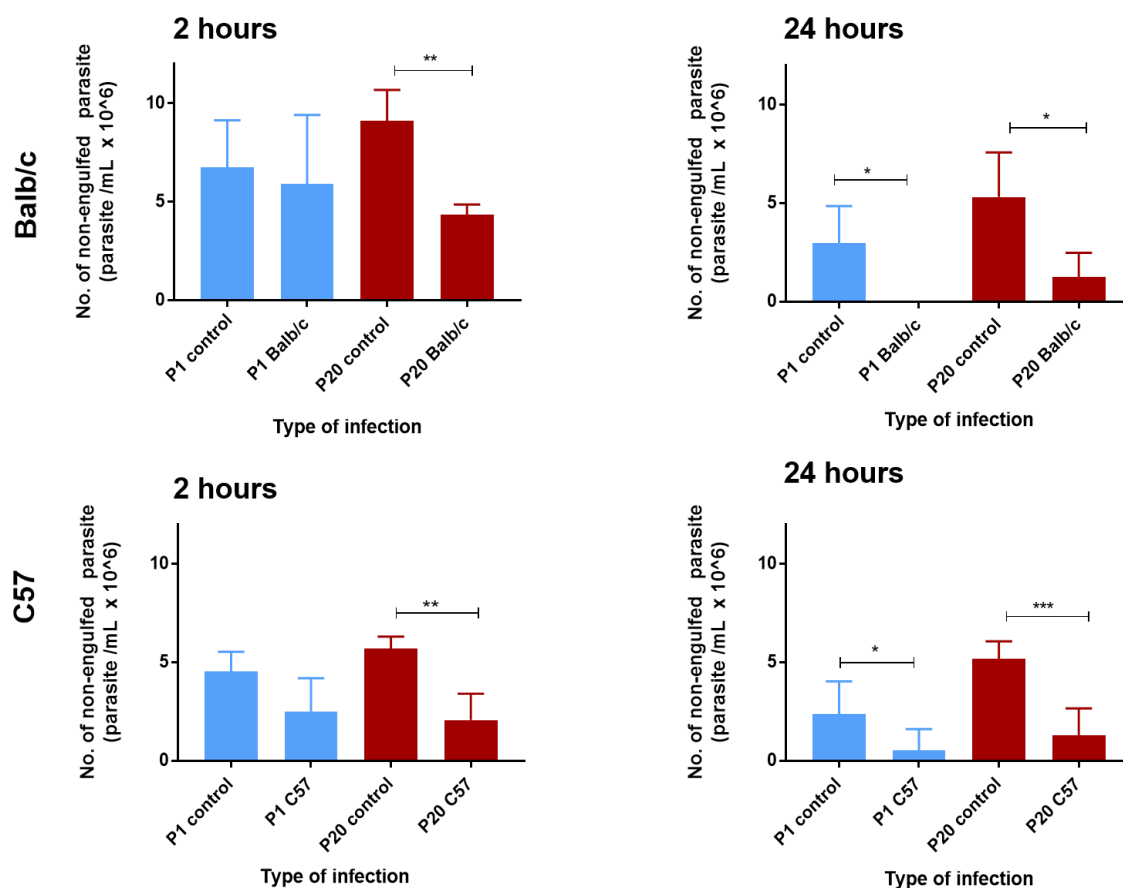


**Figure 4. 1: Estimation of numbers of non-engulfed P1 and P20 *L. mexicana* parasites after interaction with Balb/c and C57 BMDM for 2- and 24-hours at 37°C by using Neubauer haemocytometer**

Approximately one million Balb/c BMDM were infected with  $20 \times 10^6$  P1 and P20 promastigotes. All infected and control non-infected flasks were incubated in 95% v/v humidity at 37 °C in 5% v/v CO<sub>2</sub> incubator for 2, and 24 hours. Free parasites were counted by Neubauer haemocytometer. Statistically significant differences between pairs of groups represented by \* $p < 0.05$ , and \*\* $p < 0.01$  was determined by unpaired t-test. The results are average of three independent experiments and the bars represent  $\pm$  error of mean.

Estimation of P1 and P20 infectivity, by measuring the survival of non-engulfed parasite using Alamar blue after 2- and 24-hours post-infection, is an objective method and it is a more accurate estimation than haemocytometer. In the manual counting, there may be a degree of confusion between the different stages of parasites after incubation at 37°C and the number of P1 control may look lower than P20 by using haemocytometer, this could be due to rate of differentiation of promastigotes to amastigotes in the case of P1 (Appendix 7).

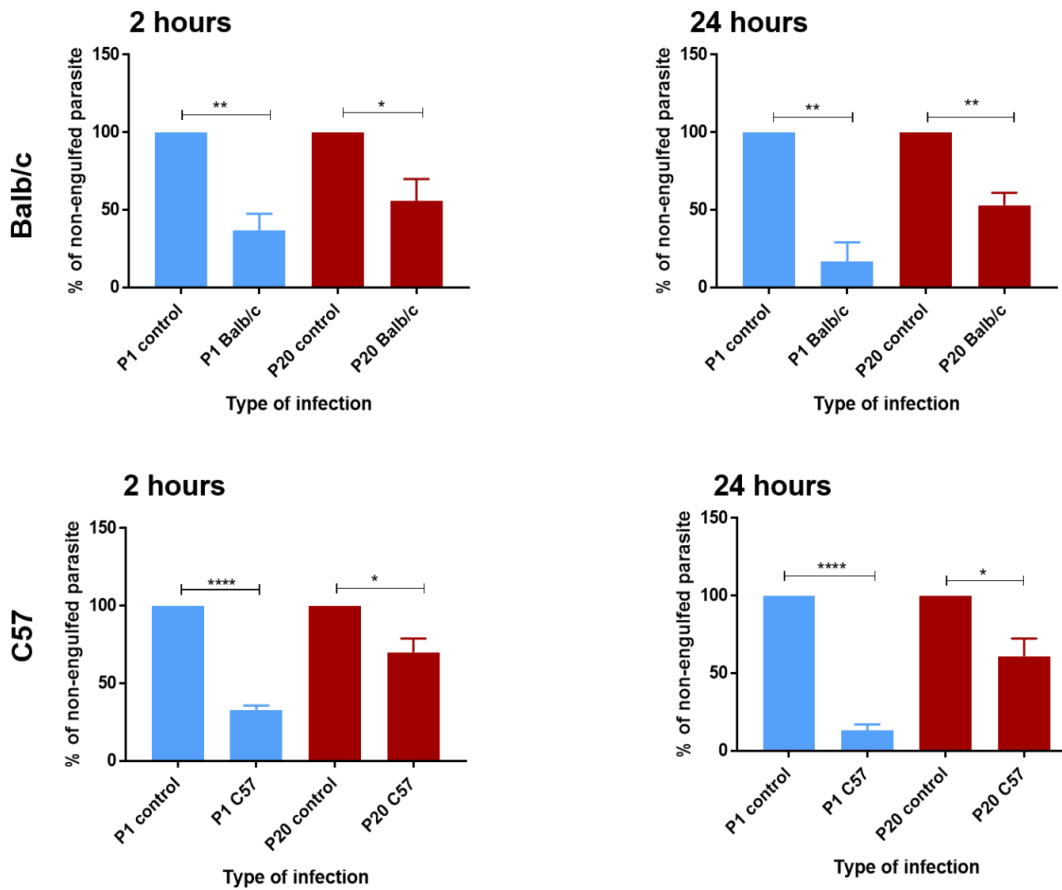


**Figure 4. 2: Estimation by Alamar blue of percentage non-engulfed P1 and P20 *L. mexicana* by Balb/c and C57 BMDM after 2 and 24 hours of infection**

Approximately one million Balb/c and C57 BMDM were infected with  $20 \times 10^6$  P1 and P20 promastigotes. All infected and control non-infected flasks were incubated in 95% v/v humidity at  $37^\circ\text{C}$  in 5% v/v  $\text{CO}_2$  incubator for 2, and 24 hours. All media containing non-engulfed free parasites were collected after 2 and 24 hours of interaction, from infected and control parasites alone were spun down at 800 g for 10 minutes. Pellets were resuspended in 300  $\mu\text{L}$  fresh RPMI medium 10% v/v HIFCS and transferred into 3 wells flat bottom 96 well plate 100  $\mu\text{L}$  in each well. 10  $\mu\text{L}$  of Alamar blue were added in all wells. Plates were sealed by cling film and wrapped by foil then incubated at  $25^\circ\text{C}$  for 2 hours. After incubation, plate was read by plate reader at 570 nm and 600 nm. Absorbance readings were calculated as mentioned in methods and then normalized with control parasite alone. Statistically significant differences between pairs of groups represented by \* $p < 0.05$ , \*\* $p < 0.001$ . p value was determined by unpaired t-test. The results are average of three independent experiments and the bars represent  $\pm$  standard error of mean.

## **4.2.2 The fate of P1 and P20 *L.mexicana* in Balb/c and C57 BMDM**

### **4.2.2.1 Live images of Balb/c and C57 BMDM infected with P1 and P20 *L.mexicana***

The ability of the P1 and P20 *L.mexicana* to infect and survive inside Balb/c and C57 BMDM was investigated. Macrophages were infected with P1 and P20 and examined daily for the presence of parasites inside macrophages for seven days. A further experiment was set up by staining of P1 and P20 with FITC in order to visualise parasites inside macrophages by fluorescent microscopy.

The results of infection of Balb/c and C57 BMDM with virulent P1 and avirulent P20 *L.mexicana* promastigotes for a period of up to 7 days have shown considerable differences in parasite infectivity, survival and multiplication, (figure 4.3 and 4.5).

The pictures of Balb/c BMDM infected with P1 and P20 *L.mexicana* promastigotes for 2 hours (figure 4.3), illustrate that both P1 and P20 promastigotes were firmly adhered/attached to macrophages (white arrows). After 24 hours, P1 parasites that differentiated to amastigotes (blue arrows) were detected outside the infected macrophage cells. However, avirulent P20 promastigotes failed to differentiate into amastigotes (white arrows) outside the cells. The majority of P20 parasites remained outside the macrophages cells as promastigotes.

The pictures clearly illustrate infectivity of parasites in macrophages, internalisation and formation of PVs inside macrophages that are infected with P1 but not P20. In addition, after 3 and 7 days, very few signs of infection were observed in macrophages infected with P20, whereas macrophages infected with P1 became enlarged and rounded with a noticeable increase in PV size. A similar pattern of results was also observed in C57 BMDM infected with P1 and P20 *L.mexicana* parasites (figure 4.4).

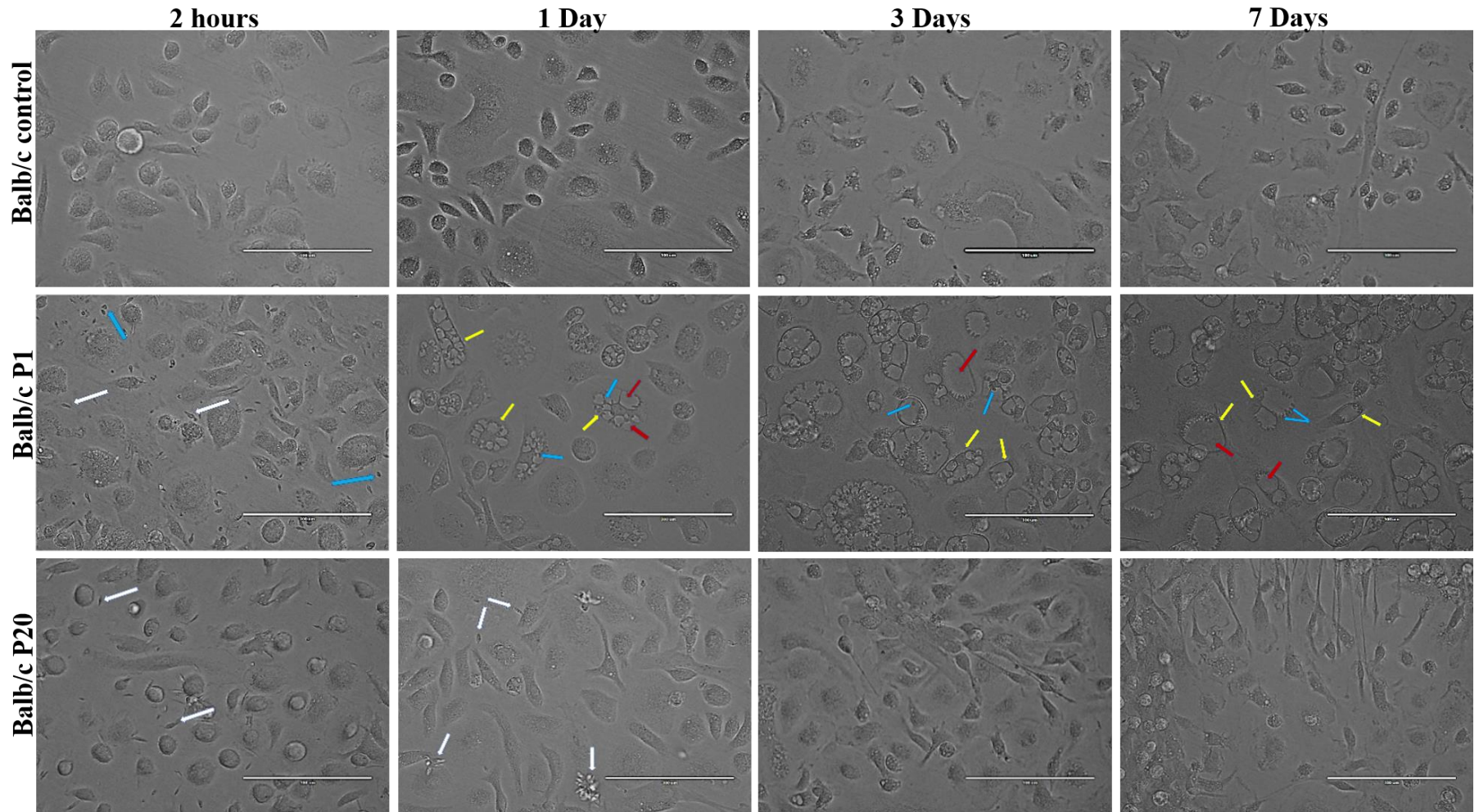


**Figure 4. 3: Live images of Balb/c BMDM infected with P1 and P20 at 2 hours and 1, 3 and 7 days**

Approximately one million Balb/c BMDM were infected with  $20 \times 10^6$  P1 and P20 promastigotes in 2.5 mL RPMI 1640 medium 10% v/v HIFCS and incubated in 95% v/v humidity at 37 °C in 5% v/v CO<sub>2</sub> incubator for 2 hours, 1, 3 and 7 days; non infected macrophages were used as control. live images were taken by EVOS microscope life technology light cubes: transmission, 40 x objective at each time point. The white arrows indicate promastigotes, blue arrows indicate amastigotes, yellow arrows indicate infected macrophages and red arrows indicate PV. (Scale bar = 100  $\mu$ ).

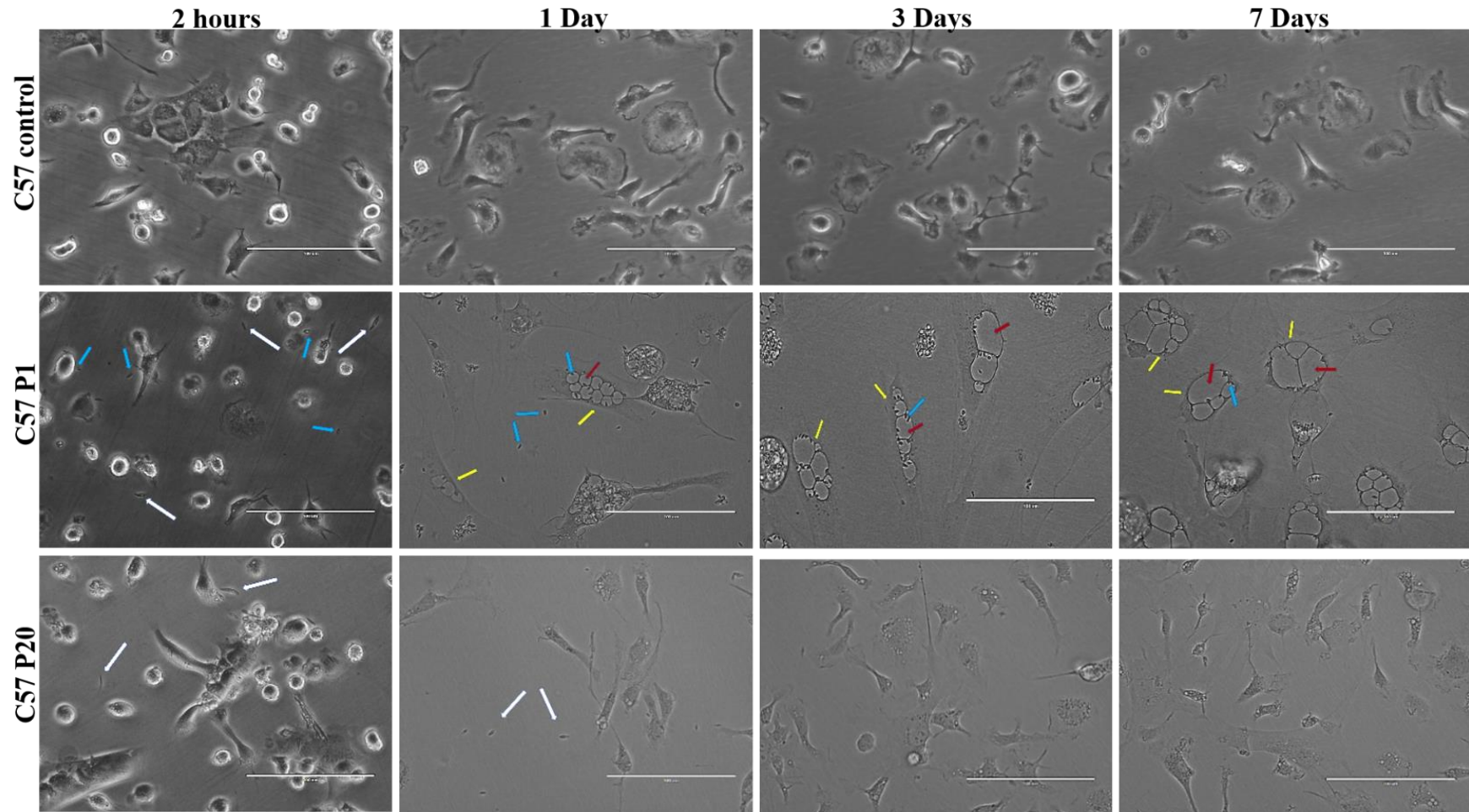


**Figure 4. 4: Live images of C57 BMDM infected with P1 and P20 *L.mexicana* at two 2 and 24 hours.**

Approximately one million C57 BMDM were infected with  $20 \times 10^6$  P1 and P20 promastigotes in 2.5 mL RPMI 1640 medium 10% v/v HIFCS and incubated in 95% v/v humidity at 37 °C in 5% v/v CO<sub>2</sub> incubator for 2 hours, 1, 3 and 7 days; non infected macrophages were used as control. Live images were taken by EVOS microscope life technology light cubes: transmission, 40 x objective at each time points. The white arrows indicate promastigotes, blue arrows indicate amastigotes, yellow arrows indicate infected macrophages and red arrows indicate PV (Scale bar = 100 μm).

After two hours of C57 and Balb/c BMDM infection, we cannot observe infected macrophages either with P1 or P20. Some P1 but not P20 promastigotes (white arrows) were differentiated into amastigotes (blue arrows) outside macrophages. Both P1 and P20 promastigotes (white arrows) made a firm attachment to the macrophages. After 24 hours, a clear infection in BMDM with P1 but not P20 parasites (yellow arrows) can be observed inside macrophages (figure 4.3 and 4.4). P1 differentiate into amastigotes (blue arrows) and survive inside PV (red arrows), whereas, P20 remained in their promastigote form and formed rosettes outside BMDM.

After 3 and 7 days, the number of infected macrophages, as well as the number of parasites inside macrophages, increased. In contrast, the number of PV per cell was decreased, and the shape of macrophages became large and round due to being filled with PV. However, no infected macrophages with P20 have been observed under a light microscope. Giemsa stained images of Balb/c and C57 BMDM infected with P1 and P20 *L.mexicana* at 2 and 24 hours.

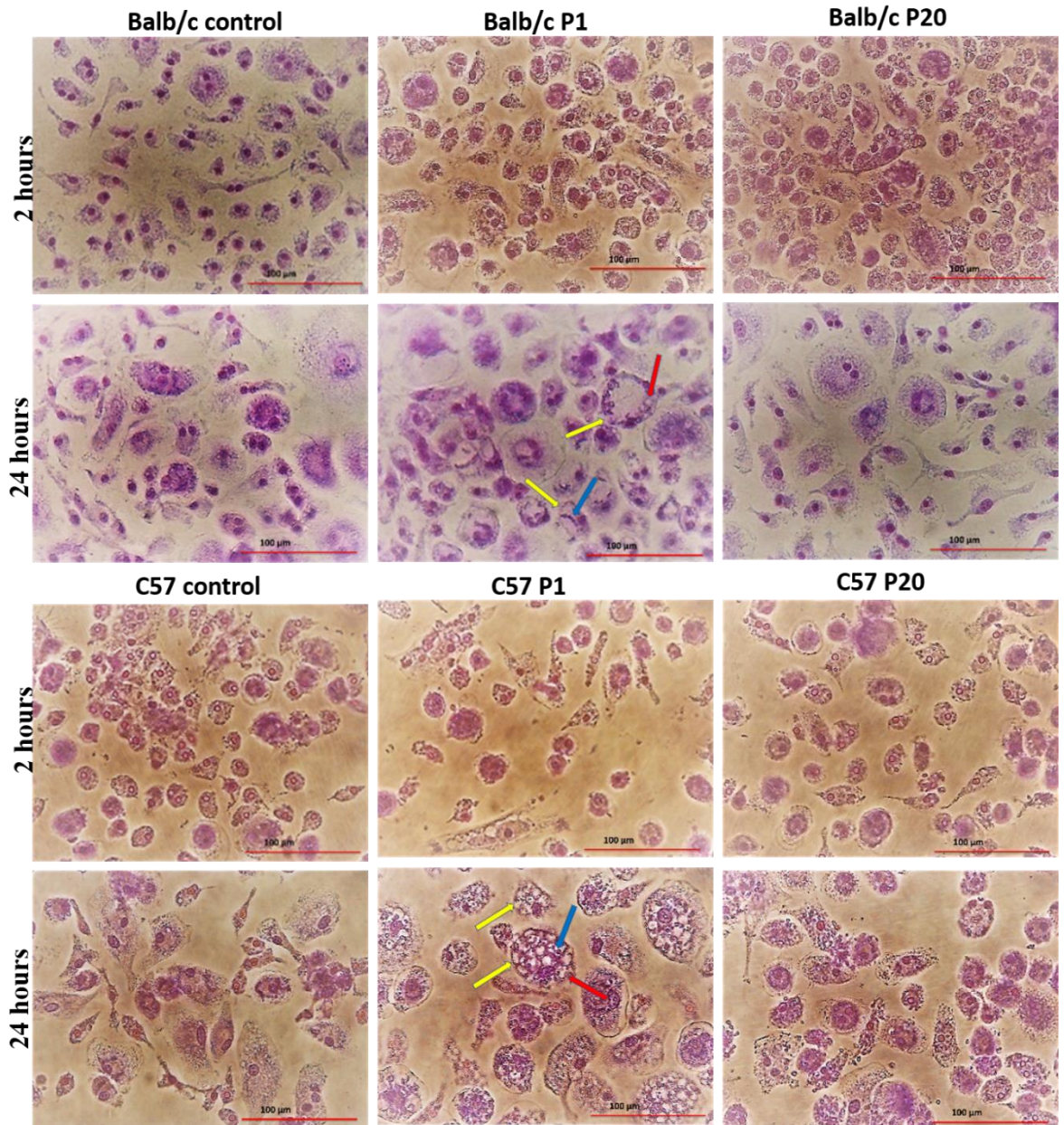


**Figure 4. 5: Giemsa stained images of Balb/c and C57 BMDM infected with P1 and P20 *L.mexicana* at 2 and 24 hours.**

Approximately one million Balb/c and C57 BMDM were infected with  $20 \times 10^6$  P1 and P20 promastigotes in 2.5 mL RPMI 1640 medium 10% v/v HIFCS and incubated in 95% v/v humidity at 37 °C in 5% v/v CO<sub>2</sub> incubator for 2 and 24 hours. Non infected macrophages were used as control. All flasks were stained with Giemsa stain, images were taken by Nikon microscope transmission, 40 x objectives at each time points. The blue arrows indicate amastigotes, yellow arrows indicate infected macrophages and red arrows indicate PV.

Non-engulfed parasites (P1 and P20) in infected Balb/c and C57 BMDM, were estimated by manual counting and Alamar blue assay after 2, and 24 hours post-infection. The results clearly show that there was a significant reduction in non-engulfed P1 and P20 parasite compared with controls (parasite without mammalian cells) after 2 and 24 hours (figure 4.1

and 4.2.). Live and Giemsa stained pictures did not detect whether P20 were engulfed by macrophages.

Light microscope and Giemsa staining pictures demonstrated the ability of virulent *L.mexicana* (P1) to infect BMDM derived from both susceptible Balb/c and resistant C57. On the other hand, the avirulent (P20) *L.mexicana* demonstrated very little to no infection in BMDM derived from both susceptible Balb/c and resistant C57.

### **4.2.3 Fluorescent microscopic images of Balb/c and C57 BMDM infected with P1 and P20 *L.mexicana* after 24 hours**

In order to investigate whether P20 can infect Balb/c and C57 BMDM, P1 and P20 promastigotes were stained with CFSE and used to infect Balb/c and C57 BMDM for 24 hours (figure 4.6 and 4.7). The results clearly show that Balb/c and C57 macrophages can engulf both P1 and P20 promastigotes, but P20 couldn't create PV and subsequently did not survive inside macrophages. After 24 hours of infection, some of P1 promastigotes differentiate into amastigotes inside macrophages. Hence, P20 promastigotes could infect both Balb/c and C57 BMDM but failed to survive inside macrophages.

Microscopically, no infected Balb/c and C57 BMDM were noticed after 2 hours infection, but after 24 hours a clear infection with P1 in both Balb/c and C57 BMDM (figure 4.3) was noticed. To confirm this, other experiments were designed to analyse infectivity of P20 in BMDM by using FITC (CFSE) labelled parasites. Interestingly, the results show that P20 promastigotes were successfully engulfed by both Balb/c and C57 BMDM but failed to differentiate into amastigotes and to survive in both Balb/c and C57 BMDM cells. In addition, diffuse fluorescence inside macrophages was observed suggesting degradation of P20 inside macrophages (figure 4.6 and 4.7).

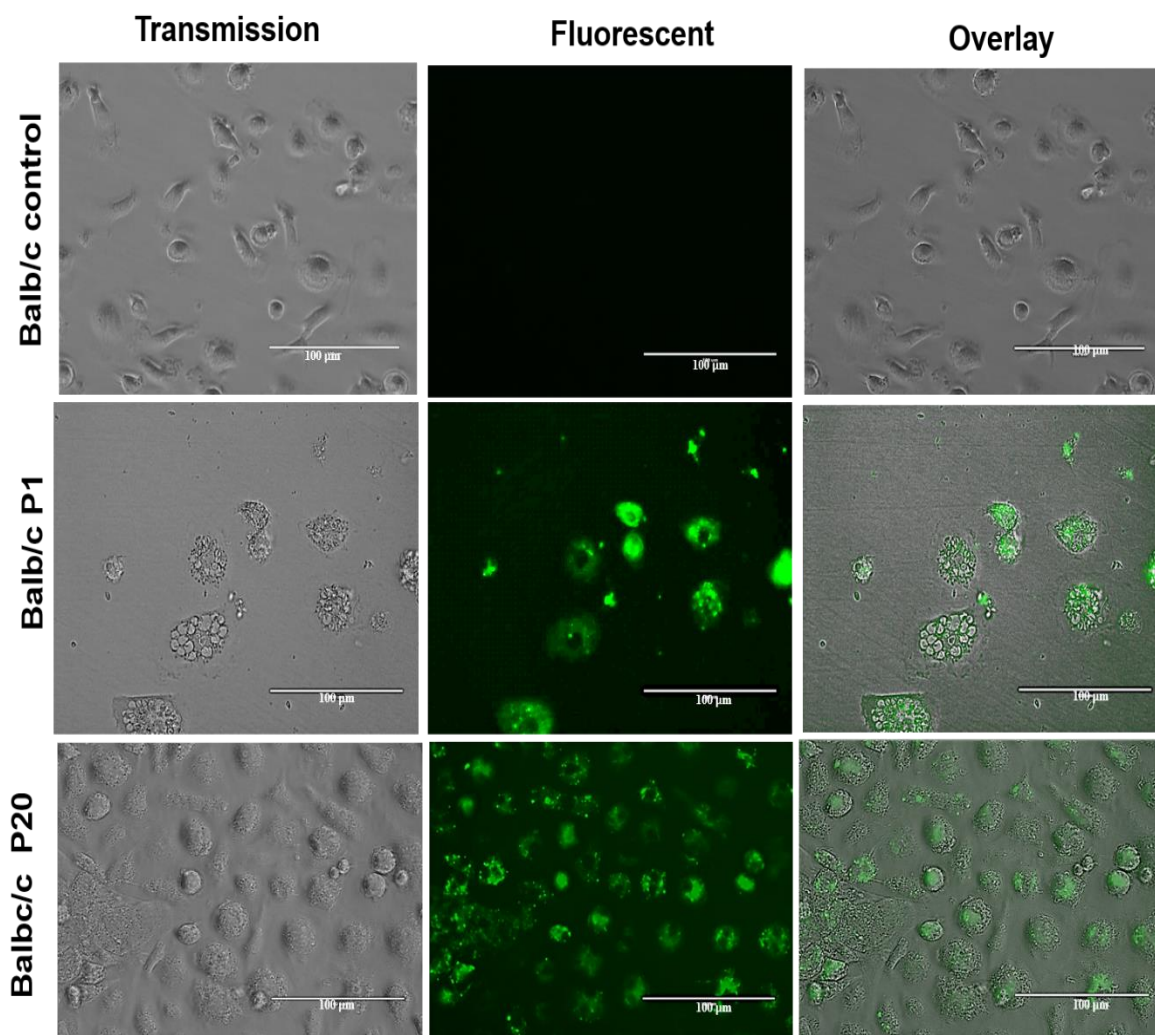


**Figure 4. 6: Infectivity of P1 and P20 *L. mexicana* promastigotes in Balb/c BMDM measured by fluorescent microscope after 24 hours**

20 x 10<sup>6</sup> P1 and P20 promastigotes were labelled with 50 ng/mL CFSE in RPMI 1640 media containing 10% v/v HIFCS. After 1-hour incubation at 25°C, promastigotes were washed three times with PBS. One million Balb/c macrophages were infected with CFSE labelled promastigotes and incubated at 95% v/v humidity at 37°C in 5% v/v CO<sub>2</sub> incubator for 24 hours. Free parasites were removed and replaced by fresh medium. Photos were taken by fluorescent microscope EVOS life technology light cubes: GFP (470/22 nm Excitation; 510/42 nm Emission) and at transmission. The results clearly showed that macrophages engulf both P1 and P20 but P20 could not create PV and did not survive inside macrophages.

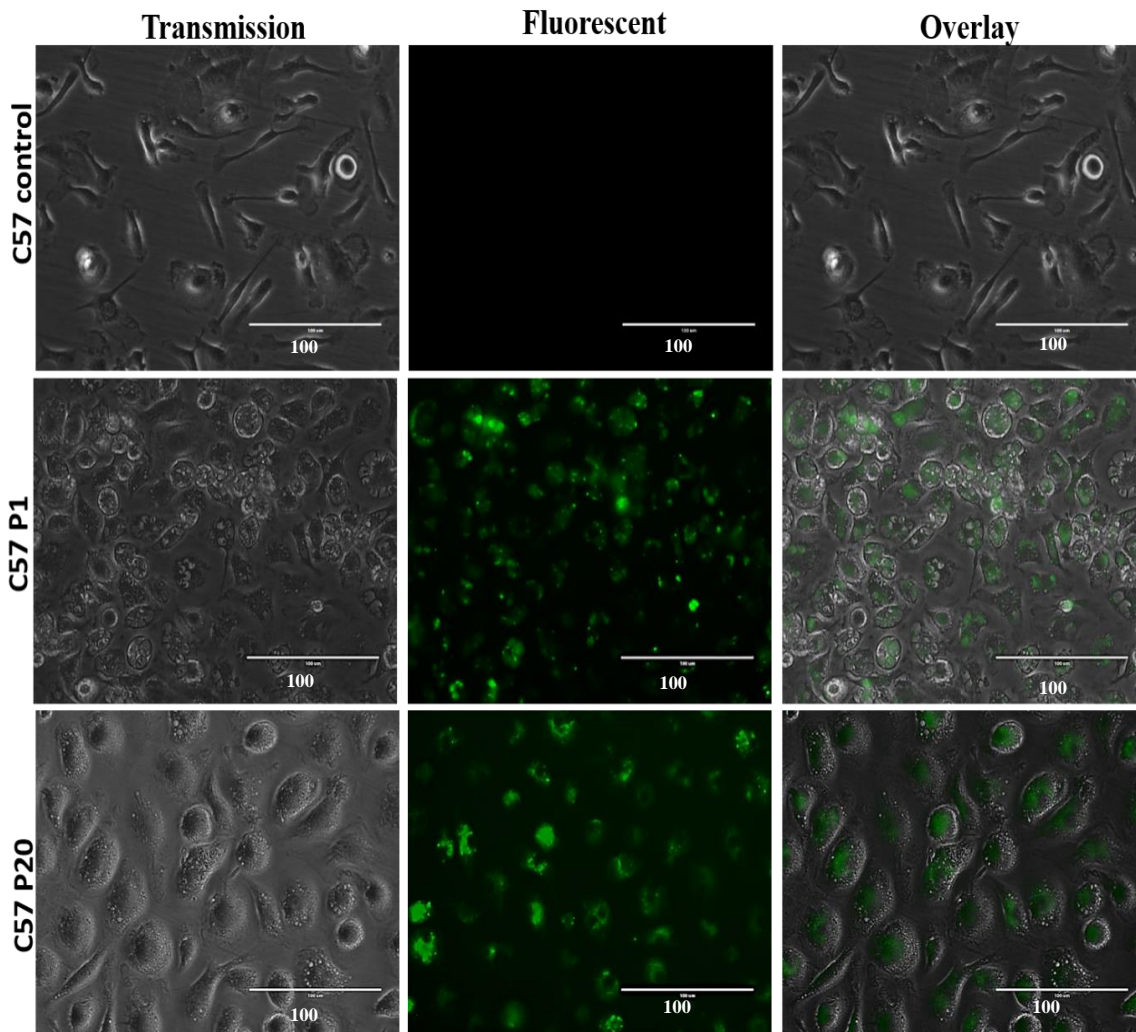


**Figure 4. 7: Infectivity of P1 and P20 *L. mexicana* promastigotes to C57 BMDM measured by fluorescent microscope after 24 hours**

20 x 10<sup>6</sup> P1 and P20 promastigotes were labelled with 50 ng /mL CFSE in RPMI 1640 media containing 10% v/v HIFCS. After 1-hour incubation at 25 °C promastigotes were washed three times with PBS. C57 macrophages were infected with CFSE labelled promastigotes and incubated at 95% v/v humidity at 37 °C in 5% v/v CO<sub>2</sub> incubator for 24 hours. Free parasites with whole medium were removed and replaced by fresh medium. Photos were taken by fluorescent microscope EVOS life technology light cubes: GFP (470/22 nm Excitation; 510/42 nm Emission) and at transmission. The results clearly showed that macrophages engulf both P1 and P20 but P20 could not create PV and did not survive inside macrophages.

#### 4.2.4 The fate of engulfed *L. mexicana* P1 and P20 in Balb/c and C57

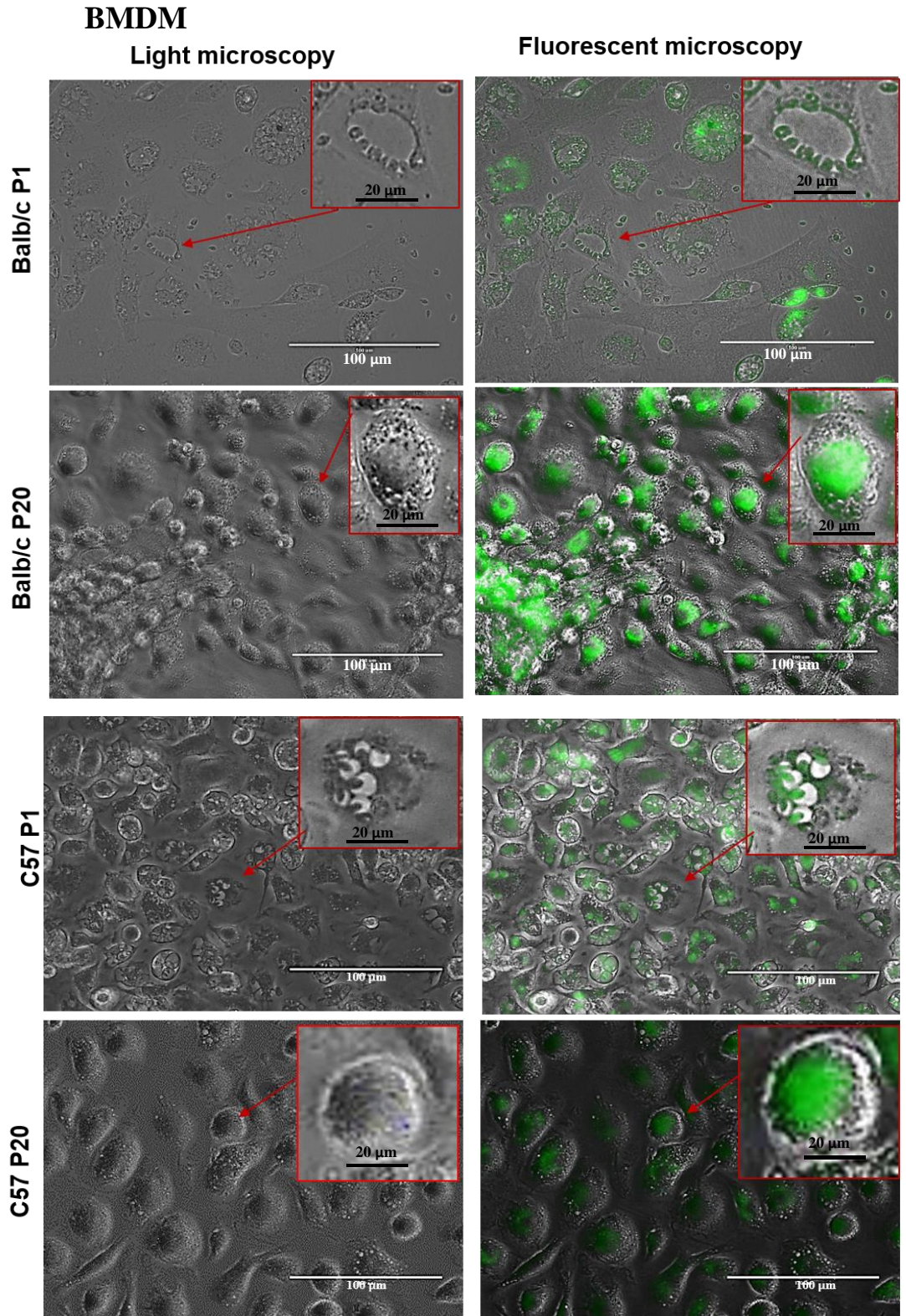


**Figure 4. 8: Fate of P1 and P20 *L. mexicana* promastigotes in Balb/c and C57 BMDM was measured by fluorescent microscope.**

20 x 10<sup>6</sup> P1 and P20 promastigotes were stained with 50 ng/mL CFSE in RPMI containing 10% v/v HIFCS. After 1-hour incubation at 25 °C promastigotes were washed three times with PBS. Balb/c and C57 BMDM were infected with CFSE labelled promastigotes and incubated at 95% v/v humidity at 37 °C in 5% v/v CO<sub>2</sub> incubator for 24 hours. After that free parasites were removed and replaced by fresh medium. Photos were taken by fluorescent microscope (EVOS life technology) light cubes: GFP and at transmission.

The picture clearly illustrate that P20 promastigotes were engulfed by both Balb/c and C57 BMDM but failed to differentiate into amastigotes whereas, P1 differentiated into amastigotes and created PV in both Balb/c and C57 BMDM (figure 4.8). In addition, diffuse fluorescence was observed inside macrophages infected with P20 suggesting degeneration of P20 inside macrophages.

#### 4.2.5 Survival of P1 *L.mexicana* in Balb/c and C57 BMDM

Survival of P1 in Balb/c and C57 BMDM was investigated by visual examination of infected target cells at 1, 3- and 7-days post-infection by using a light microscope. The percentage of infected cells, number of amastigotes, number of PVs per infected, and number of amastigotes per PV and infectivity index were calculated.

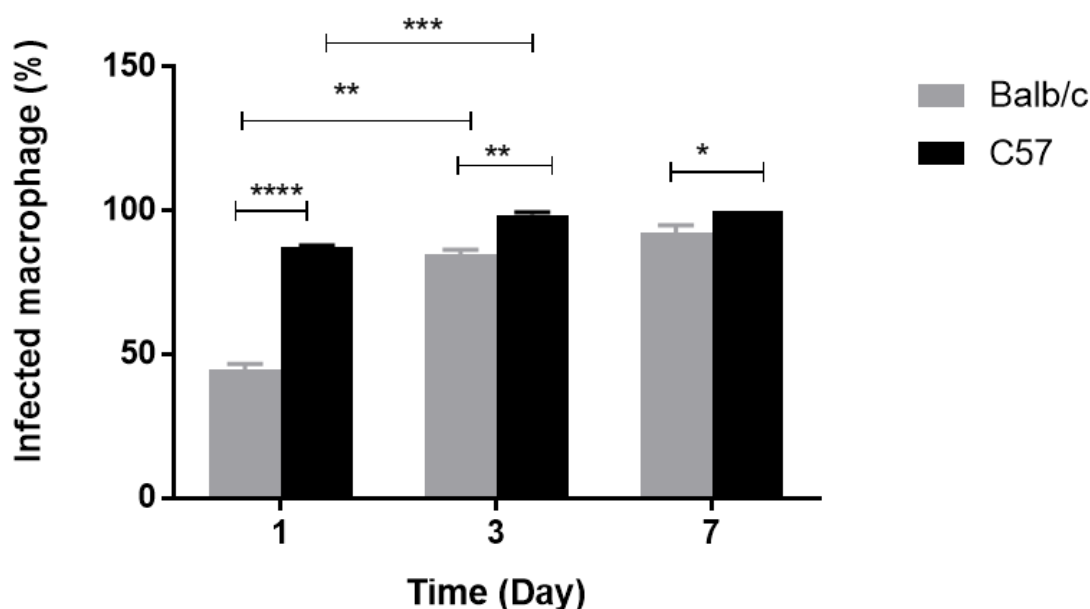


**Figure 4. 9: Infectivity of P1 *L.mexicana* promastigotes in Balb/c and C57 BMDM at 1,3- and 7-days of infection**

Approximately one million Balb/c and C57 BMDM were infected with  $20 \times 10^6$  P1 promastigotes in 2.5 mL RPMI 1640 medium supplemented with 10% v/v HIFCS and incubated in 95% v/v humidity at 37 °C in 5% v/v CO<sub>2</sub> incubator for 1,3 and 7 days. Live images were taken by light microscope (EVOS life technology) 40 x objective at each time point. To calculate the percentage of infected cells, the numbers of infected and non-infected cells were counted. The number of infected cells was divided by the number of total infected and non-infected cells and multiplied by 100. The data were analysed by using GraphPad Prism 7. Statistically significant differences between pairs of groups represented by \* $p < 0.05$ , \*\* $p < 0.001$ , \*\*\* $p < 0.0001$  and \*\*\*\* $p < 0.00001$  and determined by paired t-test. The results are average of three independent experiments and bars represent  $\pm$  SEM.

The internalisation of P1 promastigotes in Balb/c and C57 BMDM has been observed after 24 hours of infection (figure 4.3 and 4.4) and (Appendix 8). Throughout the experiment, the percentage of BMDM infected with P1 was significantly higher in C57 than Balb/c. (figure

4.9) After 3 days, the percentage of infected macrophages was significantly increased in both Balb/c and C57 BMDM. Engulfment of P1 by C57 is significantly higher than Balb/c BMDM.

The number of P1 amastigotes per cell steadily increased with time in both Balb/c and C57 suggesting that the amastigotes multiplied in both mice strains macrophages *in vitro*. The number of P1 amastigotes per infected cell was generally higher in C57 than Balb/c BMDM after 24 hours and 7 days. On the other hand, on the third day, the number of amastigotes per cell was higher in Balb/c than C57BMDM. In Balb/c BMDM, the number of P1 amastigotes per cell significantly increased on the third day compared with the first day. On the seventh day, there was no significant increase in the number of amastigotes per cell. Meanwhile, in C57 BMDM the number of P1 amastigotes per cell did not show a significant difference on the third compared to the first day. On the seventh day, the number of amastigotes per cell significantly increased (figure 4.11A). The pictures clearly show PVs in both Balb/c and C57 BMDM infected with P1 but not P20, promastigotes, which formed after 24 hours of infection (figure 4.3, 4.4).

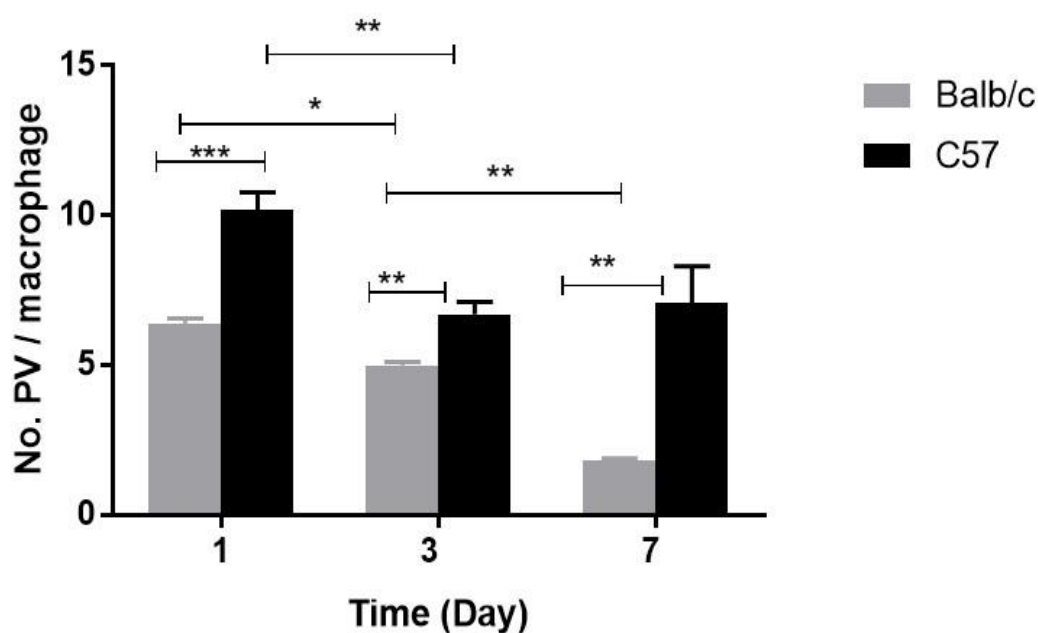


**Figure 4. 10: Number of PV per Balb/c and C57 BMDM infected with P1 after 1, 3- and 7-days of infection**

Approximately one million Balb/c and C57 BMDM were infected with  $20 \times 10^6$  P1 promastigotes in RPMI 1640 medium supplemented with 10% v/v HIFCS and incubated in 95% v/v humidity at 37 °C in 5% v/v CO<sub>2</sub> incubator for 1,3 and 7 days. Live images were taken by light microscope (EVOS life technology), 40 x objectives at each time points. To calculate the number of PV per infected cell, the number of PV was divided by the number of infected cells. The data were analysed by using GraphPad Prism 7. Statistically significant differences between pairs of groups represented by \*p <0.05, \*\*p<0.001 and \*\*\*p<0.0001. p values were determined by unpaired t-test. The results are average of three independent experiments; bars represent  $\pm$  SEM.

The percentage of infected macrophages after 3 and 7 days increased and the number of parasites was also increased; in contrast, the number of PV decreased, and macrophages appeared congested with PVs. However, no macrophage infected with P20 was observed. Throughout the experiment, the number of PV per infected cell was significantly higher in C57 than Balb/c BMDM. The number of PV per cell in C57 BMDM significantly decreased on the first 3 days of infection then remained unchanged, whereas, the number of PV per cell in Balb/c BMDM significantly decreased for the duration of the experiment. The number of PV steadily decreased with time over the period of the experiment in Balb/c and C57 BMDM, which may be due to fusion between PVs and formation of large PV. However, they were higher in C57 than Balb/c BMDM.

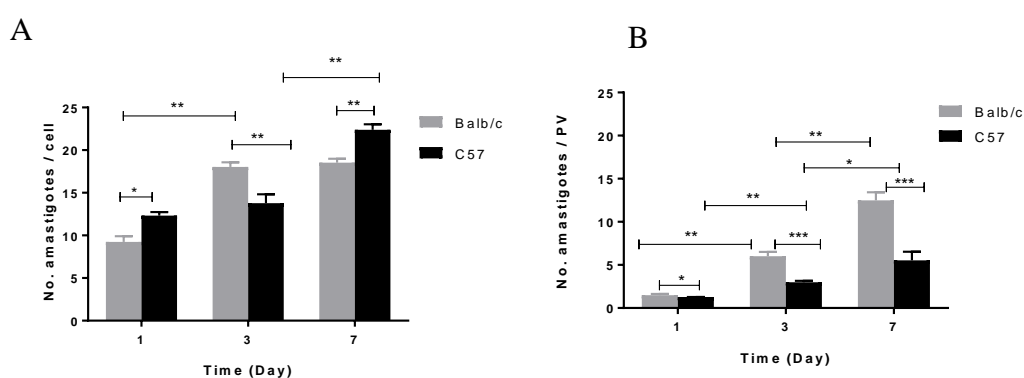


**Figure 4. 11: Number of amastigotes per PV and cell in Balb/c and C57 BMDM infected with P1 *L.mexicana* promastigotes**

Approximately one million Balb/c and C57 BMDM were infected with  $20 \times 10^6$  P1 promastigotes in RPMI 1640 medium supplemented with 10% v/v HIFCS and incubated in 95% v/v humidity at 37 °C in 5% v/v CO<sub>2</sub> incubator for 1,3 and 7 days. Live images were taken by light microscope (EVOS life technology) 40 x objectives at each time point. The number of amastigotes per cell and per PV were counted, the average of amastigotes divided by the average number of infected cells and PV. (A) The number of amastigotes per cell. (B) The number of amastigotes per PV. The data were analysed by using GraphPad Prism 7. Statistically significant differences between pairs of groups represented by \* $p < 0.05$  \*\* $p < 0.001$  \*\*\* $p < 0.0001$ . p values were determined by unpaired t-test. The results are average of three independent experiments the bars represent  $\pm$  SEM.

When Balb/c and C57 BMDM were infected by the parasites, the number of amastigotes inside PVs significantly increased with the time of incubation (figure 4.11B). In addition, the number of amastigotes and PVs per cell was significantly higher in Balb/c than C57 BMDM (figure 4.11B), suggesting proliferation of amastigotes in both Balb/c and C57 BMDM. The multiplication inside susceptible (Balb/c) was higher than in resistant (C57) BMDM.

The results clearly show that the number of amastigotes per PV was significantly higher in Balb/c than C57 BMDM at all 3 time points examined. In addition, the number of

amastigotes in PV was significantly increased with time in both Balb/c and C57 BMDM (figure 4.11B). It was also noticed that individual PVs were of different sizes and number of amastigotes (figure 4.3 and 4.4). Number of PVs was higher in C57 than Balb/c BMDM and significantly decreased with time of incubation in both strains (figure 4.10).

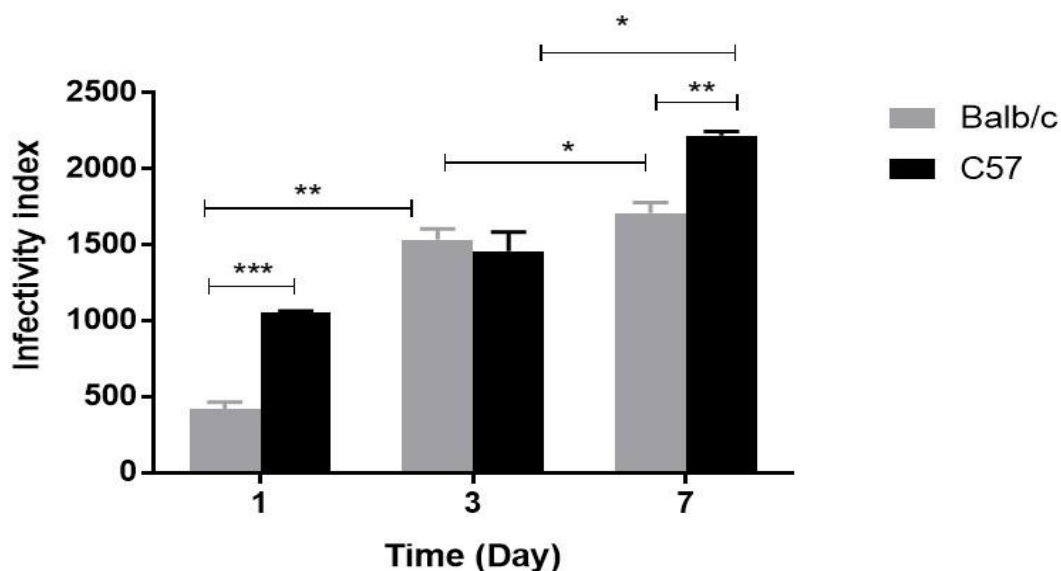


**Figure 4. 12: Infectivity index of P1 in Balb/c and C57 BMDM after 1, 3- and 7-days infection**

Approximately one million Balb/c and C57 BMDM were infected with  $20 \times 10^6$  P1 promastigotes in RPMI 1640 medium supplemented with 10% v/v HIFCS and incubated in 95% v/v humidity at 37°C in 5% v/v CO<sub>2</sub> incubator for 1,3 and 7 days. Live images were taken by light microscope (EVOS life technology) 40 x objectives at each time points. The infectivity index was calculated by multiplying the percentage of infected cells by the mean number of parasites (amastigotes) per infected cell (Tripathi and Gupta., 2003; DaMata *et al.*, 2015). The data were analysed by using GraphPad Prism 7. Statistically significant differences between pairs of groups represented by \* $p < 0.05$ , \*\* $p < 0.001$  and was determined by paired t-test. The results are average of three independent experiments; and the bars represent  $\pm$  SEM.

The results clearly show that the infectivity index of Balb/c BMDM infected with P1 was significantly increased after 1, 3 and 7 days of infection while that of C57 BMDM was significantly increased between day 3 and 7 of infection.

The number of amastigotes per infected macrophage ranged between 8 to 23 (figure 4.10) with a significant increase with time of incubation. Number of amastigotes per PV significantly increased with time (figure 4.11B). Infectivity index increased with time of infection (figure 4.12) and it was higher in C57 than Balb/c BMDM in the first and seventh day of infection. Results clearly suggest that P1 but not P20 can survive and multiply in both Balb/c and C57 BMDM *in vitro*.

## 4.2.6 Apoptosis in Balb/c and C57 BMDM in response to infection with P1 and P20 *L.mexicana* promastigotes

### 4.2.6.1 The effect of removing GMCSF from Balb/c and C57 BMDM culture on apoptosis

Macrophages were cultured in the presence or absence of GMCSF for 24 hours before use for infection with parasites. To assess whether infection with P1 and P20 *L.mexicana* promastigotes was able to inhibit apoptosis in Balb/c and C57 BMDM, macrophages were washed after 24 hours infection in order to remove all non-engulfed parasites and re-incubated for a further 24 hours. The results clearly show that incubation of Balb/c and C57 BMDM for 24 hours without GMCSF induced more apoptosis compared with controls (incubated with GMCSF). Therefore, in further experiments, GMCSF was removed to induce apoptosis in BMDM of both strains and was used to test the ability of P1 and P20 promastigotes to inhibit apoptosis after 24 hours infection (Appendix 9).

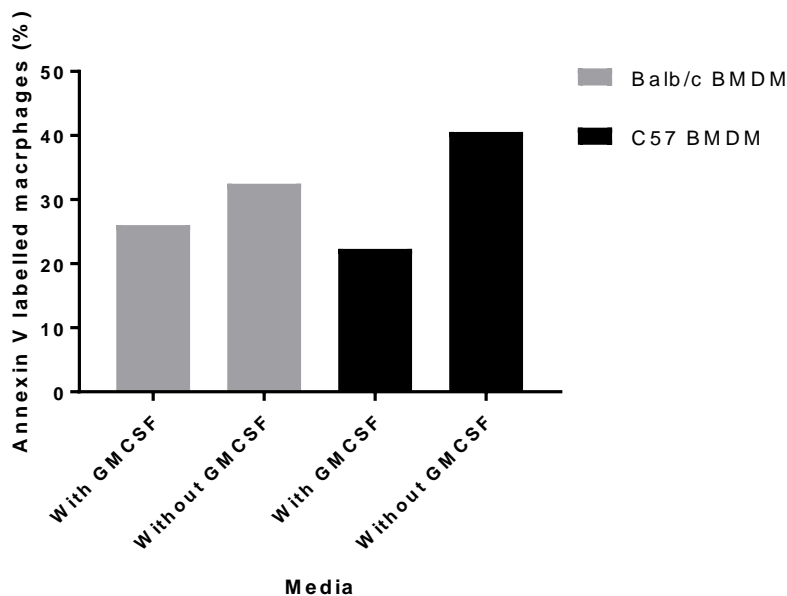


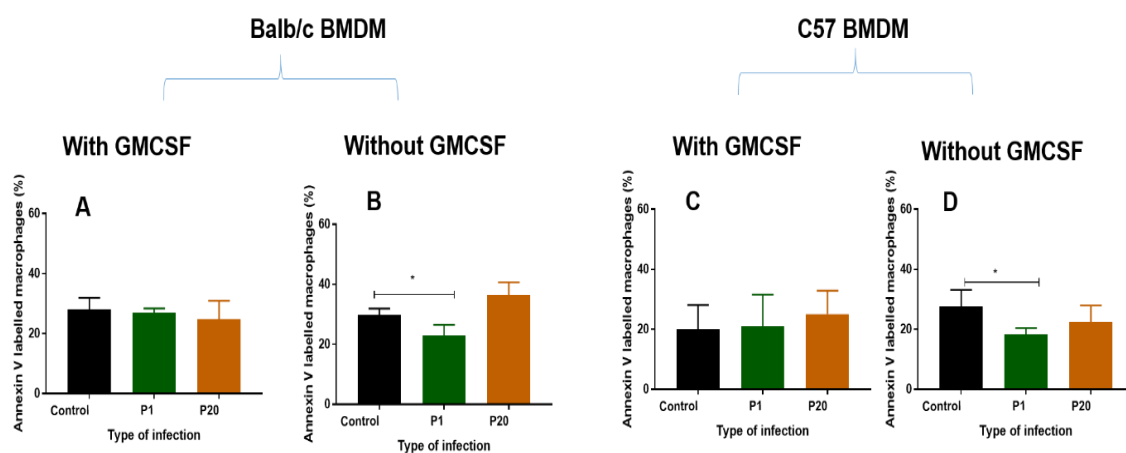
**Figure 4. 13: Effect of removing of GMCSF from control Balb/c and C57 BMDM culture apoptosis**

Approximately one million Balb/c and C57 differentiated BMDM at day 7<sup>th</sup> were cultured in T25 tissue culture flasks in RPMI1640 media. All flasks were divided into two groups with and without GMCSF. All flasks were incubated at 95% v/v humidity at 37°C in 5% v/v CO<sub>2</sub> incubator for 24 hours. All cells were harvested by cell scraper and washed with 1x PBS. 0.5 x 10<sup>6</sup> cells were stained with Annexin V for early apoptosis detection and incubated in the dark at room temperature for 15 minutes. Cells were stained with propidium iodide (PI) for dead cell detection immediately before running flow cytometry analysis (Beckman Coulter). The flow cytometry results were analysed by Beckman Coulter Kaluza software USA. The results represent two independent experiments.

#### **4.2.6.2 Effect of infection with P1 and P20 *L.mexicana* on apoptosis in Balb/c and C57 BMDM**

Infected and control non-infected Balb/c and C57 BMDM macrophages were divided into two groups, with and without GMCSF and subjected to flow cytometry analysis in order to assess levels of apoptosis and necrosis using two different stains (Annexin V and PI respectively) in the presence or absence of GMCSF in culture media respectively (figure. 4.14) and (Appendix 10 A and B). Staining of Balb/c and C57 BMDM with Annexin V showed no significant difference between control and those infected with P1 or P20 (figure. 4.14 A and D). After inducing of apoptosis by depletion of GMCSF, results show that infection with P1 promastigotes of Balb/c (figure. 4.14 (B) and C57 BMDM (figure. 4.14 D) induced significantly less apoptosis than control (non-infected macrophages) while infection with P20 did not significantly change the level of apoptosis compared with control. However, as for necrosis assessed by PI stain only significant inhibition of necrosis was observed in C57 BMDM cultured in the absence of GMCSF and infected with P1 (figure. 4.14 H).

## Apoptosis



## Necrosis

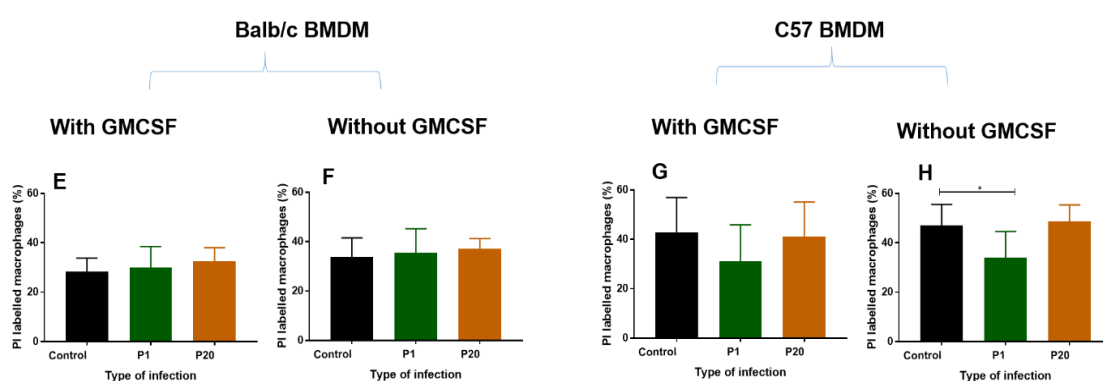


**Figure 4. 14: Apoptosis in Balb/c and C57 BMDM after infection with P1 and P20 *L.mexicana* promastigotes**

Approximately one million Balb/c and C57 BMDMs were cultured in T25 tissue culture flasks. At day 7 cells were infected with  $20 \times 10^6$  P1 and P20 *L. mexicana* promastigotes and incubated at 95% v/v humidity at 37°C in 5% v/v CO<sub>2</sub> incubator for 24 hours. Non-engulfed parasites were removed by washing with RPMI 1640 medium. All flasks were divided into two groups, first group was replaced with fresh medium containing GMCSF, whereas the media in the second group was replaced with new fresh medium but without GMCSF and re incubated for another day. All cells were harvested by cell scraper and washed with 1 x PBS.  $0.5 \times 10^6$  cells were stained with Annexin V for early apoptosis detection and incubated in the dark at room temperature for 15 minutes. Cells were stained with PI for dead cell detection directly before running flow cytometry (Beckman Coulter). The flow cytometry results were analysed by Beckman Coulter Kaluza software USA. The data were analysed by GraphPad Prism 7. Statistically significant differences between groups represented by \* $p < 0.05$  and determined by unpaired t-test. The results are average of three independent experiments and bars represent  $\pm$  SEM.

#### 4.2.6.3 Effect of infection with P1 and P20 *L.mexicana* on apoptosis associated genes regulation in Balb/c and C57 BMDM

In order to understand why P1 but not P20 inhibits apoptosis in Balb/c and C57 BMDM, it is worthwhile to evaluate the effect of P1 and P20 infection on the expression of apoptosis-associated genes in Balb/c and C57 BMDM. mRNA was extracted from Balb/c and C57 BMDM infected with P1 and P20 and control (non-infected) and converted into cDNA and used for qPCR analysis. Figure. 4.15 illustrates the gene expression profile of six apoptosis-associated genes in Balb/c and resistant C57 BMDM infected with P1 and P20 (figure. 4.15 (A and B) respectively).

Infection of Balb/c BMDM with *L.mexicana* P1 has downregulated the expression of almost all genes tested with the exception of BCL 2 which was significantly up-regulated, while infection with P20 downregulated the expression of BCL 2, caspase 1, caspase 9 and PD-1. On the other hand, infection of C57 BMDM with P1 promastigotes significantly upregulated caspase 8, caspase 9 and PD-1 genes (figure. 4.15 B) while infection with P20 downregulated the expression of caspase 9 and PD-1. In addition, expression of BCL 2 was upregulated by infection with P1 and P20 promastigotes.

Results clearly show that there was more downregulation in Balb/c compared with C57 whether infected with P1 or P20. It seems that P20 did not modulate expression of Bax and caspase 8 in both Balb/c and C57 BMDM, but it upregulated BCL 2 gene expression in C57 and significantly downregulated it in Balb/c BMDM.

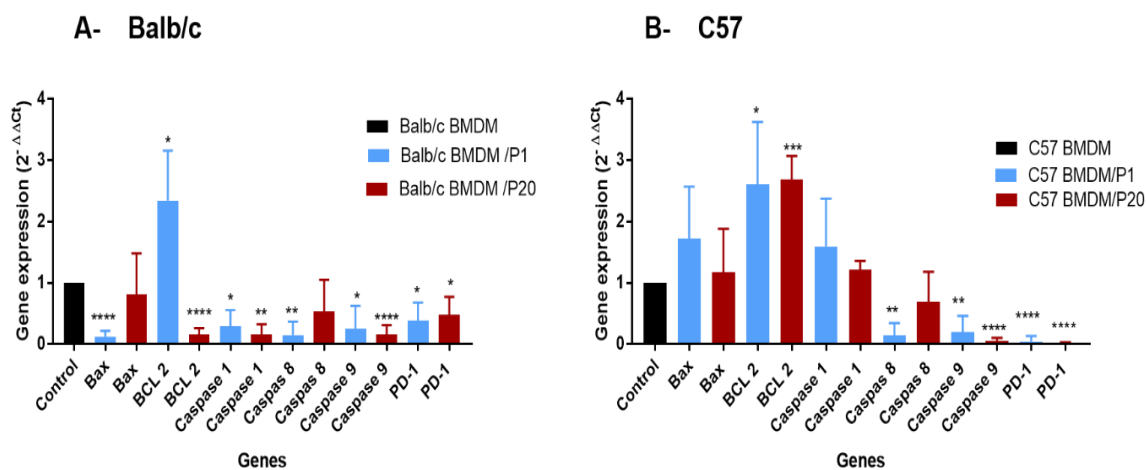


**Figure 4. 15: Apoptosis associated gene expression in Balb/c and C57 BMDM after 24 hours infection with P1 and P20 *L. mexicana* in vitro.**

Approximately one million Balb/c and C57 BMDM were cultured in 3 T25 tissue culture flasks and infected with  $20 \times 10^6$  P1 or P20 *L. mexicana* promastigotes in a total volume of 2.5 mL. Cells were harvested after 24 hours and total RNA was extracted and converted into cDNA and subjected to qPCR. qPCR results were normalized using housekeeping gene GAPDH and Ct values were calculated as  $2^{-\Delta\Delta C_t}$ . Results represent three independent experiments. The data were analysed by using GraphPad Prism 7. Statistically significant differences between groups represented by \* $p < 0.05$ , \*\* $p < 0.001$ , \*\*\* $p < 0.0001$  and determined by unpaired t-test. The results are average of five independent experiments and bars represent  $\pm$  SEM.

One can also observe from the data shown in figure. 4.15 (A and B) that caspase 8 was more downregulated in both Balb/c and C57 BMDM, infected with P1 than those infected with P20. This observation coincides with apoptosis results obtained by flow cytometry analysis (figure. 4.14). See the discussion chapter (section 4.3.5.1), for more details.

### 4.2.7 Effect of infection with P1 and P20 *L.mexicana* on cytokine gene regulation in Balb/c and C57 BMDM

Figure. 4.16 illustrates the qPCR analysis of cytokines gene regulation of IL-6, TNF- $\alpha$ , TGF- $\beta$ , and IL-1 $\beta$  of Balb/c and C57 BMDM infected with P1 and P20 after 2 and 24 hours. ELISA assay (figure. 4.17) was also used to assess TNF- $\alpha$  concentration in supernatants of Balb/c and C57 BMDM infected with P1 and P20 for 2 and 24 hours.

Infection of Balb/c BMDM with P1 for 24 hours downregulated the expression of cytokines compared with 2 hours infection except IL-6. In contrast infection of C57 BMDM for 24 hours with P1 was unable to downregulate most of the cytokine genes compared with 2 hours infection. In addition, cytokine gene expression in Balb/c, after 2 hours infection with P1 and P20 *Leishmania* promastigotes, was generally upregulated in C57. However, only infection with P1 but not P20 induced significant upregulation of IL-6, TNF- $\alpha$  IL-1  $\beta$ .

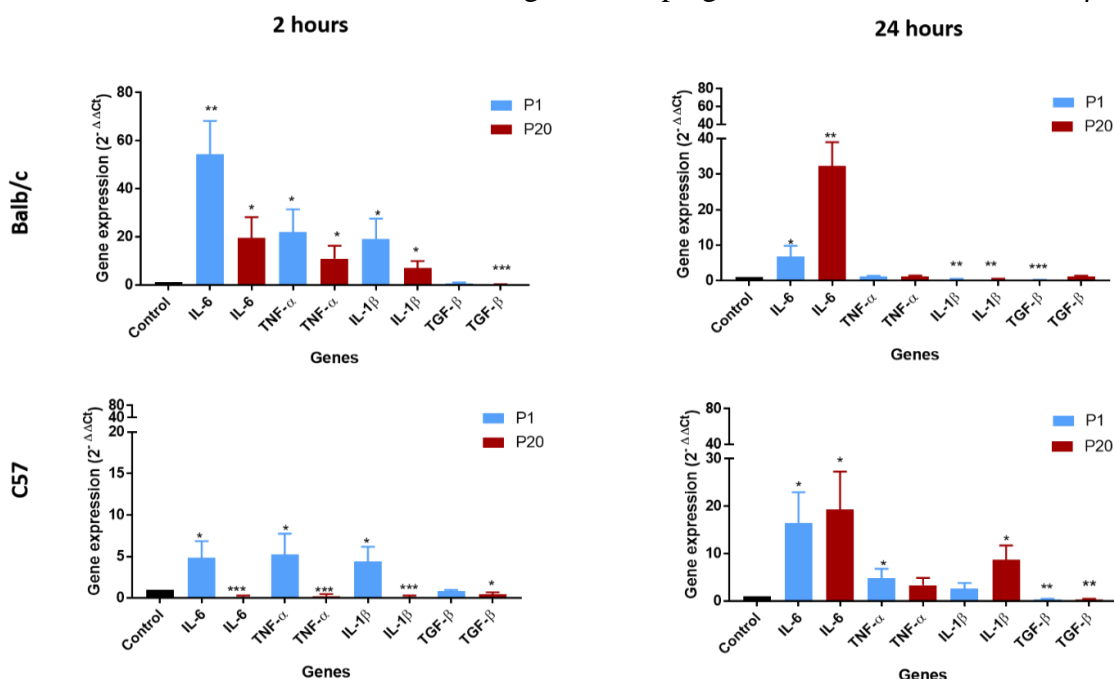


**Figure 4. 16: qPCR analysis of cytokines genes regulation of Balb/c and C57 BMDM infected with P1 and P20 promastigotes for 2 and 24 hours**

Approximately one million Balb/c and C57 BMDM were cultured in 3 T25 tissue culture flasks and infected with  $20 \times 10^6$  P1 or P20 *L. mexicana* promastigotes in a total volume of 2.5 mL. Cells were harvested after 2 and 24 hours and total RNA was extracted and converted into cDNA and subjected to qPCR. qPCR results were normalized using housekeeping gene GAPDH and Ct values were calculated as  $2^{-\Delta\Delta C_t}$ . Results represent three independent experiments. The data were analysed by using GraphPad Prism 7. Statistically significant differences between pairs of groups represented by \* $p < 0.05$ , \*\* $p < 0.001$ , \*\*\* $p < 0.0001$  and determined by un-paired t-test. The results are average of five independent experiments and bars represent  $\pm$  SEM

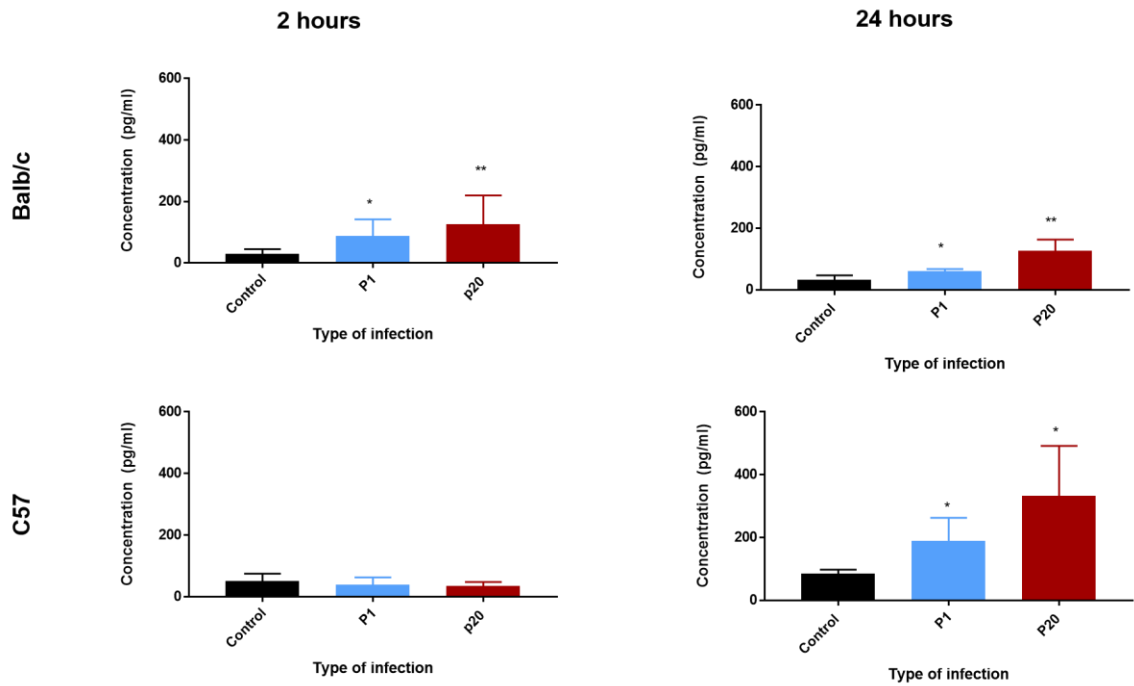


**Figure 4. 17: Estimation of TNF- $\alpha$  cytokine concentration in supernatants of Balb/c and C57 BMDM infected with P1 and P20 by ELISA**

Approximately one million Balb/c and C57 BMDM were infected with  $20 \times 10^6$  *L. mexicana* promastigotes in total volume of 2.5 mL per T25 flask. Supernatants were collected from infected and control cells. The level of secreted cytokines was estimated by ELISA according to the manufacturer's protocol. Plate absorbance was read by spectrophotometer using 450 nm. The results are average of three independent experiments. The data were analysed by using GraphPad Prism 7. Statistically significant differences between pairs of groups represented by \* $p < 0.05$ , and determined by un-paired t-test and bars represent  $\pm$  SEM

Results in figure. 4.17, illustrate the concentration of TNF- $\alpha$  in supernatants collected from Balb/c and C57 BMDM infected with P1 and P20 estimated by ELISA in order to confirm the qPCR results for this cytokine.

The pattern of TNF- $\alpha$  expression in supernatants from Balb/c BMDM contrasted with that in C57 BMDM since the expression in response to *Leishmania* infection was upregulated in C57 and downregulated in Balb/c BMDM supernatants detected by ELISA after 2- and 24-hours infection in addition level TNF- $\alpha$  was higher in C57 than Balb/c after 24 hours infection

It can be seen from this figure that the concentration of TNF- $\alpha$  of Balb/c infected with P1 and P20, after 2 hours, was significantly increased with significant changes in supernatant from C57 confirming qPCR results. The concentration of TNF- $\alpha$  of Balb/c BMDM infected with both P1 and P20 was slightly reduced after 24 hours. The concentrations of TNF- $\alpha$  in C57 BMDM infected with P1 and P20 for 24 hours have significantly increased.

#### 4.2.8 Synopsis of the infection of Balb/c and C57 BMDM with virulent P1 and avirulent P20 *L.mexicana* promastigote results

**Table 4. 1: Infection and survival of P1 and P20 *L.mexicana* in Balb/c and C57 BMDM.**

	Test	P1	P20
<b>Infectivity of P1 and P20 to Balb/c and C57 BMDM</b>	-Neubauer hemocytometer - fluorescent microscope -Alamar blue assay	Infective	Infective
<b>Survival of P1 and P20 in the Balb/c and C57 BMDM</b>	-Light microscope - fluorescent microscope	Survive up to 7 days	Fail to survive
<b>Formation of PV in Balb/c and C57 BMDM</b>	Light microscope - fluorescent microscope	Form PV	Fail to form PV

**Table 4. 2: Effect of Infection P1 and P20 *L.mexicana* in Balb/c and C57 BMDM apoptosis .**

	Test	P1	P20
<b>Apoptosis in infected Balb/c and C57 BMDM</b>	Flow cytometry	Inhibit apoptosis	Did not inhibit apoptosis
<b>Regulation of Apoptosis genes in infected Balb/c BMDM</b>	qPCR	Upregulation of BCL 2 Downregulation of Bax, Caspase 1, Caspase8, Caspase 9 and PD-1	Downregulation of BCL 2, Caspase1, Caspase 9 and PD-1
<b>Regulation of Apoptosis genes in infected C57 BMDM</b>	qPCR	Upregulation of BCL 2 Downregulation of Caspase 8, Caspase 9 and PD-1	Upregulation of BCL 2 Downregulation of Caspase9 and PD-1

**Table 4. 3: Effect of infection P1 and P20 *L.mexicana* in Balb/c and C57 BMDM cytokines.**

	Test	P1	P20
<b>Regulation of cytokine genes in infected Balb/c BMDM</b>	qPCR	-Upregulation of IL-6 after 2 and 24 hours.  -Upregulation of TNF- $\alpha$ , and IL-1 $\beta$ after 2 hours	-Upregulation of IL-6 after 2 and 24 hours.  -Upregulation of TNF- $\alpha$ , and IL-1 $\beta$ after 2 hours
<b>Regulation of cytokines genes in infected C57 BMDM</b>	qPCR	After 2 hours, upregulation of IL-6, TNF- $\alpha$ , and IL-1 $\beta$ After 24 hours, upregulation of IL-6, and TNF- $\alpha$ .	After 2 hours, downregulation of IL-6, TNF- $\alpha$ , and IL-1 $\beta$ After 24 hours, upregulation of IL-6, and IL-1 $\beta$ .
<b>Estimation of TNF-<math>\alpha</math> cytokine concentration in infected Balb/c BMDM supernatant</b>	ELISA	Increased after 2 and 24 hours	Increased after 2 and 24 hours
<b>Estimation of TNF-<math>\alpha</math> cytokine concentration in infected C57 BMDM supernatant</b>	ELISA	Increased after 24 hours with double concentration	Increased after 2 and 24 hours with double concentration

## 4.3 Discussion

### 4.3.1 Assessment of P1 and P20 *L.mexicana* infectivity

In order to assess P1 and P20 parasite internalization, free unphagocytosed parasites were counted by hemocytometry and estimated by Alamar blue assay. A haemocytometer was used by taking 10  $\mu$ L of extracellular parasites and fixed with 90  $\mu$ L 1% paraformaldehyde. Alamar blue assay was performed by taking all the medium containing extracellular parasites (2.5 mL) and the control parasite group (parasites cultured alone) then spun down and washed with RPMI1640 medium then resuspended in 300  $\mu$ L 10% HIFCS RPMI1640 medium. Parasites were transferred into a 96 well plate at 100  $\mu$ L of parasite suspension in each well and incubated at 25°C.

### 4.3.2 Assessment of P1 and P20 *L.mexicana* parasite survival in the infected macrophage

Infectivity of P20 compared with P1 revealed that both parasites can infect both mice strains Balb/c and C57 BMDM, irrespective of their susceptibility *in vitro*. After two hours of infection, there was a reduction in the number of free non-engulfed P1 and P20 parasites in both Balb/c and resistant C57 BMDM. Inspection of infected macrophages microscopically revealed the internalisation of parasites (P1) was clear after 24 but not 2 hours which means that internalisation of parasites and formation of PV need more than 2 hours which is in line with Williams *et al.*, (2006) and Real *et al.*, (2008). Moreover, P1 can survive for more than 7 days inside macrophages; however, it is reported that parasites can survive for weeks inside macrophages (Pearson *et al.*, 1983; Channon *et al.*, 1984).

Remarkably, 2 hours are also not enough time for differentiation of P1 into amastigotes (figure 3.13 and 3.14). Similar results have been observed by Williams *et al.*, (2006) who reported that *L.mexicana* need 18 to 72 hours to differentiate into amastigotes, which is concurrent with autophagy (process of differentiation of parasite to amastigote) which appears after 18 to 72 hours by increasing number of autophagosomes which is consistent with time of incubation for differentiation of parasite and consistent with time for infection. Accordingly, the results confirm previously reported data on the relationship between virulence and the ability of the parasite to differentiate into amastigotes.

Analysis by light microscopy demonstrated the infection of macrophages was accomplished by P1 but not P20, since P20 failed to survive inside both Balb/c and C57 BMDM (Section 4.2.2), while P1 can infect, survive, create PV and multiply in both mice strains. One finding of interesting in this study is that although P20 lost virulence, along with downregulation of the ten associated virulence genes (Include LPG1, LPG2, and GP63) and lost the ability to

differentiate to amastigotes, they were able to infect macrophages from Balb/c and C57 BMDM mice. A possible explanation for this observation is that the macrophages engulf P20 which may mean that the main virulence factors (*in vitro*) are factors that enable the parasite to survive inside the macrophage. Regardless of a significant difference in infectivity index between Balb/c and C57 BMDM (figure 4.9) there was no significant difference in infectivity of P1 and P20 (figure 4.2). In this incidence the use of the infectivity index is less able to illustrate the survival of the parasite in macrophages. Therefore, the current study hypothesized that the virulence factors should be ones that enable parasite to survive inside macrophages and create PVs, but not only factors that enable the parasite to infect the macrophages. Considering these findings, the main difference between virulent and avirulent parasites is the capacity of virulent parasites (P1) to differentiate into amastigotes; this finding is in line with the study by Moreira *et al.*, (2012), who reported that avirulent parasites could not differentiate into amastigotes properly.

### **4.3.3 Survival of virulent P1 *L.mexicana* in Balb/c and C57 BMDM**

*Leishmania* parasites have developed several strategies to escape the host immune response in macrophages. This strategy can be through the expression of *Leishmania* surface molecules such as LPG and GP63, inhibition of phagosome maturation biogenesis and demodulation of defence against oxidative burst. As mentioned earlier P1 but not P20 can survive in both susceptible Balb/c and resistant C57 BMDM; these results are confirmed by a previous study by Delgado-Domínguez *et al.*, (2010). Therefore, the main factor in parasite survival *in vitro* is most likely related to P1 parasite virulence factors but not mouse genetic background.

#### **4.3.3.1 Role of LPG**

One of the virulence-associated factors investigated in this study is LPG gene regulation by examining the expression of LPG1 and LPG2 by qPCR which demonstrated their downregulation in P20. In addition, a significant downregulation in LPG expression level on the surface of *Leishmania* promastigotes of P20 was observed compared with P1 as confirmed by immunofluorescence and Flow cytometry (Section 3.2.11.2). It has previously been reported that *L.mexicana* LPG1 mutant parasites failed to express LPG on their surface (Ilg, 2000). In addition, deletion of the LPG1 gene from the related species *L. infantum* impaired their ability to infect C57 BMDM and significantly reduced their survival after 72 hours of infection, concurrent with strong induction of NF- $\kappa$ B-and activation of iNOS (Lázaro-Souza *et al.*, 2018). It is of note that LPG protects promastigotes from a transient rise in ROS generated during phagocytosis (Spath *et al.*, 2003).

Results of the present study show that P1 covered with LPG survived longer in Balb/c and C57 BMDM macrophages than P20 which was deficient in LPG expression. However, this may not be the sole factor determining survival since P20 express less GP63 and CPBs as assessed by qPCR in addition to other non-tested virulence factors, which may be affected by 20 passages *in vitro*.

#### 4.3.3.2 Role of LPG and oxidative burst

The parasite is sensitive to oxidative stress either in the mammalian host or in the vector intermediate host. Therefore, parasites must defend against oxidative bursts which are a part of the host innate immunity after infection (Hancock *et al.*, 2001). It has been reported that respiratory burst or oxidative burst is the rapid release of reactive oxygen species (ROS) and reactive nitrogen species (RNS) from macrophages after a few hours interaction with *Leishmania*, which are the most effective anti-*Leishmania* molecules (Hancock *et al.*, 2001; Sardar *et al.*, 2013) in order to kill the pathogen without damaging the infected host cell. ROS include hydrogen peroxide, superoxide anions, and hydroxyl radicals which damage proteins, nucleic acids, lipids, and cell membranes. (Bokoch and Diebold, 2002; Brown *et al.*, 2003). Generation of ROS is mediated by the Nicotinamide adenine dinucleotide phosphate (NADPH) oxidase complex (Bokoch and Diebold, 2002; Brown *et al.*, 2003). Phagocytosis activates this process through several enzymes in macrophages including; NADPH for superoxide and iNOS, for NO production (Panday *et al.*, 2015; Aktan 2004). NADPH oxidase is found in the plasma membrane in all living organisms which is essential for oxidative stress defences. *Leishmania* parasites need NADPH to adapt to different host environments, and for oxidative stress defences during their infectious life cycle, as well as in the membranes of phagosomes used by macrophages to engulf microorganisms. Parasite and host interactions lead to the generation of a large amount of ROS and RNS which is toxic to the parasite, thus the parasite must consume a large amount of NADPH for detoxification of ROS and RNS to survive. Therefore, NADPH is essential for the survival of *Leishmania* parasites within the insect vectors and mammalian hosts cells (Krauth-Siegel and Comini, 2008). To avoid exposure to oxidants by the parasites, amastigotes subvert the generation of ROS within the PV through inhibition of the NADPH oxidase complex (Lodge *et al.*, 2006).

Many promastigotes are destroyed by macrophages after infection; however some escape the phagolysosome's microbiocidal power and transform this powerful organelle into a PV. As mentioned previously, *Leishmania* parasites have developed many strategies to interfere with this process, one of the most important strategies is the LPG coat that protects parasites from both ROS and RNS and subsequently delays the assembly of NADPH oxidase at the

surface of the phagolysosome in the phagocytic cup, causing suspension in the production of superoxides (Desjardins, and Descoteaux, 1997; Carneiro *et al.*, 2018). Moreover, *Leishmania* dysregulates PKC signalling through LPG, in order to promote its survival in the host cell (Descoteaux, and Turco., 1992).

Another strategy to inhibit oxidative stress is through GP63, which interferes with macrophage signalling pathways leading to NADPH and iNOS induction (Olivier *et al.*, 2012). It is noteworthy that P20 *L.mexicana* lack GP63 on their surface as reported previously by Ali *et al.*, (2013). However, it is noteworthy that *L.mexicana* amastigotes and promastigotes are more resistant to ROS than other *Leishmania* parasite species such as *L.major* and *L.donovani* (Wanasen *et al.*, 2007).

#### **4.3.3.3 Role of phosphatidylserine in infection and survival**

Phosphatidylserine (PS) is naturally expressed on the outer membrane of *Leishmania* parasites and is associated with increasing of the parasite metacyclic stage infectivity (Tripathi and Gupta, 2003; França-Costa *et al.*, 2012). *Leishmania* parasite external membrane contains relatively high levels of phosphatidylserine which may provide a mechanism for silent entry to host cells via apoptotic cell receptors without activating the immune system or proinflammatory responses (Wanderley *et al.*, 2006).

PS overexpression has an important role in parasite survival within host cell macrophages (Balb/c and C57), their dissemination and disease outcome; it is also associated with severity and persistence of the disease (França-Costa *et al.*, 2012). In addition, it has been observed that there is a positive relationship between parasite PS density and production of cytokines by macrophages e.g. IL-10 and TGF $\beta$  (Kima, 2007). The expression of apoptosis associated PS on the surface of P20 was significantly more than in P1. PS can cause opsonisation of macrophages, helping a silent entry of the parasite without triggering the immune system (van Zandbergen *et al.*, 2006; Gueirard *et al.*, 2008). It is noteworthy that PS plays a role in signalling and engulfing of the cells by macrophages (Verhoven *et al.*, 1995; Appelt *et al.*, 2005). PS is a conserved immunosuppressive signal that prevents local and systemic immune activation in microbial and parasitic infection (Birge *et al.*, 2016). The recognition of PS that is expressed on the parasite surface plays a role in deactivation of DC functions after engulfment, in a matter like that of apoptotic cell clearance (Wanderley *et al.*, 2013). PS acts as a ligand for parasite endocytosis and macrophage modulation, causing opsonisation of macrophages in a mechanism called apoptotic mimicry (Wanderley *et al.*, 2006; Wanderley *et al.*, 2013).

In this study P20 parasites were shown to express higher levels of surface PS than P1 (figure 3.22); PS may help the parasite's uptake via the host cell apoptotic receptors which

prevents the activation of immune response and may be critical for the silent entry of the parasites into the host cells (van Zandbergen *et al.*, 2006; Gueirard *et al.*, 2008). As previously reported the main receptors for the uptake of the parasite into murine macrophages *in vitro* are phosphatidylserine and Fc receptors (Wanderley *et al.*, 2005; Kima, 2007). According to Ali *et al.*, (2013) the outcome of P20 infection in Balb/c failed to form lesions (figure 1.5); this maybe due to P20 being unable to trigger immune responses due to the abundance of PS on P20, although when incubated for 24 hours at 37°C (figure 3.22), in addition losing many other virulence factors to infect and survive.

Weingärtner *et al.*, (2012) who reported that the phospholipid classes stainable by Annexin V stain that are found on *Leishmania* promastigote and amastigote surfaces are not a PS, but they are phosphatidic acid, phosphatidylinositol, phosphatidylglycerol and phosphatidylethanolamine as determined by thin-layer chromatography, mass spectrometry, nuclear magnetic resonance, and spectroscopy. However, the results of this study cannot exclude this possibility, suggesting the need to investigate these phospholipid classes including PS expressed, on P1 and P20 by other techniques such as mass spectrometry.

#### **4.3.3.4 Inhibition of the formation of phagolysosomes**

Microorganisms that can survive and multiply inside macrophages have developed different strategies to resist the hostile environment of the phagolysosome, including inhibition of formation of phagolysosomes (Finlay and Falkow, 1997). The killing of a pathogen that is engulfed by the macrophage is a dynamic process characterised by a series of fusion and fission processes of intracellular endosomal vesicles with the phagosome containing antigen, resulting in formation a phagolysosome (Desjardins *et al.*, 1994). However, the molecular mechanisms behind the arrest of phagolysosome biogenesis are still unclear for most microorganisms. It should be mentioned that the external leaflet of plasma membranes of cells contains glycolipoprotein rich in cholesterol microdomains termed lipid rafts (Korade, and Kenworthy., 2008). The lipid raft plays a central role in cellular processes by the organisation of signalling molecules, membrane fluidity and membrane protein transportation, in addition to regulation of neurotransmission and receptor trafficking (Korade, and Kenworthy., 2008; Pike, 2009). The strategy taken by *Leishmania* to survive in macrophages is by inhibition of the maturation of phagosome biogenesis (Desjardins, and Descoteaux, 1997). Inhibition of maturation of phagosomes correlates with an accumulation of periphagosomal F-actin, which leads to subversion of lipid raft function subsequently, inhibiting phagosome maturation (Winberg *et al.*, 2009) and may also form a large physical barrier that prevents phagosomes containing *Leishmania* promastigotes from interacting with endocytic vacuoles (Chang *et al.*, 2003).

The main factor that is responsible for the inhibition of maturation of the phagosome biogenesis is LPG (Desjardins, and Descoteaux, 1997). During phagocytosis, parasite LPG is transferred to the host macrophage membrane, this induces accumulation of periphagosomal F-actin which leads to the subversion of lipid raft function causing inhibition of phagosomal maturation. More precisely, inhibition of phagosomal maturation may be due to intercalation of LPG into membrane lipid rafts of the host cell membrane (Winberg *et al.*, 2009). However, targeting of lipid rafts by a drug such as anti-tumour (edelfosine) can induce cell death when lipid rafts were disrupted by sterol depletion. Villa-Pulgarín *et al.*, (2017) tested this drug by oral treatment edelfosine on four *Leishmania* species (*L.infantum*, *L.panamensis*, *L.donovani*, and *L.major*) *in vivo* and *in vitro*. They reported that edelfosine causes *Leishmania* promastigote and amastigote death within macrophages.

#### **4.3.3.5 Role of GP63 in parasite survival**

According to qPCR results, the GP63 gene was downregulated in P20 *L.mexicana* (figure 3.15) in addition, losing of surface GP63 on P20 (Ali, *et al.*, 2013). Gene methylation is another strategy that has been recently reported to enable *Leishmania* to survive inside the macrophages; by turning off genes that control macrophage physiology and microbiocidal activity through GP63 (Duque and Descoteaux, 2015). The *Leishmania* cell membrane protease GP63 cleaves AP-1 transcription factor (TF) directly (Contreras *et al.*, 2010) causing the protection of infected cells against apoptosis (Wisdom *et al.*, 1999). In addition, AP-1 plays an important role as a transcription factor in regulating the expression of many genes that are involved in activation of macrophage functions such as TNF $\alpha$ , iNOS, and IL-12 (Newell, and Lopez-Berestein, 1994; Contreras *et al.*, 2010).

The prevention of formation of phagolysosomes is another strategy taken by *Leishmania* parasites. GP63 can prevent the formation of phagolysosomes in the macrophage through cleaving of DOK proteins (Dok-1, Dok-2 and Dok-3) in order to enable the parasite to survive inside macrophage, particularly DOK-1 and DOK-2 because they are involved in phagosome maturation (de Celis *et al.*, 2015). It should be mentioned that the DOK proteins are adaptor molecules that play a major role in negative regulation of the cell signalling in response to various cytokines and growth factors (Lemay *et al.*, 2000; de Celis *et al.*, 2015). However, the mechanism of cleavage of the DOK protein by GP63 is not fully understood (De Celis *et al.*, 2015). Another strategy to inhibit the oxidative stress by GP63 is by interfering with macrophage signalling pathways leading to inhibition of NADPH oxidase and iNOS induction (Olivier *et al.*, 2012). Therefore, maybe P20 lost this strategy to overcome these stresses, due to losing GP63. Therefore, selection disruption of this

strategy has attracted many researchers to investigate this phenomenon to design drugs targeting this strategy taken by parasites (Luscher *et al.*, 2007; Birkholtz, *et al.*, 2011; Allmann *et al.*, 2013).

#### 4.3.3.6 Role of cysteine protease in parasite survival

CPB plays a vital role in the parasite's life in the amastigote stage and in interaction with its host's cells which reflect on parasite survival (Mottram *et al.*, 2004), because the lysosomal cysteine peptidase is involved in the autophagic pathway during parasites differentiation (Mottram *et al.*, 1996; Williams *et al.*, 2006). Cysteine peptidases should be abundant in the parasite for an effective autophagic pathway to induce differentiation into amastigotes, while cysteine peptidase deficient mutants of *L.mexicana* lost virulence (Williams *et al.*, 2006). The results of the current study reported that P20 which had downregulated CPB lost the ability to infect macrophages and mice which is in line with findings of Mottram *et al.*, (1996).

However, the results of Mottram *et al.*, (1996) reported that *L.mexicana* CPB is not essential for the parasite to survive in Balb/c macrophages, based on comparing between CPB null mutants and wild type *L.mexicana*. In accordance with other studies, about the importance of CPB, CPB2.8 and CPC were tested by infection of Balb/c mice *in vivo* and Balb/c mice macrophages *in vitro* with parasites deficient in CPB genes; the results showed that Balb/c mice were infected but, with reduced lesions (Mottram *et al.*, 1996; Alexander *et al.*, 1998; Frame *et al.*, 200). Denise *et al.*, (2003) suggested that multiple CPB cysteine protease genes of *L.mexicana* have complementary functions. This finding is in accordance with our finding that P20 downregulated three cysteine protease genes tested (CPB, CPB2.8 and CPC) and failed to survive in macrophages; similar findings were also reported by Ali *et al.*, (2013). Inhibition of *Leishmania* cysteine protease activity could be used as chemotherapeutic target for Leishmaniasis, because this inhibitor can kill *Leishmania* parasites at the effective dose that does not affect mammalian host cells by *in vitro* inhibition of cysteine proteases accompanied with a defect in parasite lysosomes and endosomes (Alves *et al.*, 2001). Alves *et al.*, (2001) suggest that designing efficient inhibitors for CPB is possible by manipulating the substrates. The effect of cysteine protease inhibitors such as derivatives of oxalic bis were investigated *in vivo* and *in vitro* in Balb/c mice. Mice heal and reduced disease progression with inhibition of CPB, CPA and CPC combined with shifting from a predominately Th2 into Th1 response without toxicity to the host. (Selzer *et al.*, 1999; Das *et al.*, 2001 and Bryson *et al.*, 2009). Another group of compounds targeting CPB2.8 inhibition, is  $\alpha$ -ketoheterocycles have been investigated. They have irreversible inhibition of CPB2.8 promising to be *in vivo* antiparasitic drugs (Steer *et al.*, 2010; Scala *et al.*, 2016).

However, maybe other untested virulence genes downregulated in P20 should be taken into consideration. In addition, it should be mentioned that P20 may not be representative of wild type *L.mexicana* due to large differences between these two strains and using specific depleted genes is better for comparison in this regard.

#### 4.3.4 Parasitophorous vacuoles (PV)

*Leishmania* parasites can survive inside PV through internalization in the macrophage, and maturation of the PVs by promastigotes and amastigotes. The maturation of phagosome and fusion of PV are controlled by Fc and by PS surface receptors of murine BMDM (Wanderley *et al.*, 2006; Real *et al.*, 2008). Mature PV is an adapted environment within the macrophage which supplies the parasites with nutrients and protects the parasite from the host immune system and macrophage microbiocides. Thus, parasites survive and differentiate into an amastigote form (Liévin-Le Moal, and Loiseau, 2016).

Pathogenic *Leishmania* species can survive and multiply in PV, as observed in this study. PVs were found in both Balb/c and C57 BMDM infected with P1 but not P20, and that P20 lacked LPG and GP63. It is pointed out that for *Leishmania* survival in macrophages the phagosome needs to change into a parasitophorous vacuole (PV) by pathological changes through LPG and GP63 and by inducing Th2 cytokines (Séguin and Descoteaux, 2016). Also, it has been suggested that formation of PV depends on the parasite stage and is associated with the amastigote stage molecules that changes the balance between fission and fusion such as LPG (Desjardins and Descoteaux, 1997; Courret *et al.*, 2002). Therefore, the failure of P20 to create PVs could be due to the absence of LPG and GP63 proteins in addition to the inability of P20 to differentiate into amastigotes.

Formation of PV is essential for the acquisition of nutrients and for protection of the parasite from the immune responses and dilution of the leishmanicidal NO (Wilson *et al.*, 2008). Moreover, according to Canton *et al.*, (2012), there is a positive relationship between PV size and parasite survival and proliferation with a suggestion that could work through the dilution of molecules produced by macrophages to kill the parasites. Increase of PV size is in line with this study findings (figure 4.3 and 4.4) which showed a decrease of PVs number combined with increases of amastigote number with time post-infection (figure 4.10).

These PVs were found in different size and number in each infected cell and contained a varied number of amastigotes (figure 4.3 and 4.4); this finding is in line with Chang *et al.*, (2003) who reported a similar finding of J774G8 macrophages infected with *L.amazonensis*. However, Balb/c and C57 BMDM infected with P20 did not create any PV, because the formation of PV is usually associated with a live parasite and are absent in cells infected with avirulent or killed parasites (Ramazeilles *et al.*, 1990). Therefore, maybe P20 were

killed inside macrophages according to light and fluorescent microscopic pictures (Figure 4.6, 4.7 and 4.8). PVs differed in size and number of amastigotes. The number of PVs was observed to be higher in C57 than Balb/c BMDM. PV numbers were significantly decreased with time of incubation in macrophages of both mice strains, which may be due to fusion between PVs.

#### **4.3.4.1 Fusion of parasitophorous vacuoles**

Amastigotes internalise inside PVs of macrophage, then they start multiplication by binary fission. Subsequently, PV size increased over the infection time (Liu, and Uzonna, 2012) consistent with the current study finding. Subsequently, PV size increased over the infection time which then ruptured the infected macrophages and led to the release of amastigotes to infect other surrounding macrophages (Liu, and Uzonna, 2012). Real *et al.*, (2014) who used multidimensional live cell imaging *in vitro*, reported that *L.amazonensis* amastigotes transferred from the infected cell when apoptosis was imminent. Therefore, infected macrophages may die due to apoptosis and expression of PS on the outer membrane that opsonises non-infected macrophages to engulf imminent apoptotic infected macrophages (DaMata, *et al.*, 2015).

The current study examined the fusion between PVs in Balb/c and C57 BMDM infected with *L.mexicana* by calculation of PV number per infected macrophage under a light microscope at three different time points which could provide an additional idea about the mechanism of PV membrane acquisition, fusion and vacuole growth. As observed in this study *L.mexicana* PVs carrying amastigotes can fuse with each other (figure.4.7), as well as PVs amastigotes multiplied in the PV in both Balb/c and C57 BMDM infected with P1 (figure 4.8); the multiplication of amastigotes was clear under light microscope after 2 days post-infection. Reduction in the number of PVs over time of incubation post-infection accompanied with increase of PVs size (figure 4.3 and 4.4 and 4.10 ) means there is a fusion between PVs which agrees with the study conducted by Real *et al.*, (2008) and Okuda *et al.*, (2016). However, the mechanisms of PV fusion control are still unclear (Okuda *et al.*, 2016). Interestingly, Real *et al.*, (2008) had earlier found that fusion between PVs in infected mouse bone marrow derived macrophage may be due to parasite PS which can modulate the infected cells and is associated with PV size in Balb/c and C57 BMDM (França-Costa *et al.*, 2012). On the other hand, other studies by Okuda, *et al.*, (2016) reported that the fusion of PV is not related to phosphatidylserine. However, this study results reported that P1 express PS, but it decreases significantly after differentiation into amastigotes in addition, P20 expressed higher PS and failed to create PV. Therefore, this study finding is in line in some way with findings of Okuda, *et al.*, (2016). A similar trend of amastigote growth rate per PV

was found in both Balb/c and C57 BMDM, but the multiplication rate of amastigotes was higher in Balb/c BMDM (figure 4.11B). This study reports new insights into the ability of amastigotes to multiply inside infected mammalian cells which were higher in Balb/c than C57 BMDM (figure 4.11B). PVs of *L.mexicana* complex differs from other *Leishmania* species in the size of PV, which is larger than other *Leishmania* species. Large PVs form because they contain a large number of parasites, therefore PV of *L.mexicana* are useful to investigate parasite survival and responses to chemotherapies (Real *et al.*, 2008).

### 4.3.5 Apoptosis

It is known that *Leishmania* parasites are obligate intracellular parasites that survive and multiply in the macrophages. Therefore, *Leishmania* is recognised for their manipulation of host cell defence mechanisms in order to evade the immune response in order to survive inside them. Although the parasite has developed many strategies to evade the immune system in order to survive inside macrophages, inhibition of apoptosis remains the most intriguing strategy (Aguirre-Garcia *et al.*, 2018; Solano-Gálvez, *et al.*, 2018). Apoptosis is considered as a central defence mechanism against intracellular pathogens (Barry *et al.*, 2002), However, many pathogenic microorganisms including *Leishmania* parasites have developed mechanisms to overcome apoptosis to survive inside infected host cells. It has been reported that the *Leishmania* parasite can inhibit apoptosis of different host cells such as macrophages (Akarid *et al.*, 2004).

#### 4.3.5.1 Apoptosis in Balb/c and C57 BMDM infected with P1 *L.mexicana*

Results in figure. 4.14, illustrate the apoptosis of Balb/c and C57 BMDM after infection with P1 and P20 for 24 hours, and how the removal of GMCSF enhanced apoptosis in control macrophages. It was noticed that the removal of GMCSF from media made P1 inhibit apoptosis in BMDM from both mice strains. However, there was no significant difference in apoptosis level between controls and cells infected with P20. It should be noted that P20 is supposed to be unable to stop apoptosis because it did not survive inside macrophages (figure 4.8). The ability of *L.mexicana* to inhibit apoptosis has been reported before, Valdés-Reyes *et al.*, (2009) reported that infection of monocyte-derived dendritic cells with *L.mexicana* acted as an anti-apoptotic effect with a significant reduction in caspase 3 activity after 9 hours' infection. The finding reported in this study, in which BMDM infected with P1 reduced apoptosis after the removal of GMCSF was also supported by several previous studies. Akarid *et al.*, (2004) studied apoptosis levels using *L.major* and found that apoptosis was inhibited in Balb/c and C57 BMDM after the removal of GMCSF. GMCSF is an anti-apoptotic factor that enhances the generation of ROS associated with phagocytosis (Zhang

*et al.*, 2003). Macrophages require Nicotinamide adenine dinucleotide phosphate (NADPH) to generate ROS during phagocytosis in order to kill pathogens, therefore, ROS associated with apoptosis will be significantly enhanced by increasing the oxidative burst (Hancock *et al.*, 2001; Sardar *et al.* 2013), but infection of macrophage inhibits apoptosis which in this study may be due to P1 being rich in LPG that blocks NADPH oxidase on the phagosomal membrane which will inhibit generation of ROS (Lodge *et al.*, 2006), while P20 has less LPG expressed on its surface and did not inhibit apoptosis.

A possible reason behind the inhibition of apoptosis and survival of P1 but not P20 (figure. 4.14 B and D) might be due to abundant LPG in P1 but not P20. Moore and Matlashewski, (1994) investigated apoptosis of infected BMDM with *L.donovani* and reported that *Leishmania* LPG surface molecules of the promastigote inhibited apoptosis in the macrophage and was induced by the removal of GMCSF. In addition, they also investigated purified LPG on its own (in the absence of parasite) and found similar results where the LPG inhibited apoptosis.

Inhibition of apoptosis is one of the most important defence mechanisms of the parasite to survive in the host cells. However, the full pathway of exerting an antiapoptotic effect by *Leishmania* parasite in host cells is still unclear (Solano-Gálvez, *et al.*, 2018; Abhishek 2018; Aguirre-Garcia *et al.*, 2018). The role of the anti-apoptotic effect in parasite survival and multiplication inside the infected macrophage needs further research and investigation. Therefore, in this study, the regulation of apoptosis-associated genes was investigated in Balb/c and C57 BMDM infected with P1 and P20 for 24 hours. It has been reported before that the *Leishmania* life cycle stage may have a role in modulation of host cell apoptosis and possibly parasite differentiation (Carmen and Sinai., 2007) which supports the finding already reported in this study, where avirulent P20 failed to differentiate into amastigotes and to inhibit apoptosis in infected macrophages (figure. 4.14).

Parasite outer surface membrane molecules play an important role in apoptosis inhibition. It has been reported that *Leishmania* promastigotes and amastigotes inhibit apoptosis in monocytes, dendritic cells, and macrophages (Aguirre-Garcia *et al.*, 2018). Moreover, it has been reported that some parasite membrane molecules such as LPG and GP63 inhibit apoptosis of macrophages (Moore, and Matlashewski, 1994; Hallé *et al.*, 2009). GP63 inhibits apoptosis by inhibiting the MAPK p38 apoptotic signalling pathway (Hallé *et al.*, 2009), while LPG inhibits the PKC-mediated pathways (Lisi *et al.*, 2005). It was inferred from the results reported in this study (section 3.2.11.2, figure.3.18, 3.19 and 3.20) that P1 but not P20 was rich in LPG using three different tests; qPCR, flow cytometry and Immunofluorescence. In addition, according to the results obtained from qPCR, it was found that P1 but not P20 expressed a high level of GP63. This agreed with the finding reported

by Ali *et al.*, (2013) who used qPCR and Immunofluorescence. Enrichment of P1 with both LPG and GP63 plays an important role in the inhibition of apoptosis in the infected cells where P20 (due to the lack of LPG and GP63) was not effective in apoptosis inhibition. As a result, P1 but not P20 survive inside macrophage. It should be mentioned that there might be some other differences between the effect of P1 and P20 on apoptosis which depend on other types of molecules that need to be studied further. As an example, the effect of P1 and P20 on apoptosis using CPB, CPB 2.8 and CPC was tested by qPCR but they need further confirmation as there are very few studies conducted in the literature using such types of protein in virulent and avirulent *L.mexicana*.

Interestingly, P1 but not P20 protects both Balb/c and C57 BMDM from apoptosis. This was confirmed by the removal of GM-CSF (figure. 4.14). Most of the previous work was conducted *in vivo* where the survival of parasites in infected Balb/c and C57 macrophages depends on T cell activation of Th1 or Th2 cytokines which in turn affect the pathogenicity of this disease. The results reported in this study were conducted *in vitro* (BMDM) which showed that P1 survived in both susceptible Balb/c and resistant C57 BMDM. In addition, Akarid *et al.*, (2004) reported that survival in susceptible Balb/c and resistant C57 BMDM infected with *L. major* did not depend on the genetic background of these mice. However, results of this study suggest that P1 may survive in C57 *in vitro* due to the absence of Th1 responses.

#### **4.3.5.2 Apoptotic genes regulation of Balb/c and C57 BMDM infected with P1 and P20 *L.mexicana***

As mentioned above, one of the possible reasons that P1 but not P20 inhibits apoptosis in both Balb/c and C57 BMDM was due to the difference between P1 and P20 virulence factors (such as LPG, GP63) and ability to differentiate into amastigotes. It is important at this stage to explain the regulation of the apoptotic genes in order to understand how P1 but not P20 inhibits apoptosis. The most interesting results on gene regulation of apoptosis with respect to mice background and parasite virulence are the downregulation of caspase 8 in Balb/c and C57 BMDM infected with P1 but not P20 (figure 4.15). In other words, P1 downregulates caspase 8 and survives in both mice, while P20 did not significantly affect caspase 8 regulation as well as it failed to survive in those two mouse strains. It is very clear that the only gene affected in P1 but not P20 which was downregulated in both mice was caspase 8 (figure. 4.15), indicating that this gene can be considered as a key gene in controlling the apoptosis process during infection with *L.mexicana*.

### 4.3.5.3 Caspase 8

To summarise the role of caspase 8 on apoptosis, the schematic diagram in figure. 4.18 illustrates its role in apoptosis. It is known that, under normal conditions, apoptosis is triggered through extrinsic multiple stimuli which causes activation of caspase 8 through death receptors such as FADD and TNF- $\alpha$  receptors. Activation of caspase 8 is associated with the membranes in apoptosis causing a predominance to localise with the mitochondrial membrane and release cytochrome C.

As shown in figure. 4.18, there are two apoptosis pathways; extrinsic and intrinsic. caspase 8 represents the cross talk between these two pathways. In the extrinsic pathway, activating caspase 8 will trigger the activation of a cascade of caspases (caspase 6, caspase 7 and caspase 3), leading to initiation apoptosis. In the intrinsic pathway, activation of caspase 8 will cleave BID protein which subsequently binds BAK and Bax (mitochondrial protein) causing the release of cytochrome c into the cytosol (Irmeler 1997; Chandra *et al.*, 2004). This in turns actives caspase 9 causing the activation of caspase 3, which finally triggers apoptosis. One of the interesting findings of this study was that P1 downregulated caspase 8, which suppresses apoptosis through extrinsic and intrinsic apoptosis pathways. It should be mentioned that this was observed by qPCR (figure. 4.15) and needs further confirmation using other techniques such as caspase assays or western blotting analysis.

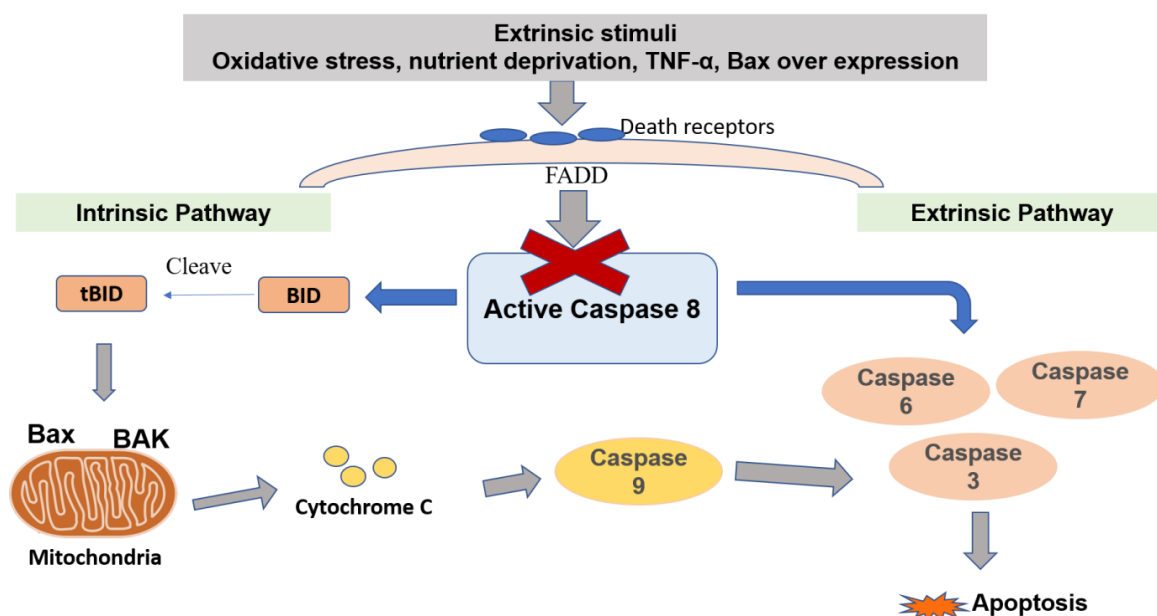


**Figure 4. 18: Diagram illustrates the possible effect of deactivation of Caspase 8 on both extrinsic and intrinsic apoptosis pathways.**

(Adapted from Chandra *et al.*, 2004 and Rampal *et al.*, 2012; with minor changes according to current study results).

There is very little known on the effect of *Leishmania* infection on caspase 8 activity in macrophages (particularly, *L.mexicana*). In addition, the approach and the results presented in this study were unique in the sense that susceptible Balb/c was compared with resistant C57 when both were infected with P1 and P20 in terms of inhibition of apoptosis and the effect of virulence of the parasite on two mouse strains.

However, there are some previous studies on the role of caspase 8 in apoptosis using different cell lines and different microorganisms. For example, Vutova *et al.*, (2007) studied the pathway of apoptosis inhibition in macrophages infected with *Toxoplasma gondii*. They found that deactivation of caspase 8 causes inhibition of apoptosis. This finding agrees with the findings of this study using virulent *L.mexicana*. Furthermore, Iwaoka *et al.*, (2006) investigated the apoptosis pathway in the macrophage-like cell line RAW264.7 and reported that apoptosis was induced by ROS. The generation and release of ROS activates caspase 8. However, infection of macrophages with *Leishmania* parasites will already stop the generation of ROS (Rodríguez-González *et al.*, 2018), leading to deactivation of caspase 8 which matches the finding reported in this study. According to recent studies conducted by Abhishek, (2018) and Zhang *et al.*, (2003), phagocytosis induces the release of ROS which activates caspase 8. They also mentioned that phagocytosis also triggers MAPK and ERK signals for the survival pathway that enhances resistance to apoptosis by downregulation of caspase 8 activation.

Huang *et al.*, (1999), who used lymphocytes and murine hepatocytes, also reported that caspase 8 and FADD were required to trigger apoptosis in those cells. Recently DaMata *et al.*, (2015) reported that inducing apoptosis in Balb/c and C57 peritoneal macrophages infected with *L. amazonensis* was concurrent with upregulation of caspase 8 (DaMata *et al.*, 2015). However, it has also been reported that *L. major* inhibits the releasing of mitochondrial cytochrome C in infected macrophages (Akarid *et al.*, 2004). The mechanisms of this inhibition are still not fully understood (Aguirre-Garcia *et al.*, 2018), suggesting the need for further investigation to determine the role of caspase 8 in inhibition of cytochrome C and apoptosis.

Although many studies focused on apoptosis, few have focused on *L.mexicana* and mitochondrial apoptosis pathways, and evidence for apoptosis inhibition in infected cells is still elusive. However, most of the studies have focused on the PI3K/Akt pathway. Considerable research on the endoplasmic reticulum pathway (unlike the pathway in this study which is mitochondrial) was conducted in the literature. For example, Balb/c BMDM infected with three *Leishmania* species *L. major*, *L. pifanoi* and *L.amazonensis* can resist apoptosis through inhibition of the PI3K/Akt signalling pathway exerting an anti-apoptotic effect in macrophages for survival after 12- and 24-hours infection (Ruhland, and Kima,

2007). Balb/c BMDM infected with *L.donovani* treated with AKT inhibitor caused an increase in host cell apoptosis and reduced parasite survival (Gupta *et al.*, 2016). Infection of RAW macrophages with *L.donovani* caused modulation of the host unfolded stress response (UPR) and PERK enzyme phosphorylation that reduces Akt phosphorylation. This can delay apoptotic induction in host macrophages and supports parasite invasion and survival (Abhishek, 2018).

#### 4.3.5.4 BCL 2

As shown in figure. 4.15, infection with P1 promastigotes upregulated the expression of BCL 2 in Balb/c and C57 BMDM and infection with P20 only upregulated this gene in C57 BMDM. Further investigation should be carried out to investigate the effect of P20 on C57 BMDM. It should be mentioned that the BCL 2 gene encodes for the anti-apoptotic BCL 2 protein. However, Bcl-xL and BCL 2 are found in the outer membrane of mitochondria and their role is to prevent apoptosis by blocking the release of cytochrome c, while the pro-apoptotic proteins such as Bax, and BAD are found in the cytosol. In response to certain stimuli, Bax, and BAD are translocated into the mitochondria, inducing outer membrane permeabilization which induces the release of cytochrome c (Frenzel *et al.*, 2009). Therefore, activation of the anti-apoptotic BCL 2 protein may interfere with Bax, and BAD protein to prevent apoptosis.

As shown in figure. 4.19, there are two apoptosis pathways: extrinsic and intrinsic. In the extrinsic pathway, unlike caspase 8, BCL 2 is only able to interfere with the apoptosis intrinsic pathway by stopping the release of cytochrome c from mitochondria.

Inhibition of apoptosis by upregulation of BCL 2 due to *Leishmania* infection has also been reported in previous studies using different host cells and different parasites species. Gutiérrez-Kobeh *et al.*, (2013) have reported that the infection of dendritic cells with *L.mexicana* causes inhibition of apoptosis and upregulation of anti-apoptotic proteins of the BCL 2 family. Also, infection of neutrophil cells with *L. major* caused a delay in apoptosis and enhanced expression of the anti-apoptotic BCL 2 proteins (Sarkar *et al.*, 2013). In a recent study conducted by Pandey *et al.*, (2016) it was reported that Balb/c peritoneal macrophages infected with *L.donovani in vitro*, causes an increase in the gene expression of BCL 2. They also used BCL 2 inhibitors in Balb/c mice *in vivo* and found that it caused an increase in NO and a reduction in the intracellular parasite survival. Therefore, they suggested that anti-BCL 2 could be used as a treatment for this disease. Moreover, infection of U937 macrophages with *L. infantum* treated with BCL 2 anti-apoptotic protein caused a significant enhancement of apoptosis with activation of caspase 3, caspase 8 and caspase 9 (Cianciulli *et al.*, 2018).



1 mRNA expression. It should be noted that both Balb/c BMDM and U937 cell lines are susceptible to *Leishmania* infection.

Activation of caspase 1 eventually leads to pyroptosis which in turn causes physical rupture of the cell and the release of DAMPs, intracellular molecules which activate the release of the proinflammatory cytokines IL-1 $\beta$  and IL-18 (Man *et al.*, 2017). The nature of the pyroptotic cell death pathway is inflammatory and is essential for the host cells to kill pathogens because parasites cannot replicate inside host cells. It is noteworthy that annexin V staining did not differentiate between apoptotic and pyroptotic cells (Jorgensen and Miao, 2015). Apoptosis or programmed cell death, on the other hand, is a defence mechanism by neutrophils, eosinophils, lymphocytes, monocytes and macrophages without triggering an immune and inflammatory response (Savill *et al.*, 2003). Apoptosis or programmed cell death is self-suicide of the cells to eliminate infected or damaged cells; therefore, apoptosis plays an important role in immune responses but, without triggering an immune and inflammatory response against the parasite (Savill, 1997; Savill *et al.*, 2003; Kono and Rock, 2008). One of the possible reasons for the resistance noticed in C57 BMDM might be due to the inability of the parasite to downregulate caspase 1. This might lead to the activation of pyroptosis which in turn could trigger an immune inflammatory response *in vivo*. In this study, caspase 1 was assessed by qPCR therefore, another technique (e.g. caspase 1 assay or western blot) should be used for further confirmation.

#### 4.3.5.6 PD-1

The gene expression of PD1 was downregulated in both mice infected with both P1 and P20 parasites (figure 4.15). This finding is fairly consistent with Roy *et al.*, (2017) who have reported that infection of Balb/c macrophages with *L.donovani* led to the downregulation of PD-1. Downregulation of PD-1 can cause the activation of pro-survival AKT (also called protein Kinase B) by phosphorylation. This subsequently leads to inhibition of the pro-apoptotic protein BAD and inhibition of apoptosis (Roy *et al.*, 2017). In addition, AKT which is a type of signal transduction pathway can promote cell survival and growth in response to extracellular signals such as cytokines, growth factors, and other stimuli (Manning, 2007). It has been reported that *Leishmania* parasite infection modulates host AKT signalling and inhibits caspase 3 which inhibits host cell apoptosis (Abhishek, 2018). It is known that the function of PD-1 is to trigger T-cell exhaustion. However, in this study, the role of PD-1 as a macrophage receptor was ambiguous in BMDM infected with *L.mexicana* because it was also downregulated in macrophages infected with P20. The role of PD-1 in macrophages is currently poorly understood, and only very recent studies have started to investigate its role.

#### 4.3.5.7 Bax

The expression of Bax was downregulated in macrophages infected with P1 in Balb/c but not C57 BMDM, while the effect of P20 is insignificant (figure. 4.15). There are no specific studies on the effect of *Leishmania* (particularly, in P1 and P20) on the gene expression of Bax. However, there is considerable research in the literature on the role of Bax in the mitochondrial pathway where cytochrome c is released by mitochondria upon binding of Bax with the outer membrane of the mitochondria, (Meier *et al.*, 2000; Zamzami and Kroemer, 2001), see also figure. 4.18. In addition, the expression of BCL 2, which is an anti-apoptotic protein, can block the action of pro-apoptotic proteins such as Bax and BAK (Rodríguez-González *et al.*, 2018).

#### 4.3.5.8 Caspase 9

The expression of caspase 9 was downregulated in both Balb/c and C57 BMDM infected with P1 and P20 irrespective of their virulence (figure. 4.15). Very few studies conducted in the literature studied the effect of *Leishmania* infection on caspase 9. caspase 9 is known for its role in the intrinsic apoptosis pathway; it can be activated by several stimuli that damage mitochondria to produce cytochrome c (Wong, 2011), with subsequent triggering of apoptosis (figure. 4.18). However, assessment of caspase 9 expression is helpful for confirmation of apoptosis because it is a sign for release of cytochrome c from the mitochondria. Contradictory to this the findings by DaMata *et al.*, (2015) reported that infection with *L. amazonensis* caused inducing of apoptosis in Balb/c and C57 BMDM concurrent with upregulation of caspase 3, caspase 8 and caspase 9.

#### 4.3.5.9 Necrosis

Figure 4.14 (H) showed that C57 but not Balb/c BMDM stained with necrotic stain (PI) was significantly less than controls after removing GMCSF. It is known that necrotic but not apoptotic cells induce inflammatory responses because of silence removal by phagocytosis (Kono and Rock, 2008). However, this may explain why lesions and clinical symptoms in Balb/c infected with *Leishmania* are more severe than that in C57 mice (Locksley *et al.*, 1992; Allenbach *et al.*, 2006). However, this finding contrasts with other studies which found that infection with *L. guyanensis* induced necrosis of Balb/c and C57 BMDM (DaMata *et al.*, 2015).

### 4.3.6 Proinflammatory cytokine gene regulation of Balb/c and C57 BMDM infected with P1 and P20 *L.mexicana*

Balb/c and C57 mice are widely used as models of choice in *Leishmania* research. However, very little is known on the role of TNF- $\alpha$  in Balb/c and C57 mice in response to *Leishmania* infection after 2 and 24 hours post-infection, hence the *L.mexicana* (P1 and P20) and Balb/c and C57 model can provide a unique opportunity to study the effect on proinflammatory cytokine modulation.

#### 4.3.6.1 TNF- $\alpha$

As already shown in results (figure. 4.17), the general trend of TNF- $\alpha$  levels in supernatants of Balb/c and C57 BMDM infected with P1 and P20 were in contrast to each other, where at 24 hours infection the concentration in the Balb/c BMDM (TNF- $\alpha$ ) decreased, in comparison to that of C57. In other words, in the susceptible Balb/c, both P1 and P20 (although P20 is avirulent) are able to modulate the infected cell in order to decrease release of TNF- $\alpha$ . In C57, both P1 and P20 failed to decrease the release of TNF- $\alpha$  after 24 hours of infection. This might be due to the differences between these mouse strain background and resistance. In general, C57 mice are known for their resistance to *Leishmania* infection, though they develop small lesions but they and self-healed, whereas Balb/c are susceptible to *Leishmania* (Locksley *et al.*, 1992; Allenbach *et al.*, 2006), and this is Th1 or Th2 response dependent. Th1 and Th2 activities depend on the modulation of pro-inflammatory cytokines such as TNF- $\alpha$ , IFN- $\gamma$ , IL-10, IL-17 and IL-4 (Soong, 2012). The secretion of TNF- $\alpha$  in the supernatant was much higher in C57 than Balb/c BMDM these findings are in agreement with other studies in the literature. C57 display a localised, small and self-healing infection lesion, combined with Th1 cytokines such as TNF- $\alpha$ , IL-1 and IFN- $\gamma$  production, while susceptible Balb/c mice have a different response to *Leishmania* infection characterised with the production of Th2 cytokines (IL-4, IL-10, and IL-13). This difference in the genetic background as a basis of susceptibility or resistance was instrumental in the development of the Th1/Th2 paradigm (Reiner, and Locksley., 1995; Gollob and Dutra., 2014; Maspi *et al.*, 2016). It has also been reported that TNF- $\alpha$  plays an important mediation role in host-protection against cutaneous Leishmaniasis in experimental murine cutaneous Leishmaniasis *in vivo* e. g. Balb/c infected with *L.major* (Titus *et al.*, 1989). Moreover, injection of anti-TNF- $\alpha$  into resistant CBA mice infected with *L.major* caused increase of the lesion size (Liew *et al.*, 1990 b) while, local injection of TNF- $\alpha$  cytokine in the skin lesion of infected CBA and Balb/c mice *in vitro* caused a reduction of the lesion and activation of macrophages to kill the parasite (Theodos *et al.*, 1991; Liew *et al.*, 1990 b). Although the trend of TNF- $\alpha$  concentration in Balb/c infected with P1 and P20 (figure.4. 18

and figure. 4.17) increased in relation to the control non-infected mice, it decreased in relation to the time from 2 to 24 hours which was confirmed by using qPCR and ELISA. Almost all studies in the literature investigated the concentration on the mammalian host cells after infection at only one time point (e.g. 24 hours, 48 hours or 72 hours). In the current study the effect of early infection with the parasite on the host cell cytokine modulation was compared at two early times; at 2 and 24 hours post-infection respectively. A similar trend of TNF- $\alpha$  gene regulation was seen in human monocytes infected with *L.mexicana* (Carrada *et al.*, 2007). Ansari *et al.*, (2006) reported that in humans infected with kala azar infection, TNF-  $\alpha$  mRNA expression was high. Infection of Balb/c BMDM with *L.donovani* promastigotes caused an increase in the expression of TNF-a (Moore, and Matlashewski, 1994). Similar results were also found in Balb/c BMDM infected with *L. major*. In addition, treatment of mice with anti-TNF- $\alpha$  was found to increase liver parasite burdens (Tumang *et al.*, 1994), whereas blocking of TNF- $\alpha$  receptor-1 in resistant C57 promoted the existence of non-healing lesions (Garcia *et al.*, 1995). Manna *et al.*, (2014) reported that infection of C57 with *L.major* caused an increase in TNF- $\alpha$ . In addition, deletion of the TNF- $\alpha$  gene in the resistant C57 infected with *L.major in vivo* caused rapid death of the infected mice combined with visceral infection with the parasites, although *L.major* is categorised as one of the causative agents of CL. As mentioned previously the resistance or susceptibility to *Leishmania* depends on anti-inflammatory cytokines that regulate Th1 or Th2. Activation of Th1 cells causes a resistance to the disease while susceptibility depends upon the activation of Th2 cells. Accordingly, linking the above ideas with the findings obtained in figure. 4.16 and 4.17, it can be reported that in Balb/c BMDM infection with P1 was able to downregulate the expression of the TNF- $\alpha$  (figure. 4.16) at both mRNA and protein levels as assessed by PCR and ELISA respectively (figure. 4.16 and 4.17), while in C57 infection with P1 failed to reduce the expression and the concentration of TNF- $\alpha$ . The increasing level of TNF- $\alpha$  in C57 could help in the activation of Th1 which in turns cause resistance to this disease (Alexander *et al.*, 1999).TNF- $\alpha$  can also be linked to apoptosis. TNF- $\alpha$  which is mainly produced by macrophages is one of the most important pro-inflammatory cytokines that is involved in the immunopathology and immunoprotection. TNF- $\alpha$  can control intracellular pathogens in CL by increasing macrophage activity and their synthesis of NO (Maspi *et al.*, 2016). Singh *et al.*, (2016) who studied the role of TNF- $\alpha$  in controlling human *L.donovani* infection reported that TNF- $\alpha$  was able to stimulate the production of IFN- $\gamma$ . Consequently, this could activate macrophages to express iNOS2 enzyme which subsequently activates the generation of NO aiding killing of the intracellular amastigotes (Sharma and Singh 2009; Singh *et al.*, 2016). TNF- $\alpha$  activates mitochondria to produce ROS which is important to activate apoptosis through different pathways such as activation of c-Jun N-terminal kinase,

activation of MKPs (Sakon *et al.*, 2003; Tobiume *et al.*, 2001; Kim *et al.*, 2010) as well as cleavage of BID protein (Deng *et al.*, 2003).

In the current study, TNF- $\alpha$  levels in Balb/c and C57 infected with P1 were less than in those infected with P20. This may cause a reduction of release of ROS (that can induce the apoptosis). This may explain why apoptosis in Balb/c and C57 infected with P1 was less than one infected with P20. It should be mentioned that one of the possible strategies for P1 to survive inside the infected cell is through the modulation of TNF- $\alpha$  and reduced production of ROS. This needs further investigation to estimate ROS concentration in Balb/c and C57 BMDM infected with P1 and P20 for 2 and 24 hours.

#### **4.3.6.2 IL-6**

The main sources of IL-6 are monocytes and macrophages; IL-6 plays an important role in inflammatory responses. Also, IL-6 is associated with *Leishmania* infection and plays a dual role in Th1 and Th2 differentiation (Diehl and Rincón *et al.*, 2002). Infection of Balb/c BMDM for two hours with P1 but not P20 caused significant upregulation of IL-6 (figure 4.16), while after 24 hours caused downregulation of IL-6 expression compared with 2 hours post-infection which means that P1 is able to modulate gene regulation of IL-6 in Balb/c but not C57 BMDM. However, a high level of IL-6 was associated with the activation of Th2 (Rincón *et al.*, 1997; Diehl and Rincón, 2002). This finding is supported in some way by Duque *et al.*, (2014) who reported that macrophages induced an early release of IL-6 in response to *Leishmania* infection *in vivo* or *in vitro*. Santos *et al.*, (2016), also reported that high blood levels of IL-6 were observed in patients infected with visceral Leishmaniasis (*L. infantum*) which was associated with severity and mortality of the disease. Similarly, a recent study by (Ramos *et al.*, 2016) also reported that there was a positive correlation between serum levels of IL-6 and clinical symptoms of infection with *L. infantum*. However, low levels of IL-6 were shown to enhance human macrophage activity against *Leishmania* parasites (Hatzigeorgiou, He *et al.*, 1993).

#### **4.3.6.3 IL-1 $\beta$**

The IL- $\beta$  cytokines which are mainly secreted by macrophages play a major role in immunopathology and inflammatory response to *Leishmania* infection, therefore IL- $\beta$  and TNF- $\alpha$  are called alarm cytokines (Charmoy *et al.*, 2016; Maspi *et al.*, 2016). IL-1 $\beta$  is a chemoattractant for granulocytes and enhances the differentiation of CD4 T cells (Ben-Sasson *et al.*, 2009). After infection, IL-1 $\beta$  stimulates the production of prostaglandin that activates the acute phase of inflammation and acts on the central nervous system to induce fever, in addition, it induces mast cells to release histamine which will cause vasodilation and localization of the inflammation (Ben-Sasson *et al.*, 2009). However, production of IL-

1 $\beta$  causes production of iNOS2 enzyme which induce NO synthesis *in vivo* and, in the macrophage, *in vitro* that lead to resistance to infection by the host cell (Lima-Junior *et al.*, 2013). According to this study finding, P1 was able to downregulate IL-1 $\beta$  expression in Balb/c but not C57 BMDM after 24 hours infection whereas, in C57 BMDM it did not change after infection with P1. Although, this result is a qPCR result and needs confirmation by another test such ELISA, the result is supported by Charmoy *et al.*, (2016) who reported that infection of C57 with *L.major* causes upregulation of IL-1 $\beta$  mRNA. Kostka *et al.*, (2006) reported that using IL-1 $\beta$  for treatment of C57 mice infected with *L.major* led to the promotion of Th1 healing of the Leishmaniasis.

#### 4.3.6.4 TGF- $\beta$

TGF-  $\beta$  is an anti-inflammatory cytokine that suppresses both Th1 and Th2 cells and promotes the function of Treg cells (Travis and Sheppard, 2014) in addition, it activates other cytokines such as TNF- $\alpha$  and IFN- $\gamma$  (NCBI RefSeq, 2016). However, TGF- $\beta$  is produced in response to infection with *Leishmania* amastigotes (Gomes *et al.*, 2014) and increases susceptibility to Leishmaniasis by inhibiting activation of macrophages and decreasing IFN- $\gamma$ . According to this study findings, TGF-  $\beta$  was downregulated in both Balb/c and C57 BMDM after infection with P1 for 24 hours infection, whereas it was upregulated in C57 infected with P20; however, to the best of my knowledge there is no study focused on the role of TGF-  $\beta$  in Balb/c and C57 BMDM infected with *L.mexicana*. The role of TGF- $\beta$  in human Leishmaniasis (*L. braziliensis*) is inhibition of Th1 responses by downregulation of IFN- $\gamma$  (Barral *et al.*, 1995). Wilson *et al.*, (1998) reported that, TGF- $\beta$  causes inhibition of Th1 in Balb/c infected with *L. chagasi*. Barral *et al.*, (1995) who compared human macrophages infected with *L. braziliensis in vitro* in tissue culture medium containing TGF- $\beta$ , reported that the number of parasites in the TGF- $\beta$  treated flask was 50% higher than controls, suggesting TGF- $\beta$  had reduced macrophage activity. Moreover, TGF-  $\beta$  is capable of changing the immune response towards Th2 by increasing IL-10, either *in vivo* or *in vitro* (Barral-Netto *et al.*, 1995). TGF- $\beta$  activates Th 17 cells which are associated with chronic inflammation and damage of tissues (Belkaid and Tarbell, 2009). In this regard TGF- $\beta$  is associated with chronic infections (Melby *et al.*, 1994), therefore the regulation of this gene may need a longer time of infection. The regulation of TGF- $\beta$  is associated with two factors, the parasite and the host. Regarding the parasite, for example, it is higher in mucosal Leishmaniasis than cutaneous Leishmaniasis (Bacellar *et al.*, 2002). Regarding the type of host cell, there is a big individual variation between hosts releasing TGF- $\beta$  cytokines in response to Leishmaniasis (Gomes *et al.*, 2014) which is supported by this study in some way that TGF- $\beta$  was upregulated in C57 BMDM and downregulated in Balb/c BMDM when they were infected with P20.

**The effect of Balb/c and C57 BMDM  
conditioned medium on P1 and P20  
*L.mexicana* promastigotes**

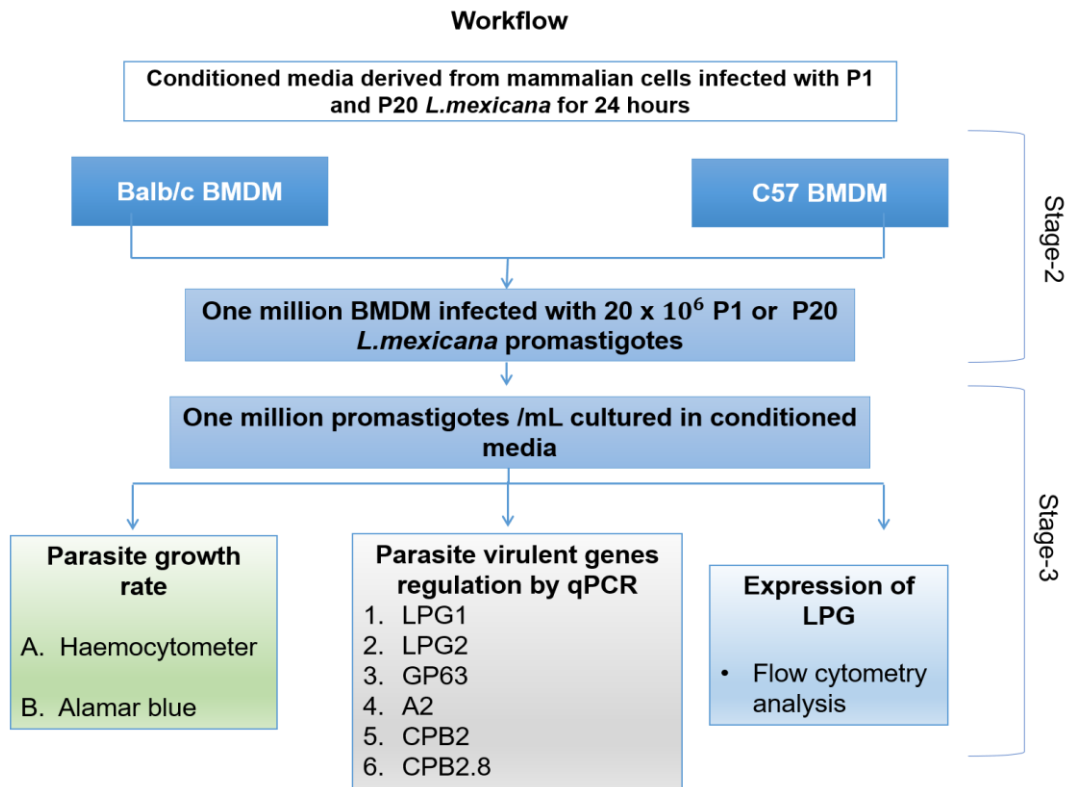


**Figure 2.4 Workflow of the effect of conditioned medium on parasite growth and virulent gene regulation (Stage-3)**

Supernatants were collected from Balb/c and C57 BMDM infected with P1 or P20 promastigotes. Briefly, one million BMDM were infected with  $20 \times 10^6$  promastigotes for 24 hours. Supernatants were collected and stored at  $-20^{\circ}\text{C}$ . The effect of conditioned medium on the promastigotes growth and virulence associated genes were investigated.

## 5.1 Introduction

Many studies have investigated the components of supernatants derived from parasites cultured on their own or from a culture of mammalian cells infected with parasites. Many approaches have been used to identify the types of proteins secreted by *Leishmania* parasites or host cells in response to infection. About 72 proteins produced by *L.mexicana* have been identified by proteomic analysis (Hassani, *et al.*, 2011), and 270 protein spots were detected by Two-Dimensional Gel Electrophoresis (Cuervo *et al.*, 2009; Garg *et al.*, 2018) from parasite cultures. *Leishmania* parasites produce molecules by two pathways: by the classical pathway and non-classical pathway, most of these proteins are secreted by the non-classical pathway (Cuervo *et al.*, 2009). The non-classical pathway involves releasing proteins by different mechanisms such as lysosomal secretion, exosome, and plasma membrane shedding (Corrales *et al.*, 2010). Many approaches have been used to assess the exosomes produced by *Leishmania* parasites. 329 proteins have been identified in *Leishmania* exosomes that can interact with macrophages and modulate the host immune system (Silverman *et al.*, 2010). *L.mexicana* at the amastigote stage secretes 1764 proteins, (Paape

*et al.*, 2010), most of them have unknown functions. Proteomic analysis of the parasite supernatant is a useful tool for studying the proteins excreted by *Leishmania* parasites and exploring of these proteins could be helpful in designing new diagnostic procedures, drugs and may help in vaccines development (Garg *et al.*, 2018).

Despite the importance of *Leishmania* extracellular secretion components in the host cell infected with the parasite which regulates the host immune responses, only a few of these extracellular proteins have been fully characterized such as LPG and GP63 (Lambertz *et al.*, 2012). Moreover, little is known about extracellular proteins which may be produced by the host which may affect parasite survival. Many studies have shown that the supernatants derived from infected mammalian cells *in vitro* contained a variety of cytokines that affect parasite-mammalian cell interaction as described by Escalona-Montaña *et al.*, (2016). Mammalian cells may produce molecules (during interaction with the parasite) that affect the growth or virulence of the parasite. Previous studies have focused on the effect of conditioned media, derived from an infected cell, on the viability of the non-infected mammalian cells such as monocytes and macrophages (Moore, and Matlashewski, 1994; Paris *et al.*, 2007). Other studies investigated the effect of supernatant on the infected cells such as Kane and Mosser, (2001).

Over the last decade, many approaches have been used to study proteins produced by the parasites, however, this study investigated the effect of supernatant components, derived from Balb/c and C57 BMDM infected with P1 and P20 *L.mexicana* on the growth characteristic of parasite promastigotes suggesting investigation of the protein or molecules that may be produced by macrophages when exposed to the parasite. Overall, little research has been conducted on the effect of supernatants derived from infected mammalian cells on *Leishmania* promastigotes. A single paper on such effect was produced by this group by Ali *et al.*, (2013). However, this study examined the effect of supernatants derived from human U937 monocytes and macrophages infected with P1 and P20 *L.mexicana* for 2 hours. However, as mentioned before in the current study parasites need about 24 hours for internalisation and to differentiate into amastigotes and to form PVs inside macrophages. Therefore, one of the unique aspects which reflects the current approach of the work is the investigation whether the infected cell can produce molecules that affect promastigote growth rate and virulence by comparing between supernatant obtained from Balb/c and C57 BMDM infection with P1 and P20 *L.mexicana* for 24 hours.

## 5.2 Results

### 5.2.1 Effect of conditioned media on the growth of P1 and P20

#### *L.mexicana* promastigotes

##### 5.2.1.1 Effect of conditioned media on the growth of P1 and P20 *L.mexicana* promastigotes measured by haemocytometer

Supernatants were collected from one million Balb/c and C57 BMDM infected with  $20 \times 10^6$  P1 or P20 *L.mexicana* promastigotes for 24 hours. The collected supernatants were used for the preparation of conditioned media. The effect of conditioned media on the growth of P1 and P20 *L.mexicana* promastigotes was investigated by using two methods; (i) manual counting of the promastigotes using haemocytometer (in this method, only 1:1 ratio supernatant and fresh RPMI1640 media was used, and (ii) Alamar blue assay, in which three different supernatant concentrations 3:4, 1:1 and 1:3 (75%, 50% and 25%) of supernatants and RPMI1640 media were used.

The conditioned medium derived from control non-infected Balb/c BMDM significantly enhanced the growth of P1 promastigotes more than that derived from Balb/c BMDM infected with P1 or P20 promastigotes when cultured for 24 hours at 25°C (figure. 5.1 A). However, the control conditioned media slightly inhibited the growth of P20 promastigotes (figure. 5.1 A). Only conditioned media derived from C57 BMDM infected with P20 significantly enhanced P20 growth (figure. 5.1B).

A similar trend of growth enhancement was also observed when the Alamar blue assay was used (which is more accurate than manual counting by haemocytometer) (figure 5.2). The most common observation of the results of the two assays, the haemocytometer (Figure. 5.1 A) and Alamar blue (figure. 5.2 A) was that the supernatant derived from non-infected Balb/c BMDM enhanced P1 growth.

In general, supernatants from control or infected Balb/c BMDM increased the growth rate of P1 in a dose-dependent manner (figure. 5.2 A, B and C) while supernatants from control or infected C57 BMDM did not show a significant enhancement on the growth of P1 promastigotes with one exception of supernatants derived from C57 BMDM infected with P1 which significantly inhibited P1 growth rate at one concentration of 1:3 (25%) (figure 5.2 E). It is clear that Balb/c supernatant influenced P20 growth rate, since P20 growth was, significantly decreased when cultured in the supernatant of Balb/c BMDM infected with P1, but significantly increased when incubated in supernatants of Balb/c BMDM infected with P20 (figure. 5.3 A, B and C).

The effect of C57 supernatant on P20 growth rate is shown in figures 5.3 D, E and F, incubation of P20 in supernatants derived from C57 BMDM control and infected with P1

caused a significant decrease in P20 growth. In contrast, incubation of P20 in supernatant derived from C57 BMDM infected with P20 caused a significant increase in their growth rate.

One of the most significant findings of this study is supernatants from Balb/c BMDM infected with virulent *L.mexicana* (P1) enhanced the growth rate of the parasite, whereas those derived from C57 BMDM infected with P1 suppressed the growth rate of virulent *L.mexicana*. In other words, supernatants from Balb/c but not C57 BMDM infected with P1 enhanced parasite growth rate.

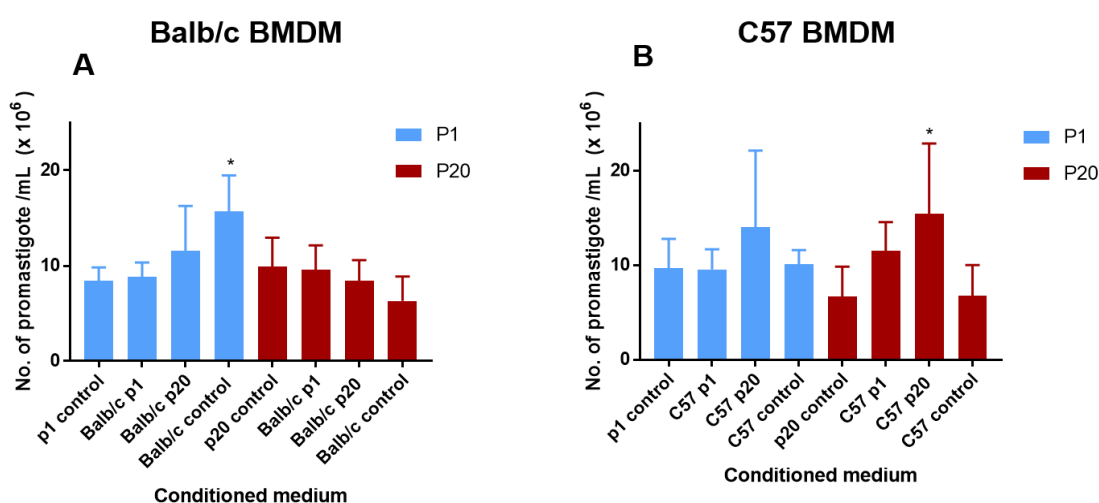


**Figure 5. 1: Effect of Balb/c and C57 BMDM conditioned medium on P1 and P20 growth by using haemocytometer.**

One million Balb/c and C57 BMDM were infected with  $20 \times 10^6$  P1 and P20 *L. mexicana* promastigotes in T25 tissue culture flasks and incubated at 95% v/v humidity at 37 °C in 5% v/v CO<sub>2</sub> incubator for 24 hours. Supernatants were collected and passed through a 0.25 µm filter to remove all parasites. Conditioned media were prepared by mixing of 1:1 ratio v/v (supernatant: fresh RPMI 1640 containing 10% v/v HIFCS) 50% supernatant. P1 and P20 promastigotes at concentration of  $10 \times 10^6$  / mL were cultured in conditioned media and incubated at 25°C for 24 hours in unvented tissue culture flasks. Parasites were collected and passed through an 18 G needle and counted manually by haemocytometer. Data were analysed by using GraphPad Prism 7, statistically significant differences between pairs of groups represented by \* $p < 0.05$ . P value was determined by unpaired t-test. The results are average of three independent experiments and the bars represent  $\pm$  standard error of mean.

### 5.2.1.2 Effect of conditioned media on P1 and P20 growth rate measured by Alamar blue assay

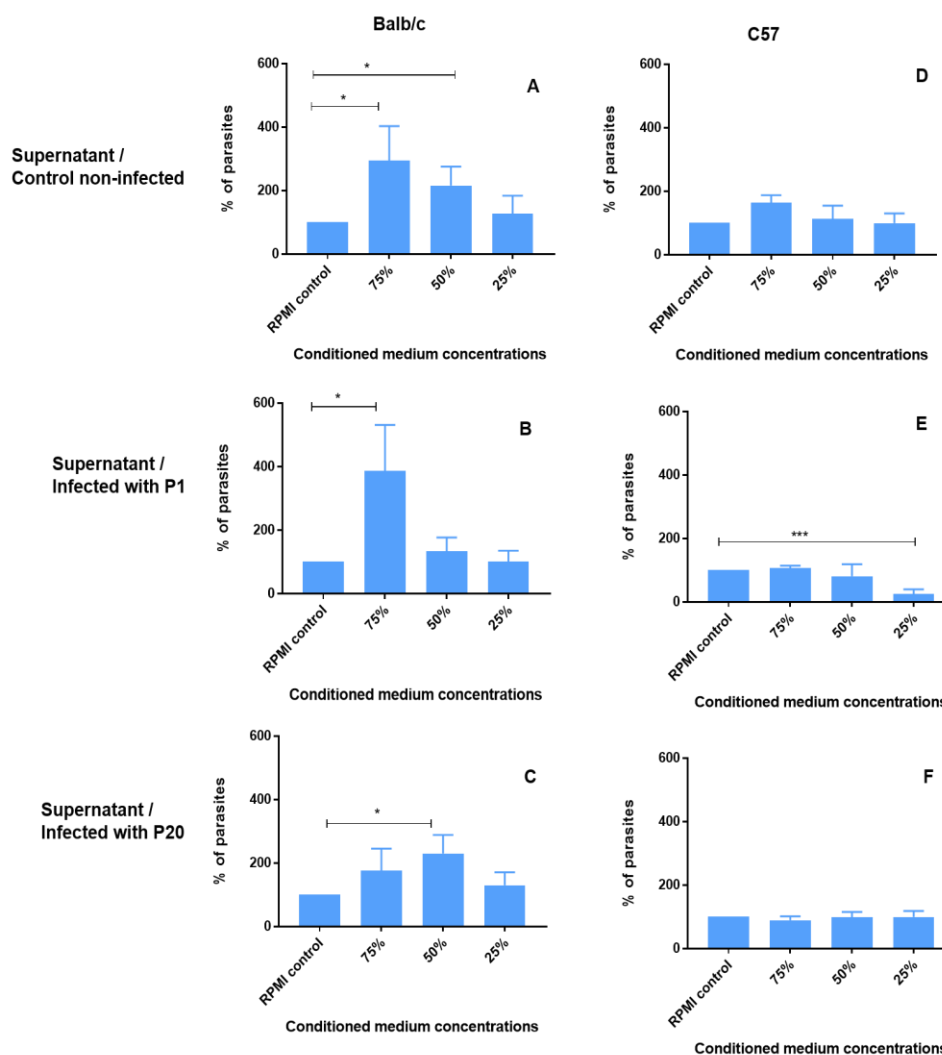


**Figure 5.2 : Effect of Balb/c and C57 BMDM conditioned medium on P1 *L.mexicana* promastigotes growth measured by Alamar blue assay.**

One million Balb/c and C57 BMDM were infected with  $20 \times 10^6$  P1 and P20 *L. mexicana* promastigotes in T25 tissue culture flasks and incubated at 95% v/v humidity at 37 °C in 5% v/v CO<sub>2</sub> incubator for 24 hours. Supernatants were collected and passed through a 0.25 µm filter. Conditioned media were prepared by mixing of fresh RPMI 1640 containing 10% v/v HIFCS and supernatant at three different concentrations 75%, 50% and 25% v/v (3:1, 1:1 and 1:3) conditioned media ratio to RPMI 1640 containing 10% v/v HIFCS respectively). One million P1 and P20 promastigotes seeded in flat bottom 96 well plate containing three different concentrations of conditioned media in 100 µL total volume, RPMI 1640 containing 10% v/v HIFCS was used as control. The plate was sealed and incubated for 24 hours at 25 °C. The concentration of promastigotes was estimated by Alamar blue assay, plate was read by spectrophotometry plate reader (Clarion star Europe) at 570 nm and 600nm. Results were calculated and normalised with control RPMI 1640 supplemented with 10% v/v HIFCS. Data were analysed by using GraphPad Prism 7, statistically significant differences between pairs of groups represented by \*p<0.05, \*\*p<0.001 and \*\*\*p<0.0001. P value was determined by unpaired t-test. The results are average of three independent experiments and the bars represent ± standard error of mean.

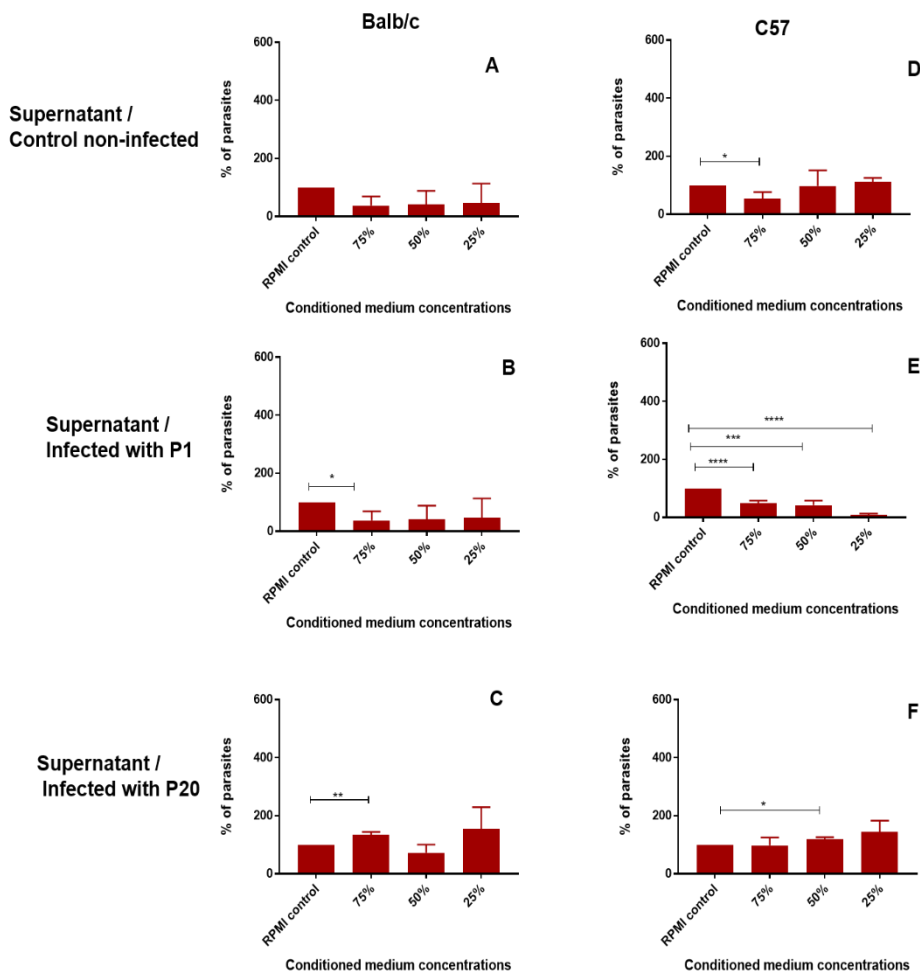


**Figure 5. 3: Effect of Balb/c and C57 BMDM conditioned medium on P20 *L.mexicana* promastigotes growth measured by Alamar blue assay**

One million Balb/c and C57 BMDM were infected with  $20 \times 10^6$  P1 and P20 *L. mexicana* promastigotes in T25 tissue culture flasks and incubated at 95% v/v humidity at 37 °C in 5% v/v CO<sub>2</sub> incubator for 24 hours. Supernatants were collected and passed through a 0.25 µm filter. Conditioned media were prepared by mixing of fresh RPMI 1640 containing 10% v/v HIFCS and supernatant at three different concentrations 75%, 50% and 25% v/v (3:1, 1:1 and 1:3) conditioned media ratio to RPMI 1640 containing 10% v/v HIFCS respectively). One million P1 and P20 promastigotes seeded in flat bottom 96 well plate containing three different concentrations of conditioned media in 100 µL total volume, RPMI 1640 containing 10% v/v HIFCS was used as control. The plate was sealed and incubated for 24 hours at 25 °C. The concentration of promastigotes was estimated by Alamar blue assay, plate was read by spectrophotometry plate reader (Clarion star Europe) at 570 nm and 600nm. Results were calculated and normalised with control RPMI 1640 supplemented with 10% v/v HIFCS Data were analysed by using GraphPad Prism 7, statistically significant differences between pairs of groups represented by \* $p < 0.05$ , \*\* $p < 0.001$  and \*\*\* $p < 0.0001$ . P value was determined by unpaired t-test. The results are average of three independent experiments and the bars represent  $\pm$  standard error of mean.

## 5.2.2 Effect of conditioned media on P1 and P20 *L.mexicana* promastigotes virulence associated gene regulation

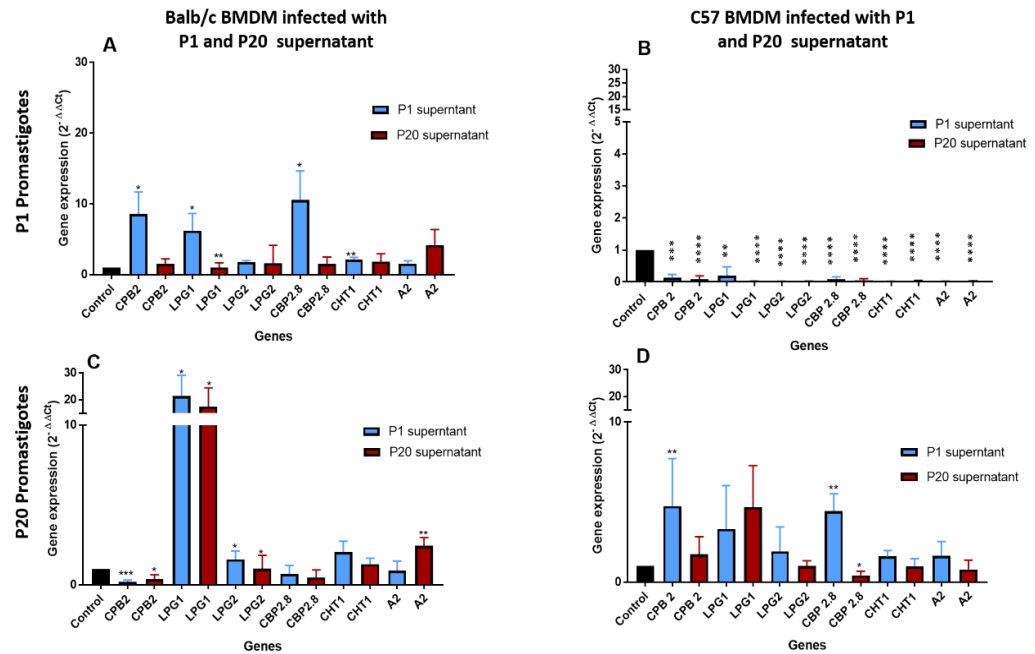


**Figure 5. 4: Effect of Balb/c and C57 BMDM conditioned medium on P1 and P20 virulence gene regulation.**

One million Balb/c and C57 BMDM were cultured in 2.5 mL RPMI 1640 containing 10% v/v HIFCS in T25 tissue culture flasks. Cells were infected with  $20 \times 10^6$  P1 and P20 *L. mexicana* promastigotes and incubated at 95% v/v humidity at 37°C in 5% v/v CO<sub>2</sub> incubator for 24 hours. Supernatants were collected, passed through 0.25 μm filters to remove any parasites and mixed with equal volume of RPMI 1640 containing 10% v/v HIFCS.  $40 \times 10^6$  P1 and P20 promastigotes were cultured in conditioned media at 1:1 concentration ratio RPMI 1640 containing 10% v/v HIFCS and incubated at 25°C for 24 hours in unvented tissue culture flasks. 4 mL of fresh RPMI 1640 containing 10 v/v HIFCS was the control medium. Cells were harvested, and total mRNA was extracted, then converted into cDNA and subjected to qPCR. qPCR results were normalized using the housekeeping gene GAPDH and Ct values were calculated as  $2^{-\Delta\Delta C_t}$ . Data were analysed by using GraphPad Prism 7. Statistically significant differences between pairs of groups represented by \* $p < 0.05$ , \*\* $p < 0.001$  and \*\*\* $p < 0.0001$ . P value was determined by unpaired t-test. The results are average of three independent experiments and the bars represent  $\pm$  standard error of mean.

The effect of conditioned media on virulence associated genes of P1 and P20 *L.mexicana* promastigotes were investigated by qPCR (CPB2, CPB2.8, LPG, LPG2, CHAT1 and A2). Supernatants were collected from one million Balb/c and C57 BMDM infected with  $20 \times 10^6$  P1 or P20 *L.mexicana* promastigotes for 24 hours. The collected supernatants were used for the preparation of conditioned media (in this method, 1:1 ratio supernatant and fresh RPMI1640 media were used), P1 and P20 *L.mexicana* promastigotes were incubated in the

conditioned medium at 25°C for 24 hours in unvented flasks. Total RNA was extracted and transcribed into cDNA then subjected to qPCR.

The results show that supernatants derived from C57BMDM infected with P1 and P20 significantly downregulated CPB2, LPG, LPG2, CHAT1 and A2 in p1 promastigotes (figure 5.4 B). In contrast, supernatants from Balb/c infected with P1 significantly upregulated a number of virulence associated genes (LPG1 CPB2 and CPB2.8). Collectively, in light of these findings, C57 BMDM may produce molecules that can downregulate virulence associated genes of the promastigotes. However, LPG1 and LPG2 in P20 but not P1 promastigotes were not affected by incubation in C57 BMDM infected with P1 or P20 conditioned medium (figure 5.4 D).

### 5.2.3 Effect of Balb/c and C57 conditioned medium on the expression of LPG in P1 and P20 promastigotes measured by flow cytometry

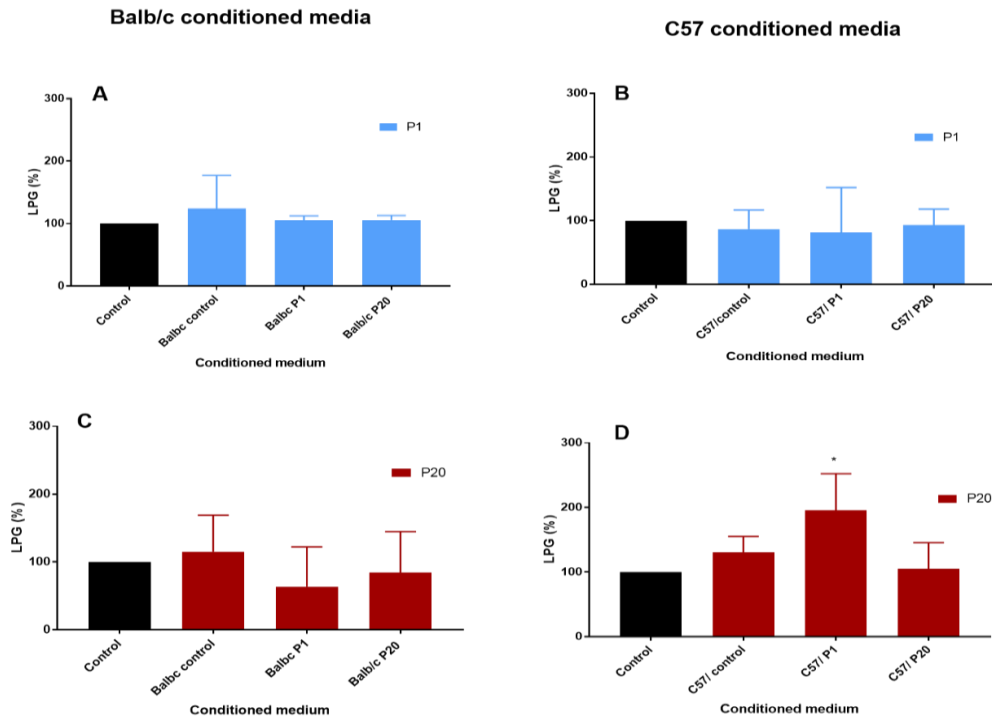


**Figure 5. 5: Effect of Balb/c and C57 BMDM conditioned medium on LPG expression on P1 and P20 *L.mexicana* promastigotes**

One million Balb/c and C57 BMDM were cultured in 2.5 mL RPMI 1640 containing 10% v/v HIFCS in T25 tissue culture flasks. Cells were infected with  $20 \times 10^6$  P1 and P20 *L. mexicana* promastigotes and incubated at 95% v/v humidity at 37°C in 5% v/v CO<sub>2</sub> incubator for 24 hours. Supernatants were collected, passed through 0.25 µm filter to remove any parasite and mixed with equal volume of RPMI 1640 containing 10% v/v HIFCS.  $0.5 \times 10^6$  P1 and P20 promastigotes at stationary phase were washed and incubated in conditioned medium at 1:1 concentration ratio RPMI 1640 containing 10% v/v HIFCS and incubated at 25°C for 24 hours in unvented tissue culture flasks. Parasites were washed twice with PBS, stained with CA7AE mouse anti *Leishmanial* LPG (Bio-Rad) primary antibody and incubated at 4°C for 30 minutes. Tubes were washed twice with PBS and stained with (secondary antibody) Alexa fluor goat anti-mouse IgG FITC antibody (Thermo Fisher Scientific) was added into all tubes and incubated at room temperature for 30 minutes. All tubes were washed 3 times with PBS and resuspended in 400 µL flow cytometry fluid and analysed by flow cytometry using Beckman Coulter Kaluza software USA. Results were normalised to the control incubated in RPMI 1640 supplemented with 10% v/v HIFCS. Data were analysed by using GraphPad Prism 7. Statistically significant differences between pairs of groups represented by \* $p < 0.05$ . The P value was determined by unpaired t-test. The results are average of three independent experiments and the bars represent  $\pm$  standard error of mean.

Results in figure. 5.5, illustrate that the conditioned medium derived from Balb/c and C57 BMDM infected with either P1 or P20 promastigotes did not significantly affect the expression of LPG by P1 promastigotes. However, conditioned medium derived from C57 BMDM infected with P1 caused significant increase in LPG expression by P20 promastigotes by flow cytometry analysis. Conditioned medium derived from Balb/c BMDM did not significantly affect the expression of LPG on either P1 or P20 promastigotes.

## 5.2.4 Synopsis of effects of conditioned media on the virulent P1 and avirulent P20 *L. mexicana* promastigotes

**Table 5. 1: Effect of Balb/c and C57 BMDM conditioned medium on the P1 and P20 *L. mexicana* promastigotes growth**

	Test	P1	P20
Effect of control Balb/c conditioned medium on promastigote growth	-Neubauer hemocytometer	Enhanced	No effect
	-Alamar blue assay		
Effect of Balb/c infected with P1 conditioned medium on promastigotes growth	-Neubauer hemocytometer	Enhanced	Inhibited
	-Alamar blue assay		
Effect of Balb/c infected with P20 conditioned medium on promastigotes growth	-Neubauer hemocytometer	Enhanced	Enhanced
	-Alamar blue assay		
Effect of control C57 BMD conditioned medium on promastigotes growth	-Neubauer hemocytometer	No effect	Inhibited
	-Alamar blue assay		
Effect of C57 BMDM infected with P1 conditioned medium on promastigotes growth	-Neubauer hemocytometer	Inhibited	Inhibited
	-Alamar blue assay		
Effect of C57 BMDM infected with P20 conditioned medium on promastigotes growth	-Neubauer hemocytometer	No effect	Enhanced
	-Alamar blue assay		

**Table 5. 2: Effect of conditioned media on P1 and P20 *L. mexicana* promastigote virulence associated gene regulation**

	Test	P1	P20
Effect of Balb/c infected with P1 conditioned medium	qPCR	Upregulation of LPG1, CHT1, CPB2 and CPB2.8	Upregulation of LPG1 and LPG2 Downregulation of CPB2
Effect of Balb/c infected with P20 conditioned medium	qPCR	Upregulation of LPG1	Upregulation of LPG1, LPG2 and A2 Downregulation of CPB2
Effect of C57 BMDM infected with P1 conditioned medium	qPCR	Downregulation of CPB2, LPG1, LPG2, CPB2.8, CHT1 and A2	Upregulation of CPB2 and CPB2.8
Effect of C57 BMDM infected with P20 conditioned medium	qPCR	Downregulation of CPB2, LPG1, LPG2, CPB2.8, CHT1 and A2	Downregulation of CPB2.8.

**Table 5. 3: Effect of Balb/c and C57 conditioned medium on P1 and P20 *L. mexicana* promastigotes LPG expression**

	Test	P1	P20
Effect of Balb/c control conditioned medium	Flow cytometry	No effect	No effect
Effect of Balb/c infected with P1 conditioned medium	Flow cytometry	No effect	No effect
Effect of Balb/c infected with P20 conditioned medium	Flow cytometry	No effect	No effect
Effect of C57 control conditioned medium	Flow cytometry	No effect	No effect
Effect of C57 BMDM infected with P1 conditioned medium	Flow cytometry	No effect	Increased
Effect of C57 BMDM infected with P20 conditioned medium	Flow cytometry	No effect	No effect

### 5.3 Discussion

The main findings of this chapter are that supernatant derived from Balb/c BMDM infected with virulent *L.mexicana* (P1) enhanced promastigote growth, while supernatant derived from C57 BMDM infected with P1 inhibited the growth of virulent *L.mexicana* (P1). This might indicate that Balb/c produced molecules that could enhance the growth of P1, whereas, the resistant C57 BMDM may generate growth inhibitor components. Further investigation is recommended of the supernatant's content in more depth using different techniques such as mass spectrometry.

As mentioned earlier, no studies have compared the effect of conditioned media derived from Balb/c and C57 post 24 hours infection on the parasite growth. Results in this study were obtained by using two different assessment methods, namely; manual counting by haemocytometer as well as by Alamar blue. The most relevant study was reported by Ali *et al.*, (2013) who used conditioned media derived from U937 monocytes and macrophages infected with P1 and P20 *L.mexicana* for only 2 hours using a manual counting technique (haemocytometer). Ali *et al.*, (2013) reported that conditioned media derived from U937 infected with P1 or P20 did not affect the growth of P1. Although both Balb/c and U937 macrophages are susceptible to *Leishmania*, the findings of the current study clearly show that conditioned media derived from Balb/c BMDM infected with P1 caused a significant increase in the growth of P1. It should be mentioned that Ali *et al.*, (2013) used only a 50 % supernatant concentration and a haemocytometer. At this concentration (and by using the haemocytometer method), the same findings obtained by Ali *et al.*, (2013) was also observed in the current study (see figure. 5.1). However, by using a 75% supernatant concentration (3:1ratio) and Alamar blue (see figure. 5.2 B), a significant effect on the growth of P1 was observed. Alamar blue technique seems more accurate and reproducible than manual counting by haemocytometer. In addition, Ali *et al.*, (2013) used conditioned media obtained after 2 hours while in the current study, conditioned media was obtained after 24 hours infection. Furthermore, it was already mentioned (section 4.2.2) that 2 hours was not enough for internalisation of the parasite inside infected cells. It noteworthy to mention it was found that the modulation of the gene regulation of proinflammatory cytokines needs approximately 24 hours to modulate the host cell (section 4.2.6). The growth factors or inhibitors may also require more than 2 hours to be generated and released. These results are in line in some way with those of Kane and Mosser, (2001) who reported that treatment of infected macrophages with supernatant from macrophages infected with *L. major* caused enhancement of parasites number inside infected macrophages.

Another phenomenon that has also been observed is that C57 BMDM infected with P1 and P20 may produce molecules which can significantly downregulate virulence associated

genes (CPB2, LPG, LPG2, CHAT1 and A2) in P1 promastigotes (figure 5.4 B). However, these results need further confirmation by another test such as flow cytometry or western blot. LPG1 and LPG2 expression in P20 promastigotes were not significantly affected after incubation in the supernatant of C57 BMDM infected with P1 or P20 (figure 5.4 D). LPG expression significantly increased after incubation in the supernatant of C57 BMDM infected with P1.

Approximately 2000 spots of soluble proteins that were released extracellularly were detected during differentiation of parasite promastigotes into the amastigote stage (Bente *et al.*, 2003; Garg *et al.*, 2018) However, the current study's results showed that the effect of conditioned media derived from control and infected Balb/c but not C57 BMDM can increase P1 promastigote growth rate. This enhancement of parasite growth rate could be due to the presence of molecules produced by Balb/c BMDM because it is observed in infected and non-infected macrophages.

It has been reported before that *Leishmania* infection can stimulate production of costimulatory molecules such as B7-1 and B7-2 on macrophages which can induce production of either Th1 or Th2 cytokines (Kuchroo *et al.*, 1995; Elloso *et al.*, 1999). No study has been directly focused on molecules that are produced by macrophages and their effect on promastigotes. However, these results may shed some light on other molecules that may be produced by infected macrophages that may inhibit promastigote growth or may affect parasite virulence induced during infection. Extracellular protein studies could be useful in the investigation of new drugs or vaccine development (Garg *et al.*, 2018).

It has been reported that understanding the nature of extracellular proteins secreted by *Leishmania* parasites at a particular time of infection or stage in its life cycle could clarify the mechanisms used by the parasite for infection and survival inside infected cells. Also, by revealing the importance of extracellular proteins or molecules, detailed knowledge may provide a novel strategy for drug or vaccine design and development (Corrales *et al.*, 2010). This study reported that Balb/c but not C57 BMDM may produce a molecule that enhanced virulent P1 growth. Further investigation of these molecules is required.

Collectively, Balb/c BMDM infected with P1 supernatants enhance P1 promastigotes growth combined with upregulation of LPG1, CHT1, CPB2 and CPB2.8 while C57 infected with P1, inhibit P1 promastigotes growth and caused downregulation of LPG1, LPG2 CPB2, CPB2.8, CHT1 and A2. This suggests that Balb/c BMDM produce molecules that enhance the infection while C57 BMDM produce molecules which inhibit the infection, however further investigation is needed for this phenomenon.

**Chapter 6:**

**General Discussion, Conclusion,  
Application and Future Work**

## 6.1 General Discussion

Cutaneous Leishmaniasis is caused by many species of the Trypanosomatidae including *L.mexicana* which is transmitted by injection of metacyclic promastigotes into the dermis of the skin, released into the bloodstream of the skin wound, phagocytosed by blood dendritic cells, monocytes, and macrophages where they finally differentiate into amastigotes (Rittig and Bogdan, 2000; Laskay *et al.*, 2008; Soulat and Bogdan, 2017). Amastigotes survive and multiply in phagocytic cells and are transported through the lymph and bloodstream to other tissues, depending on *Leishmania* species, and the host immune response. For survival of parasites in the infected mammalian hosts, *Leishmania* parasites should quickly adapt to the new host environment. *Leishmania* amastigotes should develop additional strategies to escape the host defence mechanisms of host immune response.

Phagocytic cells, such as neutrophils, dermal dendritic cells, and macrophages are the first immune cells to interact with the promastigotes inoculated into the skin by sand flies. These cells produce primary anti-leishmanial molecules; they also represent the cellular housing for *Leishmania* promastigotes to escape the complement system (Atayde *et al.*, 2016). The macrophages are the final host cell, harbouring the parasites where they survive and multiply. In this study a model system has been developed to study parasite virulence and its interaction with host (BMDM). Avirulent *L.mexicana* passage twenty (P20) was produced by sub culturing of *L.mexicana* passage one (P1) twenty times *in vitro*.

The phenotype of P20 can be interpreted as being due to a defect in differentiation to amastigotes, and attribution to downregulation of a considerable number of virulence-associated genes. The main findings of this study provide an explanation as to why P20 *L.mexicana* lack virulence.

After 20 continuous passages of *L.mexicana* promastigotes *in vitro* at 25°C, ten virulence associated genes (LPG1, LPG2, A2, CHAT1, CPB2, CPB2.8, CPC, GP63, LACK and MAPK9) were assessed by qPCR. Results showed that all tested genes were significantly downregulated in P20 compared with P1 promastigotes. P20 lost the LPG coat that protects parasite from the complement system *in vivo* and plays a role during infection and survival in the host cell. In addition, it plays a crucial role in modulation of the host immune response during interaction and establishment of macrophage infection (Desjardins and Descoteaux, 1997; Ferguson, 1999; Duque *et al.*, 2014). P20 also lost the ability to differentiate into amastigotes and thus to survive in the macrophages. Considering these findings, P20 may be killed before being phagocytosed by macrophages when used in *in vivo* experiments, whereas *in vitro* P1 and P20 can infect both susceptible Balb/c and resistant C57 BMDM. Ability to infect C57 BMDM could be due to absence of other factors that are found *in vivo* such as the role of complement, neutrophils, and dendritic cells.

Under the same conditions, P20 but not P1 failed to differentiate into amastigotes inside macrophages *in vitro*. Hence, P20 significantly lost its ability to differentiate into amastigotes under different tested conditions compared with P1. Understanding the growth characteristics and life cycle under each growth condition inside vector and mammalian host cells could be helpful in controlling this disease (Wheeler *et al.*, 2011) in addition, using the P1 and P20 model could be helpful in this regard.

The *Leishmania* parasites, during their life cycle, are exposed to two different growth conditions that significantly differ between the insect vector and mammalian host including temperature, pH and nutrients. In this study, changes in temperature was the main factor that triggered the differentiation from promastigotes into amastigotes. In addition, the decrease of pH after incubation of parasites at a concentration  $8 \times 10^6$  per mL was a contributing factor (See results 3.2.10), however changing the type of growth medium from Schneider's *Drosophila* to RPMI1640 medium and changing pH without shifting temperature did not affect the differentiation of P1 and P20. More precisely, P1 but not P20 promastigotes were able to differentiate into amastigotes when incubated under similar conditions. The main difference between virulent and avirulent parasites is the capacity of virulent parasites (P1) to differentiate into amastigotes, this finding is in line with the study of Moreira *et al.*, (2012) who reported that the avirulent parasite could not properly differentiate into amastigotes *in vitro*. Regarding the time of infection, light microscopic observations of infected macrophages with P1 for 2 hours post-infection revealed that 2 hours is not enough time to create a PV, this result is in agreement with a study by Real *et al.*, (2008) and it is not enough for parasites to differentiate into amastigotes as well, which agrees with Williams *et al.*, (2006). Roles of LPG in establishing successful Leishmaniasis are still controversial. *L.mexicana* parasites (P1) do not differ from other intracellular pathogen promastigotes, it prevents the maturation process of the phagosome and creates an environment for differentiation of promastigotes to amastigotes where the LPG surface plays a central role in this process. Comparing between P1 and P20 may provide new insights into our knowledge of the biology of the *Leishmania* parasites, as well as the biology of phagolysosome biogenesis.

### 6.1.1 Apoptosis

It is known that *Leishmania* parasites are obligate intracellular parasites that survive and multiply in macrophages. Virulent *Leishmania* parasite were shown to inhibit the apoptosis of macrophages (Akarid *et al.*, 2004). Results illustrate apoptosis was inhibited in Balb/c and C57 BMDM infected with P1 but not P20, P20 that failed to differentiate into amastigotes did not inhibit the apoptosis in infected macrophages. It has been reported that

the stage of *Leishmania* life cycle may have a role in modulation of host cell apoptosis and possibly parasite differentiation (Carmen and Sinai, 2007) which supports the finding of this study, where avirulent P20 failed to differentiate into amastigotes and to inhibit apoptosis in infected macrophages (figure. 4.14).

Inhibition of apoptosis is one of the most important defence mechanisms of the parasite to survive in the host cells. However, the full pathway of exerting an antiapoptotic effect by *Leishmania* parasite in host cells is still unclear (Solano-Gálvez, *et al.*, 2018; Abhishek 2018; Aguirre-Garcia *et al.*, 2018). The role of the anti-apoptotic effect of the parasite inside the infected macrophage needs further research. Therefore, in this study, the regulation of apoptosis-associated genes was investigated in Balb/c and C57 BMDM infected with P1 and P20 for 24 hours.

P1 but not P20 inhibits apoptosis in both Balb/c and C57 BMDM and that may be due to the differences between P1 and P20 virulence factors particularly LPG (Moore, and Matlashewski, 1994), and ability to differentiate into amastigotes. It is important at this stage to explain the regulation of the apoptotic genes in order to understand how P1 but not P20 inhibits apoptosis. P1 downregulates caspase 8 while P20 did not significantly affect caspase 8 regulation as well as it failed to survive in those two mouse strains indicating that this gene can be considered as a key gene in controlling the apoptosis process during infection with *L.mexicana*.

### **6.1.2 Role of Balb/c and C57 mouse genetic background in parasite survival**

P20 failed to differentiate to the metacyclic promastigote stage, as shown by calculations of metacyclic stage by using the promastigotes physical measurement of body length, width, and flagella using two different methods (figure 3.10), which is consistent with losing the ability to differentiate into amastigotes and consistent with the theory that LPG coat protects the parasites (Descoteaux and Turco, 2002; Naderer *et al.*, 2004). The argument can be put forward to explain why promastigotes of P20 fail to survive in BMDM of both Balb/c and C57, whereas amastigotes of P1 can survive in both Balb/c and C57 BMDM. It is known that mouse genetic background influences the pathological and immunological outcome of *Leishmania* infection. Although, Balb/c and C57 differ in their genetic background, virulent P1 can infect, survive and multiply in both these strains *in vitro* with minor differences. It has been reported that although C57 is resistant to *Leishmania* infection, it can be infected but with small self-healing lesions (Gollob *et al.*, 2014). It is also pointed out that both Balb/c and C57 have skin lesions with no difference in nitric oxide (NO) blood level during infection with *L.mexicana* (Diaz *et al.*, 2003), However, elimination of *Leishmania* parasites

in mammalian host depends on the both innate and adaptive immune response which is absent in the *in vitro* model.

### 6.1.3 Limitations of *in vitro* modelling

*In vivo*, there are a lot of factors and differences in immune cells which are part of complex biological system that interfere with parasites after infection. When promastigotes are injected into the skin, the first phagocytic cells that interact with promastigotes are polymorphonuclear, dendritic cells, and macrophages. To invade these cells *Leishmania* needs to escape from humoral immune components (e.g. complement) subsequently, infected cells produce anti-leishmanial molecules to kill the parasite (Bogdan and Rölinghoff, 1998; Atayde *et al.*, 2016). Polymorphonuclear cells that play a role in antigen presentation, and early recruitment of T cells (Appelberg, 2007) in addition, induce anti-microbial activity of macrophages (Appelberg, 2007; Ribeiro-Gomes *et al.*, 2007).

The role of Polymorphonuclear cells is to cooperate with macrophages to avoid the development of this disease. In a study by Novais *et al.*, (2009) which has addressed neutrophil and macrophage cooperation against *L. braziliensis* in infected susceptible Balb/c, reported that neutrophils play an important role in the elimination of the parasite through collaboration with macrophages through TNF- $\alpha$  and superoxide production.

Virulent *L. mexicana* promastigotes (equivalent to P1) are rapidly engulfed by neutrophils and macrophages *in vivo* after the sand fly bites. After a few hours of infection *L. mexicana* promastigotes are found in neutrophils but without differentiation into amastigotes like in macrophages (Peters and Sacks 2009). One of the neutrophil's roles in parasite infection is to bridge between innate and adaptive immune response (Appelberg, 2007; Nathan, 2006) which is absent in *in vitro* studies.

Another factor found in natural *L. mexicana* infection is that secretion of substances by the fly's midgut called proteophosphoglycans, which are inoculated along with parasite infection plays a role in stimulation of macrophages (Rogers *et al.*, 2009). In addition, the role of sand fly saliva plays a role in pro-inflammatory immune suppression (De Moura *et al.*, 2010). It was also shown that sand fly saliva inhibits the release of protective Th1 cytokines such as IL-12 and IFN- $\gamma$  and enhances the release of Th2 cytokines such as IL-4, IL-6, and IL-10, which enhance *Leishmania* parasite survival (Sacks, and Anderson 2004; Carregaro *et al.*, 2013). However, the absence of protective Th1 cytokines response in this study may be one of the most important factors that are common between Balb/ and C57 BMDM.

According to this study's results, P1 can infect and survive in BMDM from both mice strains *in vitro*, that could be due to missing roles of other cells such as neutrophils, which is

supported by previous study conducted by Van Zandbergen *et al.*, (2004) who reported that establishment of infection in macrophages is dependent on the parasites ability to infect and survive inside neutrophils, and the entry of *L. major* parasites into macrophage is achieved by engulfing of infected neutrophils as there is no direct contact between the parasite and macrophage receptors. The engulfing of apoptotic neutrophils by macrophage leads to silent infection.

Moreover, neutrophils release an elastase during inflammation in the exudate (Rainger *et al.*, 1998) which in turn induces killing of *L. major* in resistant mice macrophages *in vivo* by producing ROS in the macrophages (Ribeiro-Gomes *et al.*, 2004) which is missing in *in vitro* infection. The role of neutrophil elastase in interactions between Balb/c and C57 peritoneal macrophages and neutrophils infected with the *L. major* parasite was investigated by Ribeiro-Gomes *et al.*, (2007) who reported that neutrophil elastase plays a protective role in host macrophage responses to *L. major* infection, by activation of the macrophages and inducing microbicidal activity dependent on secretion of TNF- $\alpha$  in resistant C57 hosts. Also, activation of macrophages by inflammatory neutrophils induced the killing of *L. major* through recruitment of TLR-4 by neutrophil elastase. Hurrell *et al.*, (2015) who tested *L. mexicana*'s role in neutrophils in infected C57 and Balb/c *in vivo*, using C57 mice depleted of neutrophils reported that the presence of the neutrophils during the first day post *L. mexicana* infection prevents the parasite from inducing lesions. Therefore, regulation of neutrophils during infection could be a strategy to promote lesion healing.

According to this study findings, P20 failed to differentiate into amastigotes and to survive in macrophages, which agrees with previous studies (Thomas *et al.*, 2018). Notably, differentiation of parasites to amastigotes is regulated through autophagy which is important for adaptation of parasites to survive in mammalian cell conditions (Barak *et al.*, 2005; Reithinger, *et al.*, 2007). It is of note that the differentiation of parasites to amastigotes is influenced by the stage of parasites (stationary phase). It is also pointed out that the abundance of autophagosomes in *L. mexicana* was higher in the stationary phase which contains the highest percentage of metacyclic stages than early log phase. Thus, there is a relationship between increasing number of autophagosomes and starting differentiation of the parasite (Williams *et al.*, 2006). Current study data about P20 including; CPB downregulation, loss of metacyclic stage, loss of the ability to differentiate into amastigotes and to survive in the macrophages are all consistent with the absence of autophagy in P20. Notably, *Leishmania* survives in both murine and human macrophages (Kaye and Scott, 2011). Autophagy is one of the main differences between virulent and avirulent parasites, therefore, comparing between P1 and P20 ability to differentiate to amastigotes and autophagy could be helpful to understand wild *Leishmania* virulence.

#### 6.1.4 LPG and cytokines

Macrophages within infected tissue play an essential role in the initiation, resolution and development of inflammation (Yu *et al.*, 2012). The main roles of macrophages are to clean up pathogens and damaged cells by phagocytosis and activation of other immune cells, such as monocytes, macrophages, dendritic cells, neutrophils and T cells, in response to the pathogens. Activation or deactivation of macrophages during inflammatory processes depend on the type of signalling molecules produced. Stimulation signals include extracellular pathogen matrix proteins such as LPG and cytokines such as IL-1 and TNF- $\alpha$ . This interaction takes place through a variety of macrophage membrane receptors that are expressed on the surfaces of macrophages, including PRRs and TLRs (Batbayar, *et al.*, 2012; Ibraim *et al.*, 2013). Macrophage receptors recognise the activation signals and then subsequently activate downstream protein kinases, leading to the stimulation of transcription factors including AP-1 and NF- $\kappa$ B (Yang *et al.*, 2014). LPG protein, which is mainly found on P1 but not P20 (figure 3.19 and 3.20), is transferred from parasite membranes to macrophage cell membrane promoting lipid microdomain and disruption of PKC activation and ROS generation (de Morais *et al.*, 2015).

Inflammation can be initiated by intracellular proteins such as p38 proteins, which are a class of MAPKs, especially in the macrophage. p38 is a protein that will be phosphorylated rapidly in response to LPG stimulation (Ibraim *et al.*, 2013; Rojas-Bernabé, *et al.*, 2014). *L. mexicana* LPG binds TLR-2 and TLR-4 macrophage receptors, causing the production of TNF- $\alpha$ , IL-1 $\beta$ , and IL-10 proinflammatory cytokines and phosphorylation of ERK and p38 MAP kinase signalling cascades (Becker *et al.*, 2003; Rojas-Bernabé *et al.*, 2014; Aguirre-Garcia *et al.*, 2018). The upregulation of p38 expression was in response to inflammatory mediators such as cytokines, which are involved in cell differentiation, autophagy, and apoptosis (Clark and Dean, 2012; Huh *et al.*, 2013; Yang *et al.*, 2014; Segalés *et al.*, 2016).

However, results of this study demonstrated that P1 promastigotes were rich with LPG, it can induce inflammation and modulate apoptosis through p38 while P20, which lacks LPG, is unable to initiate inflammatory responses and modulate apoptosis and may explain why P20 failed to produce lesions in *in vivo* infection of Balb/c mice (Ali *et al.*, 2013).

Although C57 is resistant, P1 can infect and survive in C57 BMDM *in vitro*. However, the ability of P1 to modulate pro-inflammatory cytokine regulation in Balb/c was higher than C57, a similar trend was observed in apoptotic gene regulation. These results are also in line with previous results that in which demonstrate association of resistance to *Leishmania* parasites with Th1/Th2 modulation of gene regulation of infected macrophages by virulent parasites.

## 6.2 Conclusion

Continuous passaging of *L.mexicana* for twenty passages *in vitro* caused major morphological and functional changes. Cells became rounded and elongated, increased in body size, and their growth was inhibited in RPMI1640 medium. This was accompanied by a loss of metacyclic stage promastigotes, the ability to differentiate into amastigotes and virulence and the downregulation of all ten virulence-associated genes tested (LPG1, LPG2, A2, CHAT1, CPB2, CPB2.8, CPC, GP63, LACK, and MAPK9). Expression of lipophosphoglycan (LPG) and phosphatidylserine (PS) on the surfaces *L.mexicana* promastigotes was affected by 20 passages, the expression of LPG was significantly decreased, whereas the expression of PS significantly increased in P20. Therefore, this is a point to consider when preparing a vaccine from old culture parasites.

Virulent (P1) *L.mexicana* can infect and survive in both Balb/c and C57 bone marrow derived macrophages *in vitro*. Although avirulent (P20) *L.mexicana* was engulfed by both Balb/c and C57 bone marrow derived macrophages *in vitro*, it failed to differentiate into amastigotes and failed in the formation PV, subsequently it did not survive inside the macrophage. Therefore 20 passages did not affect the infectivity of *L.mexicana* but affects the survival of parasites which was noticed in both resistant and susceptible mice strains.

The strategy to survive in the macrophages may be a result of parasite virulence factors such as LPG, GP63. Virulent *L.mexicana* was able to modulate gene regulation in Balb/c more than that in C57 BMDM. P1 was able to modulate pro-inflammatory cytokine gene regulation in Balb/c, which was also confirmed by detection of TNF- $\alpha$  by ELISA. The generation and secretion of TNF- $\alpha$  cytokines (that activate Th1) was decreased by cytokines in Balb/c and increased in C57 after 24 hours infection. Virulent *L.mexicana* can inhibit apoptosis in both infected Balb/c and C57 Balb/c BMDM combined with downregulation of caspase 8 and upregulation of BCL 2 by qPCR.

P1 promastigote, treated with supernatants derived from Balb/c BMDM infected with P1 for 24 hours enhanced their growth and upregulated LPG1, CHT1, CPB2 and CPB2.8, while when treated with supernatant derived from C57 infected with P1 inhibited their growth and caused downregulation of LPG1, LPG2, CPB2, CPB2.8, CHT1 and A2.

## 6.3 Application

- These results are extremely relevant for *Leishmania* parasite vaccine development strategies since the majority of vaccine studies did not take in consideration changes in parasite properties *in vitro* cultures. Attenuation by long incubation (20 passages) may make the parasite lose the metacyclic stage which is the infective stage, this may activate the immune system against irrelevant antigens.
- Only P1 parasites formed PV and survived inside infected Balb/c and C57 macrophages, therefore targeting PV or their nutrient pathways by drugs could be key for killing the parasite e.g. targeting of rafts. Activation of apoptosis to prevent survival of the parasite could be another key factor for drug design by further investigation of caspase 8 and BCL 2.
- The results suggest that incubation of the parasite ( $8 \times 10^6$  /mL) at 37°C for 24 hours is the ideal growth condition for them to differentiate into amastigotes.

## 6.4 Future work

- DNA Sequencing of the whole P20 genome may give better knowledge about the effect of 20 passages on virulence associated genes regulation.
- Identification of the phospholipid classes including PS that are found on P1 and P20 *L.mexicana* surfaces by using thin-layer chromatography, mass spectrometry, nuclear magnetic resonance and spectroscopy.
- Sphingolipids play important roles in signal transmission and cell recognition (Chun *et al.*, 2010). However, the interplay between sphingolipids and autophagy in *Leishmania* is still unclear. Therefore, comparing between P1 and P20 could be helpful to study the metacyclogenesis, amastigote differentiation and autophagy
- Investigation of autophagy in P20 compared to P1 by quantifying autophagosomes in *L.mexicana* P20 at different stages by using electronic microscopy and ATG8 as a marker for autophagosomes could clarify the autophagy mechanism.
- Examination of virulence genes GP63, A2, CPB2, CPB2.8, CHAT1 and MAPK9, by other techniques such as western blotting or ELISA or Immunofluorescence to confirm PCR results.
- Confirmation of qPCR results of caspase 8 and BCL 2 by using western blotting and caspase activity assays.
- Estimation of IL-6 cytokines levels by ELISA to confirm the qPCR results.

- Estimation of ROS concentration in Balb/c and C57 BMDM infected with P1 and P20 for 2 and 24 hours.
- Using mass spectrometry for analysing the nature of supernatants obtained from BMDM infected with the virulent P1 and avirulent P20 parasite. For identifying specific proteomic or biomolecules.

#### **Improvement of this model**

- The findings of this study could be strengthened by using known specific gene knock-outs instead of P20, in addition to use of human derived macrophages.
- The findings of this study could be further confirmed by using more phagocytic cells such as neutrophils or neutrophils and macrophages in co-culture.
- The results of this study have demonstrated P20 but not P1 did not grow in RPMI1640 medium supplemented with 10 % HIFCS. Comparing between these two strains and studying the effect of ingredients of these two media (RPMI1640 and Schneider's *Drosophila*) would help to understand the differences between these parasites regarding food requirement and metabolism.

## References

Abhishek, K., Das, S., Kumar, A., Kumar, A., Kumar, V., Saini, S., Mandal, A., Verma, S., Kumar, M. and Das, P., 2018. Leishmania donovani induced Unfolded Protein Response delays host cell apoptosis in PERK dependent manner. *PLoS neglected tropical diseases*, 12(7), p.e0006646.

Acosta-Rodriguez, E.V., Napolitani, G., Lanzavecchia, A. and Sallusto, F., 2007. Interleukins 1 $\beta$  and 6 but not transforming growth factor- $\beta$  are essential for the differentiation of interleukin 17–producing human T helper cells. *Nature immunology*, 8(9), pp.942-949.

Adams, J.M., 2003. Ways of dying multiple pathways to apoptosis. *Genes & development*, 17(20), pp.2481-2495.

Agency for Toxic Substances and Disease Registry (ATSDR) (2011), [online] [21 September 2016] available from <http://www.atsdr.cdc.gov/substances/toxsubstance.asp?toxid=58>

Aguirre-Garcia, M.M., Escalona-Montaña, A.R., Wilkins-Rodríguez, A.A. and Gutiérrez-Kobeh, L., 2018. Immune Evasion Strategies. *Leishmaniasis as Re-emerging Diseases*, p.39.

Akarid, K., Arnoult, D., Micic-Polianski, J., Sif, J., Estaquier, J. and Ameisen, J.C., 2004. Leishmania major-mediated prevention of programmed cell death induction in infected macrophages is associated with the repression of mitochondrial release of cytochrome c. *Journal of leukocyte biology*, 76(1), pp.95-103.

Akhoundi, M., Kuhls, K., Cannet, A., Votýpka, J., Marty, P., Delaunay, P. & Sereno, D. 2016, "A Historical Overview of the Classification, Evolution, and Dispersion of Leishmania Parasites and Sandflies", *PLoS Negl Trop Dis*, vol. 10, no. 3, pp. e0004349.

Aktan, F. 2004. iNOS-mediated nitric oxide production and its regulation. *Life Sci*. 75:639.

Alcolea, P.J., Alonso, A., Gómez, M.J., Moreno, I., Domínguez, M., Parro, V. and Larraga, V., 2010 a. Transcriptomics throughout the life cycle of Leishmania infantum: high down-regulation rate in the amastigote stage. *International journal for parasitology*, 40(13), pp.1497-1516.

Alexander, J., Coombs, G.H. and Mottram, J.C., 1998. Leishmania mexicana cysteine proteinase-deficient mutants have attenuated virulence for mice and potentiate a Th1 response. *The Journal of Immunology*, 161(12), pp.6794-6801.

Alexander, J., Satoskar, A.R. and Russell, D.G., 1999. Leishmania species: models of intracellular parasitism. *J Cell Sci*, 112(18), pp.2993-3002.

Ali K. S., Rees R. C., Terrell-Nield C., ALI S. A., 2013. ‘Virulence loss and amastigote transformation failure determine host cell responses to Leishmania mexicana’ *Parasite Immunology*, 35, 441–456.

Allenbach, C., Zufferey, C., Perez, C., Launois, P., Mueller, C. and Tacchini-Cottier, F., 2006. Macrophages induce neutrophil apoptosis through membrane TNF, a process amplified by Leishmania major. *The Journal of Immunology*, 176(11), pp.6656-6664.

Allmann, S., Morand, P., Ebikeme, C., Gales, L., Biran, M., Hubert, J., Brennan, A., Mazet, M., Franconi, J.M., Michels, P.A. and Portais, J.C., 2013. Cytosolic NADPH homeostasis in glucose-starved procyclic *Trypanosoma brucei* relies on malic enzyme and the pentose phosphate pathway fed by gluconeogenic flux. *Journal of Biological Chemistry*, pp.jbc-M113.

Almeida-Souza, F., de Souza, C.D.S.F., Taniwaki, N.N., Silva, J.J.M., de Oliveira, R.M., Abreu-Silva, A.L. and da Silva Calabrese, K., 2016. *Morinda citrifolia* Linn. fruit (Noni) juice induces an increase in NO production and death of *Leishmania amazonensis* amastigotes in peritoneal macrophages from BALB/c. *Nitric Oxide*, 58, pp.51-58.

Alves, L.C., Melo, R.L., Sanderson, S.J., Mottram, J.C., Coombs, G.H., Caliendo, G., Santagada, V., Juliano, L. and Juliano, M.A., 2001. S1 subsite specificity of a recombinant cysteine proteinase, CPB, of *Leishmania mexicana* compared with cruzain, human cathepsin L and papain using substrates containing non-natural basic amino acids. *European journal of biochemistry*, 268(5), pp.1206-1212.

American Academy of Family Physicians (2016) [online] [21 September 2016] available from ( <http://www.aafp.org/afp/2004/0315/p1455.html>).

Ameyar, M., Wisniewska, M. and Weitzman, J.B., 2003. A role for AP-1 in apoptosis: the case for and against. *Biochimie*, 85(8), pp.747-752.

Ansari, N.A., Ramesh, V. and Salotra, P., 2006. Interferon (IFN)- $\gamma$ , Tumor Necrosis Factor- $\alpha$ , Interleukin-6, and IFN- $\gamma$  Receptor 1 Are the Major Immunological Determinants Associated with Post-Kala Azar Dermal Leishmaniasis. *The Journal of infectious diseases*, 194(7), pp.958-965.

Antonelli, L.R.D.V., Dutra, W.O., Almeida, R.P.D., Bacellar, O. and Gollob, K.J., 2004. Antigen specific correlations of cellular immune responses in human leishmaniasis suggests mechanisms for immunoregulation. *Clinical & Experimental Immunology*, 136(2), pp.341-348.

Appelberg, R. 2007. Neutrophils and intracellular pathogens: beyond phagocytosis and killing. *Trends Microbiol.* 15: 87-92.

Appelt, U., Sheriff, A., Gaipf, U.S., Kalden, J.R., Voll, R.E. and Herrmann, M., 2005. Viable, apoptotic and necrotic monocytes expose phosphatidylserine: cooperative binding of the ligand Annexin V to dying but not viable cells and implications for PS-dependent clearance. *Cell death and differentiation*, 12(2), p.194.

Atayde, V., Hassani, K., da Silva Lira Filho, A., Borges, A., Adhikari, A., Martel, C. and Olivier, M., 2016. *Leishmania* exosomes and other virulence factors: Impact on innate immune response and macrophage functions. *Cellular Immunology*, 309, pp.7-18.

Bacellar, O., Lessa, H., Schriefer, A., Machado, P., de Jesus, A.R., Dutra, W.O., Gollob, K.J. and Carvalho, E.M., 2002. Up-regulation of Th1-type responses in mucosal Leishmaniasis patients. *Infection and immunity*, 70(12), pp.6734-6740.

Bahr, V., Stierhof, Y.D., Ilg, T., Demar, M., Quinten, M. and Overath, P., 1993. Expression of lipophosphoglycan, high-molecular weight phosphoglycan and glycoprotein 63 in promastigotes and amastigotes of *Leishmania mexicana*. *Molecular and biochemical parasitology*, 58(1), pp.107-121.

Barak, E., Amin-Spector, S., Gerliak, E., Goyard, S., Holland, N. and Zilberstein, D., 2005. Differentiation of *Leishmania donovani* in host-free system: analysis of signal perception and response. *Molecular and biochemical parasitology*, 141(1), pp.99-108.

Baroja-Mazo, A., Martín-Sánchez, F., Gomez, A.I., Martínez, C.M., Amores-Iñesta, J., Compan, V., Barberà-Cremades, M., Yagüe, J., Ruiz-Ortiz, E., Antón, J. and Buján, S., 2014. The NLRP3 inflammasome is released as a particulate danger signal that amplifies the inflammatory response. *Nature immunology*, 15(8), p.738.

Barral, A., Barral-Netto, M., Yong, E.C., Brownell, C.E., Twardzik, D.R. and Reed, S.G., 1993. Transforming growth factor beta as a virulence mechanism for *Leishmania braziliensis*. *Proceedings of the National Academy of Sciences*, 90(8), pp.3442-3446.

Barral, A., Teixeira, M., Reis, P., Vinhas, V., Costa, J., Lessa, H., Bittencourt, A.L., Reed, S., Carvalho, E.M. and Barral-Netto, M., 1995. Transforming growth factor-beta in human cutaneous leishmaniasis. *The American journal of pathology*, 147(4), p.947.

Barral-Netto, M., da Silva, J.S., Barral, A. and Reed, S., 1995. Up-regulation of T helper 2 and down-regulation of T helper 1 cytokines during murine retrovirus-induced immunodeficiency syndrome enhances susceptibility of a resistant mouse strain to *Leishmania amazonensis*. *The American journal of pathology*, 146(3), p.635.

Barry, M. and Bleackley, R.C., 2002. Cytotoxic T lymphocytes: all roads lead to death. *Nature Reviews Immunology*, 2(6), p.401.

Batbayar, S., Lee, D.H. and Kim, H.W., 2012. Immunomodulation of fungal  $\beta$ -glucan in host defense signaling by dectin-1. *Biomolecules & therapeutics*, 20(5), p.433.

Bates, P.A., 1994. Complete developmental cycle of *Leishmania mexicana* in axenic culture. *Parasitology*, 108(1), pp.1-9.

Bates, P.A., 2007. Transmission of *Leishmania* metacyclic promastigotes by phlebotomine sand flies. *International journal for parasitology*, 37(10), pp.1097-1106.

Bates, P.A., Robertson, C.D., Tetley, L. and Coombs, G.H., 1992. Axenic cultivation and characterization of *Leishmania mexicana* amastigote-like forms. *Parasitology*, 105(2), pp.193-202.

Beck, J.A., Lloyd, S., Hafezparast, M., Lennon-Pierce, M., Eppig, J.T., Festing, M.F. and Fisher, E.M., 2000. Genealogies of mouse inbred strains. *Nature genetics*, 24(1), p.23.

Becker, I., Salaiza, N., Aguirre, M., Delgado, J., Carrillo-Carrasco, N., Kobeh, L.G., Ruiz, A., Cervantes, R., Torres, A.P., Cabrera, N. and González, A., 2003. *Leishmania* lipophosphoglycan (LPG) activates NK cells through toll-like receptor-2. *Molecular and biochemical parasitology*, 130(2), pp.65-74.

Bee, A., Culley, F.J., Alkhalife, I.S., Bodman-Smith, K.B., Raynes, J.G. and Bates, P.A., 2001. Transformation of *Leishmania mexicana* metacyclic promastigotes to amastigote-like forms mediated by binding of human C-reactive protein. *Parasitology*, 122(5), pp.521-529.

Belkaid, Y. and Tarbell, K., 2009. Regulatory T cells in the control of host-microorganism interactions. *Annual review of immunology*, 27, pp.551-589.

Beneke, T., Madden, R., Makin, L., Valli, J., Sunter, J. and Gluenz, E., 2017. A CRISPR Cas9 high-throughput genome editing toolkit for kinetoplastids. *Royal Society open science*, 4(5), p.170095.

Bengs, F., Scholz, A., Kuhn, D. and Wiese, M., 2005. LmxMPK9, a mitogen-activated protein kinase homologue affects flagellar length in *Leishmania mexicana*. *Molecular microbiology*, 55(5), pp.1606-1615.

Ben-Sasson, S.Z., Hu-Li, J., Quiel, J., Cauchetaux, S., Ratner, M., Shapira, I., Dinarello, C.A. and Paul, W.E., 2009. IL-1 acts directly on CD4 T cells to enhance their antigen-driven expansion and differentiation. *Proceedings of the National Academy of Sciences*, 106(17), pp.7119-7124.

Bente, M., Harder, S., Wiesgigl, M., Heukeshoven, J., Gelhaus, C., Krause, E., Clos, J. and Bruchhaus, I., 2003. Developmentally induced changes of the proteome in the protozoan parasite *Leishmania donovani*. *Proteomics*, 3(9), pp.1811-1829.

Berghe, T.V., Vanlangenakker, N., Parthoens, E., Deckers, W., Devos, M., Festjens, N., Guerin, C.J., Brunk, U.T., Declercq, W. and Vandenabeele, P., 2010. Necroptosis, necrosis and secondary necrosis converge on similar cellular disintegration features. *Cell death and differentiation*, 17(6), p.922.

Besteiro, S., Williams, R.A., Coombs, G.H. and Mottram, J.C., 2007. Protein turnover and differentiation in *Leishmania*. *International journal for parasitology*, 37(10), pp.1063-1075.

Besteiro, S., Williams, R.A., Coombs, G.H. and Mottram, J.C., 2007. Protein turnover and differentiation in *Leishmania*. *International journal for parasitology*, 37(10), pp.1063-1075.

Beutler, B.A., 1999. The role of tumor necrosis factor in health and disease. *The journal of rheumatology*. Supplement, 57, pp.16-21.

Biegel, D., Topper, G. and Rabinovitch, M., 1983. *Leishmania mexicana*: temperature sensitivity of isolated amastigotes and of amastigotes infecting macrophages in culture. *Experimental parasitology*, 56(3), pp.289-297.

Birge, R.B., Boeltz, S., Kumar, S., Carlson, J., Wanderley, J., Calianese, D., Barcinski, M., Brekken, R.A., Huang, X., Hutchins, J.T. and Freimark, B., 2016. Phosphatidylserine is a global immunosuppressive signal in efferocytosis, infectious disease, and cancer. *Cell death and differentiation*, 23(6), p.962.

Birkholtz, L.M., Williams, M., Niemand, J., Louw, A.I., Persson, L. and Heby, O., 2011. Polyamine homeostasis as a drug target in pathogenic protozoa: peculiarities and possibilities. *Biochemical Journal*, 438(2), pp.229-244.

Blackwell, J.M., 1985. Role of macrophage complement and lectin-like receptors in binding *Leishmania* parasites to host macrophages. *Immunology letters*, 11(3-4), pp.227-232.

Bogdan, C. and Röllinghoff, M., 1998. The immune response to *Leishmania*: mechanisms of parasite control and evasion. *International Journal for Parasitology*, 28(1), pp.121-134.

Bokoch, G.M. and Diebold, B.A., 2002. Current molecular models for NADPH oxidase regulation by Rac GTPase. *Blood*, 100(8), pp.2692-2695.

Bourreau, E., Pascalis, H., Prévot, G., Kariminia, A., Jolly, N., Milon, G., Buffet, P., Michel, R., Meynard, J.B., Boutin, J.P. and Aschimoff, D., 2003. Increased Production of Interferon- $\gamma$  by Leishmania Homologue of the Mammalian Receptor for Activated C Kinase-Reactive CD4+ T cells among Human Blood Mononuclear Cells: An Early Marker of Exposure to Leishmania?. *Scandinavian journal of immunology*, 58(2), pp.201-210.

Bourreau, E., Prévot, G., Gardon, J., Pradinaud, R., Hasagewa, H., Milon, G. and Launois, P., 2002. LACK-specific CD4+ T cells that induce gamma interferon production in patients with localized cutaneous leishmaniasis during an early stage of infection. *Infection and immunity*, 70(6), pp.3122-3129.

Brandão-Filho SP, Campbell-Lendrum D, Brito ME, Shaw JJ, Davies CR. 1999. Epidemiological surveys confirm an increasing burden of cutaneous leishmaniasis in north-east Brazil. *Trans R Soc Trop Med Hyg*, 93 : 488–94.

Brentnall, M., Rodriguez-Menocal, L., De Guevara, R.L., Cepero, E. and Boise, L.H., 2013. Caspase-9, caspase-3 and caspase-7 have distinct roles during intrinsic apoptosis. *BMC cell biology*, 14(1), p.32.

Brittingham, A., Morrison, C. J., McMaster, W. R., McGwire, B. S., Chang, K. P., & Mosser, D. M., 1995. Role of the Leishmania surface protease gp63 in complement fixation, cell adhesion, and resistance to complement-mediated lysis. *The Journal of Immunology*, 155(6), 3102-3111.

Brown, G.E., Stewart, M.Q., Liu, H., Ha, V.L. and Yaffe, M.B., 2003. A novel assay system implicates PtdIns (3, 4) P<sub>2</sub>, PtdIns (3) P, and PKC $\delta$  in intracellular production of reactive oxygen species by the NADPH oxidase. *Molecular cell*, 11(1), pp.35-47.

Bryson, K., Besteiro, S., McGachy, H.A., Coombs, G.H., Mottram, J.C. and Alexander, J., 2009. Overexpression of the natural inhibitor of cysteine peptidases in Leishmania mexicana leads to reduced virulence and a Th1 response. *Infection and immunity*, 77(7), pp.2971-2978

Cafasso J. 2019. Healthline [online] available from <https://www.healthline.com/health/leishmaniasis> [Accessed 16 February 2019].

Calegari-Silva, T.C., Pereira, R.M., De-Melo, L.D.B., Saraiva, E.M., Soares, D.C., Bellio, M. and Lopes, U.G., 2009. NF- $\kappa$ B-mediated repression of iNOS expression in Leishmania amazonensis macrophage infection. *Immunology letters*, 127(1), pp.19-26.

Cameron, P., McGachy, A., Anderson, M., Paul, A., Coombs, G.H., Mottram, J.C., Alexander, J. and Plevin, R., 2004. Inhibition of lipopolysaccharide-induced macrophage IL-12 production by Leishmania mexicana amastigotes: the role of cysteine peptidases and the NF- $\kappa$ B signaling pathway. *The Journal of Immunology*, 173(5), pp.3297-3304.

Canton, J., Ndjamen, B., Hatsuzawa, K. and Kima, P.E., 2012. Disruption of the fusion of Leishmania parasitophorous vacuoles with ER vesicles results in the control of the infection. *Cellular microbiology*, 14(6), pp.937-948.

Carmen, J.C. and Sinai, A.P., 2007. Suicide prevention: disruption of apoptotic pathways by protozoan parasites. *Molecular microbiology*, 64(4), pp.904-916.

Carneiro, M.B., Roma, E.H., Ranson, A.J., Doria, N.A., Debrabant, A., Sacks, D.L., Vieira, L.Q. and Peters, N.C., 2018. NOX2-derived reactive oxygen species control inflammation during *Leishmania amazonensis* infection by mediating infection-induced neutrophil apoptosis. *The Journal of Immunology*, 200(1), pp.196-208.

Carrada, G., Caneda, C., Salaiza, N., Delgado, J., Ruiz, A., Sanchez, B., Guti rrez-kobeh, L., Aguirre, M. and Becker, I., 2007. Monocyte cytokine and costimulatory molecule expression in patients infected with *Leishmania mexicana*. *Parasite immunology*, 29(3), pp.117-126.

Carregaro, V., Costa, D.L., Brodskyn, C., Barral, A.M., Barral-Netto, M., Cunha, F.Q. and Silva, J.S., 2013. Dual effect of *Lutzomyia longipalpis* saliva on *Leishmania braziliensis* infection is mediated by distinct saliva-induced cellular recruitment into BALB/c mice ear. *BMC microbiology*, 13(1), p.102.

Casgrain, P.A., Martel, C., McMaster, W.R., Mottram, J.C., Olivier, M. and Descoteaux, A., 2016. Cysteine peptidase B regulates *Leishmania mexicana* virulence through the modulation of GP63 expression. *PLoS pathogens*, 12(5), p.e1005658.

Castellucci, L., Menezes, E., Oliveira, J., Magalh es, A., Guimar es, L.H., Lessa, M., Ribeiro, S., Reale, J., Noronha, E.F., Wilson, M.E. and Duggal, P., (2006) IL6- 174 G/C promoter polymorphism influences susceptibility to mucosal but not localized cutaneous Leishmaniasis in Brazil. *Journal of Infectious Diseases*, 194(4), pp.519-527.

Centers for Disease Control and Prevention CDC , 2018. Leishmaniasis, Epidemiology and risk factors [Online] [16 February 2019] available from <http://www.cdc.gov/parasites/leishmaniasis/epi.html>.

Chandra, D., Choy, G., Deng, X., Bhatia, B., Daniel, P. and Tang, D.G., 2004. Association of active caspase 8 with the mitochondrial membrane during apoptosis: potential roles in cleaving BAP31 and caspase 3 and mediating mitochondrion-endoplasmic reticulum cross talk in etoposide-induced cell death. *Molecular and cellular biology*, 24(15), pp.6592-6607.

Chang, K.P., Reed, S.G., McGwire, B.S. and Soong, L., 2003. *Leishmania* model for microbial virulence: the relevance of parasite multiplication and pathoantigenicity. *Acta Tropica*, 85(3), pp.375-390.

Channon, J.Y., Roberts, M.B. and Blackwell, J.M., 1984. A study of the differential respiratory burst activity elicited by promastigotes and amastigotes of *Leishmania donovani* in murine resident peritoneal macrophages. *Immunology*, 53(2), p.345.

Chaplin, D.D., 2010. Overview of the immune response. *Journal of Allergy and Clinical Immunology*, 125(2), pp.S3-S23.

Charmoy, M., Hurrell, B.P., Romano, A., Lee, S.H., Ribeiro-Gomes, F., Riteau, N., Mayer-Barber, K., Tacchini-Cottier, F. and Sacks, D.L., 2016. The Nlrp3 inflammasome, IL-1 $\beta$ , and neutrophil recruitment are required for susceptibility to a nonhealing strain of *Leishmania major* in C57BL/6 mice. *European journal of immunology*, 46(4), pp.897-911.

Chatelain R., S. Mauze, R.L. Coffman, 1999. Experimental *Leishmania major* infection in mice: role of IL-10. *Parasite Immunology*, 21 pp. 211-218.

Chun, J. and Hartung, H.P., 2010. Mechanism of action of oral fingolimod (FTY720) in multiple sclerosis. *Clinical neuropharmacology*, 33(2), p.91.

Cienciulli, A., Porro, C., Calvello, R., Trotta, T. and Panaro, M.A., 2018. Resistance to apoptosis in *Leishmania infantum*-infected human macrophages: a critical role for anti-apoptotic Bcl-2 protein and cellular IAP1/2. *Clinical and experimental medicine*, 18(2), pp.251-261.

Clark, A.R. and Dean, J.L., 2012. Suppl 2: The p38 MAPK Pathway in Rheumatoid Arthritis: A Sideways Look. *The open rheumatology journal*, 6, p.209.

Cleary, M.L., Smith, S.D. and Sklar, J., 1986. Cloning and structural analysis of cDNAs for bcl-2 and a hybrid bcl-2/immunoglobulin transcript resulting from the t (14; 18) translocation. *Cell*, 47(1), pp.19-28.

Cobo F. 2014. Leishmaniasis. Imported Infectious Diseases (pp.227-240) Woodhead Publishing 1st edition.

Contreras, I., Gómez, M.A., Nguyen, O., Shio, M.T., McMaster, R.W. and Olivier, M., 2010. Leishmania-induced inactivation of the macrophage transcription factor AP-1 is mediated by the parasite metalloprotease GP63. *PLoS pathogens*, 6(10), p.e1001148.

Coombs, G.H., Tetley, L., Moss, V.A. and Vickerman, K., 1986. Three dimensional structure of the *Leishmania* amastigote as revealed by computer-aided reconstruction from serial sections. *Parasitology*, 92(1), pp.13-23.

Corrales, R.M., Sereno, D. and Mathieu-Daudé, F., 2010. Deciphering the *Leishmania* exoproteome: what we know and what we can learn. *FEMS Immunology & Medical Microbiology*, 58(1), pp.27-38.

Courret, N., Fréhel, C., Gouhier, N., Pouchelet, M., Prina, E., Roux, P. and Antoine, J.C., 2002. Biogenesis of *Leishmania*-harbouring parasitophorous vacuoles following phagocytosis of the metacyclic promastigote or amastigote stages of the parasites. *J Cell Sci*, 115(11), pp.2303-2316.

Cuervo, P., De Jesus, J.B., Saboia-Vahia, L., Mendonça-Lima, L., Domont, G.B. and Cupolillo, E., 2009. Proteomic characterization of the released/secreted proteins of *Leishmania* (*Viannia*) *braziliensis* promastigotes. *Journal of proteomics*, 73(1), pp.79-92.

Cull, B., Prado Godinho, J.L., Fernandes Rodrigues, J.C., Frank, B., Schurigt, U., Williams, R.A., Coombs, G.H. and Mottram, J.C., 2014. Glycosome turnover in *Leishmania* major is mediated by autophagy. *Autophagy*, 10(12), pp.2143-2157.

Da Silva, I.A., Morato, C.I., Quixabeira, V.B.L., Pereira, L.I.D.A., Dorta, M.L., de Oliveira, M.A.P., Horta, M.F. and Ribeiro-Dias, F., 2015. In vitro metacyclogenesis of *Leishmania* (*Viannia*) *braziliensis* and *Leishmania* (*Leishmania*) *amazonensis* clinical field isolates, as evaluated by morphology, complement resistance, and infectivity to human macrophages. *BioMed research international*.

Dagger, F., Bengio, C., Martinez, A. and Ayesta, C., 2018. *Leishmania mexicana* differentiation involves a selective plasma membrane autophagic-like process. *Cell Stress and Chaperones*, 23(4), pp.783-789.

DaMata, J.P., Mendes, B.P., Maciel-Lima, K., Menezes, C.A.S., Dutra, W.O., Sousa, L.P. and Horta, M.F., 2015. Distinct macrophage fates after in vitro infection with different species of *Leishmania*: induction of apoptosis by *Leishmania (Leishmania) amazonensis*, but not by *Leishmania (Viannia) guyanensis*. *PLoS one*, 10(10), p.e0141196.

Daneshvar, H., Coombs, G.H., Hagan, P. and Phillips, R.S., 2003. *Leishmania mexicana* and *Leishmania major*: attenuation of wild-type parasites and vaccination with the attenuated lines. *The Journal of infectious diseases*, 187(10), pp.1662-1668.

Danial, N.N. and Korsmeyer, S.J., 2004. Cell death: critical control points. *Cell*, 116(2), pp.205-219.

Das, L., Datta, N., Bandyopadhyay, S. and Das, P.K., 2001. Successful therapy of lethal murine visceral leishmaniasis with cystatin involves up-regulation of nitric oxide and a favorable T cell response. *The Journal of Immunology*, 166(6), pp.4020-4028.

De Celis, H.Á., Gomez, C.P., Descoteaux, A. and Duplay, P., 2015. Dok proteins are recruited to the phagosome and degraded in a GP63-dependent manner during *Leishmania major* infection. *Microbes and infection*, 17(4), pp.285-294.

De Luca, L., Ferro, S., Buemi, M.R., Monforte, A.M., Gitto, R., Schirmeister, T., Maes, L., Rescifina, A. and Micale, N., 2018. Discovery of benzimidazole-based *Leishmania mexicana* cysteine protease CPB 2.8  $\Delta$  CTE inhibitors as potential therapeutics for leishmaniasis. *Chemical biology & drug design*, 92(3), pp.1585-1596.

De Moraes, C.G.V., Castro Lima, A.K., Terra, R., dos Santos, R.F., Da-Silva, S.A.G. and Dutra, P.M.L., 2015. The dialogue of the host-parasite relationship: *Leishmania* spp. and *Trypanosoma cruzi* infection. *BioMed research international*, 2015, pp.1-19.

De Moura, T.R., Oliveira, F., Rodrigues, G.C., Carneiro, M.W., Fukutani, K.F., Novais, F.O., Miranda, J.C., Barral-Netto, M., Brodskyn, C., Barral, A. and de Oliveira, C.I., 2010. Immunity to *Lutzomyia intermedia* saliva modulates the inflammatory environment induced by *Leishmania braziliensis*. *PLoS neglected tropical diseases*, 4(6), p.e712.

De Moura, T.R., Santos, M.L.B., Braz, J.M., Santos, L.F.V., Aragão, M.T., de Oliveira, F.A., Santos, P.L., da Silva, Â.M., de Jesus, A.R. and de Almeida, R.P., 2016. Cross-resistance of *Leishmania infantum* isolates to nitric oxide from patients refractory to antimony treatment, and greater tolerance to antileishmanial responses by macrophages. *Parasitology research*, 115(2), pp.713-721

Delgado-Domínguez, J., González-Aguilar, H., Aguirre-García, M., Gutiérrez-Kobeh, L., Berzunza-Cruz, M., Ruiz-Remigio, A., Robles-Flores, M. and Becker, I., 2010. *Leishmania mexicana* lipophosphoglycan differentially regulates PKC $\alpha$ -induced oxidative burst in macrophages of BALB/c and C57BL/6 mice. *Parasite immunology*, 32(6), pp.440-449.

Deng, Y., Ren, X., Yang, L., Lin, Y. and Wu, X., 2003. A JNK-dependent pathway is required for TNF $\alpha$ -induced apoptosis. *Cell*, 115(1), pp.61-70.

Deretic, V., Saitoh, T. and Akira, S., 2013. Autophagy in infection, inflammation and immunity. *Nature Reviews Immunology*, 13(10), p.722.

Descoteaux, A. and Turco, S.J., 2002. Functional aspects of the *Leishmania donovani* lipophosphoglycan during macrophage infection. *Microbes and Infection*, 4(9), pp.975-981.

Descoteaux, A., Matlashewski, G. and Turco, S.J., 1992. Inhibition of macrophage protein kinase C-mediated protein phosphorylation by *Leishmania donovani* lipophosphoglycan. *The Journal of Immunology*, 149(9), pp.3008-3015.

Desjardins, M., and Descoteaux, A., 1997. Inhibition of phagolysosomal biogenesis by the *Leishmania* lipophosphoglycan. *J. Exp. Med.* 185, 2061–2068.

Desjardins, M., Huber, L.A., Parton, R.G. and Griffiths, G., 1994. Biogenesis of phagolysosomes proceeds through a sequential series of interactions with the endocytic apparatus. *The Journal of cell biology*, 124(5), pp.677-688.

Diehl, S. and Rincón, M., 2002 The two faces of IL-6 on Th1/Th2 differentiation. *Molecular immunology*, 39(9), pp.531-536.

Donovan, M.J., Maciuba, B.Z., Mahan, C.E. and McDowell, M.A., 2009. *Leishmania* infection inhibits cycloheximide-induced macrophage apoptosis in a strain-dependent manner. *Experimental parasitology*, 123(1), pp.58-64.

Dos Santos, P.L., de Oliveira, F.A., Santos, M.L.B., Cunha, L.C.S., Lino, M.T., de Oliveira, M.F., Bomfim, M.O., Silva, A.M., de Moura, T.R., de Jesus, A.R. and Duthie, M.S., 2016. The severity of visceral leishmaniasis correlates with elevated levels of serum IL-6, IL-27 and sCD14. *PLoS neglected tropical diseases*, 10(1), p.e0004375.

Dragovich, T., Rudin, C.M. and Thompson, C.B., 1998. Signal transduction pathways that regulate cell survival and cell death. *Oncogene*, 17(25), p.3207.

Duque, G.A. and Descoteaux, A., 2015. *Leishmania* survival in the macrophage: where the ends justify the means. *Current opinion in microbiology*, 26, pp.32-40.

Duque, G.A., Fukuda, M., Turco, S.J., Stäger, S. and Descoteaux, A., 2014. *Leishmania* promastigotes induce cytokine secretion in macrophages through the degradation of synaptotagmin XI. *The Journal of Immunology*, 193(5), pp.2363-2372.

Edinger, A.L. and Thompson, C.B., 2004. Death by design: apoptosis, necrosis and autophagy. *Current opinion in cell biology*, 16(6), pp.663-669.

EFSA AHAW Panel (EFSA Panel on Animal Health and Welfare), 2015. Scientific Opinion on canine leishmaniosis. *EFSA Journal* 2015;13(4):4075, 77 pp.

Elloso, M.M. and Scott, P., 1999. Expression and contribution of B7-1 (CD80) and B7-2 (CD86) in the early immune response to *Leishmania* major infection. *The Journal of Immunology*, 162(11), pp.6708-6715.

Escalona-Montaña, A.R., Ortiz-Lozano, D.M., Rojas-Bernabé, A., Wilkins-Rodriguez, A.A., Torres-Guerrero, H., Mondragón-Flores, R., Mondragón-Gonzalez, R., Becker, I., Gutiérrez-Kobeh, L. and Aguirre-Garcia, M.M., 2016. *Leishmania mexicana*: promastigotes and amastigotes secrete protein phosphatases and this correlates with the production of inflammatory cytokines in macrophages. *Parasitology*, 143(11), pp.1409-1420.

European Food Safety Authority, 2015 [online] [21 September 2016] available from <http://www.efsa.europa.eu/en/efsajournal/pub/4075>.

Evan, G. and Littlewood, T., 1998. A matter of life and cell death. *Science*, 281(5381), pp.1317-1322.

Fadeel, B. and Orrenius, S., 2005. Apoptosis: a basic biological phenomenon with wide-ranging implications in human disease. *Journal of internal medicine*, 258(6), pp.479-517.

Fantuzzi, G. and Dinarello, C.A., 1999. Interleukin-18 and interleukin-1 $\beta$ : two cytokine substrates for ICE (caspase-1). *Journal of clinical immunology*, 19(1), pp.1-11.

Favila, M.A., Geraci, N.S., Jayakumar, A., Hickerson, S., Mostrom, J., Turco, S.J., Beverley, S.M. and McDowell, M.A., 2015. Differential impact of LPG-and PG-deficient *Leishmania* major mutants on the immune response of human dendritic cells. *PLoS Negl Trop Dis*, 9(12), p.e0004238.

Ferguson, M. A., 1999. The structure, biosynthesis and functions of glycosylphosphatidylinositol anchors, and the contributions of trypanosome research. *J. Cell Sci.* 112(Pt 17), 2799–2809.

Fernández-Figueroa, E.A., Rangel-Escareño, C., Espinosa-Mateos, V., Carrillo-Sánchez, K., Salaiza-Suazo, N., Carrada-Figueroa, G., March-Mifsut, S. and Becker, I., 2012. Disease severity in patients infected with *Leishmania mexicana* relates to IL-1 $\beta$ . *PLoS Negl Trop Dis*, 6(5), p.e1533.

Fiebig, M., Kelly, S. and Gluenz, E., 2015. Comparative life cycle transcriptomics revises *Leishmania mexicana* genome annotation and links a chromosome duplication with parasitism of vertebrates. *PLoS pathogens*, 11(10), p.e1005186.

Fink, S.L. and Cookson, B.T., 2005. Apoptosis, pyroptosis, and necrosis: mechanistic description of dead and dying eukaryotic cells. *Infection and immunity*, 73(4), pp.1907-1916.

Fink, S.L. and Cookson, B.T., 2006. Caspase-1-dependent pore formation during pyroptosis leads to osmotic lysis of infected host macrophages. *Cellular microbiology*, 8(11), pp.1812-1825.

Finlay, B.B. and Falkow, S., 1997. Common themes in microbial pathogenicity revisited. *Microbiol. Mol. Biol. Rev.*, 61(2), pp.136-169.

Firestein, G.S., Budd, R., Gabriel, S.E., McInnes, I.B. and O'Dell, J.R., 2016. *Kelley and Firestein's Textbook of Rheumatology E-Book*. Elsevier Health Sciences.

Forde, J.A. and Dale, T.C., 2007. Glycogen synthase kinase 3: a key regulator of cellular fate. *Cellular and molecular life sciences*, 64(15), pp.1930-1944.

Forestier, C.L., Gao, Q. and Boons, G.J., 2015. *Leishmania* lipophosphoglycan: how to establish structure-activity relationships for this highly complex and multifunctional glycoconjugate?. *Frontiers in cellular and infection microbiology*, 4, p.193.

Frame, M.J., Mottram, J.C. and Coombs, G.H., 2000. Analysis of the roles of cysteine proteinases of *Leishmania mexicana* in the host-parasite interaction. *Parasitology*, 121(4), pp.367-377.

França-Costa, J., Wanderley, J.L.M., Deolindo, P., Zarattini, J.B., Costa, J., Soong, L., Barcinski, M.A., Barral, A. and Borges, V.M., 2012. Exposure of phosphatidylserine on *Leishmania amazonensis* isolates is associated with diffuse cutaneous *Leishmaniasis* and parasite infectivity. *PloS one*, 7(5), p.e36595.

Franco, L.H., Beverley, S.M. and Zamboni, D.S., 2012. Innate immune activation and subversion of mammalian functions by *Leishmania* lipophosphoglycan. *Journal of parasitology research*, 2012.

Frenzel, A., Grespi, F., Chmelewskij, W. and Villunger, A., 2009. Bcl2 family proteins in carcinogenesis and the treatment of cancer. *Apoptosis*, 14(4), pp.584-596.

Garcia, I., Miyazaki, Y., Araki, K., Araki, M., Lucas, R., Grau, G.E., Milon, G., Belkaid, Y., Montixi, C., Lesslauer, W. and Vassalli, P., 1995. Transgenic mice expressing high levels of soluble tnf-r1 fusion protein are protected from lethal septic shock and cerebral malaria, and are highly sensitive to *Listeria monocytogenes* and *Leishmania major* infections. *European journal of immunology*, 25(8), pp.2401-2407.

Garg, G., Singh, K. and Ali Dr, V., 2018. Proteomic approaches unravel the intricacy of secreted proteins of *Leishmania*: An updated review. *Biochimica et Biophysica Acta (BBA)-Proteins and Proteomics*.

Gaur, U., Showalter, M., Hickerson, S., Dalvi, R., Turco, S.J., Wilson, M.E. and Beverley, S.M., 2009. *Leishmania donovani* lacking the Golgi GDP-Man transporter LPG2 exhibit attenuated virulence in mammalian hosts. *Experimental parasitology*, 122(3), pp.182-191.

Ghedini, E., Zhang, W.W., Charest, H., Sundar, S., Kenney, R.T. and Matlashewski, G., 1997. Antibody response against a *Leishmania donovani* amastigote-stage-specific protein in patients with visceral leishmaniasis. *Clinical and diagnostic laboratory immunology*, 4(5), pp.530-535.

Gillespie, S. and Pearson, R.D. eds., 2003. *Principles and practice of clinical parasitology*. John Wiley & Sons.

Gilmore, T.D., 2006. Introduction to NF- $\kappa$ B: players, pathways, perspectives. *Oncogene*, 25(51), p.6680.

Gollob, K.J., Viana, A.G. and Dutra, W.O., 2014. Immunoregulation in human American *Leishmaniasis*: balancing pathology and protection. *Parasite immunology*, 36(8), pp.367-376.

Gomes, C.B., Souza-Silva, F., dos Santos Charret, K., Pereira, B.A.S., Finkelstein, L.C., Santos-de-Souza, R., de Castro Côrtes, L.M., Pereira, M.C.S., de Oliveira Jr, F.O.R. and Alves, C.R., 2017. Increasing in cysteine proteinase B expression and enzymatic activity during in vitro differentiation of *Leishmania* (*Viannia*) *braziliensis*: First evidence of modulation during morphological transition. *Biochimie*, 133, pp.28-36.

Gomes, C.M., Avila, L.R., Pinto, S.A., Duarte, F.B., Pereira, L.I.A., Abrahamsohn, I.A., Dorta, M.L., Vieira, L.Q., Ribeiro-Dias, F. and Oliveira, M.A.P., 2014. *Leishmania braziliensis* amastigotes stimulate production of IL-1 $\beta$ , IL-6, IL-10 and TGF- $\beta$  by peripheral blood mononuclear cells from nonendemic area healthy residents. *Parasite immunology*, 36(5), pp.225-231.

Gorczynski, R.M., 1985. Immunization of susceptible BALB/c mice against *Leishmania braziliensis*: II. Use of temperature-sensitive avirulent clones of parasite for vaccination purposes. *Cellular immunology*, 94(1), pp.11-20.

Grimm, F., Brun, R. and Jenni, L., 1991. Promastigote infectivity in *Leishmania infantum*. *Parasitology research*, 77(3), pp.185-191.

Gueirard, P., Laplante, A., Rondeau, C., Milon, G. and Desjardins, M., 2008. Trafficking of *Leishmania donovani* promastigotes in non-lytic compartments in neutrophils enables the subsequent transfer of parasites to macrophages. *Cellular microbiology*, 10(1), pp.100-111.

Gupta, P., Srivastav, S., Saha, S., Das, P.K. and Ukil, A., 2016. *Leishmania donovani* inhibits macrophage apoptosis and pro-inflammatory response through AKT-mediated regulation of  $\beta$ -catenin and FOXO-1. *Cell death and differentiation*, 23(11), p.1815.

Gurunathan, S., Sacks, D.L., Brown, D.R., Reiner, S.L., Charest, H., Glaichenhaus, N. and Seder, R.A., 1997. Vaccination with DNA encoding the immunodominant LACK parasite antigen confers protective immunity to mice infected with *Leishmania major*. *Journal of Experimental Medicine*, 186(7), pp.1137-1147.

Gutiérrez-Kobeh, L., De Oyarzabal, E., Argueta, J., Wilkins, A., Salaiza, N., Fernández, E., López, O., Aguirre, M. and Becker, I., 2013. Inhibition of dendritic cell apoptosis by *Leishmania mexicana* amastigotes. *Parasitology research*, 112(4), pp.1755-1762.

Hallé, M., Gomez, M.A., Stuiblé, M., Shimizu, H., McMaster, W.R., Olivier, M. and Tremblay, M.L., 2009. The *Leishmania* surface protease GP63 cleaves multiple intracellular proteins and actively participates in p38 mitogen-activated protein kinase inactivation. *Journal of Biological Chemistry*, 284(11), pp.6893-6908.

Hancock, J.T., R. Desikan, S.J. Neill, 2001. Role of Reactive Oxygen Species in Cell Signaling Pathways. *Biochemical and Biomedical Aspects of Oxidative Modification*, 29(2):345-350.

Handler, M.Z., Patel, P.A., Kapila, R., Al-Qubati, Y. and Schwartz, R.A., 2015. Cutaneous and mucocutaneous leishmaniasis: differential diagnosis, diagnosis, histopathology, and management. *Journal of the American Academy of Dermatology*, 73(6), pp.911-926.

Handman, E., 2001. Leishmaniasis: current status of vaccine development. *Clinical microbiology reviews*, 14(2), pp.229-243.

Hassani, K., Antoniak, E., Jardim, A. and Olivier, M., 2011. Temperature-induced protein secretion by *Leishmania mexicana* modulates macrophage signalling and function. *PloS one*, 6(5), p.e18724.

Hatzigeorgiou, D.E., He, S.U.H.U.I., Sobel, J., Grabstein, K.H., Hafner, A. and Ho, J.L., 1993. IL-6 down-modulates the cytokine-enhanced antileishmanial activity in human macrophages. *The Journal of Immunology*, 151(7), pp.3682-3692.

Hernandez, A.G., Arguello, C., Ayesta, C., Dagger, F., Infante, R.B., Stojanovich, D., Dawidowicz, K., Riggione, F. and La Riva, G., 1981. The surface membrane of *Leishmania*. In *The biochemistry of parasites* (pp. 47-65).

Hess, J., Angel, P. and Schorpp-Kistner, M., 2004. AP-1 subunits: quarrel and harmony among siblings. *Journal of cell science*, 117(25), pp.5965-5973.

Holdhoff, M., Kreuzer, K.A., Appelt, C., Scholz, R., Na, I.K., Hildebrandt, B., Riess, H., Jordan, A., Schmidt, C.A., Van Etten, R.A. and Dörken, B., 2005. Imatinib mesylate radiosensitizes human glioblastoma cells through inhibition of platelet-derived growth factor receptor. *Blood Cells, Molecules, and Diseases*, 34(2), pp.181-185.

Huang, D.C., Hahne, M., Schroeter, M., Frei, K., Fontana, A., Villunger, A., Newton, K., Tschopp, J. and Strasser, A., 1999. Activation of Fas by FasL induces apoptosis by a mechanism that cannot be blocked by Bcl-2 or Bcl-xL. *Proceedings of the National Academy of Sciences*, 96(26), pp.14871-14876.

Huh, J.E., Jung, I.T., Choi, J., Baek, Y.H., Lee, J.D., Park, D.S. and Choi, D.Y., 2013. The natural flavonoid galangin inhibits osteoclastic bone destruction and osteoclastogenesis by suppressing NF- $\kappa$ B in collagen-induced arthritis and bone marrow-derived macrophages. *European journal of pharmacology*, 698(1-3), pp.57-66.

Hurrell, B.P., Schuster, S., Grün, E., Coutaz, M., Williams, R.A., Held, W., Malissen, B., Malissen, M., Yousefi, S., Simon, H.U. and Müller, A.J., 2015. Rapid sequestration of *Leishmania mexicana* by neutrophils contributes to the development of chronic lesion. *PLoS pathogens*, 11(5), p.e1004929.

Ibraim, I.C., de Assis, R.R., Pessoa, N.L., Campos, M.A., Melo, M.N., Turco, S.J. and Soares, R.P., 2013. Two biochemically distinct lipophosphoglycans from *Leishmania braziliensis* and *Leishmania infantum* trigger different innate immune responses in murine macrophages. *Parasites & vectors*, 6(1), p.54.

Ilg, T., 2000. Lipophosphoglycan is not required for infection of macrophages or mice by *Leishmania mexicana*. *The EMBO journal*, 19(9), pp.1953-1962.

Informatics.jax.org., 2019. MGI - Inbred Strains: BALB. [online] [8 Mar. 2019] available from ([http://www.informatics.jax.org/inbred\\_strains/mouse/docs/BALB.shtml](http://www.informatics.jax.org/inbred_strains/mouse/docs/BALB.shtml)).

Irmeler, M., Thome, M., Hahne, M., Schneider, P., Hofmann, K., Steiner, V., Bodmer, J.L., Schröter, M., Burns, K., Mattmann, C. and Rimoldi, D., 1997. Inhibition of death receptor signals by cellular FLIP. *Nature*, 388(6638), p.190.

Isnard, A., Shio, M.T. and Olivier, M., 2012. Impact of *Leishmania* metalloprotease GP63 on macrophage signaling. *Frontiers in cellular and infection microbiology*, 2, p.72.

Iwaoka, S., Nakamura, T., Takano, S., Tsuchiya, S. and Aramaki, Y., 2006. Cationic liposomes induce apoptosis through p38 MAP kinase-caspase-8-Bid pathway in macrophage-like RAW264. 7 cells. *Journal of leukocyte biology*, 79(1), pp.184-191.

Jacobson, M.D., Weil, M. and Raff, M.C., 1997. Programmed cell death in animal development. *Cell*, 88(3), pp.347-354.

Jaffe CL, Grimaldi G, McMahon-Pratt D.,1984. The cultivation and cloning of *Leishmania*. In: Morel CM (ed) Genes and antigen of parasites. A laboratory manual, 2nd edn. Fundac,ao Oswaldo Cruz, Rio de Janeiro, pp 47–91.

Janeway, C. A., Travers, P., Walport, M. & Shlomchik, M. J. 2001 *Immunobiology: The Immune System in Health and Disease*, New York: Garland Science.

Jeddi, F., Piarroux, R. and Mary, C., 2011. Antimony resistance in *Leishmania*, focusing on experimental research. *Journal of tropical medicine*.

Jorgensen, I. and Miao, E.A., 2015. Pyroptotic cell death defends against intracellular pathogens. *Immunological reviews*, 265(1), pp.130-142.

Joshi, M.B., Rogers, M.E., Shakarian, A.M., Yamage, M., Al-Harthi, S.A., Bates, P.A. and Dwyer, D.M., 2005. Molecular Characterization, Expression, and in Vivo Analysis of LmexCht1 the chitinase of the human pathogen, *leishmania mexicana*. *Journal of Biological Chemistry*, 280(5), pp.3847-3861.

Kane, M.M. and Mosser, D.M., 2001. The role of IL-10 in promoting disease progression in leishmaniasis. *The Journal of Immunology*, 166(2), pp.1141-1147.

Karin, M., 1990. Too many transcription factors: positive and negative interactions. *The New Biologist*, 2(2), pp.126-131.

Karin, M., Liu, Z.G. and Zandi, E., 1997. AP-1 function and regulation. *Current opinion in cell biology*, 9(2), pp.240-246.

Kaye, P., and Scott, P., 2011. Leishmaniasis: complexity at the host-pathogen interface. *Nat. Rev. Microbiol.* 9, 604–615.

Kedzierski, L., Zhu, Y. and Handman, E., 2006. *Leishmania* vaccines: progress and problems. *Parasitology*, 133(S2), pp.S87-S112.

Kerr, J.F., Wyllie, A.H. and Currie, A.R., 1972. Apoptosis: a basic biological phenomenon with wideranging implications in tissue kinetics. *British journal of cancer*, 26(4), p.239.

Khamesipour, A., Rafati, S., Davoudi, N., Maboudi, F. and Modabber, F., 2006. *Leishmaniasis* vaccine candidates for development: a global overview. *Indian Journal of Medical Research*, 123(3), p.423.

Killick-Kendrick R. 1999. The biology and control of phlebotomine sandfl ies. *Clin Dermatol*; 17: 279–89.

Kim, J.J., Lee, S.B., Park, J.K. and Yoo, Y.D., 2010. TNF- $\alpha$ -induced ROS production triggering apoptosis is directly linked to Romo1 and Bcl-X L. *Cell death and differentiation*, 17(9), p.1420.

Kima, P.E., 2007. The amastigote forms of *Leishmania* are experts at exploiting host cell processes to establish infection and persist. *International journal for parasitology*, 37(10), pp.1087-1096.

Kima, P.E., Constant, S.L., Hannum, L., Colmenares, M., Lee, K.S., Haberman, A.M., Shlomchik, M.J. and McMahon-Pratt, D., 2000. Internalization of *Leishmania*

mexicana complex amastigotes via the Fc receptor is required to sustain infection in murine cutaneous leishmaniasis. *The Journal of experimental medicine*, 191(6), pp.1063-1068.

Kono, H. and Rock, K., 2008. How dying cells alert the immune system to danger. *Nature Reviews Immunology*, 8(4), pp.279-289.

Korade, Z. and Kenworthy, A.K., 2008. Lipid rafts, cholesterol, and the brain. *Neuropharmacology*, 55(8), pp.1265-1273.

Kostka, S.L., Knop, J., Konur, A., Udey, M.C. and von Stebut, E., 2006. Distinct roles for IL-1 receptor type I signaling in early versus established *Leishmania major* infections. *Journal of investigative dermatology*, 126(7), pp.1582-1589.

Krauth-Siegel, R.L. and Comini, M.A., 2008. Redox control in trypanosomatids, parasitic protozoa with trypanothione-based thiol metabolism. *Biochimica et Biophysica Acta (BBA)-General Subjects*, 1780(11), pp.1236-1248.

Kruidering, M. and Evan, G.I., 2000. Caspase-8 in apoptosis: the beginning of "the end"? *IUBMB life*, 50(2), pp.85-90.

Kuchroo, V.K., Das, M.P., Brown, J.A., Ranger, A.M., Zamvil, S.S., Sobel, R.A., Weiner, H.L., Nabavi, N. and Glimcher, L.H., 1995. B7-1 and B7-2 costimulatory molecules activate differentially the Th1/Th2 developmental pathways: application to autoimmune disease therapy. *Cell*, 80(5), pp.707-718.

Kuida, K., 2000. Caspase-9. *The international journal of biochemistry & cell biology*, 32(2), pp.121-124.

Kuwana, T. and Newmeyer, D.D., 2003. BCL2-family proteins and the role of mitochondria in apoptosis. *Current opinion in cell biology*, 15(6), pp.691-699.

Kweider, M., Lemesre, J.L., Darcy, F., Kusnierz, J.P., Capron, A. and Santoro, F., 1987. Infectivity of *Leishmania braziliensis* promastigotes is dependent on the increasing expression of a 65,000-dalton surface antigen. *The Journal of Immunology*, 138(1), pp.299-305.

Kweider, M., Lemesre, J.L., Darcy, F., Kusnierz, J.P., Capron, A. and Santoro, F., 1987. Infectivity of *Leishmania braziliensis* promastigotes is dependent on the increasing expression of a 65,000-dalton surface antigen. *The Journal of Immunology*, 138(1), pp.299-305.

Lachaud, L., Bourgeois, N., Plourd, M., Leproho, P., Bastien, P. and Ouellette, M., 2009. Parasite susceptibility to amphotericin B in failures of treatment for visceral leishmaniasis in patients coinfecting with HIV type 1 and *Leishmania infantum*. *Clinical Infectious Diseases*, 48(2), pp.e16-e22.

Lambertz, U., Silverman, J.M., Nandan, D., McMaster, W.R., Clos, J., Foster, L.J. and Reiner, N.E., 2012. Secreted virulence factors and immune evasion in visceral leishmaniasis. *Journal of leukocyte biology*, 91(6), pp.887-899.

Laskay, T., van Zandbergen, G. and Solbach, W., 2008. Neutrophil granulocytes as host cells and transport vehicles for intracellular pathogens: apoptosis as infection-promoting factor. *Immunobiology*, 213(3-4), pp.183-191.

Lázaro-Souza, M., Matte, C., Lima, J.B., Arango Duque, G., Quintela-Carvalho, G., de Carvalho Vivarini, Á., Moura-Pontes, S., Figueira, C.P., Jesus-Santos, F.H., Gazos Lopes, U. and Farias, L.P., 2018. Leishmania infantum Lipophosphoglycan-Deficient Mutants: A Tool to Study Host Cell-Parasite Interplay. *Frontiers in microbiology*, 9, p.626.

Le Feuvre, R.A., Brough, D., Iwakura, Y., Takeda, K. and Rothwell, N.J., 2002. Priming of macrophages with lipopolysaccharide potentiates P2X7-mediated cell death via a caspase-1-dependent mechanism, independently of cytokine production. *Journal of Biological Chemistry*, 277(5), pp.3210-3218.

Lemay, S., Davidson, D., Latour, S. and Veillette, A., 2000. Dok-3, a novel adapter molecule involved in the negative regulation of immunoreceptor signaling. *Molecular and cellular biology*, 20(8), pp.2743-2754.

Liburkin-Dan, T., Schlisselberg, D., Fischer-Weinberger, R., Pescher, P., Inbar, E., Ephros, M., Rentsch, D., Späth, G.F. and Zilberstein, D., 2018. Stage-specific expression of the proline-alanine transporter in the human pathogen Leishmania. *Molecular and biochemical parasitology*, 222, pp.1-5.

Liévin-Le Moal, V. and Loiseau, P.M., 2016. Leishmania hijacking of the macrophage intracellular compartments. *The FEBS journal*, 283(4), pp.598-607.

Liew, F.Y., Millott, S., Parkinson, C., Palmer, R.M. and Moncada, S., 1990 A. Macrophage killing of Leishmania parasite in vivo is mediated by nitric oxide from L-arginine. *The Journal of Immunology*, 144(12), pp.4794-4797.

Liew, F.Y., Parkinson, C., Millott, S., Severn, A. and Carrier, M., 1990 B. Tumour necrosis factor (TNF alpha) in leishmaniasis. I. TNF alpha mediates host protection against cutaneous leishmaniasis. *Immunology*, 69(4), p.570.

Lima-Junior, D.S., Costa, D.L., Carregaro, V., Cunha, L.D., Silva, A.L., Mineo, T.W., Gutierrez, F.R., Bellio, M., Bortoluci, K.R., Flavell, R.A. and Bozza, M.T., 2013. Inflammasome-derived IL-1 $\beta$  production induces nitric oxide-mediated resistance to Leishmania. *Nature medicine*, 19(7), p.909.

Liou, W., Geuze, H.J., Geelen, M.J., and Slot, J.W. (1997) The autophagic and endocytic pathways converge at the nascent autophagic vacuoles. *J Cell Biol* 136: 61–70.

Lisi, S., Sisto, M., Acquafredda, A., Spinelli, R., Schiavone, M.A., Mitolo, V., Brandonisio, O. and Panaro, M.A., 2005. Infection with Leishmania infantum Inhibits actinomycin D-induced apoptosis of human monocytic cell line U-937. *Journal of Eukaryotic Microbiology*, 52(3), pp.211-217.

Liu, D. and UZONNA, J.E., 2012. The early interaction of Leishmania with macrophages and dendritic cells and its influence on the host immune response. *Frontiers in cellular and infection microbiology*, 2, p.83.

Locksley, R. M., and J. A. Louis. 1992. Immunology of leishmaniasis. *Curr. Opin. Immunol.* 4: 413–418.

Lodge, R., Diallo, T.O. and Descoteaux, A., 2006. Leishmania donovani lipophosphoglycan blocks NADPH oxidase assembly at the phagosome membrane. *Cellular microbiology*, 8(12), pp.1922-1931.

Lopez-Castejon, G. and Brough, D., 2011. Understanding the mechanism of IL-1 $\beta$  secretion. *Cytokine & growth factor reviews*, 22(4), pp.189-195.

Luo, X., Budihardjo, I., Zou, H., Slaughter, C. and Wang, X., 1998. Bid, a Bcl2 interacting protein, mediates cytochrome c release from mitochondria in response to activation of cell surface death receptors. *Cell*, 94(4), pp.481-490.

Luscher, A., De Koning, H.P. and Maser, P., 2007. Chemotherapeutic strategies against *Trypanosoma brucei*: drug targets vs. drug targeting. *Current pharmaceutical design*, 13(6), pp.555-567.

Ma, D., Russell, D.G., Beverley, S.M. and Turco, S.J., 1997. Golgi GDP-mannose Uptake Requires Leishmania LPG2 a member of a eukaryotic family of putative nucleotide-sugar transporters. *Journal of Biological Chemistry*, 272(6), pp.3799-3805.

Machado de Oliveira, S.A., 2016. Complement receptor 1 mediated control of Leishmania infection in inflammatory human macrophages (Doctoral dissertation, Mainz, Univ., Diss., 2016).

Man, S.M., Karki, R. and Kanneganti, T.D., 2017. Molecular mechanisms and functions of pyroptosis, inflammatory caspases and inflammasomes in infectious diseases. *Immunological reviews*, 277(1), pp.61-75.

Manna, P.P., Hira, S.K., Basu, A. and Bandyopadhyay, S., 2014. Cellular therapy by allogeneic macrophages against visceral leishmaniasis: role of TNF- $\alpha$ . *Cellular immunology*, 290(1), pp.152-163.

Manning, B.D. and Cantley, L.C., 2007. AKT/PKB signaling: navigating downstream. *Cell*, 129(7), pp.1261-1274.

Markle, W.H. and Makhoul, K., 2004. Cutaneous leishmaniasis: recognition and treatment. *American family physician*, 69(6), pp.1455-1464.

Marletta, M.A., 1993. Nitric oxide synthase structure and mechanism. *American Society for Biochemistry and Molecular Biology*. 268: 12231-4.

Marth, T. and Kelsall, B.L., 1997. Regulation of interleukin-12 by complement receptor 3 signaling. *The Journal of experimental medicine*, 185(11), pp.1987-1995.

Martinez, F.O. and Gordon, S., 2014. The M1 and M2 paradigm of macrophage activation: time for reassessment. *F1000prime reports*, 2014; 6: 13.

Maspi, N., Abdoli, A. and Ghaffarifar, F., 2016. Pro-and anti-inflammatory cytokines in cutaneous leishmaniasis: a review. *Pathogens and global health*, 110(6), pp.247-260.

McConville, M.J. and Ferguson, M.A., 1993. The structure, biosynthesis and function of glycosylated phosphatidylinositols in the parasitic protozoa and higher eukaryotes. *Biochemical Journal*, 294(Pt 2), p.305.

McConville, M.J. and Homans, S.W., 1992. Identification of the defect in lipophosphoglycan biosynthesis in a non-pathogenic strain of *Leishmania major*. *Journal of Biological Chemistry*, 267(9), pp.5855-5861.

McConville, M.J. and Menon, A.K., 2000. Recent developments in the cell biology and biochemistry of glycosylphosphatidylinositol lipids. *Molecular membrane biology*, 17(1), pp.1-16.

McIlwain, D.R., Berger, T. and Mak, T.W., 2013. Caspase functions in cell death and disease. *Cold Spring Harbor perspectives in biology*, 5(4), p.a008656.

McLuskey, K. and Mottram, J.C., 2015. Comparative structural analysis of the caspase family with other clan CD cysteine peptidases. *Biochemical Journal*, 466(2), pp.219-232.

McMahon-Pratt, D., Ueda-Nakamura, T. and Traub-Csekö, Y.M., 2010. Megasomes in Leishmania. In *Structures and Organelles in Pathogenic Protists* (pp. 131-148). Springer, Berlin, Heidelberg.

Meier, P., Finch, A. and Evan, G., 2000. Apoptosis in development. *Nature*, 407(6805), p.796.

Melby, P.C., Andrade-Narvaez, F.J., Darnell, B.J., Valencia-Pacheco, G., Tryon, V.V. and Palomo-Cetina, A., 1994. Increased expression of proinflammatory cytokines in chronic lesions of human cutaneous leishmaniasis. *Infection and immunity*, 62(3), pp.837-842.

Mikus, J. and Steverding, D. 2000. A simple colorimetric method to screen drug cytotoxicity against *Leishmania* using the dye Alamar Blue®. *Parasitology International*, 48(3), pp.265-269.

Mills, C., 2012. M1 and M2 macrophages: oracles of health and disease. *Critical Reviews™ in Immunology*, 32(6).

Mishra, J. and Singh, S., 2013. Miltefosine resistance in *Leishmania donovani* involves suppression of oxidative stress-induced programmed cell death. *Experimental parasitology*, 135(2), pp.397-406.

Mitchell, G.F., Handman, E. and Spithill, T.W., 1984. Vaccination against cutaneous leishmaniasis in mice using nonpathogenic cloned promastigotes of *Leishmania major* and importance of route of injection. *Immunology and Cell Biology*, 62(2), p.145.

Modabber, F., 2010. Leishmaniasis vaccines: past, present and future. *International journal of antimicrobial agents*, 36, pp.S58-S61.

Moore, K.J. and Matlashewski, G., 1994. Intracellular infection by *Leishmania donovani* inhibits macrophage apoptosis. *The Journal of Immunology*, 152(6), pp.2930-2937.

Moreira, D., Santarém, N., Loureiro, I., Tavares, J., Silva, A.M., Amorim, A.M., Ouassiss, A., Cordeiro-da-Silva, A. and Silvestre, R., 2012. Impact of continuous axenic cultivation in *Leishmania infantum* virulence. *PLoS neglected tropical diseases*, 6(1), p.e1469.

Morizot, G., Jouffroy, R., Faye, A., Chabert, P., Belhouari, K., Calin, R., Charlier, C., Miaillhes, P., Siriez, J.Y., Mouri, O. and Yera, H., 2016. Antimony to cure visceral leishmaniasis unresponsive to liposomal amphotericin B. *PLoS neglected tropical diseases*, 10(1), p.e0004304.

Mosser, D. M. and Rosenthal, L. A. 1994. Divergent strategies used by the promastigote and amastigote forms of *Leishmania* to invade mammalian cells. In *Strategies for Intracellular Survival of Macrophages. Baillière's Clinical Infectious Diseases*, vol. 1 (ed. D. G. Russell), pp. 191-212. W. B. Saunders.

Mosser, D. M., T. A. Springer, and M. S. Diamond. 1992. *Leishmania* promastigotes require opsonic complement to bind to the human leukocyte integrin Mac-I (CD11b/CD18). *J. Cell Biol.* 116:511.

Mosser, D.M. and Edelson, P.J., 1984. Activation of the alternative complement pathway by *Leishmania* promastigotes: parasite lysis and attachment to macrophages. *The Journal of Immunology*, 132(3), pp.1501-1505.

Mottram, J.C., Coombs, G.H. and Alexander, J., 2004. Cysteine peptidases as virulence factors of *Leishmania*. *Current opinion in microbiology*, 7(4), pp.375-381.

Mottram, J.C., Frame, M.J., Brooks, D.R., Tetley, L., Hutchison, J.E., Souza, A.E. and Coombs, G.H., 1997. The Multiple cpb Cysteine Proteinase Genes of *Leishmania mexicana* Encode Isoenzymes That Differ in Their Stage Regulation and Substrate Preferences. *Journal of Biological Chemistry*, 272(22), pp.14285-14293.

Mottram, J.C., Souza, A.E., Hutchison, J.E., Carter, R., Frame, M.J. and Coombs, G.H., 1996. Evidence from disruption of the *lmcpb* gene array of *Leishmania mexicana* that cysteine proteinases are virulence factors. *Proceedings of the National Academy of Sciences*, 93(12), pp.6008-6013.

MuÈller, K., Zandbergen, G., Hansen, B., Laufs, H., Jahnke, N., Solbach, W. and Laskay, T., 2001. Chemokines, natural killer cells and granulocytes in the early course of *Leishmania major* infection in mice. *Medical microbiology and immunology*, 190(1-2), pp.73-76.

Mukhopadhyay, N.K., Saha, A.K., Lovelace, J.K., Da Silva, R.O.S.A.N.G.E.L.A., Sacks, D.L. and Glew, R.H., 1988. Comparison of the Protein Kinase and Acid Phosphatase Activities of Five Species of *Leishmania* 1. *The Journal of protozoology*, 35(4), pp.601-607.

Mul, F.P., Zuurbier, A.E., Janssen, H., Calafat, J., van Wetering, S., Hiemstra, P.S., Roos, D. and Hordijk, P.L., 2000. Sequential migration of neutrophils across monolayers of endothelial and epithelial cells. *Journal of leukocyte biology*, 68(4), pp.529-537.

Naderer, T. and McConville, M.J. 2008 The *Leishmania*–macrophage interaction: a metabolic perspective. *Cell. Microbiol.* 10, 301–308.

Naderer, T. and McConville, M.J., 2011. Intracellular growth and pathogenesis of *Leishmania* parasites. *Essays in biochemistry*, 51, pp.81-95.

Naderer, T., Vince, J.E. and McConville, M.J., 2004. Surface determinants of *Leishmania* parasites and their role in infectivity in the mammalian host. *Current molecular medicine*, 4(6), pp.649-665.

Nagill, R. and Kaur, S., 2011. Vaccine candidates for leishmaniasis: a review. *International immunopharmacology*, 11(10), pp.1464-1488.

Nathan, C. 2006. Neutrophils and immunity: challenges and opportunities. *Nat.Rev. Immunol.* 6: 173–182.

Nathan, C.F. and Hibbs, J.B., 1991. Role of nitric oxide synthesis in macrophage antimicrobial activity. *Current opinion in immunology*, 3(1), pp.65-70.

NCBI RefSeq, 2016. [online] available from <https://www.ncbi.nlm.nih.gov/gene/7040> [Accessed 10 January 2017].

NCBI RefSeq, 2008. [online] available from <http://www.ncbi.nlm.nih.gov/gene/3553> [Accessed 20 December 2015].

NCBI RefSeq, 2017. [online] available from <http://www.ncbi.nlm.nih.gov/gene/7124> [Accessed 10 January 2017].

Newell, C.L., Deisseroth, A.B. and Lopez-Berestein, G., 1994. Interaction of nuclear proteins with an AP-1/CRE-like promoter sequence in the human TNF- $\alpha$  gene. *Journal of Leukocyte Biology*, 56(1), pp.27-35.

Novais, F.O., Santiago, R.C., Báfica, A., Khouri, R., Afonso, L., Borges, V.M., Brodskyn, C., Barral-Netto, M., Barral, A. and de Oliveira, C.I., 2009. Neutrophils and macrophages cooperate in host resistance against *Leishmania braziliensis* infection. *The journal of immunology*, 183(12), pp.8088-8098.

Novusbio.com., 2018. p38 Signaling Interactive Pathway: Novus Biologicals. [online] [24 Dec. 2018] available from (<https://www.novusbio.com/p38mapkpathway.html>).

O'brien, J., Wilson, I., Orton, T. and Pognan, F., 2000. Investigation of the Alamar Blue (resazurin) fluorescent dye for the assessment of mammalian cell cytotoxicity. *The FEBS Journal*, 267(17), pp.5421-5426.

O'Daly, J.A. and Rodriguez, M.B., 1988. Differential growth requirements of several *Leishmania* spp. in chemically defined culture media. *Acta tropica*, 45(2), pp.109-126.

Okuda, K., Tong, M., Dempsey, B., Moore, K.J., Gazzinelli, R.T. and Silverman, N., 2016. *Leishmania amazonensis* engages CD36 to drive parasitophorous vacuole maturation. *PLoS pathogens*, 12(6), p.e1005669.

Olivier, M., Atayde, V. D., Isnard, A., Hassani, K. and Shio, M. T. 2012. *Leishmania* virulence factors: focus on the metalloprotease GP63. *Microbes Infect.* 14:1377.

Olivier, M., Gregory, D.J. and Forget, G., 2005. Subversion mechanisms by which *Leishmania* parasites can escape the host immune response: a signaling point of view. *Clinical microbiology reviews*, 18(2), pp.293-305.

Oltval, Z.N., Milliman, C.L. and Korsmeyer, S.J., 1993. Bcl-2 heterodimerizes in vivo with a conserved homolog, Bax, that accelerates programmed cell death. *Cell*, 74(4), pp.609-619.

Overholtzer, M., Mailloux, A.A., Mouneimne, G., Normand, G., Schnitt, S.J., King, R.W., Cibas, E.S. and Brugge, J.S., 2007. A nonapoptotic cell death process, entosis, that occurs by cell-in-cell invasion. *Cell*, 131(5), pp.966-979.

Paape, D., Barrios-Llerena, M.E., Le Bihan, T., Mackay, L. and Aebischer, T., 2010. Gel free analysis of the proteome of intracellular *Leishmania mexicana*. *Molecular and biochemical parasitology*, 169(2), pp.108-114.

Palatnik-de-Sousa, C.B., 2008. Vaccines for leishmaniasis in the fore coming 25 years. *Vaccine*, 26(14), pp.1709-1724.

Panday, A., Sahoo, M. K., Osorio, D. and Batra, S. 2015. NADPH oxidases: an overview from structure to innate immunity-associated pathologies. *Cell. Mol. Immunol.* 12:5.

Pandey, B.D., Pandey, K., Kaneko, O., Yanagi, T., Hirayama, K., 2009. Relapse of visceral leishmaniasis after miltefosine treatment in a Nepalese patient. *Am. J. Trop. Med. Hyg.* 80, 580–582.

Pandey, R.K., Mehrotra, S., Sharma, S., Gudde, R.S., Sundar, S. and Shaha, C., 2016. *Leishmania donovani*-induced increase in macrophage Bcl-2 favors parasite survival. *Frontiers in immunology*, 7, p.456.

Pandya, S., Verma, R.K., Khare, P., Tiwari, B., Srinivasarao, D.A., Dube, A., Goyal, N. and Misra, A., 2016. Supplementation of host response by targeting nitric oxide to the macrophage cytosol is efficacious in the hamster model of visceral leishmaniasis and adds to efficacy of amphotericin B. *International Journal for Parasitology: Drugs and Drug Resistance*, 6(2), pp.125-132.

Paris, C., Bertoglio, J. and Bréard, J., 2007. Lysosomal and mitochondrial pathways in miltefosine-induced apoptosis in U937 cells. *Apoptosis*, 12(7), pp.1257-1267.

Park, J.S., Tamayo, M.H., Gonzalez-Juarrero, M., Orme, I.M. and Ordway, D.J., 2006. Virulent clinical isolates of *Mycobacterium tuberculosis* grow rapidly and induce cellular necrosis but minimal apoptosis in murine macrophages. *Journal of leukocyte biology*, 79(1), pp.80-86.

Parsons, M., Carter, V., Muthiani, A. and Murphy, N., 1995. *Trypanosoma congolense*: developmental regulation of protein kinases and tyrosine phosphorylation during the life cycle. *Experimental parasitology*, 80(3), pp.507-514.

Pearson, R.D. and de Queiroz Sousa, A., 1996. Clinical spectrum of leishmaniasis. *Clinical infectious diseases*, pp.1-11.

Pearson, R.D., Harcus, J.L., Roberts, D. and Donowitz, G.R., 1983. Differential survival of *Leishmania donovani* amastigotes in human monocytes. *The Journal of Immunology*, 131(4), pp.1994-1999.

Perez-Victoria, F.J., Castanys, S., Gamarro, F., 2003. *Leishmania donovani* resistance to miltefosine involves a defective inward translocation of the drug. *Antimicrob. Agents Chemother.* 47, 2397–2403.

Perkins, N.D., 2007. Integrating cell-signalling pathways with NF- $\kappa$ B and IKK function. *Nature reviews Molecular cell biology*, 8(1), p.49.

Perl, M., Chung, C.S., Lomas-Neira, J., Rachel, T.M., Biffl, W.L., Cioffi, W.G. and Ayala, A., 2005. Silencing of Fas, but not caspase-8, in lung epithelial cells ameliorates pulmonary apoptosis, inflammation, and neutrophil influx after hemorrhagic shock and sepsis. *The American journal of pathology*, 167(6), pp.1545-1559.

Perry, M.R., Prajapati, V.K., Menten, J., Raab, A., Feldmann, J., Chakraborti, D., Sundar, S., Fairlamb, A.H., Boelaert, M. and Picado, A., 2015. Arsenic exposure and outcomes of antimonial treatment in visceral leishmaniasis patients in Bihar, India: a retrospective cohort study. *PLoS neglected tropical diseases*, 9(3), p.e0003518.

Peters, C., Aebischer, T., Stierhof, Y. D., Fuchs, M., & Overath, P., 1995. The role of macrophage receptors in adhesion and uptake of *Leishmania mexicana* amastigotes. *Journal of cell science*, 108(12), 3715-3724.

Peters, N.C. and Sacks, D.L., 2009. The impact of vector-mediated neutrophil recruitment on cutaneous leishmaniasis. *Cellular microbiology*, 11(9), pp.1290-1296.

Pike, L.J., 2009. The challenge of lipid rafts. *Journal of lipid research*, 50(Supplement), pp.S323-S328.

Pimenta, P.F.P., Modi, G.B., Pereira, S.T., Shahabuddin, M., Sacks D.L., 1997. A novel role for the peritrophic matrix in protecting *Leishmania* from the hydrolytic activities of the sand fly midgut. *Parasitology* 115, 359–369.

Planchon, S.M., Pink, J.J., Tagliarino, C., Bornmann, W.G., Varnes, M.E. and Boothman, D.A., 2001.  $\beta$ -Lapachone-induced apoptosis in human prostate cancer cells: involvement of NQO1/xip3. *Experimental cell research*, 267(1), pp.95-106.

Proskuryakov, S.Y., Konoplyannikov, A.G. and Gabai, V.L., 2003. Necrosis: a specific form of programmed cell death?. *Experimental cell research*, 283(1), pp.1-16.

Pupkis, M.F., Tetley, L. and Coombs, G.H., 1986. *Leishmania mexicana*: amastigote hydrolases in unusual lysosomes. *Experimental parasitology*, 62(1), pp.29-39.

Rainger, G. E., A. F. Rowley, and G. B. Nash. 1998. Adhesion-dependent release of elastase from human neutrophils in a novel, flow-based model: specificity of different chemotactic agents. *Blood* 92: 4819–4827.

Ramazeilles, C., Juliano, L., Chagas, J.R. and Rabinovitch, M., 1990. The anti-leishmanial activity of dipeptide esters on *Leishmania amazonensis* amastigotes. *Parasitology*, 100(2), pp.201-207.

Ramos, I., Alonso, A., Marcen, J.M., Peris, A., Castillo, J.A., Colmenares, M. and Larraga, V., 2008. Heterologous prime-boost vaccination with a non-replicative vaccinia recombinant vector expressing LACK confers protection against canine visceral leishmaniasis with a predominant Th1-specific immune response. *Vaccine*, 26(3), pp.333-344.

Ramos, P.K., Carvalho, K.I., Rosa, D.S., Rodrigues, A.P., Lima, L.V., Campos, M.B., Gomes, C.M.C., Laurenti, M.D., Corbett, C.E. and Silveira, F.T., 2016. Serum Cytokine Responses over the Entire Clinical-Immunological Spectrum of Human *Leishmania (L.) infantum* chagasi Infection. *BioMed research international*.

Rampal, G., Khanna, N., Thind, T.S., Arora, S. and Vig, A.P., 2012. Role of isothiocyanates as anticancer agents and their contributing molecular and cellular mechanisms. *Med. Chem. Drug Discovery*, 3, pp.79-93.

Ravikumar, B., Sarkar, S., Davies, J.E., Futter, M., Garcia-Arencibia, M., Green-Thompson, Z.W., Jimenez-Sanchez, M., Korolchuk, V.I., Lichtenberg, M., Luo, S. and Massey, D.C., 2010. Regulation of mammalian autophagy in physiology and pathophysiology. *Physiological reviews*, 90(4), pp.1383-1435.

Real, F., Florentino, P.T.V., Reis, L.C., Ramos-Sanchez, E.M., Veras, P.S.T., Goto, H. and Mortara, R.A., 2014. Cell-to-cell transfer of *Leishmania amazonensis* amastigotes is mediated by immunomodulatory LAMP-rich parasitophorous extrusions. *Cellular microbiology*, 16(10), pp.1549-1564.

Real, F., Pouchelet, M. and Rabinovitch, M., 2008. *Leishmania* (L.) *amazonensis*: fusion between parasitophorous vacuoles in infected bone-marrow derived mouse macrophages. *Experimental parasitology*, 119(1), pp.15-23.

Real, F.E.R.N.A.N.D.O., Vidal, R.O., Carazzolle, M.F., Mondego, J.M.C., Costa, G.G.L., Herai, R.H., Würtele, M.A.R.T.I.N., De Carvalho, L.M., e Ferreira, R.C., Mortara, R.A. and Barbiéri, C.L., 2013. The genome sequence of *Leishmania* (*Leishmania*) *amazonensis*: functional annotation and extended analysis of gene models. *DNA research*, 20(6), pp.567-581.

Reddy, G.S., Mukhopadhyay, A.G. and Dey, C.S., 2017. The p38 MAP kinase inhibitor, PD 169316, inhibits flagellar motility in *Leishmania donovani*. *Biochemical and biophysical research communications*, 493(4), pp.1425-1429.

Reggiori, F. and Klionsky, D.J., 2005. Autophagosomes: biogenesis from scratch?. *Current opinion in cell biology*, 17(4), pp.415-422.

Reiner, S.L. and Locksley, R.M., 1995. The regulation of immunity to *Leishmania major*. *Annual review of immunology*, 13(1), pp.151-177.

Reithinger, R., Dujardin, J.C., Louzir, H., Pirmez, C., Alexander, B. and Brooker, S., 2007. Cutaneous leishmaniasis. *The Lancet infectious diseases*, 7(9), pp.581-596.

Reyland, M.E. and Bradford, A.P., 2010. PKC and the Control of Apoptosis. In *Protein Kinase C in Cancer Signaling and Therapy* (pp. 189-222). Humana Press, Totowa, NJ.

Ribeiro-Gomes, F. L., A. C. Otero, N. A. Gomes, M. C. Moniz-De-Souza, L. Cysne-Finkelstein, A. C. Arnholdt, V. L. Calich, S. G. Coutinho, M. F. Lopes, and G. A. DosReis. 2004. Macrophage interactions with neutrophils regulate *Leishmania major* infection. *J. Immunol.* 172: 4454–4462.

Ribeiro-Gomes, F.L., Moniz-de-Souza, M.C.A., Alexandre-Moreira, M.S., Dias, W.B., Lopes, M.F., Nunes, M.P., Lungarella, G. and DosReis, G.A., 2007. Neutrophils activate macrophages for intracellular killing of *Leishmania major* through recruitment of TLR4 by neutrophil elastase. *The Journal of Immunology*, 179(6), pp.3988-3994.

Ricardo-Carter, C., Favila, M., Polando, R.E., Cotton, R.N., Bogard Horner, K., Condon, D., Ballhorn, W., Whitcomb, J.P., Yadav, M., Geister, R.L. and Schorey, J.S., 2013. *Leishmania major* inhibits IL-12 in macrophages by signalling through CR3 (CD11b/CD18) and down-regulation of ETS-mediated transcription. *Parasite immunology*, 35(12), pp.409-420.

Rincón, M., Anguita, J., Nakamura, T., Fikrig, E. and Flavell, R.A., 1997. Interleukin (IL)-6 directs the differentiation of IL-4-producing CD4+ T cells. *The Journal of experimental medicine*, 185(3), pp.461-470.

Rittig MG, Bogdan C. *Leishmania*-host-cell interaction: complexities and alternative views. *Parasitol Today* (2000) 16:292–7. doi:10.1016/S0169-4758(00)01692-6.

Rivier, D., Shah, R., Bovay, P. and Mauel, J., 1993. Vaccine development against cutaneous leishmaniasis. Subcutaneous administration of radioattenuated parasites protects CBA mice against virulent *Leishmania major* challenge. *Parasite immunology*, 15(2), pp.75-84.

Rizvi, F.S., Ouaiissi, M.A., Marty, B., Santoro, F. and Capron, A., 1988. The major surface protein of *Leishmania promastigotes* is a fibronectin-like molecule. *European journal of immunology*, 18(3), pp.473-476.

Rodrigues, J.C.F., Seabra, S.H. and de Souza, W., 2006. Apoptosis-like death in parasitic protozoa. *Brazilian Journal of Morphological Sciences*, 23(1), pp.87-98.

Rodríguez-González, J., Wilkins-Rodríguez, A.A. and Gutiérrez-Kobeh, L., 2018. Role of glutathione, ROS, and Bcl-xL in the inhibition of apoptosis of monocyte-derived dendritic cells by *Leishmania mexicana promastigotes*. *Parasitology research*, 117(4), pp.1225-1235.

Rogers, M., Kropf, P., Choi, B.S., Dillon, R., Podinovskaia, M., Bates, P. and Müller, I., 2009. Proteophosphoglycans regurgitated by *Leishmania*-infected sand flies target the L-arginine metabolism of host macrophages to promote parasite survival. *PLoS pathogens*, 5(8), p.e1000555.

Rogers, M.E. 2012. The role of *Leishmania* proteophosphoglycans in sand fly transmission and infection of the mammalian host. *Microbiology*, 3(223), pp.1-13.

Rogers, M.E., Chance, M.L. and Bates, P.A., 2002. The role of promastigote secretory gel in the origin and transmission of the infective stage of *Leishmania mexicana* by the sandfly *Lutzomyia longipalpis*. *Parasitology*, 124(5), pp.495-507.

Rojas-Bernabé, A., Garcia-Hernández, O., Maldonado-Bernal, C., Delegado-Dominguez, J., Ortega, E., Gutiérrez-Kobeh, L., Becker, I. and Aguirre-Garcia, M., 2014. *Leishmania mexicana* lipophosphoglycan activates ERK and p38 MAP kinase and induces production of proinflammatory cytokines in human macrophages through TLR2 and TLR4. *Parasitology*, 141(6), pp.788-800.

Rojas-Bernabé, A., Garcia-Hernández, O., Maldonado-Bernal, C., Delegado-Dominguez, J., Ortega, E., Gutiérrez-Kobeh, L., Becker, I. and Aguirre-Garcia, M., 2014. *Leishmania mexicana* lipophosphoglycan activates ERK and p38 MAP kinase and induces production of proinflammatory cytokines in human macrophages through TLR2 and TLR4. *Parasitology*, 141(6), pp.788-800.

Rosenthal, L.A., Sutterwala, F.S., Kehrl, M.E. and Mosser, D.M., 1996. *Leishmania major*-human macrophage interactions: cooperation between Mac-1 (CD11b/CD18) and complement receptor type 1 (CD35) in promastigote adhesion. *Infection and immunity*, 64(6), pp.2206-2215.

Roy, S., Gupta, P., Palit, S., Basu, M., Ukil, A. and Das, P.K., 2017. The role of PD-1 in regulation of macrophage apoptosis and its subversion by *Leishmania donovani*. *Clinical & translational immunology*, 6(5), p.e137.

Royal Society of Chemistry (2016) [online] [21 September 2016] available from <http://www.rsc.org/periodic-table/element/51/antimony>

Ruhland, A., Leal, N. and Kima, P.E., 2007. *Leishmania* promastigotes activate PI3K/Akt signalling to confer host cell resistance to apoptosis. *Cellular microbiology*, 9(1), pp.84-96.

Russell, D.G. and Wright, S.D., 1988. Complement receptor type 3 (CR3) binds to an Arg-Gly-Asp-containing region of the major surface glycoprotein, gp63, of *Leishmania* promastigotes. *Journal of Experimental Medicine*, 168(1), pp.279-292.

Ryan, K.A., Garraway, L.A., Descoteaux, A., Turco, S.J. and Beverley, S.M., 1993. Isolation of virulence genes directing surface glycosyl-phosphatidylinositol synthesis by functional complementation of *Leishmania*. *Proceedings of the National Academy of Sciences*, 90(18), pp.8609-8613.

Sacks D. L., Pimenta P. F., Mcconville M. J., Schneider P., Turco S. J., 1995. Stage-specific binding of *Leishmania donovani* to the sand fly vector midgut is regulated by conformational changes in the abundant surface lipophosphoglycan. *J. Exp. Med.* 181, 685–697.

Sacks, D. and Anderson, C., 2004. Re-examination of the immunosuppressive mechanisms mediating non-cure of *Leishmania* infection in mice. *Immunological reviews*, 201(1), pp.225-238.

Sacks, D. and Kamhawi, S., 2001. Molecular aspects of parasite-vector and vector-host interactions in leishmaniasis. *Annual reviews in microbiology*, 55(1), pp.453-483.

Saha, G., Khamar, B.M., Singh, O.P., Sundar, S. and Dubey, V.K., 2019. *Leishmania donovani* evades Caspase 1 dependent host defense mechanism during infection. *International journal of biological macromolecules*, 126, pp.392-401.

Sakon, S., Xue, X., Takekawa, M., Sasazuki, T., Okazaki, T., Kojima, Y., Piao, J.H., Yagita, H., Okumura, K., Doi, T. and Nakano, H., 2003. NF- $\kappa$ B inhibits TNF-induced accumulation of ROS that mediate prolonged MAPK activation and necrotic cell death. *The EMBO journal*, 22(15), pp.3898-3909.

Sánchez-Sampedro, L., Gómez, C.E., Mejías-Pérez, E., Pérez-Jiménez, E., Oliveros, J.C. and Esteban, M., 2013. Attenuated and replication competent Vaccinia Virus strains M65 and M101 with distinct biology and immunogenicity as potential vaccine candidates against pathogens. *Journal of virology*, pp.JVI-03013.

Sanger Institute 2018 [online] [18 Aug. 2018] available from (<https://www.sanger.ac.uk/resources/downloads/protozoa/leishmania-mexicana.html>)

Santos, D.O., Coutinho, C.E., Madeira, M.F., Bottino, C.G., Vieira, R.T., Nascimento, S.B., Bernardino, A., Bourguignon, S.C., Corte-Real, S., Pinho, R.T. and Rodrigues, C.R., 2008. Leishmaniasis treatment—a challenge that remains: a review. *Parasitology research*, 103(1), pp.1-10.

Sardar, A.H., Kumar, S., Kumar, A., Purkait, B., Das, S., Sen, A., Kumar, M., Sinha, K.K., Singh, D., Equbal, A. and Ali, V., 2013. Proteome changes associated with *Leishmania donovani* promastigote adaptation to oxidative and nitrosative stresses. *Journal of proteomics*, 81, pp.185-199.

Sarkar, A., Aga, E., Bussmeyer, U., Bhattacharyya, A., Möller, S., Hellberg, L., Behnen, M., Solbach, W. and Laskay, T., 2013. Infection of neutrophil granulocytes with *Leishmania major* activates ERK 1/2 and modulates multiple apoptotic pathways to inhibit apoptosis. *Medical microbiology and immunology*, 202(1), pp.25-35.

Saunders, E.C., Ng, W.W., Kloehn, J., Chambers, J.M., Ng, M. and McConville, M.J., 2014. Induction of a stringent metabolic response in intracellular stages of *Leishmania mexicana* leads to increased dependence on mitochondrial metabolism. *PLoS pathogens*, 10(1), p.e1003888.

Savill, J., 1997. Apoptosis in resolution of inflammation. *Journal of Leukocyte Biology* 61, 375–380.

Savill, J., Gregory, C. and Haslett, C., 2003. Cell biology. Eat me or die. *Science* 308, 1516–1517.

Scala, A., Micale, N., Piperno, A., Rescifina, A., Schirmeister, T., Kesselring, J. and Grassi, G., 2016. Targeting of the *Leishmania mexicana* cysteine protease CPB2. 8 $\Delta$ CTE by decorated fused benzo [b] thiophene scaffold. *RSC Advances*, 6(36), pp.30628-30635.

Scheller, J., Chalaris, A., Schmidt-Arras, D. and Rose-John, S., 2011. The pro-and anti-inflammatory properties of the cytokine interleukin-6. *Biochimica et Biophysica Acta (BBA)-Molecular Cell Research*, 1813(5), pp.878-888.

Schlein, Y., Jacobson, R.L. and Shlomai, J., 1991. Chitinase secreted by *Leishmania* functions in the sandfly vector. *Proceedings of the Royal Society of London. Series B: Biological Sciences*, 245(1313), pp.121-126.

Schroit, A.J. and Zwaal, R.F., 1991. Transbilayer movement of phospholipids in red cell and platelet membranes. *Biochimica et Biophysica Acta (BBA)-Reviews on Biomembranes*, 1071(3), pp.313-329.

Segalés, J., Perdiguero, E. and Muñoz-Cánoves, P., 2016. Regulation of muscle stem cell functions: a focus on the p38 MAPK signaling pathway. *Frontiers in cell and developmental biology*, 4, p.91.

Segovia, M., Artero, J.M., Mellado, E. and Chance, M.L., 1992. Effects of long-term in vitro cultivation on the virulence of cloned lines of *Leishmania major* promastigotes. *Annals of Tropical Medicine & Parasitology*, 86(4), pp.347-354.

Séguin, O. and Descoteaux, A., 2016. *Leishmania*, the phagosome, and host responses: The journey of a parasite. *Cellular Immunology*, 309, pp.1-6.

Selzer, P.M., Pingel, S., Hsieh, I., Ugele, B., Chan, V.J., Engel, J.C., Bogyo, M., Russell, D.G., Sakanari, J.A. and McKerrow, J.H., 1999. Cysteine protease inhibitors as chemotherapy: lessons from a parasite target. *Proceedings of the National Academy of Sciences*, 96(20), pp.11015-11022.

Sharma, U. and Singh, S., 2009. Immunobiology of leishmaniasis. *Indian J Exp Biol.* 47(6):412–23.

Sher, A., Pearce, E. and Kaye, P. 2003. Shaping the immune response to parasites: role of dendritic cells. *Curr Opin Immunol*, 15, 421-429.

Silverman, J.M., Clos, J., de'Oliveira, C.C., Shirvani, O., Fang, Y., Wang, C., Foster, L.J. and Reiner, N.E., 2010. An exosome-based secretion pathway is responsible for protein export from *Leishmania* and communication with macrophages. *J Cell Sci*, 123(6), pp.842-852.

Singh, N., Kumar, R., Nylén, S., Sacks, D. and Sundar, S., 2016. The effect of TNF- $\alpha$  neutralization on parasite load and cytokine production in human visceral leishmaniasis. *International Journal of Infectious Diseases*, 45, p.62.

Solano-Gálvez, S., Abadi-Chiriti, J., Gutiérrez-Velez, L., Rodríguez-Puente, E., Konstat-Korzenny, E., Álvarez-Hernández, D.A., Franyuti-Kelly, G., Gutiérrez-Kobeh, L. and Vázquez-López, R., 2018. Apoptosis: Activation and Inhibition in Health and Disease. *Medical Sciences*, 6(3), p.54.

Solbach, W., and T. Laskay., 2000. The host response to *Leishmania* infection. *Adv. Immunol.* 74:275.

Soong, L., 2012. Subversion and utilization of host innate defense by *Leishmania amazonensis*. *Frontiers in immunology*, 3, p.58.

Soulat, D. and Bogdan, C., 2017. Function of Macrophage and Parasite Phosphatases in Leishmaniasis. *Frontiers in immunology*, 8, p.1838.

Späth, G.F., Garraway, L.A., Turco, S.J. and Beverley, S.M., 2003. The role (s) of lipophosphoglycan (LPG) in the establishment of *Leishmania* major infections in mammalian hosts. *Proceedings of the National Academy of Sciences*, 100(16), pp.9536-9541.

Sperandio S, de Belle I, Bredesen DE, 2000 An alternative, non-apoptotic form of programmed cell death. *Proc Natl Acad Sci (USA)* 97: 14376–81.

Sperandio S, Poksay K, de Belle I, Lafuente MJ, Liu B, Nasir J, Bredesen DE, 2004. "Paraptosis: mediation by MAP kinases and inhibition by AIP-1/Alix". *Cell Death and Differentiation*. 11 (10): 1066–75.

Steert, K., Berg, M., Mottram, J.C., Westrop, G.D., Coombs, G.H., Cos, P., Maes, L., Joossens, J., Van der Veken, P., Haemers, A. and Augustyns, K., 2010.  $\alpha$ -Ketoheterocycles as Inhibitors of *Leishmania mexicana* Cysteine Protease CPB. *ChemMedChem*, 5(10), pp.1734-1748.

Stenger, S., Thüring, H., Rölinghoff, M. and Bogdan, C., 1994. Tissue expression of inducible nitric oxide synthase is closely associated with resistance to *Leishmania major*. *The Journal of experimental medicine*, 180(3), pp.783-793.

Stillwell, W., 2016. *An Introduction to Biological Membranes: Composition, Structure and Function*. Elsevier 2<sup>nd</sup> ed.pp.423-451.

Stossel, T.P., 1978. Contractile proteins in cell structure and function. *Annual review of medicine*, 29(1), pp.427-457.

Streit, J.A., Recker, T.J., Gueiros Filho, F., Beverley, S.M. and Wilson, M.E., 2001. Protective immunity against the protozoan *Leishmania chagasi* is induced by subclinical cutaneous infection with virulent but not avirulent organisms. *The Journal of Immunology*, 166(3), pp.1921-1929.

Stricker, J., Falzone, T. and Gardel, M.L., 2010. Mechanics of the F-actin cytoskeleton. *Journal of biomechanics*, 43(1), pp.9-14.

Sullivan, D.E., Ferris, M., Nguyen, H., Abboud, E. and Brody, A.R., 2009. TNF- $\alpha$  induces TGF- $\beta$ 1 expression in lung fibroblasts at the transcriptional level via AP-1 activation. *Journal of cellular and molecular medicine*, 13(8b), pp.1866-1876.

Sundar, S., Jha, T.K., Thakur, C.P., Engel, J., Sindermann, H., Fischer, C., Junge, K., Bryceson, A., Berman, J., 2002. Oral miltefosine for Indian visceral leishmaniasis. *N. Engl. J. Med.* 347, 1739–1746.

Sundar, S., Pai, K., Kumar, R., Pathak-Tripathi, K., Gam, A.A., Ray, M. and Kenney, R.T., 2001. Resistance to treatment in Kala-azar: speciation of isolates from northeast India. *The American journal of tropical medicine and hygiene*, 65(3), pp.193-196.

Tauber, A.I., 2003. Metchnikoff and the phagocytosis theory. *Nature Reviews Molecular Cell Biology*, 4(11), p.897.

Taylor, R.C., Cullen, S.P. and Martin, S.J., 2008. Apoptosis: controlled demolition at the cellular level. *Nature reviews Molecular cell biology*, 9(3), p.231.

Teixeira, D.E., Benchimol, M., Rodrigues, J.C., Crepaldi, P.H., Pimenta, P.F. and de Souza, W., 2013. The cell biology of *Leishmania*: how to teach using animations. *PLoS pathogens*, 9(10), p.e1003594.

the lipidweb, 2019 [online] [1 Oct. 2019] available from (<https://www.lipidhome.co.uk/lipids/complex/ps/index.htm>).

Theodos, C.M., Povinelli, L., Molina, R., Sherry, B. and Titus, R.G., 1991. Role of tumor necrosis factor in macrophage leishmanicidal activity in vitro and resistance to cutaneous leishmaniasis in vivo. *Infection and immunity*, 59(8), pp.2839-2842.

Thiakaki, M., Kolli, B., Chang, K.P. and Soteriadou, K., 2006. Down-regulation of gp63 level in *Leishmania amazonensis* promastigotes reduces their infectivity in BALB/c mice. *Microbes and infection*, 8(6), pp.1455-1463.

Thomas, S.A., Nandan, D., Kass, J. and Reiner, N.E., 2018. Countervailing, time-dependent effects on host autophagy promotes intracellular survival of *Leishmania*. *Journal of Biological Chemistry*, 293(7), pp.2617-2630.

Thornberry, N.A. and Lazebnik, Y., 1998. Caspases: enemies within. *Science*, 281(5381), pp.1312-1316.

Titus, R.G., Sherry, B. and Cerami, A., 1991. The involvement of TNF, IL-1 and IL-6 in the immune response to protozoan parasites. *Parasitology Today*, 7(3), pp.13-16.

Titus, R.G., Sherry, B.A.R.B.A.R.A. and Cerami, A.N.T.H.O.N.Y., 1989. Tumor necrosis factor plays a protective role in experimental murine cutaneous leishmaniasis. *Journal of Experimental Medicine*, 170(6), pp.2097-2104.

Tobiume, K., Matsuzawa, A., Takahashi, T., Nishitoh, H., Morita, K.I., Takeda, K., Minowa, O., Miyazono, K., Noda, T. and Ichijo, H., 2001. ASK1 is required for sustained activations of JNK/p38 MAP kinases and apoptosis. *EMBO reports*, 2(3), pp.222-228.

Tolson, D.L., Turco, S.J. and Pearson, T.W., 1990. Expression of a repeating phosphorylated disaccharide lipophosphoglycan epitope on the surface of macrophages infected with *Leishmania donovani*. *Infection and immunity*, 58(11), pp.3500-3507.

Töttemeyer, S., Sheppard, M., Lloyd, A., Roper, D., Dowson, C., Underhill, D., Murray, P., Maskell, D. and Bryant, C., 2006. IFN- $\gamma$  enhances production of nitric oxide from macrophages via a mechanism that depends on nucleotide oligomerization domain-2. *The Journal of Immunology*, 176 (8), 4804-4810.

Travis, M.A. and Sheppard, D., 2014. TGF- $\beta$  activation and function in immunity. *Annual review of immunology*, 32, pp.51-82.

Tripathi, A. and Gupta, C.M., 2003. Transbilayer translocation of membrane phosphatidylserine and its role in macrophage invasion in *Leishmania promastigotes*. *Molecular and biochemical parasitology*, 128(1), pp.1-9.

Tsujimoto, K., Ono, T., Sato, M., Nishida, T., Oguma, T. and Tadakuma, T., 2005. Regulation of the expression of caspase-9 by the transcription factor activator protein-4 in glucocorticoid-induced apoptosis. *Journal of Biological Chemistry*, 280(30), pp.27638-27644.

Tsujimoto, Y., Finger, L.R., Yunis, J., Nowell, P.C. and Croce, C.M., 1984. Cloning of the chromosome breakpoint of neoplastic B cells with the t (14; 18) chromosome translocation. *Science*, 226(4678), pp.1097-1099.

Tumang, M.C., Keogh, C., Moldawer, L.L., Helfgott, D.C., Teitelbaum, R., Hariprashad, J. and Murray, H.W., 1994. Role and effect of TNF-alpha in experimental visceral leishmaniasis. *The Journal of Immunology*, 153(2), pp.768-775.

Turco, S.J. and Descoteaux, A., 1992. The lipophosphoglycan of *Leishmania* parasites. *Annual review of microbiology*, 46(1), pp.65-92.

Turco, S.J., Späth, G.F. and Beverley, S.M., 2001. Is lipophosphoglycan a virulence factor? A surprising diversity between *Leishmania* species. *Trends in parasitology*, 17(5), pp.223-226.

Tyler, K.M. and Engman, D.M., 2001. The life cycle of *Trypanosoma cruzi* revisited. *International journal for parasitology*, 31(5), pp.472-481.

Ueda-Nakamura, T., Attias, M. and de Souza, W., 2001. Megasome biogenesis in *Leishmania amazonensis*: a morphometric and cytochemical study. *Parasitology research*, 87(2), pp.89-97.

Ueno, N. and Wilson, M.E., 2012. Receptor-mediated phagocytosis of *Leishmania*: implications for intracellular survival. *Trends in parasitology*, 28(8), pp.335-344.

Ueno, N., Bratt, C.L., Rodriguez, N.E. and Wilson, M.E., 2009. Differences in human macrophage receptor usage, lysosomal fusion kinetics and survival between logarithmic and metacyclic *Leishmania infantum* chagasi promastigotes. *Cellular microbiology*, 11(12), pp.1827-1841.

Unanue, E R. and Allen P M.,1987. The basis for the immunoregulatory role of macrophages and other accessory cells. *Sciences*, 236(4801), 551-557.

Valdés-Reyes, L., Argueta, J., Morán, J., Salaiza, N., Hernández, J., Berzunza, M., Aguirre-García, M., Becker, I. and Gutiérrez-Kobeh, L., 2009. *Leishmania mexicana*: inhibition of camptothecin-induced apoptosis of monocyte-derived dendritic cells. *Experimental parasitology*, 121(3), pp.199-207.

van Zandbergen, G., Bollinger, A., Wenzel, A., Kamhawi, S., Voll, R., Klinger, M., 2006 *Leishmania* disease development depends on the presence of apoptotic promastigotes in the virulent inoculum. *Proc Natl Acad Sci USA* 103: 13837–13842.

van Zandbergen, G., Klinger, M., Mueller, A., Dannenberg, S., Gebert, A., Solbach, W. and Laskay, T., 2004. Cutting edge: neutrophil granulocyte serves as a vector for *Leishmania* entry into macrophages. *The Journal of Immunology*, 173(11), pp.6521-6525.

Verhoven, B., Schlegel, R. and Williamson, P., 1995. Mechanisms of phosphatidylserine exposure, a phagocyte recognition signal, on apoptotic T lymphocytes. *Journal of Experimental Medicine*, 182(5), pp.1597-1601.

Villa-Pulgarín, J.A., Gajate, C., Botet, J., Jimenez, A., Justies, N., Varela-M, R.E., Cuesta-Marbán, Á., Müller, I., Modolell, M., Revuelta, J.L. and Mollinedo, F., 2017. Mitochondria and lipid raft-located FOF1-ATP synthase as major therapeutic targets in the antileishmanial and anticancer activities of ether lipid edelfosine. *PLoS neglected tropical diseases*, 11(8), p.e0005805.

Von Stebut, E., Ehrchen, J.M., Belkaid, Y., Kostka, S.L., Mölle, K., Knop, J., Sunderkötter, C. and Udey, M.C., 2003. Interleukin 1 $\alpha$  promotes Th1 differentiation and inhibits disease progression in *Leishmania major*-susceptible BALB/c mice. *The Journal of experimental medicine*, 198(2), pp.191-199.

Vukosavic, S., Dubois-Dauphin, M., Romero, N. and Przedborski, S., 1999. Bax and Bcl-2 interaction in a transgenic mouse model of familial amyotrophic lateral sclerosis. *Journal of neurochemistry*, 73(6), pp.2460-2468.

Vutova, P., Wirth, M., Hippe, D., Gross, U., Schulze-Osthoff, K., Schmitz, I. and Lüder, C.G., 2007. *Toxoplasma gondii* inhibits Fas/CD95-triggered cell death by inducing aberrant processing and degradation of caspase 8. *Cellular microbiology*, 9(6), pp.1556-1570.

Wanasen, N., MacLeod, C.L., Ellies, L.G. and Soong, L., 2007. L-arginine and cationic amino acid transporter 2B regulate growth and survival of *Leishmania amazonensis* amastigotes in macrophages. *Infection and immunity*, 75(6), pp.2802-2810.

Wanderley, J.L., Benjamin, A., Real, F., Bonomo, A., Moreira, M.E., Barcinski, M.A., 2005. Apoptotic mimicry: an altruistic behavior in host/*Leishmania* interplay. *Brazilian Journal of Medical and Biological Research* 38, 807–881.

Wanderley, J.L., Moreira, M.E., Benjamin, A., Bonomo, A.C. and Barcinski, M.A., 2006. Mimicry of apoptotic cells by exposing phosphatidylserine participates in the establishment of amastigotes of *Leishmania (L) amazonensis* in mammalian hosts. *The Journal of Immunology*, 176(3), pp.1834-1839.

Wanderley, J.L.M., Thorpe, P.E., Barcinski, M.A. and Soong, L., 2013. Phosphatidylserine exposure on the surface of *Leishmania amazonensis* amastigotes modulates in vivo infection and dendritic cell function. *Parasite immunology*, 35(3-4), pp.109-119.

Wang, G., Petzke, M.M., Iyer, R., Wu, H. and Schwartz, I., 2008. Pattern of proinflammatory cytokine induction in RAW264. 7 mouse macrophages is identical for virulent and attenuated *Borrelia burgdorferi*. *The Journal of Immunology*, 180(12), pp.8306-8315.

Wang, Y., Yang, D., Song, L., Li, T., Yang, J., Zhang, X. and Le, W., 2012. Mifepristone-inducible caspase-1 expression in mouse embryonic stem cells eliminates tumor formation but spares differentiated cells in vitro and in vivo. *Stem Cells*, 30(2), pp.169-179.

Wei, X.Q., Charles, I.G., Smith, A., Ure, J., Feng, G.J., Huang, F.P., Xu, D., Mullers, W., Moncada, S. and Liew, F.Y., 1995. Altered immune responses in mice lacking inducible nitric oxide synthase. *Nature*, 375(6530), p.408.

Weingärtner, A., Kemmer, G., Müller, F.D., Zampieri, R.A., dos Santos, M.G., Schiller, J. and Pomorski, T.G., 2012. *Leishmania* promastigotes lack phosphatidylserine but bind annexin V upon permeabilization or miltefosine treatment. *PloS one*, 7(8), p.e42070.

Westphal, D., Kluck, R.M. and Dewson, G., 2014. Building blocks of the apoptotic pore: how Bax and BAK are activated and oligomerize during apoptosis. *Cell death and differentiation*, 21(2), p.196.

Wheeler, R.J., Gluenz, E. and Gull, K., 2011. The cell cycle of *Leishmania*: morphogenetic events and their implications for parasite biology. *Molecular microbiology*, 79(3), pp.647-662.

Wiese, M., 1998. A mitogen-activated protein (MAP) kinase homologue of *Leishmania mexicana* is essential for parasite survival in the infected host. *The EMBO Journal*, 17(9), pp.2619-2628.

Williams, R.A., Tetley, L., Mottram, J.C. and Coombs, G.H., 2006. Cysteine peptidases CPA and CPB are vital for autophagy and differentiation in *Leishmania mexicana*. *Molecular microbiology*, 61(3), pp.655-674.

Wilson, J., Huynh, C., Kennedy, K.A., Ward, D.M., Kaplan, J., Aderem, A. and Andrews, N.W., 2008. Control of parasitophorous vacuole expansion by LYST/Beige restricts the intracellular growth of *Leishmania amazonensis*. *PLoS pathogens*, 4(10), p.e1000179.

Wilson, M.E., Young, B.M., Davidson, B.L., Mente, K.A. and McGowan, S.E., 1998. The importance of TGF- $\beta$  in murine visceral leishmaniasis. *The Journal of Immunology*, 161(11), pp.6148-6155.

Winberg, M.E., Holm, Å., Särndahl, E., Vinet, A.F., Descoteaux, A., Magnusson, K.E., Rasmusson, B. and Lerm, M., 2009. Leishmania donovani lipophosphoglycan inhibits phagosomal maturation via action on membrane rafts. *Microbes and infection*, 11(2), pp.215-222.

Winter, G., Fuchs, M., McConville, M.J., Stierhof, Y.D. and Overath, P., 1994. Surface antigens of Leishmania mexicana amastigotes: characterization of glycoinositol phospholipids and a macrophage-derived glycosphingolipid. *Journal of Cell Science*, 107(9), pp.2471-2482.

Wisdom, R., Johnson, R.S. and Moore, C., 1999. c-Jun regulates cell cycle progression and apoptosis by distinct mechanisms. *The EMBO journal*, 18(1), pp.188-197.

Wong, R.S., 2011. Apoptosis in cancer: from pathogenesis to treatment. *Journal of Experimental & Clinical Cancer Research*, 30(1), p.87.

World Health Organisation WHO (2013) [online] [20 January 2016] available from ([http://www.who.int/leishmaniasis/about\\_disease/en/](http://www.who.int/leishmaniasis/about_disease/en/)).

World Health Organisation WHO (2018) Fact Sheet N°375 [online] available from (<https://www.who.int/en/news-room/fact-sheets/detail/leishmaniasis>).

Wozencraft, A.O., Sayers, G. and Blackwell, J.M., 1986. Macrophage type 3 complement receptors mediate serum-independent binding of Leishmania donovani. Detection of macrophage-derived complement on the parasite surface by immunoelectron microscopy. *The Journal of experimental medicine*, 164(4), pp.1332-1337.

WWW<sup>1</sup>,[http://www.who.int/leishmaniasis/burden/Status\\_of\\_endemicity\\_of\\_CL\\_worldwide\\_2015\\_with\\_imported\\_cases.pdf?ua=1](http://www.who.int/leishmaniasis/burden/Status_of_endemicity_of_CL_worldwide_2015_with_imported_cases.pdf?ua=1)

Yang, Y., Kim, S.C., Yu, T., Yi, Y.S., Rhee, M.H., Sung, G.H., Yoo, B.C. and Cho, J.Y., 2014. Functional roles of p38 mitogen-activated protein kinase in macrophage-mediated inflammatory responses. *Mediators of Inflammation*, 2014.

Yang, Z.; Klionsky, D.J. 2010, Eaten alive: A history of macroautophagy. *Nat. Cell Biol.* 12, 814–822.

Yu, T., Yi, Y.S., Yang, Y., Oh, J., Jeong, D. and Cho, J.Y., 2012. The pivotal role of TBK1 in inflammatory responses mediated by macrophages. *Mediators of inflammation*, 2012.

Zakai, H.A., Chance, M.L. and Bates, P.A., 1998. In vitro stimulation of metacyclogenesis in *Leishmania braziliensis*, *L. donovani*, *L. major* and *L. mexicana*. *Parasitology*, 116(4), pp.305-309.

Zamora-Chimal, J., Fernández-Figueroa, E.A., Ruiz-Remigio, A., Wilkins-Rodríguez, A.A., Delgado-Domínguez, J., Salaiza-Suazo, N., Gutiérrez-Kobeh, L. and Becker, I., 2016. NKT cell activation by Leishmania mexicana LPG: Description of a novel pathway. *Immunobiology*.

Zamzami, N. and Kroemer, G., 2001. The mitochondrion in apoptosis: how Pandora's box opens. *Nature reviews Molecular cell biology*, 2(1), p.67.

Zhang, B., Hirahashi, J., Cullere, X. and Mayadas, T.N., 2003. Elucidation of molecular events leading to neutrophil apoptosis following phagocytosis cross-talk between caspase 8, reactive oxygen species, and MAPK/ERK activation. *Journal of Biological Chemistry*, 278(31), pp.28443-28454.

Zhang, K., Showalter, M., Revollo, J., Hsu, F.F., Turk, J. and Beverley, S.M., 2003. Sphingolipids are essential for differentiation but not growth in *Leishmania*. *The EMBO journal*, 22(22), pp.6016-6026.

Zhang, W.W. and Matlashewski, G., 1997. Loss of virulence in *Leishmania donovani* deficient in an amastigote-specific protein, A2. *Proceedings of the National Academy of Sciences*, 94(16), pp.8807-8811.

Zhang, W.W., Charest, H., Ghedin, E. and Matlashewski, G., 1996. Identification and overexpression of the A2 amastigote-specific protein in *Leishmania donovani*. *Molecular and biochemical parasitology*, 78(1-2), pp.79-90.

Zhang, X., Goncalves, R. and Mosser, D.M., 2008. The isolation and characterization of murine macrophages. *Current protocols in immunology*, 83(1), pp.14-1.

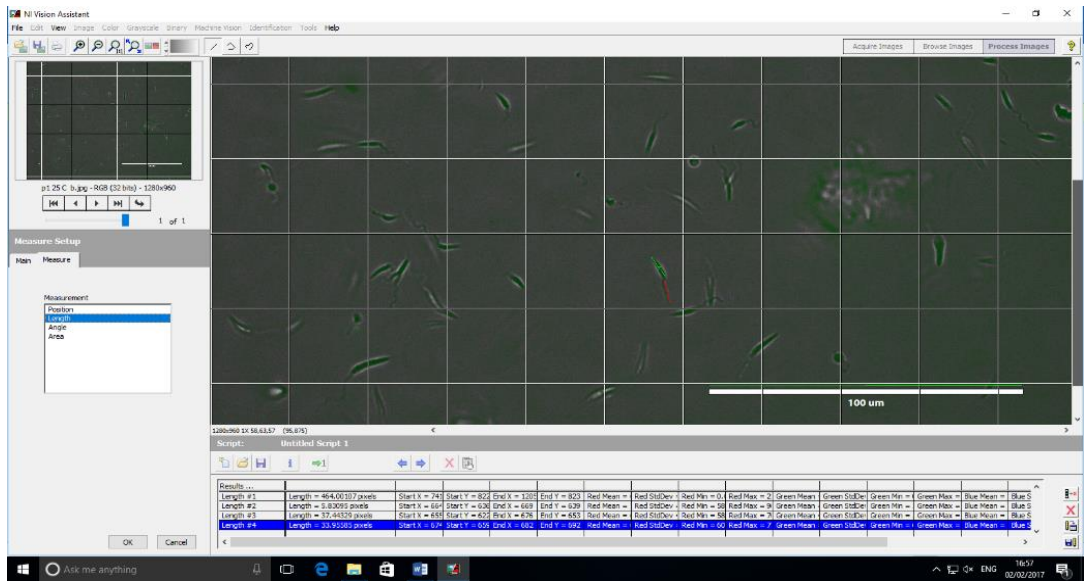
Zhu, H., Zhang, Y., Shi, Z., Lu, D., Li, T., Ding, Y., Ruan, Y. and Xu, A., 2016. The neuroprotection of liraglutide against ischaemia-induced apoptosis through the activation of the PI3K/AKT and MAPK pathways. *Scientific reports*, 6, p.26859.

Zilberstein, D. and Shapira, M., 1994. The role of pH and temperature in the development of *Leishmania* parasites. *Annual Reviews in Microbiology*, 48(1), pp.449-470.

Zwingenberger, K., Harms, G., Pedrosa, C., Pessoa, M.C., Sandkamp, B., Scheibenbogen, C. and Andreesen, R., 1991. Generation of cytokines in human visceral leishmaniasis: dissociation of endogenous TNF- $\alpha$  and IL-1 $\beta$  production. *Immunobiology*, 183(1-2), pp.125-132.

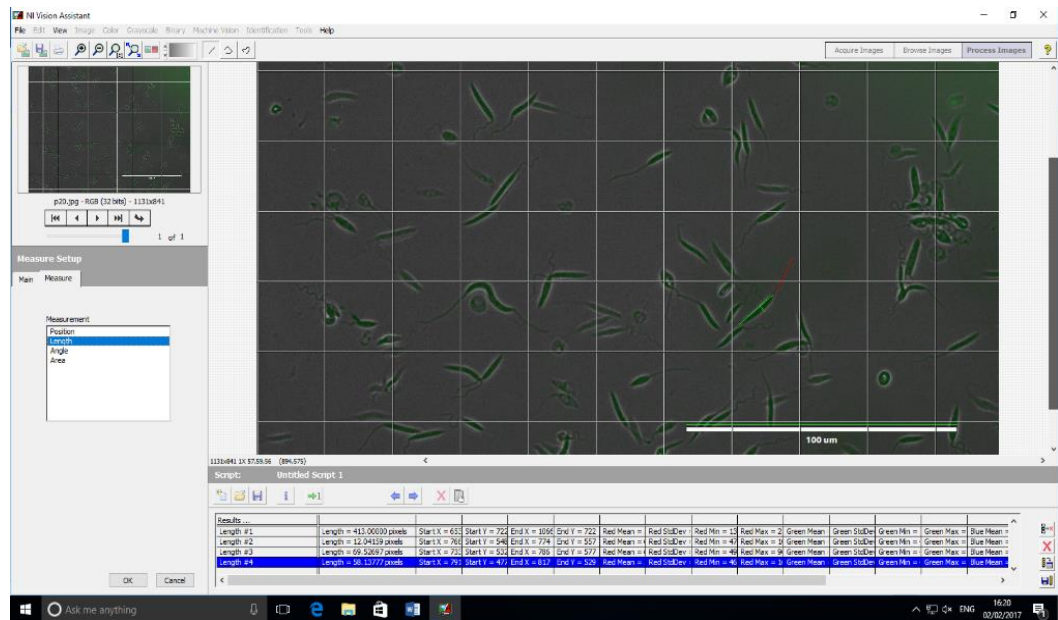
# Appendices

## Appendix 1



### Appendix 1A: physical measurement of P1 promastigotes

Screen shots of NI vision assistant software used for measurement of promastigote sizes

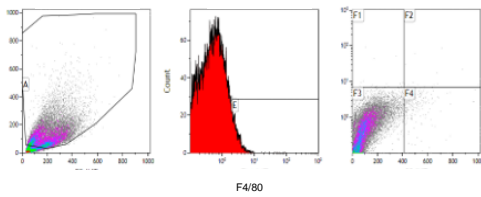


### Appendix 1B: physical measurement of P20 promastigotes

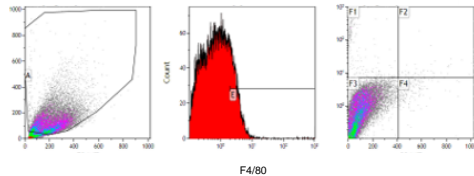
Screen shots of NI vision assistant which used for measurement of promastigote sizes

## Appendix 2

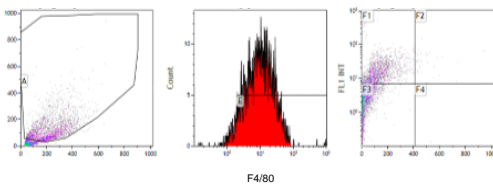
### BMDM unlabelled control



### BMDM labelled with 2° Ab control



### BMDM labelled with primary and 2° Ab



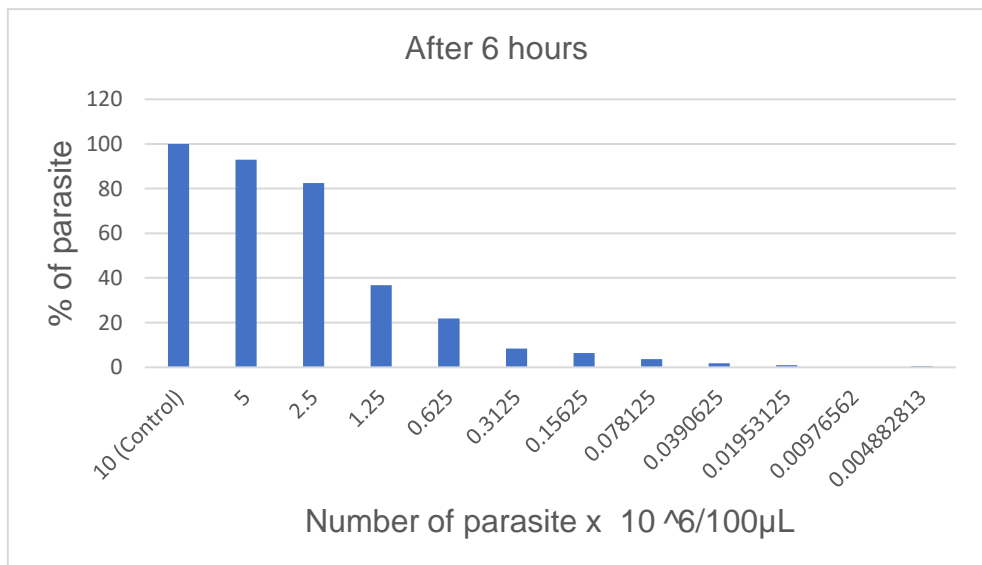
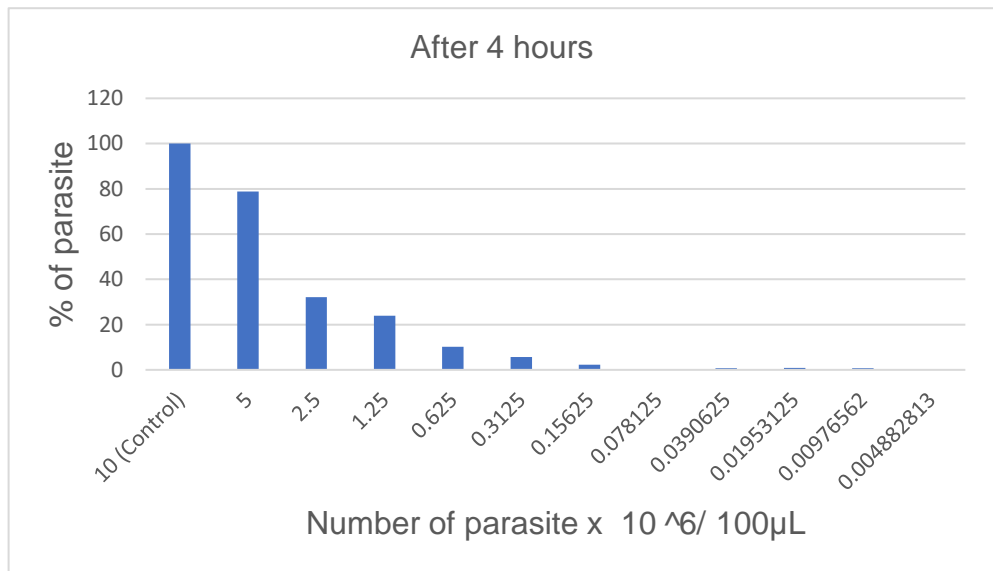
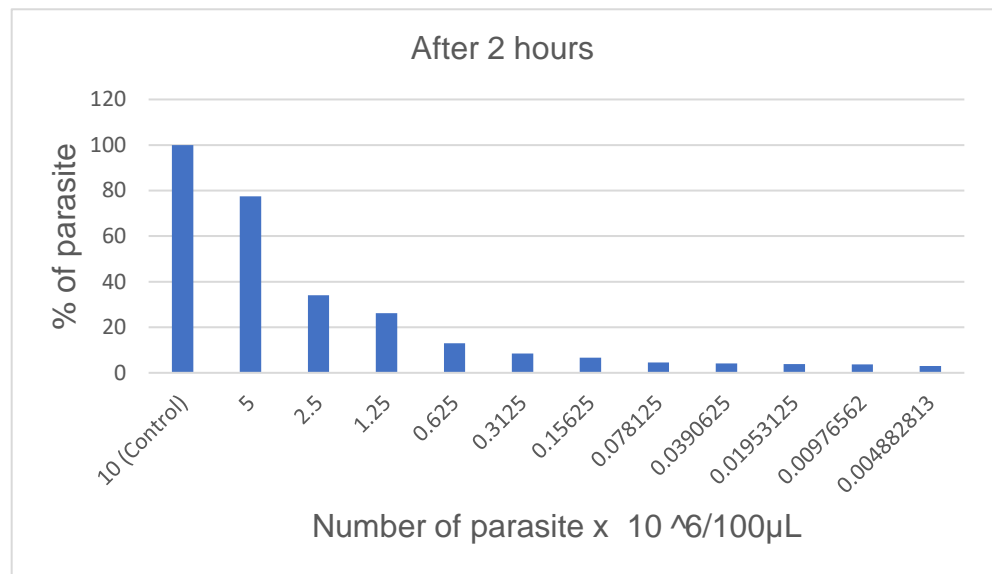
### Overlay of the result

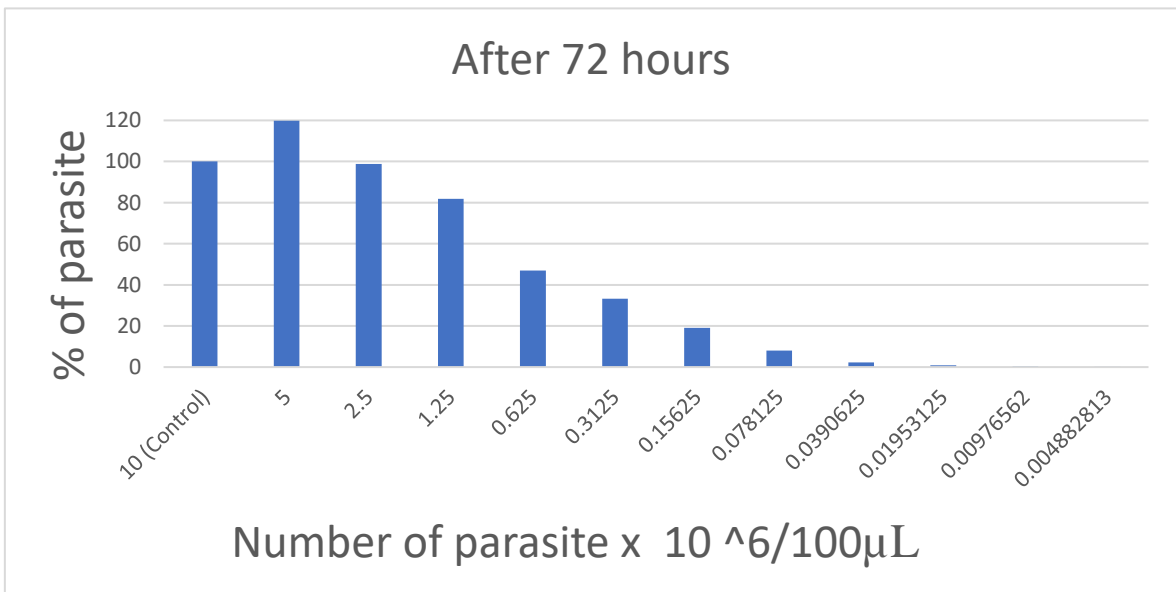
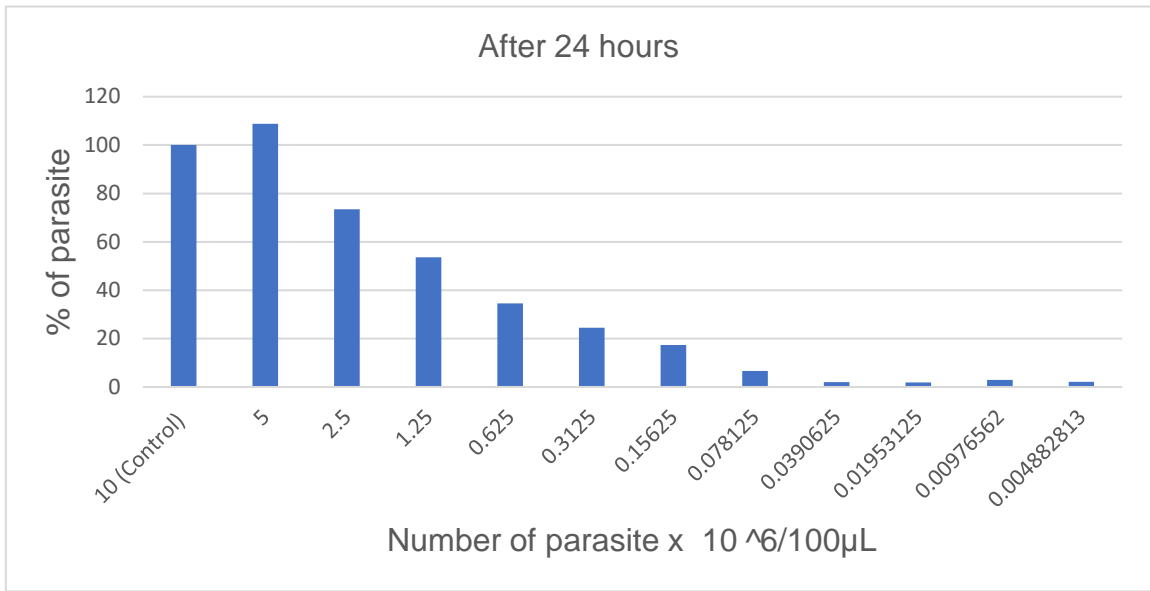


### Appendix 2 Characterisation of BMDM by flow cytometry

At the 7th day BMDM were rinsed twice with PBS adhered macrophages were detached using a tissue culture scraper. Macrophages were washed with PBS by centrifugation at 300g for 5 minutes. Pellets were re suspended in 1 mL PBS. 10  $\mu$ L cells were stained using trypan blue by mixing of 90  $\mu$ L trypan blue and 10  $\mu$ L cells. Cells were divided into three 2 mL Eppendorf tubes 250 x10<sup>5</sup> cells in each one. The first tube was stained with rat anti mouse F4/80 and incubated on ice for 30 minutes, then washed. Tubes number one and two were stained by secondary antibody Goat anti rat F(ab')<sub>2</sub> IgG:FITC and incubated on ice for 30 minutes, and 3rd control tube used non-stained macrophages. All tubes were washed and suspended in 500  $\mu$ L sheath fluid and subjected to flow cytometry analysis. The actual results are for Balb/c BMDM however similar procedure was repeated on C57 BMDM and produced similar results.

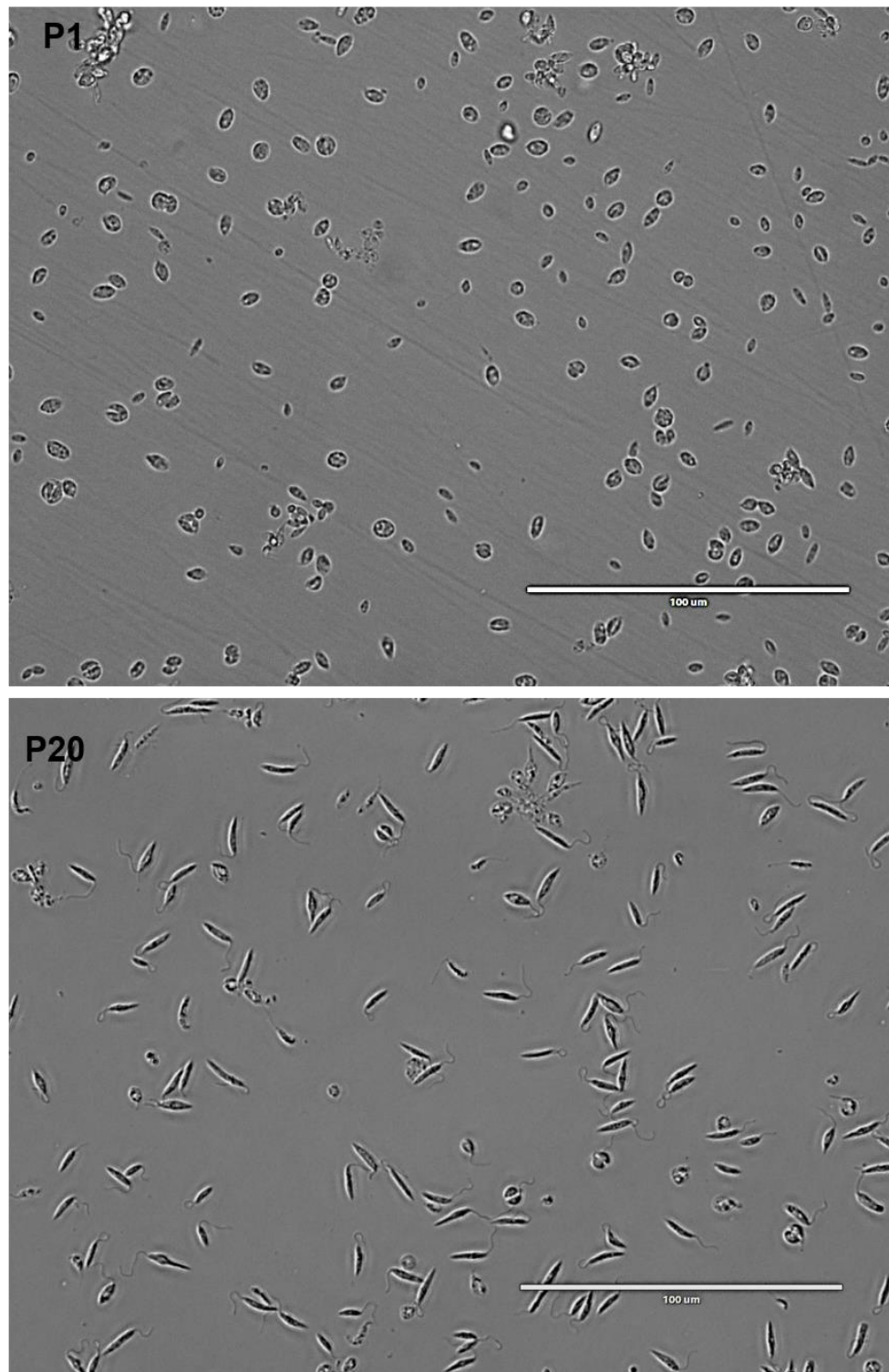
### Appendix 3





**Appendix 3 Optimisation of Alamar blue by using different numbers of parasites and different times of incubation.**

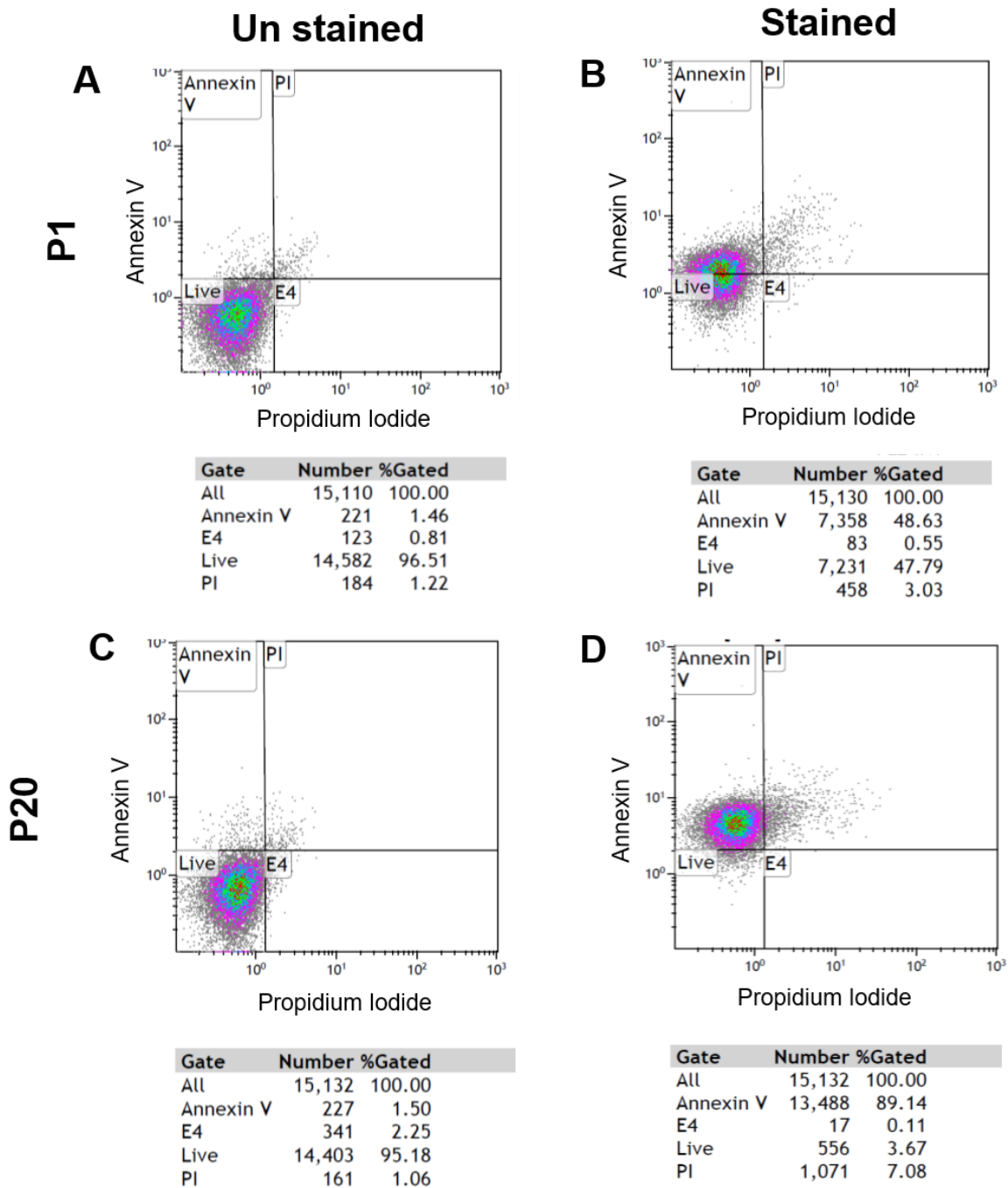
## Appendix 4



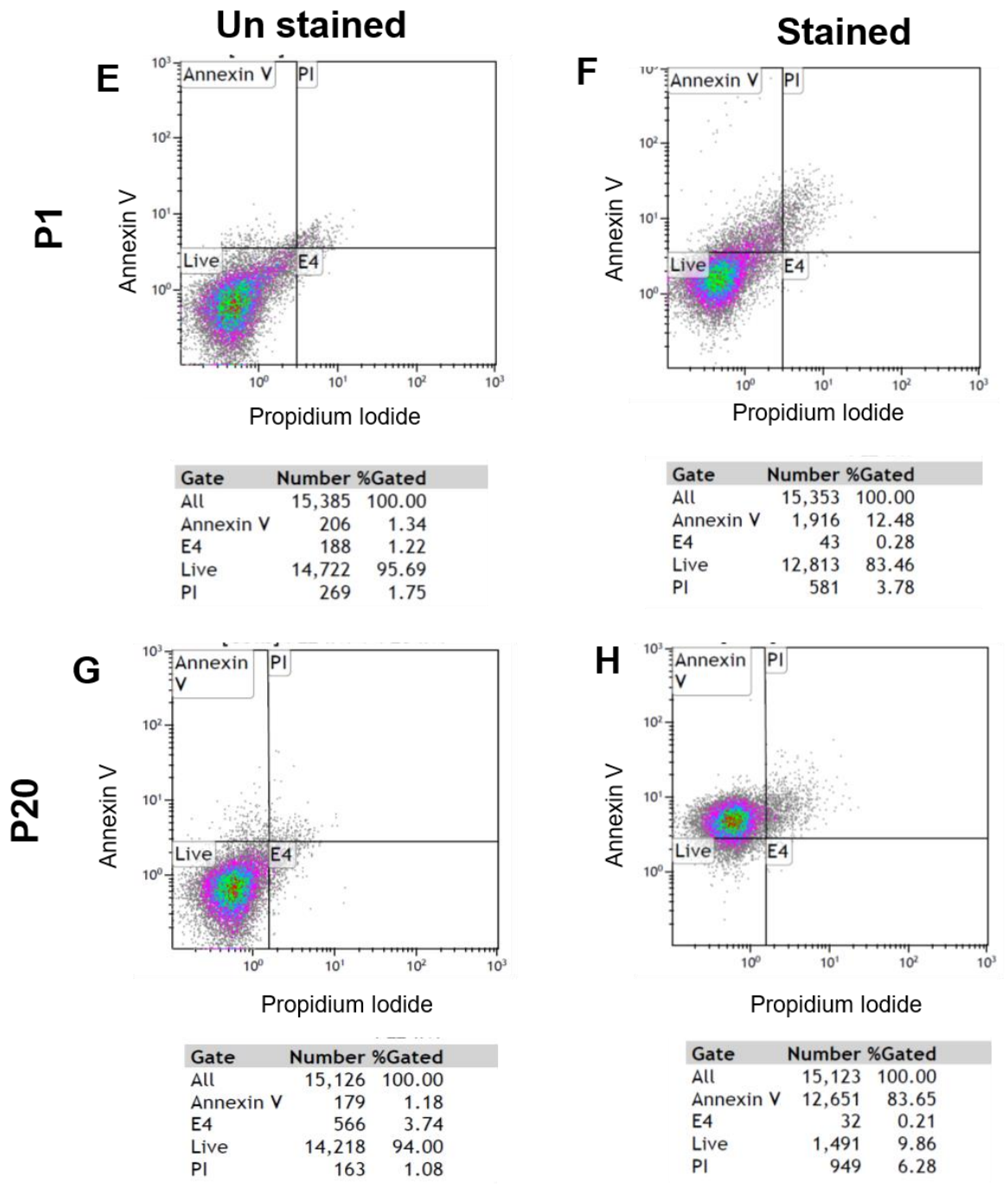
### **Appendix 4: Ability of P1 and P20 *L. mexicana* promastigotes to differentiate into amastigotes**

Ability of P1 and P20 *L. mexicana* to differentiate into amastigotes in RPMI 1640 supplemented with 10% HIFCS after incubation at 95% v/v humidity at 37 °C in 5% v/v CO<sub>2</sub> for 24 hours.

## Appendix 5

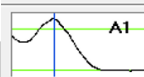
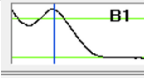
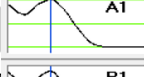
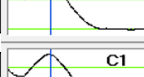


**Appendix 5A: Flow cytometry results of P1 and P20 *L.mexicana* promastigotes PS expression after incubation for 2 hours under amastigote differentiation conditions**

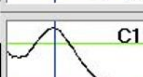
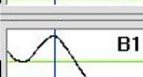
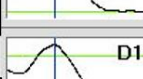


**Appendix 5B: Flow cytometry results of P1 and P20 *L.mexicana* PS expression after incubation for 24 hours under amastigote differentiation conditions**

## Appendix 6

P1 <i>L.mexicana</i> promastigotes		Sample # 2	nm 1 abs. 24.55	A-260 24.63	ng/ul 985.4
		A-280 11.82	260/280 2.08	260/230 1.80	
P20 <i>L.mexicana</i> promastigotes		Sample # 2	nm 1 abs. 12.18	A-260 12.21	ng/ul 488.5
		A-280 5.926	260/280 2.06	260/230 1.38	
P1 <i>L.mexicana</i> /2 hours incubation		Sample # 2	nm 1 abs. 20.30	A-260 20.30	ng/ul 811.9
		A-280 11.20	260/280 1.81	260/230 1.40	
P20 <i>L.mexicana</i> /2 hours incubation		Sample # 2	nm 1 abs. 14.79	A-260 14.79	ng/ul 591.8
		A-280 7.169	260/280 2.06	260/230 1.30	
P1 <i>L.mexicana</i> /24 hours incubation		Sample # 2	nm 1 abs. 14.07	A-260 14.07	ng/ul 562.8
		A-280 6.765	260/280 2.08	260/230 1.94	
P20 <i>L.mexicana</i> /24 hours incubation		Sample # 2	nm 1 abs. 9.820	A-260 9.820	ng/ul 392.8
		A-280 4.809	260/280 2.04	260/230 1.57	

**Appendix 6 A: Quantity analysis of RNA from P1 and P20 promastigotes at stationary phase cultured at standard conditions and after incubation under amastigote differentiation conditions for 2 and 24 hours using the Nano-Drop spectrophotometer**

Balb/c BMDM + P1 / 2 hours		Sample # 1	nm 1 abs. 21.43	A-260 21.43	ng/ul 857.0
		A-280 9.997	260/280 2.14	260/230 2.01	
Balb/c BMDM + P20 / 2 hours		Sample # 1	nm 1 abs. 4.271	A-260 4.271	ng/ul 170.8
		A-280 2.002	260/280 2.13	260/230 1.77	
Balb/c BMDM control / 2 hours		Sample # 1	nm 1 abs. 13.67	A-260 13.67	ng/ul 546.6
		A-280 6.521	260/280 2.10	260/230 2.02	
C57 BMDM + P1 / 2 hours		Sample # 7	nm 1 abs. 17.644	A-260 17.644	ng/ul 705.8
		A-280 8.296	260/280 2.13	260/230 1.72	
C57 BMDM + P20 / 2 hours		Sample # 7	nm 1 abs. 14.789	A-260 14.789	ng/ul 591.6
		A-280 7.054	260/280 2.10	260/230 2.09	
C57 BMDM control / 2 hours		Sample # 5	nm 1 abs. 12.200	A-260 12.200	ng/ul 488.0
		A-280 5.994	260/280 2.04	260/230 1.92	

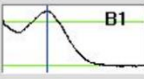
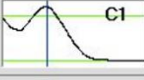
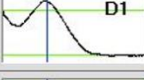
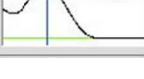
**Appendix 6B: Quantity analysis of RNA from Balb/c and C57 BMDM infected with P1 and P20 promastigotes for 2 hours using the Nano-Drop spectrophotometer**

Balb/c BMDM + P1 / 24 hours		Sample # 6	nm 1 abs. 13.484	A-260 13.484	ng/ul 539.4
		A-280 6.309	260/280 2.14	260/230 1.79	
Balb/c BMDM + P20 / 24 hours		Sample # 6	nm 1 abs. 16.476	A-260 16.476	ng/ul 659.1
		A-280 7.765	260/280 2.12	260/230 2.17	
Balb/c BMDM control/ 24 hours		Sample # 4	nm 1 abs. 10.778	A-260 10.778	ng/ul 431.1
		A-280 5.239	260/280 2.06	260/230 1.98	
C57 BMDM + P1 / 24 hours		Sample # 7	nm 1 abs. 17.644	A-260 17.644	ng/ul 705.8
		A-280 8.296	260/280 2.13	260/230 1.72	
C57 BMDM + P20 / 24 hours		Sample # 7	nm 1 abs. 14.789	A-260 14.789	ng/ul 591.6
		A-280 7.054	260/280 2.10	260/230 2.09	
C57 BMDM control / 24 hours		Sample # 5	nm 1 abs. 12.200	A-260 12.200	ng/ul 488.0
		A-280 5.994	260/280 2.04	260/230 1.92	

**Appendix 6C: Quantity analysis of RNA from Balb/c and C57 BMDM infected with P1 and P20 promastigotes for 24 hours using the Nano-Drop spectrophotometer**

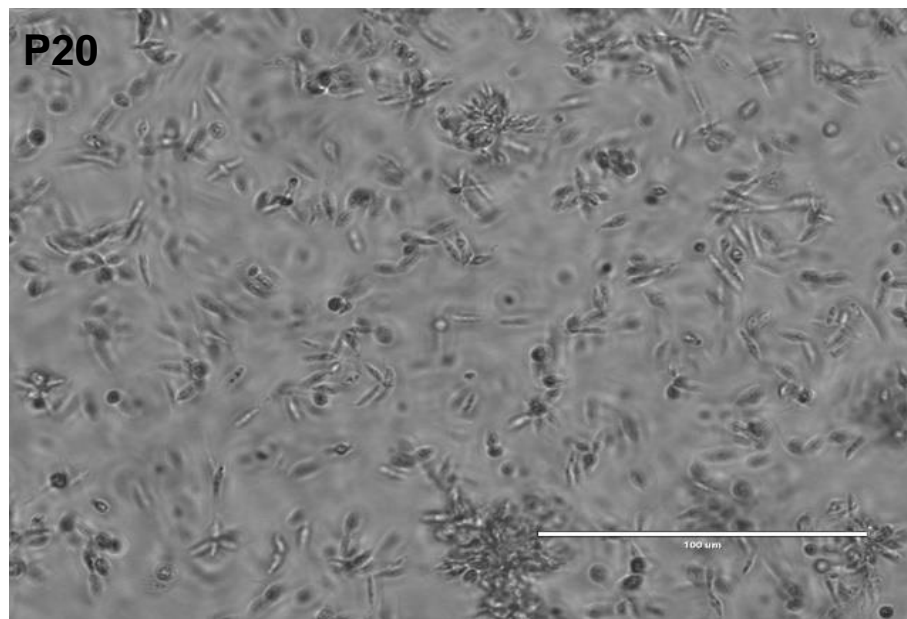
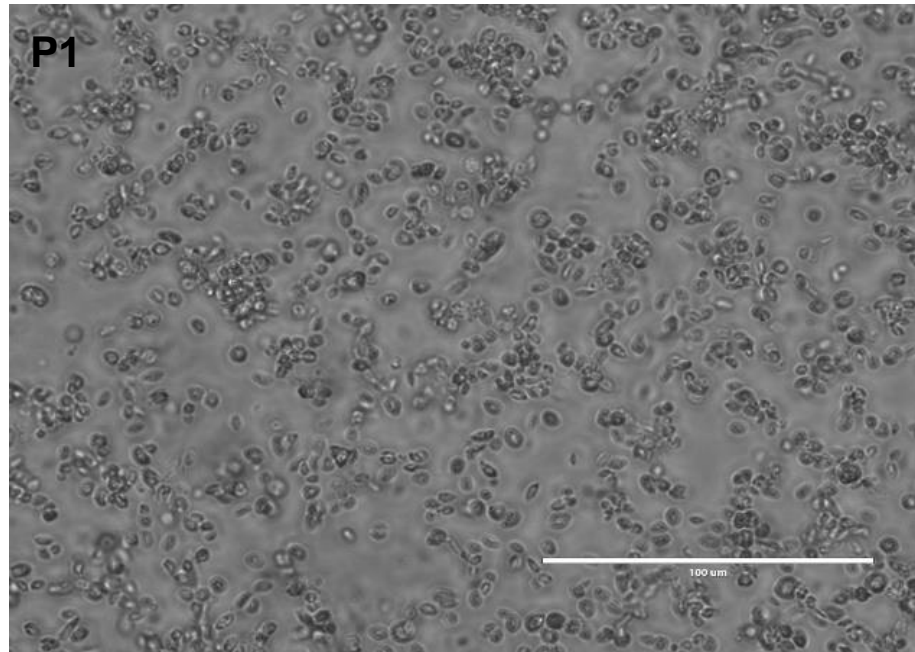
P1 in Balb/c BMDM control supernatant		Sample # 1	nm 1 abs. 10.53	A-260 10.53	ng/ul 421.1
		A-280 4.969	260/280 2.12	260/230 2.05	
P1 in Balb/c BMDM + P1 supernatant		Sample # 1	nm 1 abs. 8.185	A-260 8.185	ng/ul 327.4
		A-280 3.796	260/280 2.16	260/230 2.09	
P1 in Balb/c BMDM + P20 supernatant		Sample # 1	nm 1 abs. 11.54	A-260 11.54	ng/ul 461.7
		A-280 5.453	260/280 2.12	260/230 1.98	
P20 in Balb/c BMDM control supernatant		Sample # 1	nm 1 abs. 11.62	A-260 11.62	ng/ul 465.0
		A-280 5.522	260/280 2.10	260/230 2.26	
P20 in Balb/c BMDM + P1 supernatant		Sample # 1	nm 1 abs. 10.65	A-260 10.65	ng/ul 425.8
		A-280 5.010	260/280 2.13	260/230 1.95	
P20 in Balb/c BMDM + P20 supernatant		Sample # 1	nm 1 abs. 13.19	A-260 13.19	ng/ul 527.6
		A-280 6.232	260/280 2.12	260/230 2.37	

**Appendix 6D: Quantity analysis of RNA from P1 and P20 promastigotes incubated in Balb/c BMDM conditioned media for 24 hours using the Nano-Drop spectrophotometer**

P1 in C57 BMDM control supernatant		Sample # 2	nm 1 abs. 6.179	A-260 6.170	ng/ul 246.8
		A-280 2.969	260/280 2.08	260/230 1.57	
P1 in C57 BMDM + P1 supernatant		Sample # 2	nm 1 abs. 6.080	A-260 6.092	ng/ul 243.7
		A-280 2.793	260/280 2.18	260/230 1.72	
P1 in C57 BMDM + P20 supernatant		Sample # 2	nm 1 abs. 11.998	A-260 12.009	ng/ul 480.4
		A-280 5.620	260/280 2.14	260/230 1.78	
P20 in C57 BMDM control supernatant		Sample # 2	nm 1 abs. 9.302	A-260 9.326	ng/ul 373.0
		A-280 4.419	260/280 2.11	260/230 2.15	
P20 in C57 BMDM + P1 supernatant		Sample # 2	nm 1 abs. 8.571	A-260 8.585	ng/ul 343.4
		A-280 4.047	260/280 2.12	260/230 2.03	
P20 in C57 BMDM + P20 supernatant		Sample # 2	nm 1 abs. 12.344	A-260 12.361	ng/ul 494.5
		A-280 6.031	260/280 2.05	260/230 2.14	

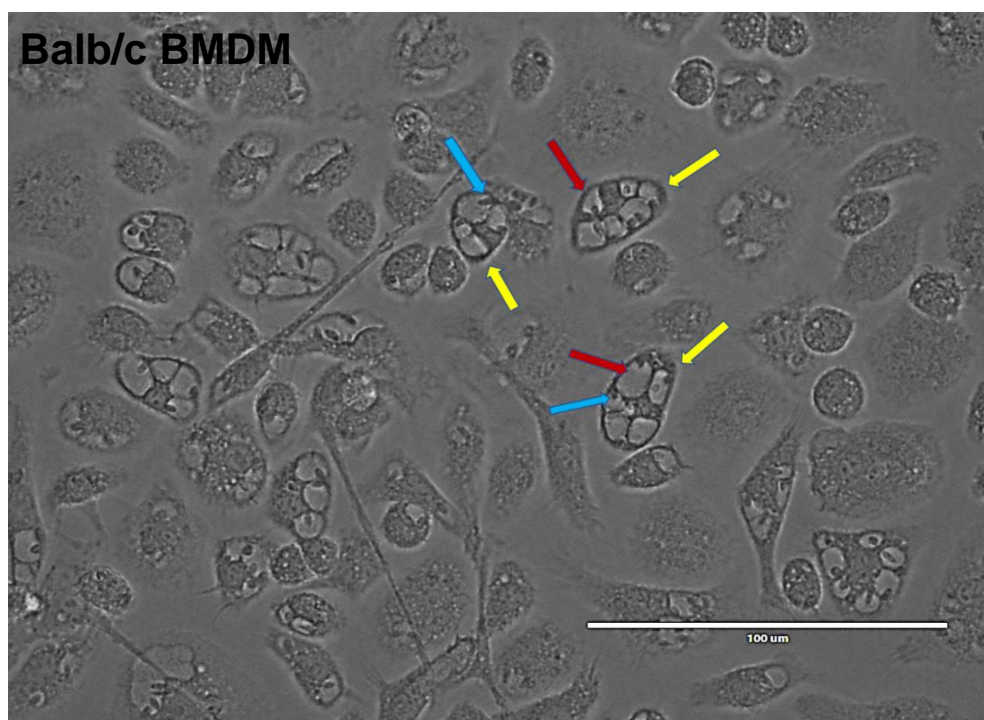
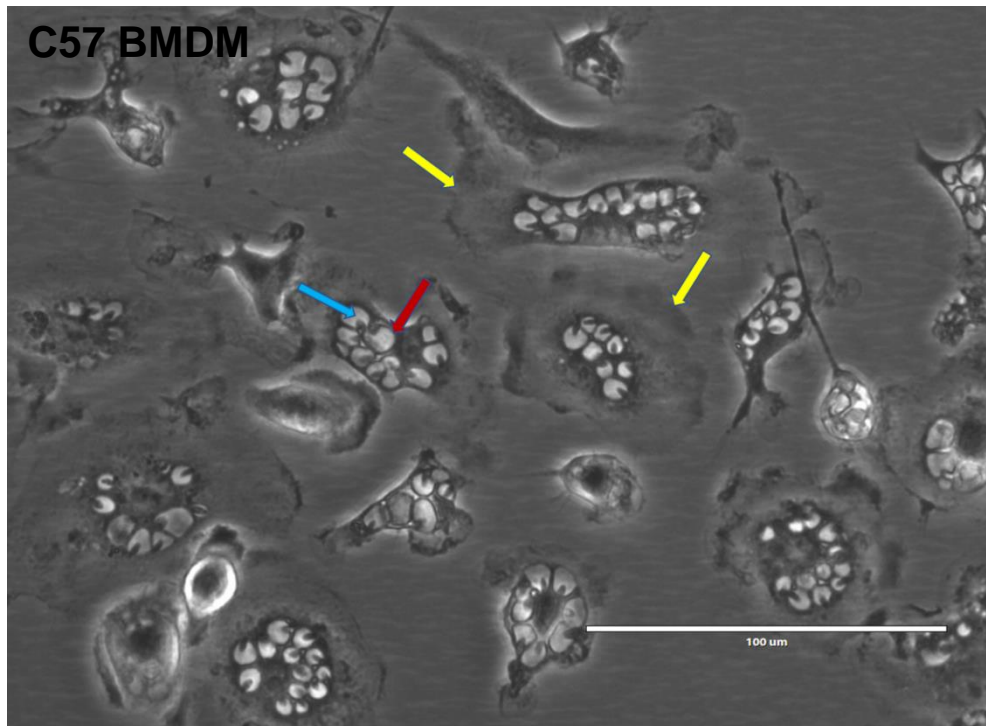
**Appendix 6E: Quantity analysis of RNA from P1 and P20 promastigotes incubated in C57 BMDM conditioned media for 24 hours using the Nano-Drop spectrophotometer**

## Appendix 7



**Appendix 7: Live image of P1 and P20 *L. mexicana* cultured alone control**  
P1 and P20 *L. mexicana* cultured and incubated at 95% v/v humidity at 37 °C in 5% v/v CO<sub>2</sub> for 24 hours without presence of BMDM . P1 lost motility due to loss of flagella in amastigote stage while, P20 was in promastigote stage and too motile.

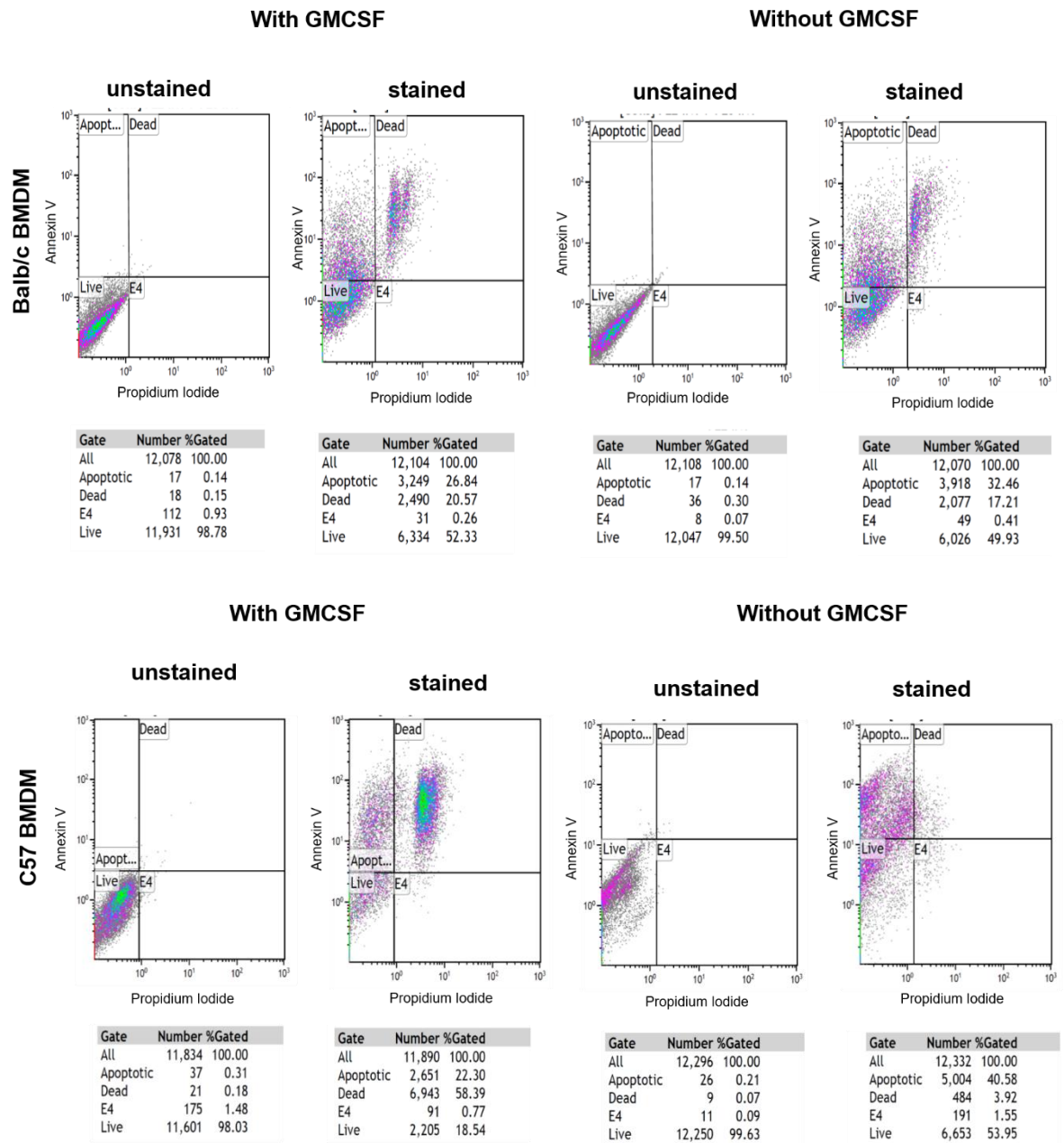
## Appendix 8



### Appendix 8: Live image of Balb/c and C57 BMDM infected with P1 for 24 hours

The blue arrows indicate amastigotes, yellow arrows indicate infected macrophage and red arrows indicate PV

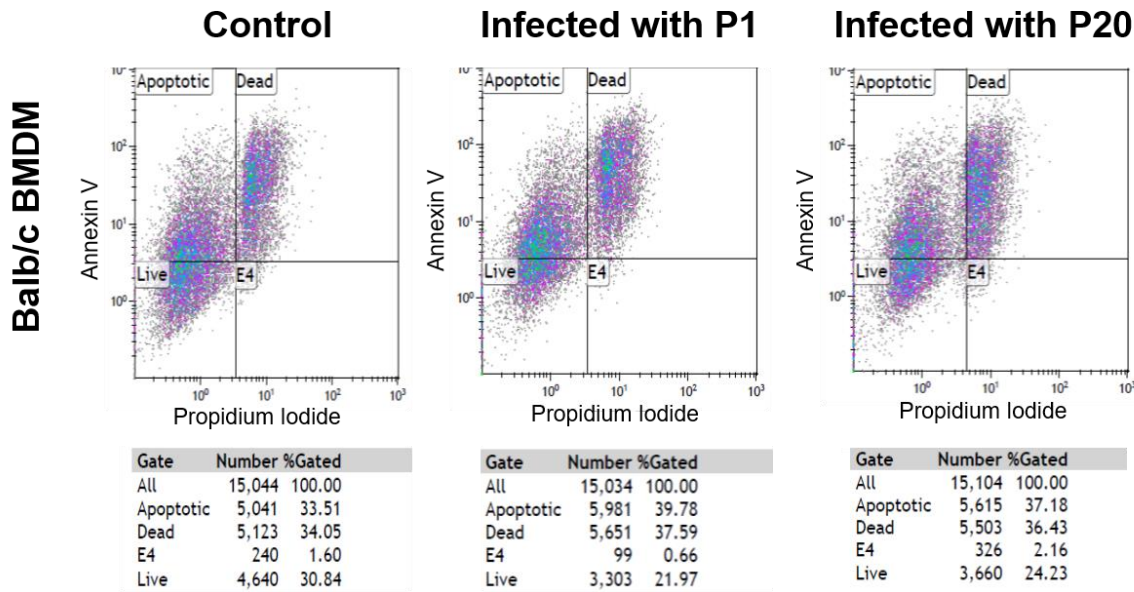
## Appendix 9



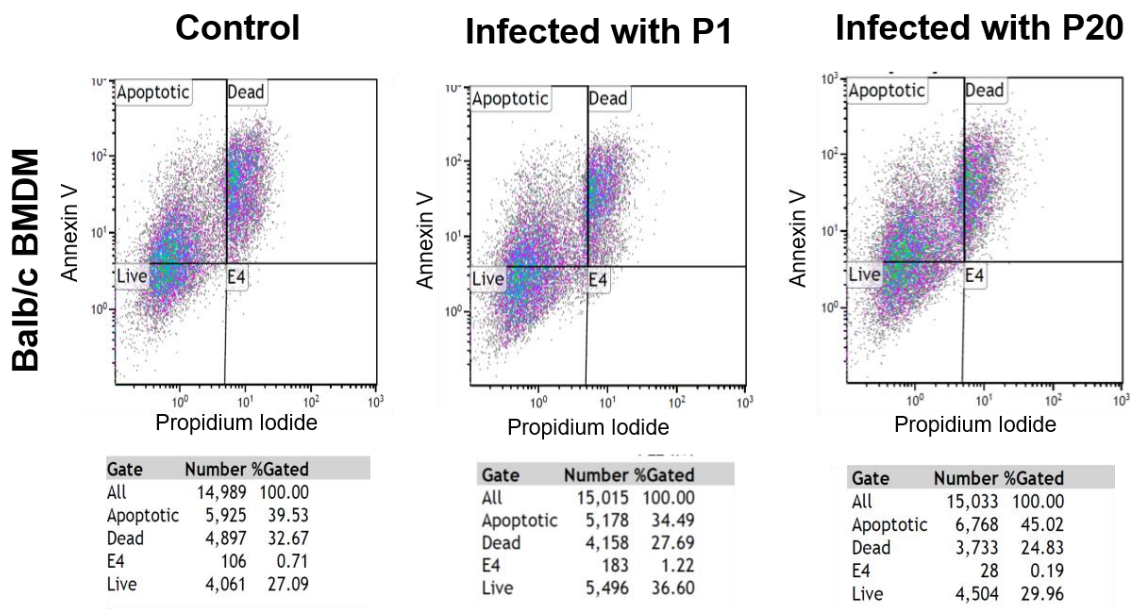
**Appendix 9: Effect of removing of GMCSF from control Balb/c and C57 BMDM culture on apoptosis by flow cytometry**  
 BMDMs were stained with Annexin V for early apoptosis detection and propidium iodide (PI) for dead cells. These results represent two independent experiment.

## Appendix 10

### With GMCSF

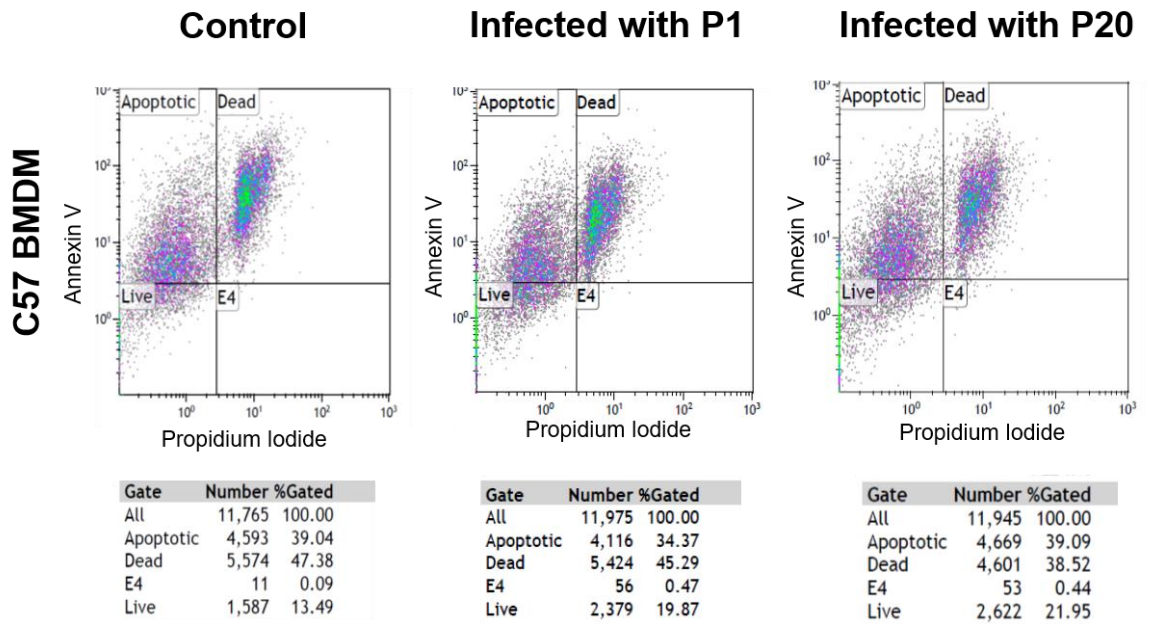


### Without GMCSF

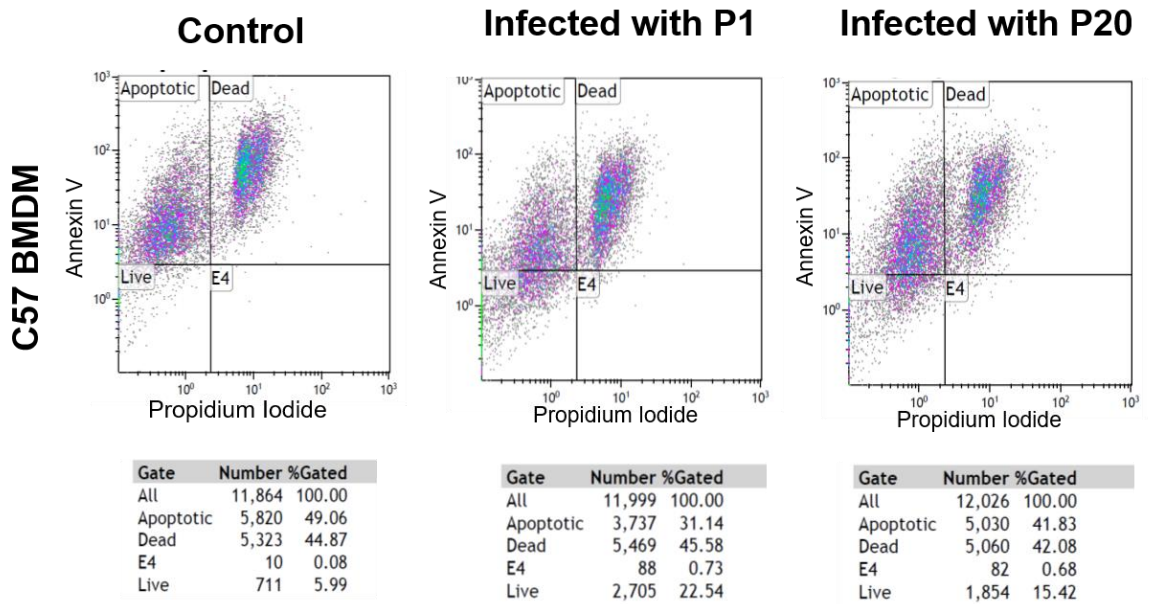


**Appendix 10A: Flow cytometry results of the effect of infection with P1 and P20 *L. mexicana* on apoptosis in Balb/c BMDM after induction of apoptosis by removing GMCSF**

**With GMCSF**



**Without GMCSF**



**Appendix 10 B: Flow cytometry results of the effect of infection with P1 and P20 *L. mexicana* on apoptosis in C57 BMDM after induction of apoptosis by removing GMCSF**